Tbx1 and *Bmp2* in the development of the ear, neural crest and pharyngeal system in mice

Filipa Pontes de Moraes

Dissertation presented to obtain the PhD degree in Biology at the
Instituto de Tecnologia Química e Biológica, Universidade Nova de Lisboa

Oeiras 2010

FCT Fundação para a Ciência e a Tecnologia
MINISTÉRIO DA CIÊNCIA, TECNOLOGIA E ENSINO SUPERIOR

Acknowledgements

First of all I would like to thank Professor Dr. Moisés Mallo for giving me the opportunity to work in his lab and supervise my PhD thesis. Thank you for being always present and for provide the first important boost of energy that triggered me to pursue a PhD in your lab. Your high level of scientific expertise, and the freedom you gave me to pursue my goals set the background in which I am built today.

A todos os actuais e ex-membros do laboratório do Moisés Mallo no Instituto Gulbenkian de Ciência: Marta Carapuço, Inês, Emília, Vanessa, Diogo, Pedro, Cristina, Filipa, Ana, Marta Costa, Tânia, Vitória, Natália, e Jennifer obrigada por todo o apoio e companheirismo.

Um obrigado especial à Marta Carapuço que me ajudou bastante nos primeiros passos de Biologia de Desenvolvimento. Obrigada Tânia pela partilha nestes últimos anos. Nati *gracias* pelo companheirismo e energia, a tua forma de saborear a vida é inspiradora. Marta Costa, tu és das pessoas que mais me orgulho de ter conhecido, a tua força e inteligência têm sido inspiradoras. Muito obrigada pela leitura crítica da tese, pela eterna disponibilidade e pela grande amizade. Jennifer, my dear friend, thank you so much! For your focused mind, for critical reviewing the thesis, for helping me in such a way... I cannot describe it here. Recently you have been the light of my days. “You are so close I can almost taste it!”.

A todo o pessoal dos servicos técnicos do IGC sem os quais este trabalho não seria possivel. Manuel Rebelo e Dolores Bonaparte do Biotério, Ana Nóvoa e Joana Bom da Unidade de transgénicos, João Garcia do Serviço de Informática e toda a Unidade de Imagiologia celular principalmente ao Gabriel Martins por todo o apoio e entusiasmo contagiante.

À Fundação para a Ciência e Tecnologia agradeço o apoio financeiro essencial a preparação desta tese (Apoio financeiro da FCT e do FSE no âmbito do Quadro Comunitário de Apoio, SFRH/BD/18620/2004).

Ao Professor António Coutinho, o seu apoio crucial em momentos chave do meu PhD abriu-me muitas janelas de oportunidades. “Prof. Coutinho tem dois minutos?” Muito obrigada por todos os minutos de conversa “roubada” que sempre se revelou desafiante e inspiradora.

Thank you to my thesis committee Jocelyne Demengeot and Joaquín León for the helpful discussions and kind advice.

To Anne Eichmann who gave me the possibility to learn new techniques and to work in such rich and friendly environment. Thank you Liz Jones for all the training and friendship.

Charles Little, your generosity and enthusiasm touched me a lot!

Um obrigado especial à Ana Tavares que sempre se mostrou disponível para discutir o meu trabalho contribuindo com discussões científicas saudáveis e motivantes.

Obrigada à Leonor Saúde por me ter sempre apoiado com energia positiva e bons conselhos.

A todos os amigos que fiz durante a minha estadia no “planeta“ IGC: Célia, ai senhora! Que bons momentos de puro disparate! Susana e Dinis, obrigada pela força e disponibilidade, Boston é um *must*! Santiago estás no coração, amigo! Margarida “cheia de dengo”, tenho saudades. Patrícia, estejas onde estiveres sinto-te sempre presente, obrigada pelo apoio incondicional. Paulo e Fátima obrigada pelas conversas e pela paciência. *Gracias* Beatriz pela eterna disponibilidade. Daniel, estavas lá e não me deixaste cair, sei que posso contar sempre contigo, obrigada. Obrigada Rita pela revisão critica dos textos, pela força e amizade. Raquel obrigada pelo companheirismo nestes últimos anos, és

uma pessoa muito especial para mim! Mariana "'bora ao Avante?", obrigada pela energia e força. Catch, sabendo-te longe mas à distância de um click, sentia-te perto... Obrigada pela paciência e por todas as conversas, foste uma ajuda preciosa.

Laura amiga, este último ano foi de prova para ambas. Tem sido muito bom saber que posso contar contigo sem preconceitos, com ternura e com uma extraordinária compreensão. Obrigada pela companhia, por todo o apoio e generosidade e por me ajudares a percorrer este e muitos outros caminhos;)

Ao João agradeço todos os anos de companheirismo e por se mostrar sempre disponível para ajudar. E sabes uma coisa? Sei que vais conseguir!

Agradeço ao Paulo por me ter proporcionado momentos de pura gargalhada neste último ano. "Tu vais chumbar!!"

Aos amigos do teatro e da dança Catarina, Rita, Elisa, Pêpê, Zé, Sofia N. e Peter M. que me proporcionaram momentos de pura criação essenciais para manter uma "insanidade saudável".

Aos meus pais obrigada pelo apoio que me deram. Ao Luis e à Isabel obrigada pelo interesse e pela força.

A ti Rui, obrigada por teres estado sempre presente e por me aceitares como sou. Obrigada pela ternura, e pela força inspiradora que és. Tem sido bom ter-te por perto.... sou mais feliz ao teu lado.

"E a liberdade para o professor o que é?

É a liberdade de se ser plenamente aquilo que se é. Outro dia, um amigo que estava numa terra do interior e que me perguntava o que devia fazer por lá. Mandei-lhe dizer: faça favor de ser o que é e de se tornar contagioso!" *De* "Diálogos com Agostinho da Silva", 2001.

Table of Contents

Summary

Development of the vertebrate head involves complex interactions between tissues derived from the three germ layers. Significantly, alterations in the development of this region of the embryo are often associated with a wide variety of human congenital birth defects. Some of them are inherited disorders such as Treacher Collins, Branchio-oto-renal and DiGeorge syndromes. During embryonic development, morphogenesis of the craniofacial area occurs sequentially with the formation of a variety of transient structures, which then undergo complex sequential reorganization to form the adult structures. One of these transient structures is the pharyngeal system, which is formed by a series of individual pharyngeal arches (also called branchial arches), separated by ectodermal clefts and endodermal pouches. Each of the arches is composed by a mesenchymal core, which is formed by mesodermal and neural crest-derived cells, surrounded by epithelia provided by the ectoderm (in the outside) and endoderm (in the inside). In addition, branchial arches contain a cranial nerve and are transversed by a pharyngeal arch artery. Upon differentiation, the pharyngeal apparatus gives rise to structures as diverse as the facial skeleton, the heart outflow tract or organs like the thymus or the thyroid. In addition to the pharyngeal apparatus, other structures are also involved in the formation of head structures. Most notably for the purpose of this thesis, the inner ear of vertebrates derives from another transient embryonic structure, the otic vesicle, which gives rise to the organs of the hearing and equilibrium.

The main focus of this thesis was to further understand the morphogenetic events of the cell populations and the genetic players involved in the development of craniofacial area and the pharyngeal system.

Chapter 1 presents a general introduction to the pharyngeal arch region in mouse embryos and the tissues involved in the correct morphogenesis of this system. A particular section is given to the formation of the mammalian ear development.

The work described in **Chapter 2** involves characterization of the ear phenotype

of null mutant embryos for the *Tbx1* gene. *TBX1* is the major genetic determinant for the pharyngeal arch-derived defects observed in individuals with DiGeorge syndrome. The middle ear skeleton components were strongly affected in null embryos due to a combination of underdeveloped branchial arches and misrouting of neural crest cells. The inner ears of *Tbx1*$^{-/-}$ animals are hypoplastic. The strong inner ear phenotypes observed in these mutants appears to be caused by the inability of the *Tbx1*$^{-/-}$ embryos to keep properly segregated functional domains in the otocyst (Moraes et al., 2005).

Chapter 3 describes neural crest development in the absence of the *Bmp2* gene. Bone morphogenetic protein (BMP) signalling is essential for neural crest development in several vertebrates. Using several markers and a transgenic reporter approach, this chapter shows that neural crest cells are induced in *Bmp2* null mutant embryos, but that these cells fail to migrate out of the neural tube and this defect in migration is not due to apoptosis. The data also suggest that the molecular mechanisms for neural crest migration diverge among species (Correia et al., 2007).

Chapter 4 outlines the development of new imaging tools to study vascular development in mammalian embryos, in particular the arteries that pass through pharyngeal arches. We produced double transgenic reporter mouse lines with endothelial and neural crest cells expressing the fluorescent GFP and RFP proteins, respectively. These transgenic mouse lines, *Tie2-GFP* and *HtPA-RFP,* when introduced into the *Tbx1* null background, confirmed the phenotype of these mutants already described by other methods in Chapter 2. In addition, this chapter reports the development and optimization of a staining technique that enables the analyses of the vasculature of the entire embryo in 3 dimensions. Using this tecnique, the endothelial cells (anti-PECAM) and smooth muscle cells (anti-SMA) from embryonic arch arteries were observed by confocal microscopy. As a proof of principle we evaluated the phenotype of specific mutants with abnormal aortic arch development, such as *Tbx1* and *Gbx2* KO embryos. We were also able to show that the impaired development of embryonic arch arteries

was more severe in *Tbx1*$^{+/-}$;*Gbx2*$^{-/-}$ mutants than in *Gbx2*$^{-/-}$ embryos. These observations suggested that the decreased dosage of *Tbx1* in *Gbx2* mutant background leads to a cumulative effect in the development of the aortic arteries.

Chapter 5 describes the study of smooth muscle recruitment around the embryonic arch arteries. In wild type embryos the cranial arch arteries (first and second) that regress during development, never become associated with vascular smooth muscle cells (VSMCs). In contrast, the caudal arch arteries (third, fourth and sixth) that are maintained at E10.5, recruit VSMCs to their walls shortly after their formation. The embryonic arteries of two mutant strains that have abnormal development in this area were analysed. In particular, I demonstrated that the persistent second arch artery found in mutants for the endothelin receptor A is associated to the presence of VSMCs and that the prematurely regressing fourth arch artery of *Pbx1* mutants fails to recruit vascular smooth muscle cells before its regression. Finally, I show that forced differentiation of VSMCs in the rostral arches (using the transgenic embryo *HtpA-Myoc::Mkl2)* is sufficient to stabilize their normally regressing arteries. The data presented in this Chapter indicates that the physiological regression of the first and second arch arteries results from their failure to recruit VSMCs, most likely because these arches are not populated by cardiac neural crest cells, which are the source of VSMCs in this area of the embryo.

Finally, in **Chapter 6** I present a general discussion integrating some of the most relevant results obtained during the course of this work.

Overall, this work describes and interprets the ear defects in the absence of *Tbx1,* the impaired neural crest development in *Bmp2* null mutants, and shows a clear advancement in our understanding of neural crest-derived vascular smooth muscle cells in the remodelling of the embryonic arch arteries in mammalian embryos.

Resumo

O desenvolvimento da estrutura craniofacial nos vertebrados envolve interacções complexas entre os tecidos originários das três camadas germinais: endoderme, mesoderme e ectoderme. É de salientar que alterações no desenvolvimento desta região no embrião estão frequentemente associadas a um vasto espectro de defeitos congénitos nos humanos: alguns dos quais correspondem a doenças hereditárias, tais como os síndromas Branchio-oto-renal, síndrome de Teacher Collins, e o síndrome de DiGeorge. Durante o desenvolvimento embrionário, a morfogénese da região craniofacial ocorre com a formação de um vasto número de estruturas transitórias, as quais sofrem uma complexa reorganização até à formação das estruturas no adulto. Uma destas estruturas é o sistema faríngeo, o qual é constituído por uma série de arcos faríngeos (também designados por arcos branquiais) separados entre si externamente por ectoderme, e internamente por endoderme. Cada arco faríngeo consiste num centro de tecido mesênquimatoso composto por células derivadas da mesoderme e da crista neural. Para além do mesênquima, apresentam um componente nervoso e um vaso sanguíneo (arco aórtico ou artéria embrionária). A diferenciação do aparelho faríngeo dá lugar a estruturas tão diversas como o esqueleto facial, o tracto de saída do coração ou a órgãos como o timo ou a tiróide. Para além do sistema faríngeo, outros componentes constituem a estrutura craniofacial dos vertebrados. No contexto desta tese será evidenciada a formação do ouvido interno, responsável pela audição e equilíbrio. O ouvido interno é proveniente da vesícula ótica (ou otocisto), outra estrutura transitória e presente em estádios embrionários no desenvolvimento dos vertebrados.

O principal objectivo deste trabalho foi o de aprofundar o conhecimento sobre a formação das estruturas craniofaciais dos vertebrados, bem como os eventos morfogenéticos associados ao desenvolvimento do sistema faríngeo. Nomeadamente o estudo das diferentes populacões celulares e determinantes genéticos envolvidos.

No **Capítulo 1** é apresentada uma introdução sobre a formação do sistema faríngeo nos embriões de ratinho. Um enfoque particular é dado na secção sobre o desenvolvimento do ouvido nos mamíferos.

O trabalho descrito no **Capítulo 2** envolve a caracterização do fenótipo do ouvido de embriões mutantes para o gene *Tbx1*. *TBX1* é o maior determinante genético de anomalias provocadas por deformações dos arcos faríngeos. Tais anomalias são geralmente encontradas em pacientes com o síndrome de DiGeorge. Os ossículos do ouvido médio encontram-se severamente afectados devido ao desenvolvimento insuficiente dos arcos branquiais assim como a alterações na trajectória de migração da crista neural. Os ouvidos internos dos animais *Tbx1*$^{-/-}$ são hipoplásicos. As severas malformações observadas ao nível do ouvido interno parecem ser originadas pela incapacidade de nestes mutantes os diferentes grupos de células que constituem regiões funcionais distintas no otocisto se manterem separados (Moraes et al., 2005).

O **Capítulo 3** descreve o desenvolvimento da crista neural na ausência do gene *Bmp2*. A via de sinalização BMP é essencial ao desenvolvimento da crista neural em várias espécies de vertebrados. Através da caracterização molecular destes mutantes e da criação de uma linha de ratinhos transgénicos, neste capítulo é descrito que as células da crista neural dos embriões mutantes para *Bmp2* são induzidas: no entanto, estas células são incapazes de se destacar do tubo neural e migrarem para as diversas regiões do embrião. Estes resultados também sugerem que os mecanismos moleculares para a migração da crista neural divergem entre as diferentes espécies de vertebrados (Correia et al., 2007).

O **Capítulo 4** descreve novas ferramentas para estudar o desenvolvimento vascular nos embriões de mamífero, em particular o desenvolvimento das artérias embrionárias (ou arcos aórticos) presentes no sistema faríngeo. Foram produzidas linhas transgénicas de ratinhos com células endoteliais que expressam GFP (proteína verde fluorescente) e com células da crista neural que expressam RFP (proteína vermelha fluorescente). Estas linhas transgénicas (*Tie2-GFP* e *HtPA-RFP),* quando introduzidas no *background* genético mutante

para *Tbx1,* confirmam o fenótipo vascular previamente descrito por outros grupos. Também validam as alterações observadas na trajectória da migração da crista neural destes mutantes, já previamente descritas no Capítulo 2. Neste capítulo relata-se também o desenvolvimento e optimização de uma técnica de imunofluorescência, a qual permite a análise tridimensional do sistema vascular do embrião de ratinho. As células endoteliais (observadas com anti-PECAM) e as células do músculo liso (observadas com anti-SMA), que constituem os arcos aórticos, foram observadas por microscopia confocal. De modo a validar esta técnica como uma ferramenta fiável na análise dos diversos fenótipos vasculares, avaliámos o fenótipo de determinados mutantes com anomalias ao nível do desenvolvimento dos arcos aórticos, tais como os embriões mutantes para *Tbx1* e *Gbx2*. Também mostramos que as deformações dos arcos aórticos eram mais severas nos mutantes $Tbx1^{+/-};Gbx2^{-/-}$ do que as deformações observadas nos embriões $Gbx2^{-/-}$. Esta análise sugere que um baixo nível de *Tbx1* no *background* genético mutante de *Gbx2* leva a um efeito cumulativo no desenvolvimento dos arcos aórticos.

O **Capítulo 5** contém o estudo do recrutamento das células do músculo liso em volta dos arcos aórticos. Na estirpe selvagem (WT), os vasos aórticos mais anteriores (presentes no primeiro e segundo arcos faríngeos) regridem durante o desenvolvimento e nunca se encontram associados às células do músculo liso vascular (VSMCs). Pelo contrário, os arcos aórticos posteriores (presentes no terceiro, quarto e sexto arcos faríngeos), que se mantêm durante o desenvolvimento, têm capacidade de recrutar VSMCs. Estas células do músculo liso que se encontram na zona faríngea posterior do embrião, envolvem os vasos endoteliais (arcos aórticos) logo após a sua formação. Foram analisadas duas linhas de ratinhos mutantes que apresentam anomalias no desenvolvimento dos arcos aórticos. Em particular, é descrito que o segundo arco aórtico, anormalmente persistente e que se encontra em mutantes para o receptor de endotelina A, está associado à presença de células de músculo liso vascular e que nos embriões mutantes para o gene *Pbx1,* o arco aórtico que regride

prematuramente nestes embriões não consegue recrutar VSMCs. Finalmente, é observado que a diferenciação forçada de VSMCs no arcos faríngeos anteriores (usando os embriões transgénicos *HtpA-Myoc::Mkl2*) é suficiente para estabilizar as artérias, que normalmente regridem. Os resultados apresentados neste capítulo indicam que a regressão fisiológica do primeiro e segundo arcos aórticos resulta da sua incapacidade de recrutar VSMCs, sendo bastante provável que esta incapacidade resulte do facto de que estes arcos não se encontrem numa zona composta por crista neural cardíaca, que é a fonte de VSMCs na região faríngea do embrião.

Finalmente, o **Capítulo 6** corresponde a uma discussão geral que integra alguns dos resultados mais relevantes obtidos durante o curso deste trabalho.

Em resumo, este trabalho descreve e interpreta os defeitos na formação do ouvido causados pela ausência de *Tbx1,* as anomalias no desenvolvimento da crista neural em embriões mutantes para *Bmp2* para além de mostrar um claro avanço na nossa compreensão do papel das células do músculo liso vascular (originárias da crista neural cardíaca) na remodelação vascular nos embriões de mamífero.

Abreviations

AP	Antero-posterior
BMP	Bone morphogenetic protein
cDNA	Complementary DNA
CNS	Central nervous system
CVG	Cochleo-vestibular ganglion
DNA	Deoxyribonucleic acid
DGS	DiGeorge syndrome
Dlx	Distal-less related
dUTP	deoxyuridine triphosphate nucleotides
DV	Dorso-ventral
E	Embryonic day
EAA	Embryonic arch arteries
EAM	External acoustic meatus
ECE	Endothelin converter enzyme
Eph	Ephrin
EMT	Epithelial to mesenchymal transition
ErbB4	Tyrosine kinase-type cell surface receptor HER4
ET-1	Endothelin-1
ET-A	Endothelin receptor A
FGF	Fibroblast growth factor
FGFR	FGF receptor
Gbx2	Gastrulation brain homeobox-2
GFP	Green fluorescent protein
Ht-PA	Human tissue plasminogen activator
Hox	Homeobox genes
KO	Knock-out
Lfng	Lunatic fringe
ML	Medio-lateral
mRNA	Messenger RNA

Myoc	Myocardin
Mkl2 (MRTF-B)	Myocardin like 2 (Myocardin related transcription factor-B)
NC	Neural crest
N-CAM	Neural cell adhesion molecule 1
NCC	Neural crest cell
OFT	Outflow tract
PA	Pharyngeal arch
Pax	Paired-box
PBS	Phoshate buffer saline
PBT	Phosphate buffer saline – Tween20 0.1%
Pbx1	Pre-B-cell leukemia transcription factor 1
PCR	Polymerase chain reaction
PDGF	Platelet-derived growth factor
PFA	Paraformaldehyde
PTA	Persistent truncus arteriosus
RA	Retinoic acid
Raldh2	Retinaldehyde dehydrogenase 2-RA synthesizing enzyme
RNA	Ribonucleic acid
RFP	Red fluorescent protein
SMA	Smooth muscle actin
SHH	Sonic hedgehog
Srf	Serum response factor
Tbx	T box
TGFβ	Transforming growth factor beta
TUNEL	Terminal dUTP nick-end Labelling
YFP	Yellow fluorescent protein
VEGF	Vascular endothelial growth factor
VSD	Ventricular septal defect
VSMC	Vascular smooth muscle cell
WT	Wild-type

Index of Figures

Index of Tables

Chapter 1:
General Introduction

A. DEVELOPMENT OF THE PHARYNGEAL ARCHES

The pharyngeal system is a transient embryonic complex that is present in all vertebrates. It comprises the pharyngeal arches, also known as branchial arches, which are serially arranged pairs of swellings that appear along the sides of the embryonic head. They give rise to structures of the face and neck, contributing to the adult oro-pharyngeal apparatus with primary functions of breathing and feeding (Noden, 1983a; Noden, 1983b). Cells from all germ layers contribute to the development of the arches (Fig. 1.1). Each arch contains a core of paraxial mesoderm and an aortic arch artery, which are surrounded by neural crest cells (NCC). The arches are externally covered by ectoderm and internally by pharyngeal endoderm. Ectodermal clefts and endodermal pharyngeal pouches separate the arches in areas where ectodermal and endodermal cells are in direct contact (Graham, 2008). Significantly, each of these different embryonic cell types gives rise to distinct derivatives (Le Douarin et al., 2004). The ectoderm generates the epidermis and also forms thickenings called placodes which give rise to some of the sensory neurons of the cranial ganglia (D'Amico-Martel and Noden, 1983; Couly and Le Douarin, 1990). The endoderm gives rise to the pharyngeal and middle ear epithelium and the taste buds. It also forms the thymus as well as two endocrine glands: the thyroid and the parathyroid (Le Douarin and Jotereau, 1975). The mesoderm-derived mesenchyme contributes to the musculature and endothelial precursors of the pharyngeal arches (Couly et al., 1992; Trainor et al., 1994). The neural crest can give rise to a wide variety of tissues such as neurons, glial and Schwann cells of the peripheral nervous system, cartilages and bones of the head, melanocytes, connective tissue in muscle and glands and vascular smooth muscle cells of the arch arteries (Couly et al., 1993; Le Douarin et al., 1993; Jiang et al., 2000; Etchevers et al., 2001).

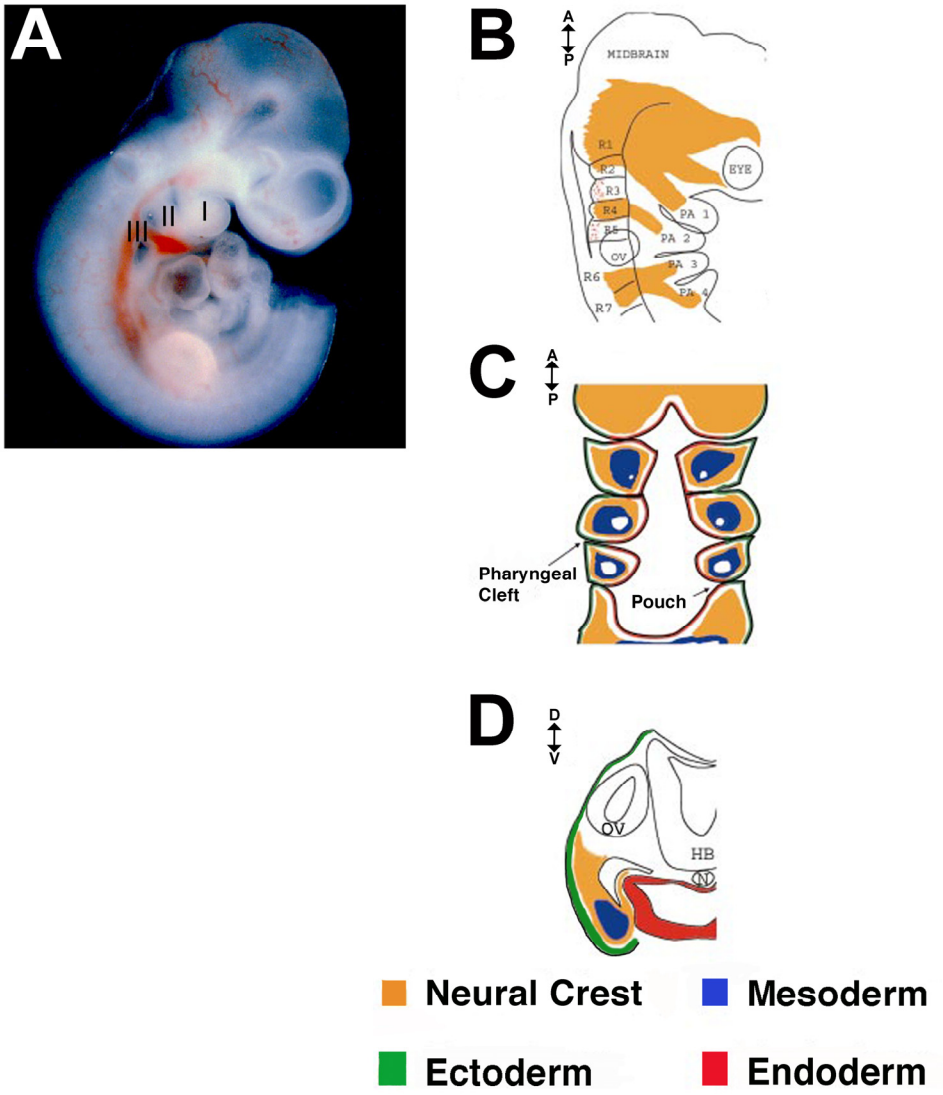

Figure 1.1 The pharyngeal arches
(A) Side view of a mouse embryo at E9.5 showing the first (I), second (II) and third pharyngeal (branchial) arches (B) Drawing representing the neural crest in yellow migrating from the hindbrain to the pharyngeal arches. The rhombomeres, are labelled R1 through to R7. The pharyngeal arches are labelled PA 1-4. The eye, midbrain and otic vesicle (ov) are also highlighted. (C) A longitudinal section through the pharyngeal arches showing the different embryonic populations that contribute to the arches. The ectoderm, which surrounds the outer face of the arches is green, while the endoderm which forms the inner surface of the pharynx is labelled red. The neural crest is shown in yellow and the mesodermal core of the arches is blue. (D) A transverse section through the second pharyngeal arch showing the relationships of the arch components to each other (adapted from Graham and Smith, 2001).

At a certain stage in its development, each pharyngeal arch contains progenitors of cartilage and bone, skeletal and smooth muscle, an aortic arch and a cranial nerve. The development of the system gives rise to structures as diverse as skeletal and muscle components of the face, the heart outflow tract or organs like the thymus or the thyroid. Although the distinct pharyngeal arches generate the same basic tissues, each arch also has its own identity and contributes to specific structures. The first most anterior arch forms structures including the malleus, incus and tympanic ring of the middle ear, maxilla, mandible and temporal bone, jaw muscles and portions of the trigeminal nerve; the second contributes to some of the bones and muscle of the neck, the stapes of the middle ear, the styloid process of the temporal bone, the facial nerve, muscles of facial expression and the stapedial artery. The third arch forms the body and the greater horn of the hyoid bone, the thymus, and the glossopharyngeal nerve; the fourth pharyngeal arch gives rise to the thyroid cartilage, superior branch of the vagus nerve (X); the sixth arch forms the cartilages and the muscles of the larynx and the laryngeal portion of vagus nerve (X). In addition all these most posterior arches (3^{rd} to 6^{th}) give rise to the aortic arteries connected to the heart. The derivatives of the pharyngeal arches are summarized in Table 1.1.

Table 1.1 Derivatives of the pharyngeal arches (PA)

PA	Skeletal derivatives (neural crest and mesoderm)	Cranial nerves (neural tube)	Muscles (mesoderm)	Arch arteries (mesoderm)
1st	Maxilla, mandible and temporal bone, malleus of the middle ear, also Meckel´s cartilage	Maxillary and mandibular divisions of trigeminal nerve (V)	Jaw muscels; muscle of the ear and soft palate	The aortic arch regress to maxillary branch of the carotid artery (to the ear, nose, and jaw
2nd	Stapes, styloid process of temporal bone, lesser horn of the hyoid bone Reichert´s membrane	Facial nerve (VII)	Muscles of facial expression; jaw and upper neck muscles	The aortic arch regresses to the stapedial artery, arteries to the ear region
3rd	Greater horn of the hyoid bone, thymus, inferior parathyroid gland	Glossopharyngeal nerve (IX)	Stylopharyngeus (to elevate the pharynx)	Common carotid artery; root of internal carotid
4th	Laryngeal cartilages Thyroid cartilage, superior parathyroid gland	Superior laryngeal branch of vagus nerve (X)	Constrictions of pharynx and vocal cords	Right 4th aortic arch: Subclavian artery Left 4th aortic arch: aortic arch
6th	Ring of cartilage around the trachea, cartilage of the larynx	Recurrent laryngeal of vagus nerve (X)	Intinsic muscles of larynx	Right 6th aortic arch: pulmonary artery. Left 6th aortic arch: Pulmonary artery and ductus arteriosus

(Adapted from Gilbert, 2003)

The development of this system involves tightly co-ordinated interactions between different embryonic cell types to generate a normal morphology, when the correct pharyngeal arch development is compromised all of the organs that it gives rise to are affected. Significantly, alterations in the development of this region of the embryo are often associated with a wide variety of human congenital birth defects, and they are evident in a number of inherited disorders such as Treacher Collins, Branchio-oto-renal and DiGeorge syndromes (Poswillo, 1988; Jerome and Papaioannou, 2001).

Here I will review the contribution of the cell populations and corresponding genetic factors involved in the correct development of the mammalian pharyngeal region. I will emphasize the role of neural crest giving an overall introduction about this important cell population characteristic of all vertebrates.

A.1 Neural crest

The neural crest was initially described in the nineteenth century by Wilhelm His as a novel longitudinal strip of cells dorsal to spinal cord lying between the dorsal ectoderm and the neural tube. This mesenchymal population was later named neural crest by Marshall in 1879 (Hall, 1999) and has been considered one of the most interesting tissues of the vertebrate embryo for a variety of reasons:

1) In evolutionary terms the neural crest has been crucial for the generation of the vertebrate head, as Gans and Northcutt pointed out on their significant paper “Neural crest and the origin of vertebrates: a new head” (Gans and Northcutt, 1983), which clearly made the point that many of the features that distinguish the vertebrates from their closest relatives have their origin in the neural crest;
2) This cell population displayed an unusual and striking degree of motility and spread throughout the body;
3) Finally these cells diversify into a wide variety of cell types, including neurons and glial cells of the peripheral nervous system, melanocytes, smooth muscle

and many of the skeletal and connective tissue of the head (Le Douarin and Kalcheim, 1999; Table 1.2).

Table 1.2 Main cell types derived from neural crest

Neurons	Peripheral nervous system (PNS): sensory, sympathetic and enteric ganglia
Glial cells	PNS satellite glial cells and Schwann cells of peripheral nerves
Pigment cells	Skin melanocytes
Mesenchymal cells	Cartilages and bone Odontoblasts Dermis Connective tissue in muscles and glands Meninges of the forebrain Adipocytes Vascular smooth muscle cells (VSMCs)

(Adapted from Dupin et al., 2007)

A.1.1 Induction of Neural crest

Neural induction (also called neurulation) occurs when a thickening of ectoderm is segregated from the rest of the embryonic ectoderm and originates the precursor region of the nervous system called the neural plate. This neural plate will invaginate and the neural folds elevate and close, forming the neural tube. Neural crest induction is the step in which a group of cells in the ectoderm receives signals that will instruct them to become specified as neural crest precursors. These cells arise at the interface between the neural plate and the surface ectoderm of the embryo; from there they delaminate and migrate along specific routes to many destinations in the vertebrate embryo (Selleck and Bronner-Fraser, 1996). The process of induction of neural crest cells has been extensively studied in different model organisms. The prevailing view is that interactions

between the neural plate and the surrounding non-neural ectoderm specify the neural crest (Moury and Jacobson, 1990; Selleck and Bronner-Fraser, 1995; Mancilla and Mayor, 1996;). Studies in several model organisms sometimes produced conflicting results in the effort to characterize the molecular mechanisms that induce neural crest formation. One of the problems when analysing this process has been separating neural crest induction from "neural induction" due in part to the close spatiotemporal association of both processes. Moreover, many of the same signals, (such as BMPs, FGFs and Wnts) implicated in neural crest formation, were also key molecules for the induction of neural tissue itself. It has been suggested recently that induction of neural plate and neural crest occur independently (Wawersik et al., 2005).

The bone morphogenetic proteins (BMPs) were among the first factors implicated in the earliest processes of neural crest development (Liem et al., 1995). BMPs are secreted proteins of the transforming growth factor beta (TGF-β) superfamily and are involved in dorsoventral patterning during early development. Experiments in chick suggested that *Bmp4* and *Bmp7*, expressed in the epidermis were implicated in neural crest induction (Liem et al., 1995). Inhibition of BMP signalling in the ectoderm leads to neural induction; when BMP is added to explants of neural epithelial tissue, BMP it is able to substitute for the crest-inducing activity of the non-neural ectoderm. Experiments in *Xenopus* animal caps (Marchant et al., 1998) and genetic analysis in zebrafish (Barth et al., 1999), suggest that neural crest induction could be explained by a response of the ectoderm to intermediate levels of BMPs: epidermis forms where BMP is high, neural plate forms where BMP signalling is low. An alternative model is that the border between neural plate and non-neuroectoderm is a competency zone – a region where neural crest can be induced (Bastidas et al., 2004). This model predicts that there are separate, sequential signals for the formation of neural crest. However, the role of BMPs in neural crest induction is not entirely clear. In chick embryos, Bmp4-soaked beads implanted in the prospective neural plate are not able to alter the specified neural fate (Streit et al., 1998). More recently,

another study showed that induction of neural crest cells *in vitro* was not only dependent of BMP signals but also depends on the simultaneous activity of other factors (Garcia-Castro et al., 2002). In addition, studies performed in chicken embryos suggested that BMPs are required for the migration rather than the induction of neural crest cells (Sela-Donenfeld and Kalcheim, 1999). Furthermore, experiments in *Xenopus* demonstrate that BMP signalling alone is not sufficient for neural crest induction *in vivo* and there is a direct requirement for a Wnt signal for this process to occur (LaBonne and Bronner-Fraser, 1998). Mouse studies have shown that null mutants for *Bmp5* are viable and display morphologic alterations in the ear, cartilage and bone elements (Kingsley et al., 1992). On the other hand, mutations in *Bmp4* or *Bmp7* do not produce obvious defects in cranial neural crest development (Dudley et al., 1995; Luo et al., 1995; Winnier et al., 1995). Even mouse embryos mutant for both *Bmp5* and *Bmp7* also present no defects in neural crest formation and migration. Nevertheless, *Bmp5* and *Bmp7* have been reported to be required in a redundant manner for the survival of posmigratory cells, as demonstrated by their increased cell death in *Bmp5;Bmp7* double mutants (Solloway and Robertson, 1999). In addition *Bmp2*, which is expressed in a small region of the surface ectoderm, is essential for the formation of migratory neural crest cells (Kanzler et al., 2000). In this study, transgenic mice expressing the BMP antagonist *Xnoggin* in the neural tube were analysed. *BMP2* signalling was blocked resulting in spatially specific ablation of the neural crest, leading to the failure of branchial arch development and an absence of cranial neural crest derivatives from the targeted regions. However it was not possible to conclude whether *Bmp2* is required for induction of neural crest cells or for their migration from the neural tube. This subject will be explored in Chapter 3 where the neural crest phenotype from *Bmp2* null mutant mouse embryos is characterized. Nevertheless it is now clear, from *in vitro* and *in vivo* experiments that levels of BMP signalling alone cannot be sufficient for neural crest induction, and that other signalling pathways are involved.

The Wnt families are also involved in neural crest induction (Ikeya et al., 1997;

LaBonne and Bronner-Fraser, 1998). Wnts are a large family of cys-rich glycoproteins that controls developmental processes such as cardiac progenitor morphogenesis and head induction. Activation of the canonical Wnt signalling pathway results in the stabilization and nuclear translocation of β catenin, which in turn activates transcription of Wnt target genes (Wu et al., 2003). Several studies in different organisms have shown the multiple roles of Wnts in neural crest formation. In the frog, gain and loss of function experiments show that activation of the canonical Wnt pathway is both sufficient and necessary for neural crest induction. Misexpression of Wnt signals in early embryos results in ectopic expression of neural crest markers in cells normally fated to become epidermis, not neural tissue (Saint-Jeannet et al., 1997; LaBonne and Bronner-Fraser, 1998). In zebrafish, mosaic analysis has shown that direct reception of a Wnt signal is required for the production of neural crest precursors (Lewis et al., 2004). *In vitro* and *in vivo* studies performed in chick embryos, showed that the Wnt signalling pathway alone is both necessary and sufficient to induce neural crest cells in the absence of added factors, and Wnt6 was suggested to be the key factor involved (Garcia-Castro et al., 2002). In mouse embryos, the results are not so clear as in chick embryos. For example genetic ablation of *Wnt1* or *Wnt3a* in mouse embryos shows significant defects in neural crest derivatives, but there was no detailed analysis at earlier stages (when neural crest induction occurs). Even so, neural crest is induced in these animals, failing to demonstrate a conserved role for Wnt signalling in murine neural crest induction (Ikeya et al., 1997). Studies on downstream factors of Wnt signalling pathway have also provided further evidence about the role of Wnt signalling in neural crest development. Targeted inactivation of β-catenin in mouse embryo neural tube leads to defects in cranial neural crest derivatives (Brault et al., 2001). Wnt signalling in mouse embryos appears to be important for differentiation rather than neural crest induction. However, several other Wnts are expressed all around in the embryo, including in domains that overlap with BMPs (Parr et al., 1993; Mani et al., 2010). Therefore the functions of Wnt signalling are likely to be complex, making it difficult to

support a simplified view about their specific role in mammalian neural crest development.

In addition to BMP and Wnt, members of FGF and Notch families have been shown to participate in the process of neural crest induction to different extents in different organisms. For example, Fgf2 combined with Bmp antagonists can induce neural crest formation in *Xenopus* (Mayor et al., 1995; LaBonne and Bronner-Fraser, 1998).

Studies in frogs and birds have shown that Delta-Notch signalling is also required upstream of BMP signalling to promote neural crest formation (Endo et al., 2002; Glavic et al., 2004).

Subsequently the signalling molecules of the Wnt, FGF and BMP families cooperate to activate a distinct combination of transcription factors at the neural plate border including Snail2 (previously known as Slug, the earliest marker of specified neural crest) Sox9/10, Pax3, Id3, Foxd3, Zic and Msx1 which constitute the neural crest specification network (reviewed in Meulemans and Bronner-Fraser, 2004; Steventon et al., 2005; Fig. 1.2). For example, *Pax* genes are expressed initially in the neural plate border and dorsal neural tube and are targets of Wnt signalling pathway (Sato et al., 2005). Another example is the group of Snail transcription factors, which are among the earliest known markers of neural crest formation and their expression has been used as a read out of neural crest induction in response to different signals. Based on expression analyses, it has been suggested that, in the mouse, *Snail1* performs the function of *Snail2* in the chicken neural crest (Sefton et al., 1998). However, contrary to observations in frog and avian embryos neither *Snail1* nor *Snail2* seem to be involved in neural crest production in mice (Murray and Gridley, 2006), suggesting that some of the mechanisms of neural crest induction are not conserved among vertebrates.

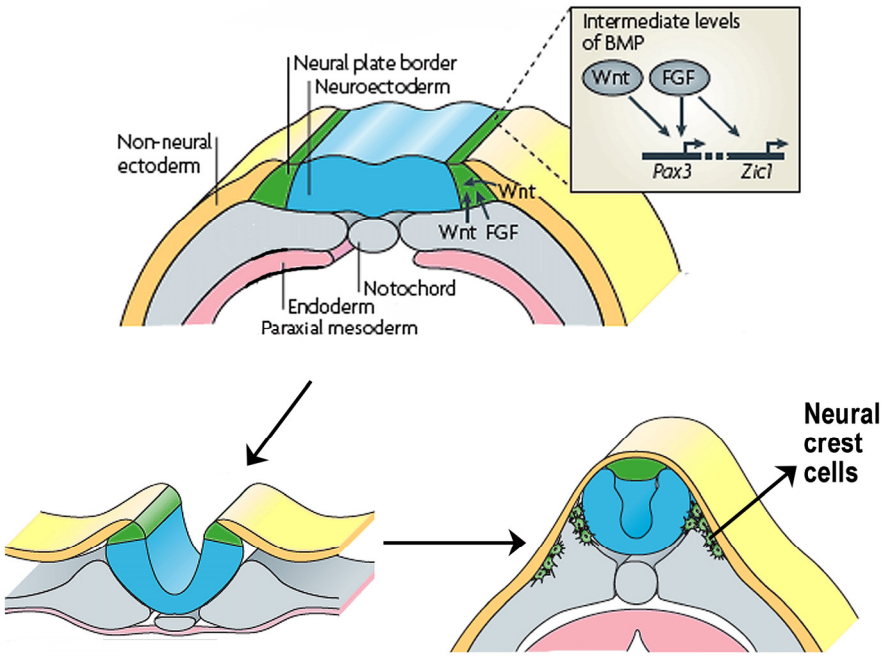

Figure 1.2 Neural crest induction, specification and delamination.
Induction initiates at the neural plate border and is mediated by signals including fibroblast growth factor (FGF) from the underlying mesoderm as well as Wnts from mesoderm and adjacent non-neural ectoderm. These signals induce the expression of individual neural plate border specifiers, such as *Pax3* and *Zic1*, in a manner that is dependent on intermediate levels of bone morphogenetic protein (BMP). Expression of these early neural crest specifiers, segregates neural crest from the dorsal neuroepithelium and control its delamination from the neural tube. Finally these cells diversify into a wide variety of cell types (Le Douarin and Kalcheim, 1999), including neurons and glial cells of the peripheral nervous system, melanocytes, smooth muscle and many of the skeletal and connective tissue of the head (adapted from Sauka-Spengler and Bronner-Fraser, 2008).

A.1.2 Delamination

Once the neural crest cells have been induced they migrate out of the neural tube. Neural crest cells lose cell-cell adhesions by undergoing a transition from epithelial to mesenchymal type, which allows them to delaminate and emigrate from the neuroepithelium. More specifically, this epithelial to mesenchymal transition (EMT) requires a switch in the repertoire of cell adhesion molecules expressed by these cells. Thus the crest cells down-regulate *N-CAM*, *N-Cadherin* and *Cadherin-6B,* which are generally expressed by cells of the neural tube and

upregulate *Cadherin-7* and *Cadherin-11* (Akitaya and Bronner-Fraser, 1992; Nakagawa and Takeichi, 1998; Cano et al., 2000). The transcriptional repressor Snail2 is thought to be crucial for the EMT and recent experiments in chick embryos show that the avian *Snail2* directly represses *Cadherin-6B* during this process (Taneyhill et al., 2007).

The delamination process is also controlled by BMP signalling. Most prominently *Bmp4*, which comes to be expressed at the dorsal midline of the neural tube. If Bmp4 is added alone to neural tube explants, it stimulates production of neural crest cells. Interestingly, inhibition of BMP4 signalling by Noggin, a BMP4-specific antagonist, in the chick spinal cord prevents crest delamination; the neural crest cells cannot escape from the neural tube and accumulate within it, demonstrating that BMP4 and Noggin act antagonistically to control neural crest delamination (Sela-Donenfeld and Kalcheim, 1999; Smith and Graham, 2001).

Studies in chicken implicate Wnt signalling in the delamination process. It has been shown that BMP signalling controls the cell cycle by modulating cyclin levels and that this effect was mediated by Wnt1 (Burstyn-Cohen et al., 2004).

A.1.3 Migration

The neural crest can be divided into cranial, trunk and vagal neural crest (the cranial more anterior and the vagal the most posterior). Each population migrates along unique pathways contributing to specific cell and tissue types (Le Douarin and Kalcheim, 1999). In this thesis I will mainly focus on the **cranial neural** crest, that play an important role in sculpting the craniofacial structures by contributing to pigment cells, the neurons and glia of the sensory ganglia, cartilage, bone, smooth muscle and connective tissue of the face (Noden, 1983b; Kontges and Lumsden, 1996). Cranial NCCs migrate into the head periphery in distinct streams that correlate with their places of origin in the different brain regions: forebrain (telencephalon and diencephalon), midbrain (mesencephalon) or hindbrain (metencephalon or rhombencephalon). The hindbrain contains seven transient segments, called rhombomeres (r1-r7) (Lumsden et al., 1991; Birgbauer et al.,

1995; Kontges and Lumsden, 1996; Fig. 1.3). These rhombomeres dictate the axial levels where patterned neural crest cells exit the hindbrain to populate the pharyngeal arches. Neural crest cells that emanate from diencephalon and anterior mesencephalon migrate to the fronto-nasal and periocular regions of the head. These neural crest cells form the head mesenchyme generating some of the bones of the face (Le Douarin and Kalcheim, 1999). Neural crest cells from posterior mesencephalon and rhombomeres r1 and r2 migrate to the first pharyngeal arch originating some of the skeletal components of the face and ear (Table 1.1). The cells arising from r4 populate the second pharyngeal arch forming the lesser horn of the hyoid cartilage as well the stapes bone of the middle ear and the styloid process. The most caudal stream of cranial NCCs migrates from r6, 7 and 8 to populate the third and more caudal pharyngeal arches giving rise to some of the cartilages and connective tissue of the neck (Fig. 1.3; Le Lievre and Le Douarin, 1975; D'Amico-Martel and Noden, 1983).

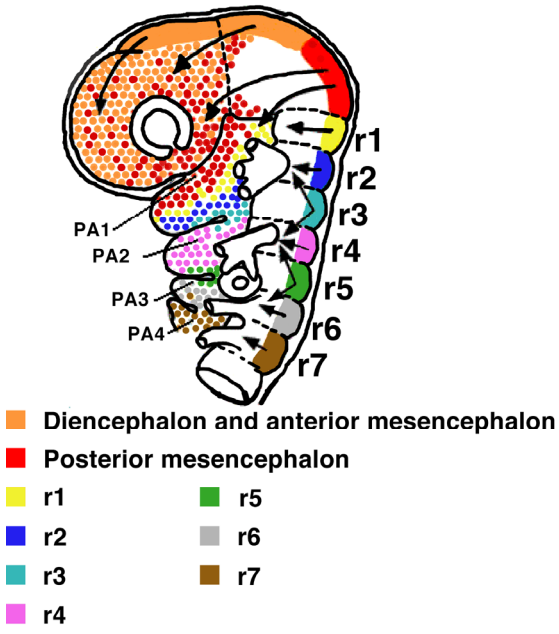

Figure 1.3 Migratory streams of neural crest
Neural crest cells from diencephalon and mesencephalon migrate to the nasofrontal and periocular area. Migratory streams from posterior mesencephalon also populate the first pharyngeal arch (PA1), which is also populated by neural crest derived from rhombomeres 1 and 2 (r1/r2) together with a small contribution from r3 crest cells. The major contribution to the second pharyngeal arch (PA2) comes from rhombomere 4 crest cells. Neural crest cells arising from r3 and r5 split into strains participating, in two adjacent arches. Neural crest from r6 and r7 migrate to PA3 and PA4. r1-r7, rhombomeres 1-7, PA1-4, pharyngeal arches 1-4 (adapted from Couly et al., 2002).

It has been reported that r3 and r5 do not form neural crest cells, although later

reports showed that, in fact, these two rhombomeres produce a small amount of neural crest cells that do not exit the hindbrain lateral to these rhombomeres but move anteriorly or posteriorly to join the streams of crest migrating from the adjacent even-number rhombomeres (Sechrist et al., 1993; Birgbauer et al., 1995). The absence of neural crest cell streams associated to r3 and r5 has a key role in reinforcing the segregation of the migratory crest cells from their adjacent rhombomeres. Previous studies in chick showed that the majority of neural crest from r3 and r5 is lost by apoptosis, and this effect is mediated by *Bmp4* expression (Graham et al., 1993; Smith and Graham, 2001). However studies in other species such as zebrafish (Schilling and Kimmel, 1994) or *Xenopus* (Hensey and Gautier, 1998; Hensey and Gautier, 1999) did not observe focal cell death in r3 and r5. Accordingly, mouse embryo studies have also suggested that the segregation of the neural crest cells into streams is not only due to induction of apoptosis in r3 and r5 as shown in chick, but also to the action of cues in the periphery, which act to reinforce and stabilize this region (Trainor et al., 2002). Genetic engineering in mice has shown several mouse embryo phenotypes with defects in cranial crest streams. *ErbB4* and *Twist* act cell non-autonomously to regulate proper neural crest migration (Golding et al., 2000; Soo et al., 2002; Ota et al., 2004). In addition, other molecules such as Sema3A expressed in both r3 and r5 act cell autonomously to regulate cell migration (Eickholt et al., 1999). Studies in frog embryos suggest that Ephrin cell signalling plays an intrinsic role in keeping the neural crest streams segregated (Smith et al., 1997). EphA4 and EphB1 receptor tyrosine kinases are expressed in neural crest cells that populate the third and fourth arches, whereas second arch cells express EphrinB2 ligands. Inhibitory and repelling interactions between these r3/5 neural crest cells and second arch cells function to prevent intermingling between cell populations and keep the neural crest in their respective arch streams (Smith et al., 1997). Interestingly, in mouse it was shown that *EphrinB1* acts cell autonomously in cranial neural crest cells and controls their migration. *EphrinB1* null neural crest displays abnormal migration by invading regions normally devoid of this cell type.

This led to defects in middle ear, nerve fasciculation and branching (Davy et al., 2004). These studies showed that the segregation of the neural crest is a central step for the correct organization of the pharyngeal system.

The **cardiac neural crest** is a subpopulation of cranial neural crest originated in the caudal region of the cranial crest. It populates the third, fourth and sixth caudal arches and produces the muscular connective tissue wall of the large arteries as they arise from the heart, as well contributing to the septum that separates the pulmonary circulation from the aorta (Le Lievre and Le Douarin, 1975; Jiang et al., 2000). They can also develop into melanocytes, neurons or cartilage. This cell population will be emphasized in the second section of this introduction, where I will review some of the aspects regulating the development of the embryonic arch arteries.

A.2 The role of neural crest in pharyngeal arch development

There has been a general interest in understanding how the different embryonic populations pattern the pharyngeal arches. In the past, several studies have suggested that the neural crest played a crucial role in coordinating the development of the pharyngeal arches and in giving specific identity to individual arches (Noden, 1983b). More specifically, it was found that if the presumptive first arch neural crest was grafted and forced to populate the second arch, the second arch in the host embryo developed derivatives resembling the skeleton characteristic of the dorsal first arch (Noden, 1983b). These classic transplantation experiments suggested that the neural crest has positional information for organizing the pharyngeal arches already in the neural primordium, before emigration. Experiments by other groups suggested that the fate determination of cranial neural crest was due in part to differential *Hox* gene expression along the hindbrain, where these cells are originated (Trainor et al., 2002). *Hox* genes are involved in establishing anterior-posterior (cranial-caudal) positional identities (Hunt et al., 1991); unique combinations of these genes are

expressed among different hindbrain rhombomeres and their associated neural crest cells (reviewed in LaBonne and Bronner-Fraser, 1998). These studies indicated that these genes were also involved in specifying the anterior-posterior identity of the neural crest cells populating each of the arches. Mutational analysis of *Hox* genes in mice, have shown that these genes are required for the normal morphogenesis of arch-derived skeletal elements (Gendron-Maguire et al., 1993; Rijli et al., 1993; Kanzler et al., 1998; Gavalas et al., 2001). This is exemplified by inactivation studies of *Hoxa2* gene, which is specifically expressed in the neural crest that originates from rhombomere 4 and populates the second pharyngeal arch. In mice mutant for *Hoxa2* neither first nor second arches express this gene and consequently multiple cranial skeletal defects were evident, in which the second arch skeletal derivatives assume first arch characteristics. These results indicate that *Hoxa2* expressed in rhombomere 4 crest cells is essential for the identity of the second arch (Gendron-Maguire et al., 1993; Rijli et al., 1993; Kanzler et al., 1998) by inhibiting the formation of skeletal elements in this arch. Hox3 group genes are expressed in the third pharyngeal arch (Hunt et al., 1991; Prince and Lumsden, 1994; Hunter and Prince, 2002). Compound mutants of *Hoxa3* and *Hoxd3*, exhibit defects in the laryngeal cartilages (Condie and Capecchi, 1994).

Other transcription factors, in particular the Dlx family can also modulate the development of the derivatives of the pharyngeal arches, more specifically the skeletal tissues derived from neural crest. *Dlx* genes are expressed in the pharyngeal arches, with *Dlx1/Dlx2* being expressed broadly and *Dlx5/6* expressed in the more distal mesenchyme (Qiu et al., 1997; Depew et al., 1999; Depew et al., 2002; Depew and Simpson, 2006). In *Dlx5/6* mutant mice some of the elements of the first pharyngeal arch fail to form, such as the lower jaw. In their place an upper jaw is formed. The authors concluded that loss of *Dlx5* and *Dlx6* resulted in a homeotic transformation of the lower jaw into an upper jaw, indicating that *Dlx5* and *Dlx6* are major determinants of the cellular identity within the pharyngeal arches (Depew et al., 2002). Although these studies support a

major role for the neural crest and their transcription factors in patterning the pharyngeal arches, recent work shows that the fate determination of cranial neural crest is strongly influenced by instructive signals provided by adjacent tissues. For example, studies in mouse embryos showed that expression of Dlx transcription factors is regulated by ET-1 signals from the epithelia of the pharyngeal arches. Endothelins (ETs 1, 2 and 3) are a family of small peptides that play important roles in neural crest cell differentiation and survival (Yanagisawa et al., 1998). More specifically, endothelin-1 (ET-1) is proteolytically generated from its inactive precursor by endothelin-converting enzyme–1 (ECE-1) and acts on the endothelin-A (ET-A) receptor. *ET-1* is expressed in the epithelium and endothelium of the pharyngeal arches (Kurihara et al., 1995), while the receptor ET-A is expressed in migrating neural crest populating the pharyngeal arches (Clouthier et al., 1998). In mouse studies, genetic disruption of this ET-1/ECE-1/ET-A pathway resulted in several developmental defects including craniofacial anomalies. More specifically, *ET-1* null embryos display homeotic transformation of the mandibular arch with downregulation of *Dlx5/Dlx6*. These observations implicate the Endothelin pathway in the patterning of the pharyngeal arch system as a positive regulator of *Dlx5/Dlx6* expression (Kurihara et al., 1994; Ozeki et al., 2004).

Even though neural crest is critical for the correct development of the pharyngeal arches, this role is more responsive than instructive. Cranial neural crest cells interact with and consequently respond to signals from endoderm (Couly et al., 2002; Cerny et al., 2004; Le Douarin et al., 2004), paraxial mesoderm (Trainor and Krumlauf, 2000) and ectoderm (Lumsden, 1988; Bobola et al., 2003) giving rise to various types of tissues. These interactions modulate prior specifications and are necessary for patterning the arches as well the correct morphogenesis of the pharyngeal arch tissues.

Below I discuss some of the interactions neural crest cells have with the other cell players as well some of the genetic factors involved.

A.3 The role of endoderm

Ablation and transplantation experiments in birds revealed that the endoderm instructs neural crest cells to form the different skeletal derivatives of the arches, having an effect on the size, shape and position of some components of the facial skeleton (Couly et al., 2002). This work strongly suggests a central role for the pharyngeal endoderm during arch morphogenesis. Several studies also propose that this role comes from the ability of the endoderm to segment the pharyngeal apparatus by forming endodermal pouches, which provide specific signals to surrounding tissues (Piotrowski and Nusslein-Volhard, 2000; Piotrowski et al., 2003; Graham et al., 2004). Endodermal pouches form in an anterior to posterior sequence, separating the mesoderm and neural crest of the arches and defining the anterior and posterior limits of each arch. The formation of the pouches indicates the correct segmentation of the pharyngeal endoderm (Crump et al., 2004; Quinlan et al., 2004). These structures are polarized and have characteristic expression of several genes. For instance, the anterior half of each pouch expresses *Bmp7*, the posterior half expresses *Fgf8* and *Pax1* is expressed in the dorsal domain of each pouch (Veitch et al., 1999). In this study, early ablation of cranial neural crest cells in chick embryos did not affect the development and function of endoderm cells and the pharyngeal arches are normally patterned and regionalized. This implies that the patterning of endoderm and the pharyngeal segmentation is not dependent on neural crest (Veitch et al., 1999). In zebrafish mutants *bonnie and clyde* (*bon*) and *casanova* (*cas*), which do not produce endoderm, the pharyngeal cartilages fail to form (David et al., 2002). Moreover, the reintroduction of endoderm in these zebrafish embryos showed that the endoderm is required for the development of neural crest cells, including their identity, survival and differentiation into arch cartilages (David et al., 2002).

There are many genetic factors expressed in the endodermal pouches known to be key players for the correct morphogenesis of the arches. Several studies have shown a major role of FGF signalling for the formation of pharyngeal pouches.

Fgf8 is expressed within the developing pharyngeal arch ectoderm and endoderm during neural crest cells migration through the arches. Mouse embryos hypomorphic for Fgf8 have impaired development of the posterior pharyngeal pouches (Abu-Issa et al., 2002). In the zebrafish doubly reduced for Fgf8 and Fgf3, the pouches fail to form (Crump et al., 2004) and it has also been shown that the neural crest cells are induced to form cartilage via the action of FGF-3 and FGF8 emanating from the endoderm (David et al., 2002; Walshe and Mason, 2003). In these studies it was evident a correlation between alterations in pouch morphology and consequent defects in cartilage derived from neural crest.

Studies perfomed in early chicken embryos showed that ablation of the endoderm before neural crest migration eliminates the facial structures (Couly et al., 2002). This study showed that the most cranial endodermal regions were required for nasal capsule morphogenesis, while the more caudal regions were required for the development of Meckel's cartilage and the mandibular joint (Couly et al., 2002).

Together, these zebrafish and chicken studies determine the causality between alterations in pharyngeal endoderm and consequent defects in cartilage derived from neural crest.

In addition, mutations of the *Sonic hedgehog* (*Shh*) gene, encoding for the morphogen Shh, have been associated to cases of holoprosencephaly in humans, a syndrome that includes a variety of malformations, such as absence of the lower jaw, cyclopia, and cleft palate (Belloni et al., 1996; Roessler et al., 1997). Recent studies, where Hedgehog signalling was blocked specifically in mouse NCCs, showed cell death of neural crest followed by severe head skeleton abnormalities (Jeong et al., 2004) suggesting that *Shh* is important for survival of the neural crest cells that populate the first pharyngeal arch. Furthermore, the absence of *Shh* in mutant mice results in strong abnormalities in the patterning of first branchial arch during development (Moore-Scott and Manley, 2005). Chicken studies showed *Shh* expression throughout the pharyngeal and gut endoderm, especially in the endoderm of the first pharyngeal arch (Brito et al., 2006). The

elimination of the anterior foregut endoderm, that expresses *Shh*, prevents upper and lower jaw development; however this phenotype can be rescued by applying a bead carrying Shh protein (Brito et al., 2006).
Therefore, all these studies show that the pharyngeal endoderm plays a crucial role in regulating the morphogenesis of pharyngeal arch derivatives.

A.4 The role of the ectoderm

The ectoderm that surrounds the neural crest mesenchyme also plays a role in regulating neural crest derivatives. Previous studies in birds showed that a zone of frontonasal ectoderm stimulated the proliferation and differentiation of underlying neural crest cells (Hu et al., 2003). A molecular boundary in the frontonasal ectoderm, defined by *Fgf8* and *Shh* expression, indicates the initial site of outgrowth of the upper beak. When transplanted to an ectopic location, the frontonasal ectodermal zone activated a cascade of molecular events that ultimately re-programmed the neural crest-derived mesenchyme, producing a duplication in the upper beak structures. This indicates the ability of the ectodermal epithelium to re-pattern skeletal elements derived from the neural crest (Hu et al., 2003). The signals with the ability to re-specify the fates of neural crest are being discovered. Although *Shh* and *Fgf8* are expressed in adjacent domains in this region it is not clear if they are the molecules that instruct the beak formation or simply molecular markers of this important boundary.
FGF signalling in the ectoderm plays critical functions in the development of the pharyngeal arch derivatives. Various studies have shown that conditional inactivation of the FGF8 signalling in the ectoderm resulted in the disappearance of the most proximal portion of the mandible (Trumpp et al., 1999) as well as cardiovascular defects derived from impaired development of the embryonic arteries (Macatee et al., 2003). Furthermore, analysis of mouse embryos hypomorphic for Fgfr1 demonstrate that ectoderm FGF signalling patterns the pharyngeal region to create a permissive environment for the entry of neural crest

cells (Trokovic et al., 2003; Trokovic et al., 2005). Moreover, pharyngeal arch explant experiments show that *Fgf8* expression in the ectoderm of the second arch interacts with *Hoxa2* positive crest cells to modulate the development of second arch skeletal derivatives (Bobola et al., 2003).
Taken together, it is clear that ectoderm mediated signalling plays an important role in determining the patterning of pharyngeal arch structures.

A.5 The role of cranial mesoderm

The cranial mesoderm generates the branchiomeric skeletal muscles of the head and neck which include muscles of mastication, derived from the first arch; muscles of facial expression, derived from the second arch; and muscles of the pharynx and larynx, derived from more caudal arches (Noden, 1983a; Couly et al., 1992; Trainor et al., 1994). It also provides sources for cardiovascular tissues such as the endothelia of the blood vessels and heart (Couly et al., 1995). Experiments in chick embryos have suggested that cranial mesoderm is able to direct cranial neural crest cell movement (Noden, 1986; Noden, 1988; Ferguson and Graham, 2004). Both cell populations have been examined in detail in the context of pharyngeal apparatus and it was observed that neural crest cells initially populate the superficial regions of each pharyngeal arch, and afterwards cover the mesodermal core tissue of the arches (Trainor and Tam, 1995). This study suggests that the consequent tissue-tissue interactions between neural crest and mesoderm could be important to organize the skeletal, myogenic and endothelial derivatives within the arches (Trainor and Tam, 1995).
Gene expression analysis of some transcription factors, such as Paraxis, Tbx1 and Hoxb1 suggest some degree of regionalization in the cranial mesoderm (Noden and Trainor, 2005). Some techniques were developed to allow the transposition of hindbrain cells in cultured mouse embryos (Trainor and Krumlauf, 2000). These experiments showed that, if neural crest from the second pharyngeal arch is transplanted into the first arch, it downregulates its expression

of *Hoxb1*. But, if it is transplanted along with second arch mesoderm, then, *Hoxb1* expression is maintained. Although the cranial mesoderm doesn´t seem to have a primary role in pharyngeal arch patterning, it is responsible to maintain the normal expected *Hox* gene expression patterns (Trainor and Krumlauf, 2000).
Overall it is clear that pharyngeal arch development is a complex process, which involves co-ordinated interactions between different cell populations in order to generate a wide range of derivatives with correct morphology. Some signalling molecules that could also be included in this section (such as Tgfβ or Retinoic acid signalling molecules) will be referred in the next section in the context of vascular development.

B. EMBRYONIC ARTERIES AND HEART OUTFLOW TRACT

B.1 Formation of blood vessels

The cardiovascular system is the first functional organ to develop in the vertebrate embryo being essential for its survival, also assuring oxygen and nutrient supply and efficiently removal of waste products. The vasculature of the mouse embryo is composed of small and large blood vessels. The smaller vessels consist only of endothelial cells (ECs) whereas, the larger vessels, are surrounded by mural cells (perycites in medium-sized and smooth muscle cells in large vessels). In the embryo the vessels can develop by two distinct processes: vasculogenesis and angiogenesis.
Vasculogenesis assures the creation of the first embryonic vasculature. It starts in the yolk sac with the specification of endothelial cell precursors (angioblasts) from mesoderm. Subsequently the angioblasts proliferate and connect to construct a primitive tubular network composed of capillaries, arteries and veins (Risau and Flamme, 1995).
There are several factors essential for vasculogenesis. Experiments in chick and quail embryos have suggested that FGF signalling is important for the initiation of

angioblast specification (Flamme et al., 1997; Cox and Poole, 2000). In addition, vascular endothelial growth factor (VEGF) is a crucial player in triggering the basic processes of vasculogenesis (reviewed in Holderfield and Hughes, 2008) having a crucial role for the differentiation and migration of endothelial cells. *VEGF-A* deficient mice die at embryonic stages and their primitive vascular structures are severely defective (Carmeliet et al., 1996; Ferrara et al., 1996). *Vegf receptor-2* is required for the migration of angioblasts to the initial sites of vasculogenesis as embryos lacking *Vegfr-2* die around E9.0 and lack development of blood vessels (Shalaby et al., 1995; Shalaby et al., 1997).

Subsequent elaboration of the embryonic vasculature occurs by **angiogenesis**, which is the sprouting, formation and growth of vessels from the pre-existing vascular network (Carmeliet and Jain, 2000). These vessels undergo stabilization and maturation through the recruitment of mural cells - vascular smooth muscle cells (VSMCs) or perycites. The majority of vessels of the developing embryo are formed through angiogenesis. The interactions between molecules of VEGF, TGF-β, and Notch signalling pathways mediate the basic processes of angiogenesis, such as endothelial cell migration, proliferation, tube formation and vessel branching (Breier et al., 1992; Carmeliet et al., 1996; Ferrara, 1999; Holderfield and Hughes, 2008). The processes of angiogenesis and remodelling will be further discussed in the context of the arch arteries development in the mammalian embryo.

B.2 Development of the embryonic arch arteries

The embryonic arch arteries (EAAs or aortic arches) are formed within the pharyngeal arches by vasculogenesis and angiogenesis. During early stages of development, six arch arteries are formed as symmetrical sets of vessels. They connect the developing heart with the dorsal aortae allowing blood to circulate throughout the embryo. A single artery is located in each pharyngeal arch. The development of the aortic arches follows a cranial-caudal sequence, beginning

around embryonic day (E) 8.5 with formation of the most cranial aortic arch (first EAA), which traverses the first pharyngeal arch (Waldo and Kirby, 1998; Hiruma et al., 2002). From E9.5 to E11.5, the second, third, fourth and sixth will appear sequentially following the formation of the pharyngeal arches through which they run (Fig. 1.4); the fifth aortic arch appears briefly and atrophies, not being associated with any independent pharyngeal arch (Waldo and Kirby, 1998; Hiruma et al., 2002).

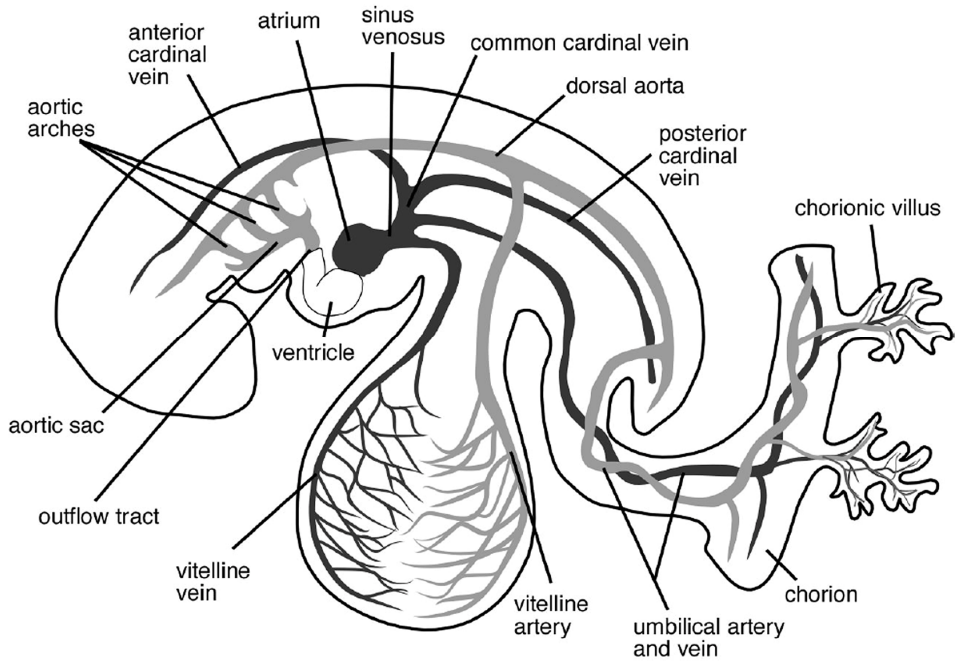

Figure 1.4 Representation of the vasculature of the mammalian embryo at E9.5.
The vessels in grey correspond to the arteries and the ones in black represent the veins (adapted from Schoenwolf et al., 2008).

The morphogenesis of the embryonic arteries inside the pharyngeal system is closely related with the proper segmentation of the pharyngeal arches. Recent work has shown that it is the pharyngeal endoderm and its related pouches that play the key role in generating pharyngeal segmentation (Piotrowski and Nusslein-Volhard, 2000; Couly et al., 2002). If the pharyngeal arches do not form

and segment, subsequently, the artery associated has severe defects being hypoplastic or even absent. Several genes are involved in the proper segmentation of the pharyngeal system and mutations in these genes cause severe defects in the development of the embryonic arteries, some of which will be referred below.

Retinoic acid (RA), the active vitamin A derivative, plays a crucial role in vertebrate embryonic development, being involved in the patterning of the anterior-posterior body axis and specification of the endoderm that assures a correct morphogenesis of the pharyngeal arches. RALDH2 (retinaldehyde dehydrogenase) is a key synthetic enzyme for the generation of retinoic acid during early development, and it has been found that inactivation of this gene in mice results in pharyngeal anomalies including defects in heart and aortic arch arteries (Duester, 2000; Niederreither et al., 2001; Niederreither et al., 2003). Enzymes of the Cyp26 family are required for RA inactivation during embryogenesis (Fujii et al., 1997). Blocking Cyp26 function in the chick embryo results in the loss of caudal pharyngeal arches and associated arteries in early embryos and the late stage embryos show heart defects including common arterial trunk and ventricular septal defects (Roberts et al., 2006).

The best-characterized *Hox* mutant with pharyngeal region defects is ***Hoxa3***. *Hoxa3* controls the differentiation and development of the third pharyngeal arch and pouch in which *Hoxa3* is expressed (Manley and Capecchi, 1995; Watari et al., 2001). The *Hoxa3* null mutant mice die shortly after birth and have severe defects in pharyngeal organ development, including absence of the thymus and parathyroid glands in addition to a broad spectrum of cardiovascular abnormalities consistent with a NCC defect (Chisaka and Capecchi, 1991; Manley and Capecchi, 1995; Kameda et al., 2002). In particular the *Hoxa3* null mutants show specific regression of the third arch artery leading to malformations of third arch artery derivatives. Several studies have suggested that *Hox* genes could act collaboratively with other transcription factor, **Pbx1**, in the development of the pharyngeal region (Selleri et al., 2001; Manley et al., 2004). It has been previously

demonstrated *in vivo* that Pbx1 functions in concert with Hox proteins during development and Pbx1–Hox interactions result in enhanced DNA binding affinities and specificities (Chan et al., 1994; Chang et al., 1995; Popperl et al., 1995; Chan et al., 1997; Maconochie et al., 1997; Lampe et al., 2008). Interestingly, null mutants for the *Pbx1* gene, which codes for a TALE-class homeodomain transcription factor (Burglin, 1997) exhibited abnormalities in pharyngeal development similar to *Hoxa3* null mutant embryos. *Pbx1*$^{-/-}$ mutant embryos display impaired development of the caudal aortic arteries (Manley et al., 2004; Chang et al., 2008).

B.3 Remodelling of the embryonic arch arteries

During development, the embryonic arch arteries undergo a complex remodelling process which involves the programmed regression or persistence of specific arch arteries that leads to the definitive adult left-sided aortic arch vascular pattern (Fig. 1.5). In this process the first two arch arteries undergo regression to form capillary beds and turn into the vasculature of the head. A small part of the first arch artery contributes to the maxillary artery and part of the second arch artery becomes the hyoidal and stapedial arteries (Hiruma et al., 2002). In mammals, the third embryonic arch artery (3rd EAA) forms the carotid artery system, the fourth arch artery forms the main part of the future left-sided aortic arch and a connection to the right subclavian artery. The sixth pharyngeal arch artery forms the pulmonary artery. On the right side the distal part of this artery disappears, whereas on the left side, this artery forms the ductus arteriosus connecting pulmonary to the systemic circulation; after birth this ductus arteriosus is closed (Cassels, 1973; Ho and Anderson, 1979). Therefore, during development, these three caudal arteries (third, fourth and sixth) are remodelled asymmetrically to complete morphogenesis of the heart outflow tract. This outflow tract (OFT) is the embryonic structure that connects the ventricles of the heart to the ascending aorta and pulmonary arteries, and gives rise to the aortic and pulmonary valves,

the aortic arch, and the outflow septum (reviewed in Restivo et al., 2006).

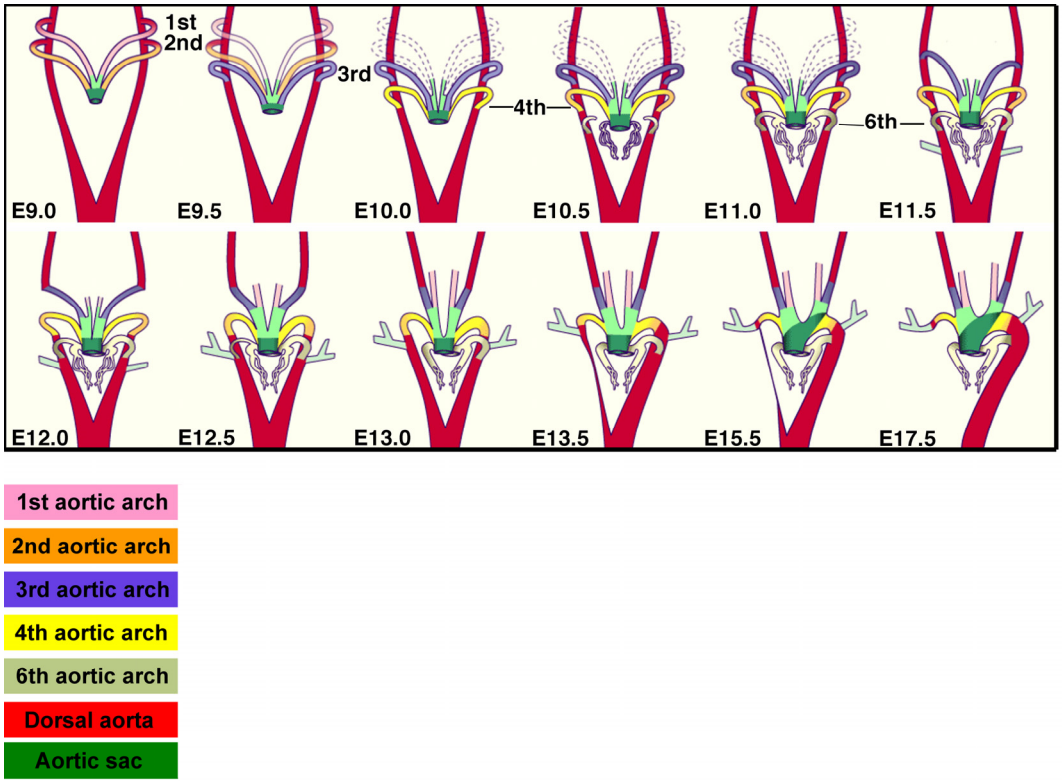

Figure 1.5 Development of the pharyngeal arch arteries (or aortic arches) in the mouse embryo.
At earlier stages (E9) two aortic arches are present (the 1st and the 2nd) that direct blood from the outflow tract into the dorsal aorta. Then the 3rd aortic arch appears already one day later. With the appearance of the 4th aortic arch the 1st arch has disappeared and the 2nd has also begun to atrophy. The 5th arch fails to develop a real vessel and atrophies very quickly. Further in development the 6 arch forms. When the aortic arches 3-6 have appeared the first two have already disappeared. During development these vessels will be remodelled asymmetrically to form the mature heart outflow tract of the newborns (E17.5), which is the system of the great arteries exiting the heart (adapted from http://www.embryology.ch and Hiruma et al. 2002).

B.4 The role of the cardiac neural crest in the remodelling of arch arteries

Experiments in chick embryos, using quail chick chimeras and DiI labelling techniques, revealed that a subpopulation of neural crest cells (NCCs) migrate to

the third, fourth, and sixth pharyngeal arches and contributes specifically to the aortico-pulmonary septation complex within the outflow tract and to the walls of the great arteries that exit the heart; these cells were called cardiac neural crest (Table 1.3; Kirby et al., 1983). Ablation of pre-migratory NCC shows subsequent loss of neural crest derivatives and resulted in cardiovascular malformations, specifically outflow misalignment, abnormal patterning of the great arteries and persistent truncus arteriosus, a phenotype that consists in a failure to properly septate (divide) the early outflow tract of the heart into distinct aortic and pulmonary channels. Therefore, proper development of the aortic arches requires the presence of cardiac neural crest cells (Kirby et al., 1983; Bockman et al., 1987; Bockman et al., 1989; Waldo et al., 1996; Waldo et al., 1998).

Table 1.3 Vascular Derivatives of the caudal pharyngeal arches

Pharyngeal arch	Mesoderm	Neural crest
3rd	Skeletal muscles, Endothelial cells of 3rd aortic arch and of their derivatives (common carotids)	Smooth muscle cells of the common carotids and aorticopulmonary septum. Mesenchyme of the thymus and parathyroid glands
4th	Skeletal muscles, Endothelial cells of 4th aortic arch and of their derivatives (arch of the aorta and part of subclavian and pulmonary arteries)	Smooth muscle cells of arch of the aorta, part of subclavian arteries and aorticopulmonary septum
6th	Skeletal muscles, Endothelial cells of 6th aortic arch and of their derivatives (part of pulmonary arteries)	Smooth muscle cells of part of the pulmonary arteries and aorticopulmonary septum

(Adapted from Mark et al., 2004)

The analysis of cardiac neural crest in mammalian species was delayed compared to chick studies mainly because the transplantation and labelling techniques used in birds are technically difficult to perform in mice. Nevertheless, fate-mapping studies with gene expression markers for neural crest (Lo et al.,

1997; Waldo et al., 1999; Jiang et al., 2000) overcame the previous lack of specific molecular markers in mice that could be used to follow cardiac neural crest cells. In addition, a series of transgenic mouse lines that included neural crest specific promoters (like P0, Pax3, Wnt1, Ht-PA) allowed lineage tracing of neural crest cells from the time of emergence into the final mature structures (Yamauchi et al., 1999; Jiang et al., 2000; Li et al., 2000; Pietri et al., 2003). These genetic fate-mapping experiments in mice have also demonstrated that cardiac neural crest cells migrate throughout the pharyngeal region in large numbers. They coalesce around the third, fourth and sixth arch embryonic arch arteries, which initially form as endothelial tubes, and subsequently, differentiate into vascular smooth muscle (Fig. 1.6).

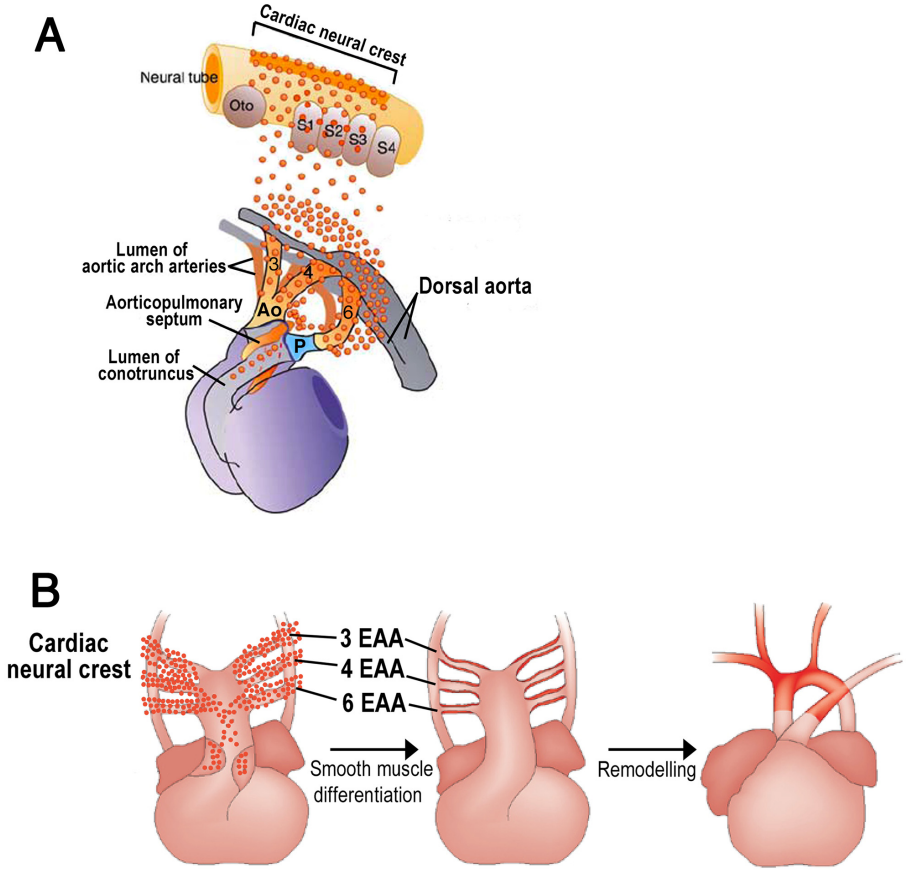

Figure 1.6 Cardiac neural crest contribution for the heart outflow tract and aortic arch artery remodelling.
(A) and (B left panel) Migration and distribution of cardiac neural crest cells from their origin in the neural tube, into the caudal pharynx and into the outflow tract.These cardiac neural crest cells differentiate to form the vascular smooth muscle layer (shown in B middle panel). Subsequently, the aortic arch arteries remodel to form the mature aortic arch, with neural-crest-derived vascular smooth muscle contributing to most of the aortic arch and its major branches (shown in the B right panel; adapted from High and Epstein, 2008; Hutson and Kirby, 2007).

In addition, they form the aorto-pulmonary septum, thus dividing the truncus arteriosus into the aorta and pulmonary artery. Smooth muscle in the aortic arch, ductus arteriosus, and carotid arteries are derived from neural crest (Jiang et al., 2000; Engleka et al., 2005).

B.5 Genetic factors involved in the remodelling of the arch arteries

Anomalies of the arch arteries are observed in several gene-targeted mice showing defective production and differentiation of neural crest cells in general or its cardiac subpopulation in particular (Epstein et al., 1991; Yanagisawa et al., 1998; Feiner et al., 2001; Abu-Issa et al., 2002; Brewer et al., 2002; Ohnemus et al., 2002; Vitelli et al., 2002; Wang et al., 2006; Varadkar et al., 2008). Nevertheless the precise role of the cardiac neural crest and the mechanisms by which these cells control development of the heart outflow tract are not clear. Several studies indicate that the ability of this neural crest cell population to generate the vascular smooth muscle cells (VSMCs) that associate with the arch arteries is among the most important factors contributing to this process. Indeed, mutations that affect differentiation of VSMCs from the cardiac neural crest cells resulted in impaired development of the structures derived from the embryonic arteries (Conway et al., 1997b; Kochilas et al., 2002; Tallquist et al., 2003; Oh et al., 2005; Wei et al., 2007; Huang et al., 2008; Varadkar et al., 2008). Mouse model observations have identified many signalling molecules and transcription factors associated with cardiac neural crest function in the correct formation and remodelling of the embryonic arch arteries. Some of them are referred to below.

TGF-beta-superfamily signalling has been strongly implicated in neural crest cell development. *Tgfβ2* is expressed in the neural crest-derived smooth muscle of all pharyngeal arch arteries (Akhurst et al., 1990; Molin et al., 2003). *Tgfβ2* null mutant mice show abnormal regression of the fourth arch arteries (Molin et al., 2002) giving rise to cardiovascular malformations while conditional inactivation of *TGFβ type II receptor* (*Tgfbr2*) in neural crest cells resulted in interruption of the aortic arch and persistent truncus arteriosus (Wurdak et al., 2005; Choudhary et al., 2006). Similarly, neural crest specific abrogation of *TGFβ type I receptor* (or *Alk5*) in mice shows cardiac and pharyngeal defects (Wang et al., 2006).

Alterations in **Endothelin** signalling have been associated with congenital heart defects in humans. Endothelin-1 has been identified as a potent vasoconstrictor

peptide produced by endothelial cells (reviewed in Beghetti et al., 2005). Mice null mutants for *ET-1* die of respiratory failure at birth and had morphologic abnormalities of the pharyngeal arch derivatives (Kurihara et al., 1994). Later studies in mouse embryos, confirmed that *ET-1* is expressed in the epithelium of the arches as well as in the endothelium of the arch arteries and cardiac outflow tract, demonstrating that *ET-1* is involved in the normal development of the heart and great vessels (Kurihara et al., 1995). Other studies observed that mice deficient in *ECE-1* or *ETA*, which is expressed in neural crest, develop defects in a subset of neural crest derivatives leading to great vessel malformations (Clouthier et al., 1998; Yanagisawa et al., 1998). The pattern of ligand and receptor expression appears to be involved in coordinating specific aspects of pharyngeal arch development. According to work in mice, studies in chick have shown that ETA specific antagonists cause aortic arch mispatterning and outflow defects (Kempf et al., 1998). Taken together these studies demonstrated that ET-1/ECE-1/ETA pathway plays an essential role in the complex process of aortic arch patterning by affecting the postmigratory cardiac neural crest cell development. Disruption of this pathway results in cardiac outflow defects and great vessel structures, such as abnormal persistence of second artery, abnormal regression of fourth and sixth arteries and enlargement of third arch artery (Kurihara et al., 1994; Kurihara et al., 1995; Clouthier et al., 1998; Yanagisawa et al., 1998).

Semaphorins represent a family of membrane bound and secreted molecules that mediate guidance for extending axons in developing nervous system. Recent work has indicated that several of the axon guidance molecules, such as Semaphorins, Ephrins and Netrins, also contribute to the patterning of the vasculature (reviewed in Carmeliet and Tessier-Lavigne, 2005; Eichmann et al., 2005; Gu et al., 2005; Weinstein, 2005). Inactivation of the class 3 semaphorin, *Sema3C*, results in interruption of the aortic arch, persistent truncus arteriosus and alterations in cardiac neural crest patterning (Feiner et al., 2001). However these mutants do not have defects in other neural crest derivatives, suggesting

that Sema3C signalling acts specifically in the cardiac neural crest. *Sema3C* is expressed within neural crest and bind to heterodimeric receptors composed of Neuropilin and Plexin subunits (Kawasaki et al., 1999; Brown et al., 2001). Recent studies have determined that there is a coordination of attractive cues provided by Sema3C through Plexin-D1, paired with repulsive cues given by other Semaphorin molecules, such as Sema6A/Sema6B through Plexin-A2, which globally orchestrate the migration of cardiac neural crest into the heart outflow tract (Toyofuku et al., 2008).

Accumulating data from human genetics and animal models implicates **Notch signalling pathway** in cardiovascular development. In mammals, the Notch pathway consists of 4 type I transmembrane receptors (Notch1 to Notch4) and 5 type I transmembrane ligands, including those of the Jagged, Serrate and Delta classes. *Jagged1* null mutant embryos die during embryogenesis and display severe vascular disorders (Xue et al., 1999) and compound *Notch2/Jagged1* heterozygotes exhibit more severe cardiac abnormalities than either heterozygote alone (McCright et al., 2002). Work from Epstein and collaborators suggests that cell-autonomous Notch signalling in neural crest is required for smooth muscle differentiation and aortic arch remodelling (High et al., 2007). Indeed, conditional ablation of Notch signalling in neural crest results in aortic arch branching defects namely abnormal development of the smooth muscle cells of the sixth aortic arch artery (High et al., 2007).

Two naturally occurring mutants **Splotch** and **Patch** show a variety of developmental abnormalities including cardiovascular phenotypes very similar to the cardiac neural crest ablation in the chick embryo (Franz, 1989; Morrison-Graham et al., 1992; Conway et al., 1997a; Conway et al., 1997b; Conway et al., 1997c). The Splotch mutation is a 32–base pair deletion of the DNA-binding transcription factor **Pax3** (Goulding et al., 1993). In mice, the homozygous *Splotch* embryos die in utero and display persistent truncus arteriosus, impaired outflow alignment, and patterning of the aortic arch arteries (Franz, 1989; Conway et al., 1997c). Cre-lox technology has been used to fate map the Pax3-expressing cells

in normal and *Splotch* mice (Epstein et al., 2000; Kwang et al., 2002). *Pax3*-expressing cells are fated to populate 3, 4 and 6 caudal pharyngeal arches, and contribute smooth muscle cells to the great vessels and mesenchymal cells to the outflow septum (Epstein et al., 2000). In this study it was observed that, in *Splotch* embryos, the neural crest is able to migrate to the pharyngeal arches and outflow tract but, there are much fewer cells than in the control mice (Epstein et al., 2000). Therefore, as in the chick ablation model, a particular threshold number of cardiac neural crest cells must reach the pharyngeal arches and then the outflow tract for proper septation. It appears that this decrease in cardiac neural crest cell numbers is the primary defect that ultimately leads to arterial smooth muscle cell and heart outflow tract defects in these mice (Epstein et al., 2000).

The other naturally occurring mouse mutant, patch (Ph), carries a deletion in the α subunit of the **platelet-derived growth factor (PDGF)** receptor (Morrison-Graham et al., 1992; Schatteman et al., 1995). Homozygous PATCH embryos have persistent truncus arteriosus that could be due to impaired neural crest development (Price et al., 2001). Interestingly, this phenotype was also observed in the mouse with a conditional deletion of *Pdgf-receptor α* in the neural crest cells (Tallquist and Soriano, 2003). These embryos display cardiac defects such as persistent truncus arteriosus and ectopic origin of the right subclavian artery. **Myocardin**, and **Mkl2** represent a family of potent transcriptional co-activators that modulate serum response factor (SRF) transcription. Many smooth muscle specific genes are regulated by SRF and its factors. *Myocardin* appears to play a critical role in most vascular smooth muscle development since KO mice display severe vascular defects (Li et al., 2003). On the other hand, inactivation of *Mkl2* results in specific defects in cardiac outflow tract that mimic common forms of congenital disease including interrupted aortic arch and persistent truncus arteriosus. Although *Mkl2* has a broad expression domain, neural crest derived vascular smooth muscle is specifically affected in the *Mkl2* null embryos (Li et al., 2005; Oh et al., 2005).

Some of the genes known to be involved in the patterning and remodelling of the pharyngeal arch arteries are summarised in Table 1.4.

Collectively, these mouse genetics approaches identified several candidate genes associated with embryonic artery defects that may mediate interactions between the pharyngeal endoderm, ectoderm and endothelial vessels and can also affect the development of cardiac neural crest cells leading to severe defects in the adult cardiovascular system. Moreover they highlight the complexity of signalling and tissue communications in the pharynx and outflow tract that are required for normal cardiovascular development. Nevertheless, several lines of evidence from these studies suggest that one common mechanism for congenital heart disease involving the outflow tract is related to deficient smooth muscle differentiation of cardiac neural crest. Actually, in Chapter 5 we further explore the roles of the neural crest derived vascular smooth muscle in the remodelling of the embryonic arch arteries.

Table 1.4 Genes involved in formation and remodelling of aortic arch arteries

GENES	EXPRESSION	PHENOTYPE	FUNCTION	REFERENCES
Mouse models with cardiac neural crest deficiency				
Pax3	Cardiac NC	Homozygous embryos die at E14 and have persistent truncus arteriosus (PTA) and ventricular septal defects.	Specification, migration and development of neural crest	(Franz, 1989; Conway et al., 1997b; Epstein et al., 2000)
PDGFRα	Cardiac NC	Most null mice die ~E16.5 due to extensive haemorrhaging. Conditional wnt1-Cre deletion results in neonatal lethality with cleft palate, aortic arch artery defects, PTA and VSD.	Development of NCC during aortic arch remodelling	(Soriano, 1997; Tallquist and Soriano, 2003)
Genes involved in DiGeorge syndrome				
Tbx1	Pharyngeal mesoderm endoderm, otic vesicle	Homozygous nulls exhibit hypoplasia of the pharynx, various anomalies of the aortic arteries and abnormal neural crest migration within AA.	Main candidate gene for DiGeorge syndrome	(Vitelli et al., 2002)
Fgf8	Ectoderm, endoderm and mesoderm of pharyngeal arches	Hypomorphic mutants have small thymus, craniofacial defects and lethal malformation of aortic arch arteries, cardiac outflow tract exhibiting PTA.	Development of NCC	(Abu-Issa et al., 2002; Frank et al., 2002)
Gbx2	Various tissues within the pharyngeal arches	Defects in fourth aortic arch development	Development of NCC, interaction of Fgf8	(Byrd and Meyers, 2005)
VEGF	Endothelial cells, pharyngeal endoderm	Various anomalies of AA	Angiogenesis	(Carmeliet et al., 1999; Stalmans et al., 2003)

GENES	EXPRESSION	PHENOTYPE	FUNCTION	REFERENCES
Crkl	Ubiquitous expression	Various anomalies of AA.	Candidate gene for DiGeorge syndrome. Regulate Fgf8 expression	(Guris et al., 2001; Guris et al., 2006; Moon et al., 2006)
Pitx2	Left pharyngeal arch mesoderm	Homozygous mutants die ~E14.5 and exhibit defects in asymmetric remodelling of AA leading to various cardiovascular defects.	Mediation of left-right assymetry of AA	(Kitamura et al., 1999; Liu et al., 2002; Yashiro et al., 2007)
TGFβ superfamily members				
Tgfβ2	SMC in AA	Defective A4 (R, L), Interrupted aortic arch.	Development of SMC	(Molin et al., 2003; Gittenberger-de Groot et al., 2006)
Alk2 (Bmptype1r)	Cardiac NCC	Regression of A3 and A6, PTA	Migration and differentiation of NCC	(Gu et al., 1999; Kaartinen et al., 2004)
Alk5 (TgfβR1)	Cardiac NCC	Embryos with Alk5 deleted in NCC die perinatally. Have abnormal AA remodelling and aortic sac development and PTA.	Survival of NCCs. Activation of Tgfβ2-Smads signal	(Wang et al., 2006)
Bmp4	Pharyngeal arch mesoderm, cardiac outflow tract	Interrupted aortic arch and PTA.	Migration of NCC	(Liu et al., 2004; Shoval et al., 2007)
Chordin	Pharyngeal endoderm	Various anomalies of AA and PTA.	Antagonist of Bmps	(Bachiller et al., 2003)

GENES	EXPRESSION	PHENOTYPE	FUNCTION	REFERENCES
Ap2α	Cardiac and cranial NC	Null mice die perinatally and exhibit defects in the outflow tract, neural tube, craniofacial skeleton, eye and cranial ganglia.	Interaction between NC and surrounding pharyngeal tissues regulating correct morphogenesis of the outflow tract.	(Brewer et al., 2002)
Endothelin				
Endothelin-1 (ET-1)	Pharyngeal mesenchyme, ectoderm, endoderm	Homozygous mutants have various aortic arch anomalies and OFT defects, VSD and enlarged right ventricle.	Development of NCC	(Kurihara et al., 1995)
ECE-1	Pharyngeal ectoderm and endothelium of AA	Null mutant embryos have cardiac OFT defects, VSD and abnormal remodelling of AA	Development of NCC	(Yanagisawa et al., 1998)
ETA	Pharyngeal mesenchyme	Knock out mice have defects in AA alignment, OFT development and craniofacial structures. Mutants are cyanotic and die shortly after birth.	Development of NCC	(Clouthier et al., 1998)
Semaphorin				
Semaphorin 3C	Cardiac NC	Mutants die shortly after birth and exhibit interrupted aortic arch and PTA.	Migration of NC; axon guidance.	(Feiner et al., 2001)
Neuropilin-1	Endothelial cells	Mutants die ~E13.5 and exhibit PTA, disorganized yolk sac, and various anomalies of AA.	Receptor for semaphorins	(Kawasaki et al., 1999)
PlexinD1	Endothelial cells	Various anomalies of AA.	Receptor for semaphorins in EC	(Gitler et al., 2004)

GENES	EXPRESSION	PHENOTYPE	FUNCTION	REFERENCES
GATA6	Cardiac neural crest derivatives	Embryos with GATA6 deleted in vascular SMC and cardiac NCC die perinatally.	Regulation of *Semaphorin3C* in the correct morphogenesis of the cardiac outflow tract.	(Lepore et al., 2006)
Retinoic acid				
RARs		Major developmetal defects in the heart, its outflow tract and the aortic arteries. Defects in the thymus, thyroid and parathyroid glands.	Alterations of gene expression in pharyngeal endoderm	(Mendelsohn et al., 1994)
Raldh2	Posterior pharyngeal mesoderm	A3, A4, A6 developmental defects	Enzyme for RA synthesis	(Niederreither et al., 2003)
Other transcription factors				
Hoxa3	Third pharyngeal arch and pouch	Null mutants exhibit defects in the third arch artery (A3)	Differentiation of the third pharyngeal arch and pouch	(Kameda et al., 2003)
Pbx1		Null embryos exhibit anomalous aortic arch arteries and outflow tract defects	Formation of 4th and 6th pharyngeal arches. Function of NC during OFT septation by regulating *Pax3* expression in cardiac NCCs.	(Chang et al., 2008)

GENES	EXPRESSION	PHENOTYPE	FUNCTION	REFERENCES
MRTF_B/Mkl2	Premigratory neural crest, in rhombomeres 3 and 5, and in the neural crest-derived mesenchyme that surrounds the aortic arch arteries.	Homozygous embryos die at E17.5 and display abnormal patterning of the aortic arch arteries, ventricular septal defects (VSD) and compromised differentiation of SMCs derived from the neural crest.	Remodelling of branchial arch arteries and smooth muscle differentiation	(Li et al., 2005; Oh et al., 2005)
Myocardin	Expressed in cardiac and differentiated SMC	Null embryos die around ~E10.5 accompanied by a loss of smooth muscle gene expression, but no apparent decrease in cardiac gene expression.	Key role in regulation of multiple SMC marker genes	(Chen et al., 2002; Du et al., 2003; Li et al., 2003; Yoshida et al., 2003)
Factors involved in EMT and migration of NC				
N-cadherin	Dynamic expression pattern during NCC development: In the dorsal region where the NCC emerge, but downregulated as EMT occurs.	Homozygous mutants die ~E10. Conditional deletion of N-cadherin results in OFT defects, including PTA. N-cadherin	Migration of NC critical for patterning of the cardiac outflow tract.	(Luo et al., 2006)

GENES	EXPRESSION	PHENOTYPE	FUNCTION	REFERENCES
Sox9	Expressed in a variety of tissues such as the neural crest, inner ear, brain, hindbrain and notochord.	Null mice die ~E11.5 from heart failure due to abnormal dilated major vessels. Embryos with Sox9 deleted in NCC exhibit abnormal NC apoptosis.	Role in epithelial-mesenchymal transition of neural crest	(Akiyama et al., 2004)

EMT Epithelial mesenchymal transition; PTA persistent truncus arteriosus, OFT outflow tract, VSD ventricular septal defect, NCC neural crest cells AAA aortic arch arteries, A3-A6 third to sixth aortic arch, SMC smooth muscle cells, ECs endothelial cells

C. *TBX1* IN MOUSE EMBRYONIC DEVELOPMENT AND IN CONGENITAL HEART DISEASE

C.1. *Tbx1* and the pharyngeal system

A considerable body of work from numerous investigators implicates *Tbx1* in the development of the pharyngeal arches and their derivatives (Lindsay et al., 2001; Merscher et al., 2001). Tbx1 is a member of the T-box-containing family of transcription factors (Bollag et al., 1994) and has been identified as a human disease gene (Yagi et al., 2003). In humans, this gene is located within a microdeletion on chromosome 22 and is the major genetic determinant for the pharyngeal arch derived defects observed in individuals with DiGeorge syndrome (Scambler, 2000; Merscher et al., 2001; Yagi et al., 2003). DiGeorge syndrome is characterized by: cardiac outflow tract defects, aortic arch abnormalities, hypoplasia or aplasia of the thymus and parathyroid glands, and craniofacial defects (Scambler, 2000). In mice, heterozygous inactivation of *Tbx1* causes milder phenotypes as those seen in the DiGeorge syndrome such as reproducible anomalies in heart outflow tract development and impairment of neural crest-derived smooth muscle cell (Lindsay et al., 2001; Merscher et al., 2001; Kochilas et al., 2002). Homozygous inactivation of *Tbx1* in mice causes a much more severe phenotype that is only rarely seen in patients. The *Tbx1* mutant embryos die before birth, have severe developmental defects in the thymus, cardiac outflow tract and aortic arteries, craniofacial area and the ear (Jerome and Papaioannou, 2001; Lindsay et al., 2001; Merscher et al., 2001; Vitelli et al., 2002a). *Tbx1* is expressed dynamically in the pharyngeal arch endoderm and mesoderm, in the distal pharyngeal ectoderm, otic vesicle and head mesenchyme (Chapman et al., 1996; Vitelli et al., 2002a; Yamagishi et al., 2003; Zhang et al., 2005). *Tbx1* inactivation studies in mice support the notion that the pharyngeal endoderm plays a crucial role in regulating the morphogenesis of pharyngeal arch

derivatives. *Tbx1* mutant mice fail to form caudal pouches, whereas the first pharyngeal pouch develops normally (Jerome and Papaioannou, 2001; Lindsay et al., 2001). Since *Tbx1* is expressed in a variety of tissues apart from endoderm it was not possible to affirm with no doubt that it was the role of *Tbx1* in the pharyngeal endoderm that was important for regulating the morphogenesis of pharyngeal arch derivatives. Nevertheless, in agreement with the mouse studies, the zebrafish *Tbx1* mutant *vgo* also displays severe segmentation defects that could be partially corrected by transplantation of wild-type endodermal cells (Piotrowski and Nusslein-Volhard, 2000; Piotrowski et al., 2003). Recent studies have shown that complete inactivation of *Tbx1* in the pharyngeal endoderm mimics the phenotype of *Tbx1* null mutants (Arnold et al., 2006). These results further support the view that the pharyngeal endoderm is a key regulator of pharyngeal arch development and *Tbx1* a major genetic player in this process.

In addition *Tbx1* expression in the mesoderm appears to be important for the correct development of the pharyngeal arch derivatives. In fact the absence of *Tbx1* function severely perturbs branchiomeric muscle development in mouse embryos (Kelly et al., 2004). Moreover conditional ablation experiments in mouse embryos where *Tbx1* had been specifically ablated from mesoderm have shown severe pharyngeal patterning defects (Zhang et al., 2006). These studies have demonstrated that expression of *Tbx1* in the mesoderm is important in morphogenesis of the pharyngeal system.

On the other hand, although it is not expressed in the neural crest, *Tbx1* null mouse embryos present several defects in the development of the neural crest derivatives. Actually, we have observed how disruption of the caudal arches in these mutants leads to poor colonisation of neural crest and misrouting of their migratory streams leading to craniofacial defects (Moraes et al., 2005). These results are developed and explored in Chapter 2.

C.2 *Tbx1* and other candidate genes for the DiGeorge syndrome

The *Tbx1* gene is expressed in various regions of the pharyngeal arches but not in the neural crest. Since ablation of pre-migratory NCCs in chick also results in phenocopies of the DiGeorge syndrome (Bockman et al., 1987; Bockman et al., 1989;) it is probable that *Tbx1* could regulate other set of genes expressed in neighbouring tissues in the pharyngeal arches which could signal to neural crest cells to promote their growth and differentiation. One way to identify this set of genes is to analyse mouse mutants carrying null alleles with equivalent defects as in *Tbx1*$^{-/-}$ mutant mice. Only some of the most relevant ones will be referred to below.

Fgf8, which belongs to the extracellular signalling fibroblast growth factor (FGF) family, is expressed in the developing pharyngeal arch ectoderm, endoderm and mesoderm (Abu-Issa et al., 2002; Frank et al., 2002). Mice deficient in *Fgf8* exhibit a typical DiGeorge syndrome phenotype, (Abu-Issa et al., 2002; Frank et al., 2002). Interestingly, *Fgf8* expression is downregulated in the pharyngeal endoderm of *Tbx1*$^{-/-}$ embryos and double heterozygous *Tbx1*$^{+/-}$*;Fgf8*$^{+/-}$ embryos display significantly higher penetrance of aortic arch artery defects when compared with *Tbx1*$^{+/-}$ embryos, indicating that *Tbx1* and *Fgf8* are genetically linked in the development of the aortic arch arteries (Vitelli et al., 2002b). Furthermore tissue–specific deletion of *Fgf8* in pharyngeal endoderm using *Tbx1-Cre* mice reproduces representative outflow tract defects associated with deficient neural crest derived smooth muscle cell differentiation (Brown et al., 2004).

Besides *Tbx1*, ***Crkl*** is also located within the microdeleted region for DiGeorge syndrome (Guris et al., 2001). *Crkl* encodes an adaptor protein that is important for intercellular signalling and homozygous mice null for *Crkl* display defects in multiple cardiac neural crest derivatives including aortic arch arteries (Guris et al., 2001; Guris et al., 2006). Double heterozygous *Crkl*$^{+/-}$*;Tbx1*$^{+/-}$ embryos have increased thymic, parathyroid, and cardiovascular defects characteristic of DiGeorge syndrome at a higher penetrance than that generated by heterozygosity

of *Crkl* or *Tbx1* alone (Guris et al., 2006). As well as identifying a dose-dependent genetic-interaction of *Tbx1* and *Crkl* in pharyngeal development, these double mutants also exhibit abnormal ectopic retinoic acid signalling (RA). Interestingly, by reducing the amount of RA in these mutants, the penetrance of thymic hypoplasia was reduced (Guris et al., 2006), reinforcing the idea that genes involved in retinoic acid signalling may act as modifiers of the syndrome.

Gbx2, a homeobox containing transcription factor is expressed in the developing pharyngeal arches (Wassarman et al., 1997; Waters and Lewandoski, 2006) and mouse embryos deficient for *Gbx2* have craniofacial anomalies, and cardiovascular defects such as the failure of remodelling the fourth arch artery (Byrd and Meyers, 2005). These defects seem to be associated with abnormal differentiation and development of neural crest cells. Furthermore *Gbx2* has been suggested to interact genetically with *Fgf8* during development of the aortic arch arteries (Byrd and Meyers, 2005). These findings suggest that *Gbx2* may be a modifying locus for DiGeorge syndrome. In fact, *Gbx2* expression is reduced in *Tbx1* null mouse embryos suggesting that *Gbx2* is a target gene for Tbx1. It would be interesting to analyse the aortic arteries development of $Tbx1^{+/-}$;$Gbx2^{+/-}$ double heterozygous in order to evaluate if there is higher penetrance compared to the single heterozygous. In fact, in Chapter 4 we analyse the embryonic arteries defects of double heterozygous $Tbx1^{+/-}$;$Gbx2^{+/-}$ mice, using a staining technique that enables a detailed visualization of the vasculature of the mouse embryo.

D. THE MAMMALIAN EAR DEVELOPMENT

The mammalian auditory system is comprised of the outer, middle and inner ears (Fig. 1.7). The process of hearing starts as the outer ear receives sound waves from the air, which are amplified and transmitted by the middle ear ossicles into the inner ear to generate vibrations in the endolymph. These vibrations excite the hair cells of the organ of Corti, located in the cochlear part of the inner ear, to generate neural impulses that are transmitted to the brain through the acoustic nerve. While the outer and middle ears are exclusively responsible for hearing, the inner ear is also involved in the processes of acceleration and balance, centered in the vestibular area. Therefore the ear is an intricate sensory organ composed of distinct structures, derived from different germ layers (Fekete and Wu, 2002). Understanding the origin of each structure and the genes involved in this process helps to understand functional anomalies associated with congenital malformations of external, middle and inner ears.

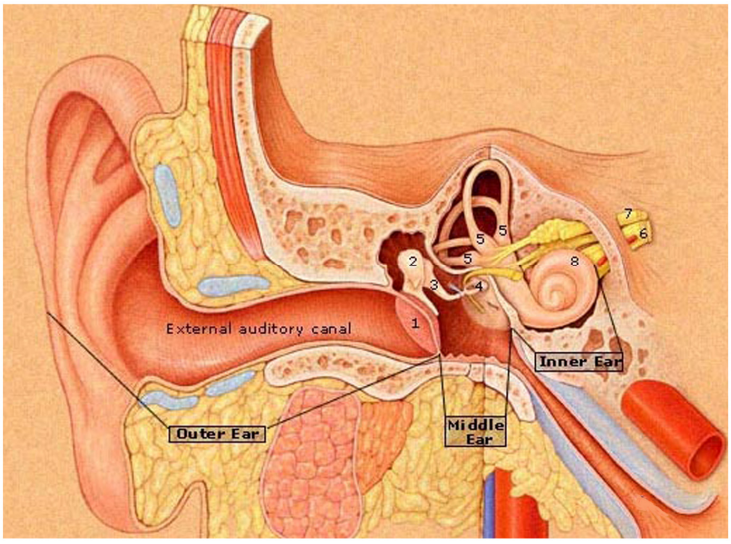

Figure 1.7 The mammalian ear
Drawing of the human ear showing the structures of the outer, middle and inner ear. (1) Tympanic membrane, (2) Malleus, (3) Incus, (4) Stapes, (5) Semicircular canals, (6) Auditory nerve, (7) Vestibular nerve, (8) Cochlea (adapted from Hain, 2008).

D.1 Outer and middle ear

The outer and middle ears develop as a result of interactions between cells in the first and second pharyngeal arches (Fig. 1.8). Their development is linked to general patterning and morphogenetic processes in the pharyngeal region, which require specific interactions between cranial neural crest and ectodermal and endodermal elements of the developing first and second arches (reviewed in Mallo, 1998; Mallo, 2001). The outer ear forms as a result of fusion of first and second pharyngeal arches that will originate the ear pinna and the external acoustic meatus (Sulik and Bream, 1995). The ear pinna develops around the first pharyngeal cleft from several protuberances (hilloks) that appear on the first and second arches. The EAM develops from the invagination of the ectoderm from the 2^{nd} pharyngeal cleft. The tympanic ring, which is originated from the neural crest first arch mesenchyme, regulates this process (Mallo and Gridley, 1996). The middle ear ossicles are also formed from the neural crest of the first two pharyngeal arches (Mallo, 1998; Mallo, 2001; see section A.1.3). The malleus, incus and tympanic ring derive from neural crest originating in caudal mesencephalon and r1 and r2 (Kontges and Lumsden, 1996) and the stapes derives from neural crest cells migrating from r4 (Le Douarin et al., 1993; Carlson, 1999). The middle ear plays an important role in converting the sound to the mechanical vibration.

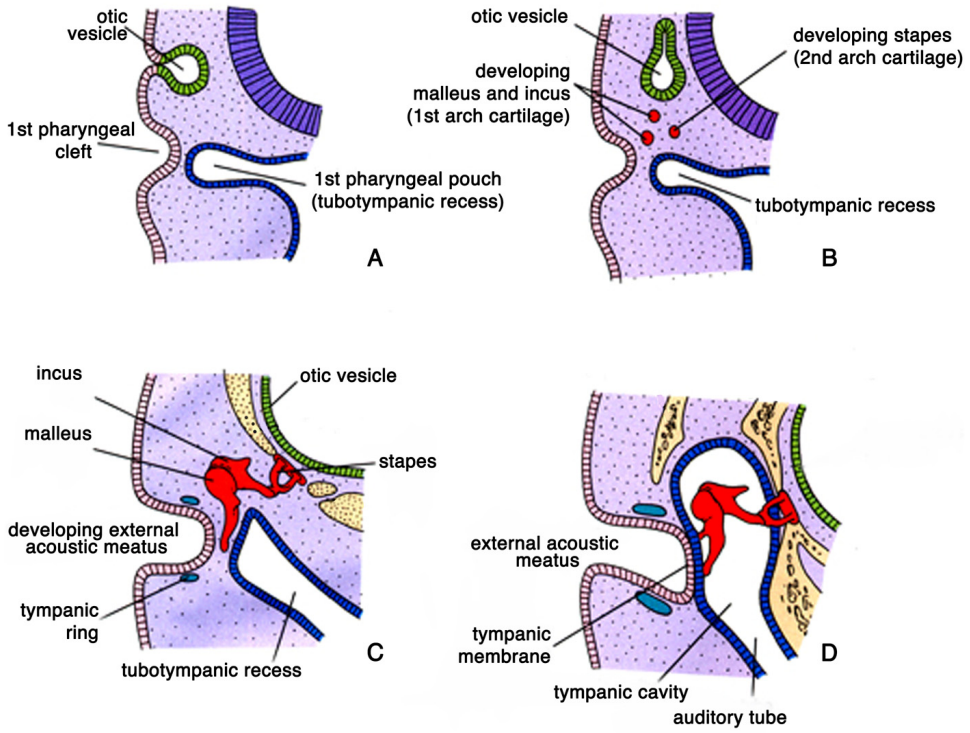

Figure 1.8 The middle ear development.
Drawing representing cross sections through a developing mouse embryo at the level of the hindbrain (dorsal towards the top). (A) The otic vesicle develops from an epithelial thickening from the ectoderm. (B) By the time the otic cup closes and pinches off to form the otic vesicle, the mesenchyme of the first and second pharyngeal arches begins to condense to form cartilage. (C) The middle ear ossicles, malleus and incus derive from the cartilage of the first pharyngeal arch and stapes derives from the second arch cartilage. In-growth of ectoderm gives rise to the first pharyngeal groove that develops into the external acoustic meatus. (D) Later, the endoderm of the first pharyngeal pouch (tubotympanic recess) enlarges and 'engulfs' the ossicles giving rise to the tympanic cavity auditory tube. The middle ear forms an ossicular chain bridge across the cavity (adapted from Moga, 2004).

D.2 Inner ear

The development of the inner ear begins with the otic placodes that originate as ectodermal thickenings on both sides of early hindbrain (Anniko and Wikstrom, 1984; Rinkwitz et al., 2001). These placodes invaginate to form the otic vesicles that eventually separate from the surface ectoderm (Fig. 1.9). Neuroblasts

delaminate from the otic placode generating the cochleo-vestibular ganglion that innervates the auditory and vestibular sensory organs of the inner ear (Streit, 2001; Schlosser, 2006). Then the otic vesicle undergoes a period of intense proliferative growth prior to differentiation. Subsequently, the otic vesicle follows an intricate series of morphogenetic and differentiation processes giving rise to three semicircular canals (and their associated sensory tissues – cristae, that detect angular acceleration), the utricle and saccule (and associated sensory tissue – macula, that detect linear acceleration), the endolymphatic duct and sac (that helps regulate endolymph homeostasis) and the cochlea (that elongates in the spiral organ of Corti - the auditory end organ). Despite its complexity and multiple functions, almost all cellular components of the inner ear epithelium derive from the embryonic otic vesicle (exception to the secretory epithelium of the cochlea, which is neural crest derived); in addition the neurons of the cochleo-vestibular ganglion also derive from the otic vesicle. Below I will review the development of the inner ear with regards to embryological, genetic and molecular data, from early inductive events to differentiation and innervations.

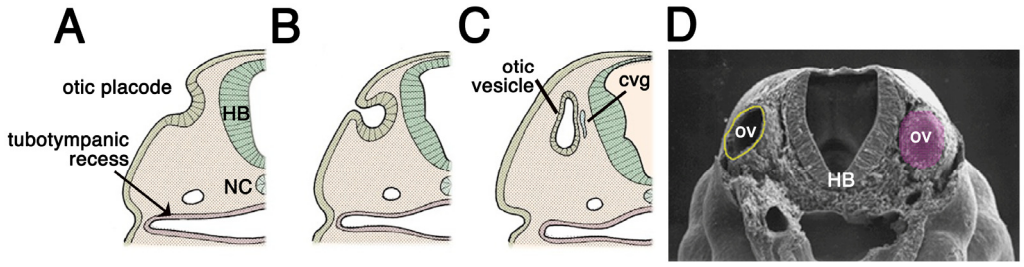

Figure 1.9 Development of the otic vesicle.
(A) Schematic view of left side of a cross section through a developing embryo at the level of the hindbrain (dorsal towards the top). The otic placode forms as a thickening of the surface ectoderm adjacent to the hindbrain (HB) and notochord (NC) (adapted with permission from Richard Dryden, Bionalogy.com). **(B)** As development continues, the placode pinch off to form the otic vesicle. **(C)** Soon after closure of the otic vesicle, neuroblasts delaminate from the anteroventral surface of the otic epithelium and give rise to the cochleo-vestibular ganglion (cvg). **(D)** Scanning electron micrograph showing a cross section of a mouse embryo, the left otic vesicle is cut while the right is intact (adapted from Sulik and Bream, 1995).

D.2.1 Induction of the otic placode

The earliest morphological event in inner ear development is the formation of the otic placode that separates from the surface ectoderm to form the otic vesicle (also called otocyst). The otic placode, is specified when it has already received inducing signals from surrounding tissues and can express otic markers in the absence of any additional signals. Classical experiments have emphasized the relevance of neural tube for otic development (Jacobson, 1963). Studies in amphibia led to the analysis of the otic inductive processes and the relative contribution of each embryonic layer (Jacobson, 1966). This work showed the sequential influence of endoderm, mesoderm and hindbrain to the induction of the otic placode. In addition, *in vitro* studies showed that formation of the otic vesicle from placodal stages requires signals from the hindbrain (Represa et al., 1991). These studies were also substantiated by tissue recombination experiments and ablation studies, as well genetic analysis in mouse and zebrafish models, which show that placodal development is directed by signals arising from the adjacent hindbrain and underlying mesenchyme (Steel, 1995; Whitfield et al., 1996; Baker and Bronner-Fraser, 2001). Furthermore the genetic mutations described in the mouse (Steel, 1995) and in zebrafish (Whitfield et al., 1996) with primary deficiencies affecting hindbrain development, have also associated inner ear defects. For example, the *kreisler* mutant mouse and the *valentino* mutant zebrafish, which carry mutations in orthologous transcription factors, expressed in the hindbrain, have otic defects that are secondary to disruption of rhombomeres 5 and 6 (Frohman et al., 1993; McKay et al., 1994; Moens et al., 1998). Therefore, the molecular identities of signals responsible for otic placode induction are a subject of strong interest to the research community. In particular members of the FGF and Wnt signalling families originate in the hindbrain or surrounding mesenchyme (periotic mesenchyme) and act as inducing agents for otic tissue in direct or indirect manner (Ladher et al., 2000; Phillips et al., 2001; Leger and Brand, 2002; Maroon et al., 2002; Wright and Mansour, 2003; Phillips et al., 2004). Fgf3 is thought to act as major otic inducing agent as *Fgf3* expression in

the hindbrain appears to be conserved across vertebrate species and disruption of Fgf3 signalling alone leads to inner ear defects (Baker and Bronner-Fraser, 2001; Noramly and Grainger, 2002; Liu et al., 2003; Schlosser, 2006). Nevertheless, in these mouse mutants, the otic placodes clearly form and other Fgfs were shown to act with *Fgf3* in a redundant fashion (Represa et al., 1991; Phillips et al., 2001). In fact, different species seem to have adopted alternate molecules for placode induction. In mammals, Fgf10 is a second placode inducing factor (Wright and Mansour, 2003), while Fgf8 plays an analogous role in zebrafish (Liu et al., 2003). In chicken, *Fgf19* and *Wnt8c* induce the expression of the placode-specific genes (Ladher et al., 2000), but in zebrafish *Wnt8c* is not sufficient for otic induction (Phillips et al., 2004). Additionally, the mouse homolog of chick *Fgf19*, *Fgf15*, is sufficient to induce expression of otic markers in chick explants, however, mouse embryos lacking *Fgf15* do not have otic abnormalities (Wright et al., 2004).

Although the majority of the genetic deletions do not lead to a complete loss of otic vesicles, these studies show how the surrounding environment is crucial for the otocyst development.

D.2.2 Patterning

Following induction, the otic placode of most vertebrates invaginates to form the otic vesicle. Within the otic epithelium, both intrinsic and extrinsic signals begin to pattern the otic vesicle in early stages (Morsli et al., 1998; Fekete and Wu, 2002; Liu et al., 2003). The patterning of the otic vesicle leads to a sequence of cell fate decisions that ultimately gives rise to neural, sensory and non-sensory cells. These early fate decisions, followed by inner ear morphogenesis, take place in a three dimensional context and are dependent of the proper establishment of the three axes of the inner ear, anteroposterior (AP), dorsoventral (DV) and mediolateral (ML) (Harrison, 1936; Wu et al., 1998; Bok et al., 2007). Acquisition of axial identity from surrounding tissues is one of the early events in inner ear formation. Formation of the AP axis is required for neurogenesis since

neuroblasts only delaminate from the anterior/lateral domain of the otic epithelium. Formation of the DV axis is necessary for development of dorsal (vestibular) and ventral (cochlear) structures. In order to better understand inner ear morphogenesis it is crucial to first identify the inductive signals that confer axial identity and their consequent molecular and cellular events. Specification of three primary axes of the inner ear was originally addressed in the salamander model using classical embryological approaches (Harrison, 1936). More recent studies have observed that establishment of inner ear axis is acquired by interactions between otic epithelium and morphogen signals produced by the surrounding tissues, such as the hindbrain, notochord, endoderm and head mesenchyme (Wu et al., 1998; Ladher et al., 2005; Bok et al., 2007). For instance, Wnts secreted from the hindbrain are required for dorsal otic patterning and morphogenesis of both dorsal and ventral otic structures (Riccomagno et al., 2005). The ventral hindbrain and the notochord are sources of Sonic Hedgehog (Shh) signalling required for the formation of ventral inner ear structures (Riccomagno et al., 2002; Bok et al., 2005). Additionaly, reciprocal epithelial-mesenchymal signalling is required for inner ear development as some transcription factors, such as *Brn4,* expressed in the mesenchymal cells surrounding the otocyst have been shown to mediate proper cochlear outgrowth (Phippard et al., 1999).

After receiving signals from surrounding tissues the otic vesicle adopts very restricted gene expression patterns. An increasing amount of work supports the concept that gene expression domains define compartments of the otic vesicle that will ultimately determine identity within the inner ear (e.g. endolymphatic duct, semicircular canals, cochlea, etc) (Fig. 1.10). The boundaries of these compartments may then be critical in the positioning of specific structures (e.g. sensory hair cell patches, the endolymphatic apparatus) and may be mediated by molecular signals transmitted across boundaries (Brigande et al., 2000a; Brigande et al., 2000b; Fekete and Wu, 2002). The search for molecular mechanisms underlying impaired development of the inner ear, led to the

assessment of expression of molecular markers for specific otic structures (e.g. genes with specific expression compartments or boundaries). In fact, in several studies describing mutant mouse embryos with impaired development of inner ear, the affected area typically reflects the gene's expression domain (Torres et al., 1996; Hadrys et al., 1998; Ma et al., 1998; Torres and Giraldez, 1998; Wang et al., 1998; Acampora et al., 1999; Depew et al., 1999; Liu et al., 2000; Riley and Phillips, 2003). Several transcription factors have been suggested to act cell autonomously to regulate positional identity, differentiation and morphogenesis within their domains of expression. This is exemplified by analysis of two transcription factors, the homeobox ***Nkx5.1*** and the paired box ***Pax2****,* that contribute to patterning processes of the inner ear. Both genes are expressed in the otic epithelium in a complementary fashion, which indicates that early segregation of the functional domains takes place already at otic vesicle stages during inner ear development (Sanyanusin et al., 1995; Schimmenti et al., 1997).

In mouse, expression of ***Pax2*** in the ventral medial regions of the otic vesicle, closer to the neural tube, correlates well with its essential role in the cochlear duct outgrowth. In fact, inner ear analyses of *Pax2*$^{-/-}$ mutants display agenesis of the mouse cochlea (Torres et al., 1996; Burton et al., 2004), which normally emerges from the ventral most portion of the *Pax2* expression domain in the otocyst. Changes in gene expression profiles in *Pax2*$^{-/-}$ inner ears indicate that the cochlear outgrowth and patterning is arrested at early stages of cochlea development. It has been suggested that this effect is due to a decrease in cell proliferation and an increase in cell death in the domains that normally express *Pax2* in the developing cochlea (Burton et al., 2004).

On the other hand ***Nkx5.1*** expression in the dorso-lateral regions of the otic epithelium and later in non-sensory epithelium of the vestibular apparatus (Rinkwitz-Brandt et al., 1996) is in agreement with fate map studies assigning vestibular cells to the lateral part of the otocyst (Li et al., 1978). This region of the otic epithelium will further develop into the three semicircular canals. The observed *Nkx5.1* mutant phenotype emphasizes this lineage relationship.

Homozygous *Nkx5.1* mutant mice presented abnormal hyperactivity and circling movement, indicating balance defects. This behaviour was caused by severe malformations of the semicircular canals of the inner ear (Hadrys et al., 1998). In contrast to the severe malformations of the vestibular system, the morphology of the cochlea appeared unaffected indicating that this *Nkx5.1* is not essential in this part of the inner ear. In conformity with this these observations, no hearing problems were observed in these adult *Nkx5.1* mutant adult mice.

Other dorsal otic genes such as ***Dlx5*** and ***Dlx6*** establish the vestibular fate in the dorsal otic region that further develops into the three semicircular canals and their associated cristae (Riccomagno et al., 2005). The inner ears of *Dlx5* single, or *Dlx5/Dlx6* double null mutants all show defects in crista and canal development (Merlo et al., 2002; Robledo and Lufkin, 2006).

Gbx2 is a homeobox transcription factor known to be a key molecule in patterning both vestibular and auditory components of the inner ear. *Gbx2* is required for normal development of the midbrain-hindbrain region, where it is expressed (Wassarman et al., 1997). *Gbx2* is also expressed in the otic placode of several species (Bouillet et al., 1995; Shamim and Mason, 1998; Su and Meng, 2002). In mice, expression of *Gbx2* in the dorso-medial region of the otocyst correlates with proper otocyst formation (Wright and Mansour, 2003). In fact, in null mutants for *Gbx2* the endolymphatic duct, which is a dorsomedial structure, is absent. As *Gbx2* is normally expressed in this region, it indicates that *Gbx2* is required cell autonomously for endolymphatic duct formation (Lin et al., 2005). In addition, these mutants display variable defects of the semicircular canals, which are dorsolateral structures. Since *Gbx2* expression is excluded from the lateral region of the otocyst, it has been suggested that *Gbx2* could have a non-cell autonomous role in the development of these structures (Lin et al., 2005).

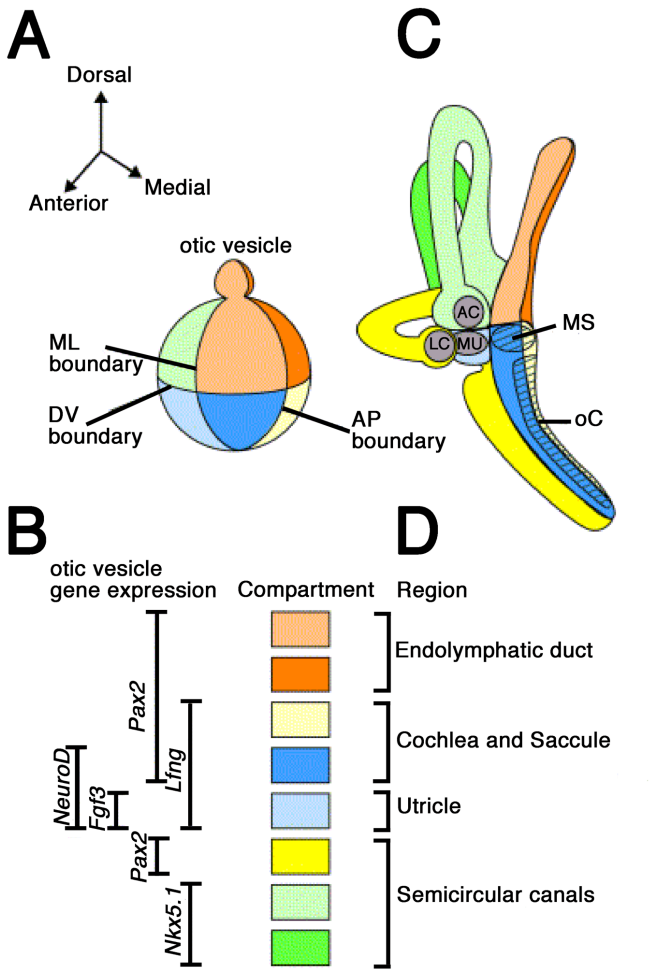

Figure 1.10 A compartment-boundary model of ear morphogenesis.
(A) Model of the compartmentalized otic vesicle divided by three boundaries, (Antero-posterior: AP; Medio-Lateral: ML; Dorsoventral: DV). The budding endolymphatic duct arises near the dorsal pole. (B) Several genes expressed in different parts of the otic vesicle are indicated, along with compartments that they are most likely to encompass. Data are compiled from studies of both mouse and chicken. (C) Predicted map from the early inner ear, showing were cells from each compartment of the early otic vesicle are expected to be located after morphogenesis. The precise location of the developing saccule and organ of Corti (oC) in mammals is uncertain and consequently these are shown as stripes. (D) Possible arrangement of the regions of the ear arising from the different developmental compartments. AC: anterior crista; LC: lateral crista; oC:organ of Corti; MS: macula from saccule; MU: macula from utricle (adapted from Fekete and Wu, 2002).

Taking together these studies, there are two consecutive developmental processes involved in patterning of the inner ear. First, evidence from several vertebrate models (chick, mouse and zebrafish) show that normal hindbrain development and cues from the hindbrain and surrounding tissues are necessary for establishing the primary axes and pattern the otocyst. Second, these cues induce specific patterns of gene expression, and mutations in these key genes result in the loss of distinct ear structures. Additionally, gene expression studies in the otic vesicle sustain the importance of gene expression compartments and boundaries in order to direct the correct development of inner ear structures.

D.2.3 Morphogenesis

D.2.3.1 Inner ear structures and function

Soon after the otic vesicle is formed, several morphogenetic movements occur in a sequential manner. At an early stage, a group of cells in the antero-ventral part of the otocyst becomes committed to a neural fate and delaminates to give rise to the neurons of the VIIIth cranial ganglion (also called the cochleo-vestibular ganglion, cvg) (Torres and Giraldez, 1998). Differential gene expression within the otic epithelium results in complex folding and growth to produce several interconnected chambers (reviewed in Torres and Giraldez, 1998). At very early stages a dorso-medial outgrowth from the otic vesicle gives rise to the endolymphatic duct. Later on, differentiation from specific areas of the otic epithelium leads to the formation of the cochlea, semicircular canals, utricle and saccule (Torres and Giraldez, 1998; Riley and Phillips, 2003). As the otic epithelium differentiates, it interacts with the surrounding mesenchyme to induce formation of a skeletal case for the inner ear.

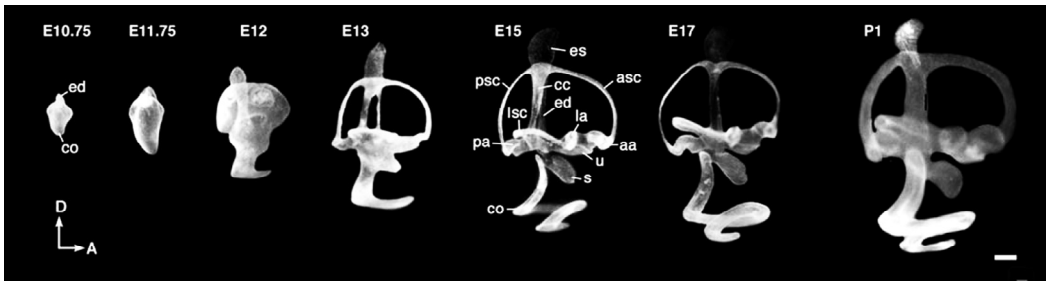

Figure 1.11 Morphogenesis of the mouse inner ear.
Lateral views of mice inner ears filled with latex paint solution from embryonic days 10.75 (E10.75) to postnatal day 1 (P1). Abbreviations: aa, anterior ampulla; asc, anterior semicircular canal; cc, common crus; co, cochlear duct; ed, endolymphatic duct; es, endolymphatic sac; la, lateral ampulla; lsc, lateral semicircular canal; pa, posterior ampulla; psc, posterior semicircular canal; s, saccule; u, utricle, D, dorsal; A, anterior. Scale bar, 200 μm (adapted from Morsli et al., 1998).

A mature inner ear is composed of two major parts, a dorsal vestibular component and a ventral auditory component (Fig. 1.11). In the vestibular component, three semicircular canals and their associated sensory tissues (cristae) housed within the ampullae, are responsible for detecting angular head movements. Two additional sensory tissues, the macula of the utricle and the macula of the saccule, are fundamental for sensing gravity and linear acceleration, respectively. The cochlea has one sensory organ, known as the organ of Corti responsible for detecting sound.

Each sensory epithelium has specific morphology but with a common characteristic: the presence of two different cell types, the hair cells and the supporting cells. Hair cells of the vertebrate inner ear are mechanosensors that detect sound, gravity and acceleration. Each hair cell has several rows of apical protrusions known as stereocilia bundles that are projected into the lumen of the ear. Hair cell function is stimulated by lateral deflection of these stereociliary bundles providing the basis for both hearing and balance (Muller and Littlewood-Evans, 2001). The function of supporting cells is less clear. Zebrafish studies indicate that supporting cells appear to have an active role in the maintenance of hair cell function and structure (Haddon et al., 1999). The sensory epithelia in the utricle and saccule, called macula, are associated with otoliths. These otoliths are

dense crystals attached to the hair cells and facilitate vestibular and auditory function by transmitting acceleration forces to hair cell cilia. By contrast, the sensory epithelia in the semicircular canals (cristae) do not have otoliths. Alternatively, hair cells from the cristae have extremely long ciliary bundles that are sensitive to fluid motion caused by angular acceleration. Electrical signals from hair cells are transduced by neurons projected from the cochleo-vestibular ganglion that innervate the various sensory patches in the developing inner ear. The fluid inside the inner ear, called endolymph, has a specific ionic balance necessary for hair cells function and its volume is regulated by flow that passes through the endolymphatic duct. Despite its complexity and multiple functions, almost all the cellular components of the otic epithelium derive from the embryonic otic vesicle. Thus, the study of the development of the inner ear is mainly the study of the otic vesicle.

D.2.3.2 Specification of neurogenic and sensory cells of the ear

Neurons from the cochleovestibular ganglion

Derivatives of the otic vesicles include various differentiated cell types. The first lineage to differentiate and the only one to leave the epithelium is the neuronal lineage. Neuroblasts delaminate from ventral areas of the otic epithelium, near the neural tube and gather together as the cochleo-vestibular ganglion (cvg). After becoming postmitotic their growth cones emerge from the ganglion to seek out targets among the sensory patches of the inner ear, eventually innervating mature hair cells. Morphologically and molecularly, the specification of some otocyst cells as neuroblasts is perhaps the earliest cell fate decision that takes place in the ear. Interestingly, the molecular basis of this decision involves transcription factors that are members of the basic helix–loop–helix (bHLH) gene family, *neurogenin-1* - *Ngn-1* and *NeuroD*. Null mouse mutants for these genes display abnormal differentiation of the otic ganglion (cvg) (Ma et al., 1998; Liu et al., 2000).

Specification of sensory cells

After neuroblast delamination, major morphogenetic events of the inner ear are correlated with the appearance of sensory organs. As already discussed, there are six major sensory organs in the vertebrate inner ear: the three cristae from the canals, maculae of the utricle and saccule and the auditory sensory organ (the organ of Corti in mammals). The molecular mechanisms underlying specification of the neurosensory domain involve ***Bmp4*** and ***Lfng*** genes, which are expressed specifically in the sensory organs of the inner ear with specific patterns for particular structures (Morsli et al., 1998). Both genes are normally expressed in the supporting cells of the three vestibular cristae, and *Lfng* is also expressed in the utricular and saccular maculae. In the cochlea, they display distinct expression patterns, *Lfng* being expressed in the supporting cells beneath the inner and outer hair cells and *Bmp4* in a more lateral domain that corresponds to the future Hensen's and/or Claudius' cells - the supporting cells that constitute the outer border of the organ of Corti (Morsli et al., 1998). It is thought that the *Bmp4*-positive cells give rise to the three cristae, while the Lfng-expressing cells give rise to the maculae and the organ of Corti (Morsli et al., 1998).

Sensory-fated cells eventually develop into hair cells or supporting cells that form the various sensory patches within the ear components. The specification of hair cell identity against supporting cells is another critical developmental decision in inner ear morphogenesis. Genetic studies in mouse have been instrumental in elucidating various stages of hair cell differentiation following specification. Mouse transcription factor **Brn3c** (also known as Pou4f3 or Brn3.1) is expressed in the hair cells present in all sensory areas of the otic vesicle (Erkman et al., 1996; Xiang et al., 1998; Hertzano et al., 2004). *Brn3c* was the first gene described to be crucial for normal differentiation and survival of the inner ear hair cells. In *Brn3c* mouse mutants, hair cells are unable to produce stereocilia and subsequently degenerate by apoptosis (Erkman et al., 1996; Xiang et al., 1998).

Figure 1.12 represents the expression domains of some of the genes commonly

associated with the formation of the sensory region of the inner ear components.

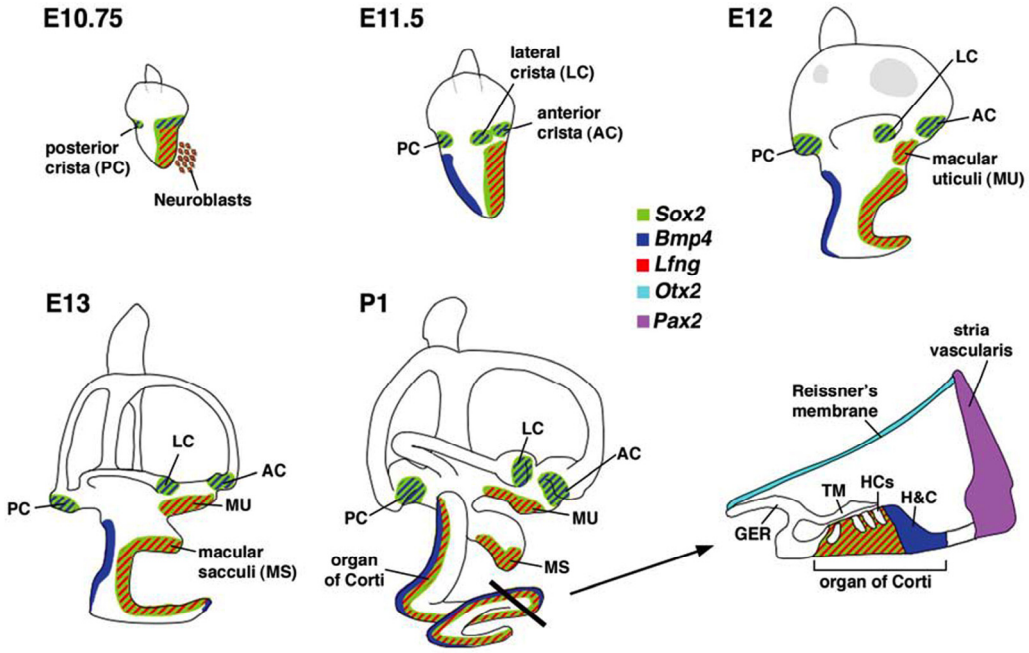

Figure 1.12 Sensory organ formation in the mouse inner ear.
At **E10.75**, Bmp4 and Lfng are expressed in subsets of cells within the larger Sox2-positive, neurosensory domain of the otic-vesicle. The *Bmp4* expression domains are associated with the three presumptive cristae. *Lfng* is expressed broadly in the anterior ventral region, associated with the macula utriculi, macula sacculi, organ of Corti and where neuroblasts delaminate. By **E11.5**, the presumptive anterior and lateral cristae are separate entities. *Bmp4* is also expressed in the non-sensory region of the developing cochlear duct. By **E12**, the broad *Lfng* expression domain splits into two distinct regions: a dorsal, macula utricle and a ventral domain that consists of the macula saccule and organ of Corti, which become distinct entities by **E13**. A cross-section view of the organ of Corti at **P1** shows that *Sox2* and *Lfng* are downregulated in sensory hair cells but strongly expressed in supporting cells. Abbreviations: GER, greater epithelial ridge; TM, tectorial membrane; HCs, hair cells; H&C, Hensen's and Claudius' cells (adapted from Bok et al., 2007).

In Chapter 2 the ear phenotype of homozygous null mutant embryos for *Tbx1* gene is characterized and some of the patterning genes crucial for correct ear development, are evaluated in this *Tbx1* mutant background.

E. SUMMARY AIMS AND GOALS

The general aim of this thesis was to better understand the development of the ear and pharyngeal arches in mouse embryos and deepen our knowledge about some of the genetic players involved in these processes. It is important to understand the mechanisms that regulate the morphogenesis of these structures and what happens when this development is compromised giving rise to several malformations in mice that usually recapitulate congenital defects in humans, thus providing an animal model for their study.

In **Chapter 2** the main objective was to determine the role of *Tbx1* in mammalian ear development. We pursued the characterization of the ear phenotype of null mutant embryos for *Tbx1* gene. The middle and inner ear phenotypes of the *Tbx1* null mice were characterized using skeletal, histologic, and molecularly analysis (Moraes, et. al 2005).

In **Chapter 3** the main objective was to discover the function of *Bmp2* in the induction of neural crest. It has been very difficult to distinguish between defects in neural crest cell induction versus a complete failure of neural crest cell migration largely because the latter depends on the former. In order to reach this objective, we did a molecular analysis of early neural crest development in *Bmp2* null mice. Moreover using a transgenic approach, we analysed *RFP*-labelled neural crest cells in *Bmp2* null genetic background using the transgenic mouse line *Tg(HtPA-RFP)* produced for this effort (Correia, et. al 2007).

Chapter 4 outlines the development of new imaging tools to study vascular development, in particular the arteries that pass through pharyngeal arches in mammalian embryos, designated by pharyngeal arch arteries (or aortic arches). Firstly, double transgenic reporter mouse lines were produced with endothelial

cells and neural crest cells expressing fluorescent proteins (GFP and RFP). Secondly, a staining technique described in this Chapter was developed and optimized. The embryonic arteries were immunostained with the endothelial specific marker PECAM and simultaneously with the vascular smooth muscle marker SMA to observe the coverage of these large vessels by vascular smooth muscle cells (VSMC) by staining with the vascular smooth muscle marker SMA.

Chapter 5 describes the study of smooth muscle recruitment around the embryonic arch arteries using the methodology developed in Chapter 4. To determine the function of vascular smooth muscle cells in the remodelling of the embryonic arteries, two mutant strains with impaired development of the arch arteries were analysed (*ETA*$^{-/-}$ *and Pbx1*$^{-/-}$). Moreover transgenic mouse embryos *HtpA-Myoc::Mkl2* were produced in order to find a correlation between the presence or absence of VSMCs and the stabilization or regression of the arch arteries.

Chapter 2:

Tbx1 is required for proper neural crest migration and to stabilize spatial patterns during middle and inner ear development

Mechanisms of Development **122**, 199-212
(2005)

Tbx1 is required for proper neural crest migration and to stabilize spatial patterns during middle and inner ear development

Filipa Moraes[1], Ana Nóvoa[1], Loydie A. Jerome-Majewska[2], Virginia E. Papaioannou[2] and Moisés Mallo[1,*]

(1) Instituto Gulbenkian de Ciência, Oeiras, Portugal
(2) Department of Genetics and Development, College of Physicians and Surgeons of Columbia University, New York, New York, USA

The work presented here was carried out in collaboration between all authors.
FM and AN performed experiments, FM and MM designed research, analysed data and wrote the paper. VP and LJ-M contributed the *Tbx1*$^{+/-}$ mouse line and reagents/analytic tools.

ABSTRACT

Tbx1 belongs to the family of T-box containing transcription factors. In humans, *TBX1* is implicated in the etiology of the DiGeorge syndrome. Inactivation of the *Tbx1* gene in mice produces a variety of malformations including abnormal branching of the heart outflow tract, deficiencies in the branchial arch derivatives, agenesis of pharyngeal glands and abnormal development of the auditory system. We analyse here the middle and inner ear phenotypes of the *Tbx1* null mice. The middle ear is strongly affected. Its skeletal components are malformed to varying degrees, some being slightly hypoplastic and others completely absent. However, a seemingly normal-looking tympanic membrane can still be recognized. Middle ear anomalies are associated with other skeletal deficiencies in the branchial arch-derived skeleton. These phenotypes derive from a combination of the failure of the posterior branchial arches to develop and the misrouting of neural crest cells. The inner ears of *Tbx1*$^{-/-}$ animals are hypoplastic. No vestibular or cochlear structures are detectable, but the endolymphatic duct, the cochleovestibular ganglia and residual sensory patches are still identifiable. Molecular analyses revealed a seemingly normal spatial distribution of a variety of patterning markers in the otic vesicles of *Tbx1* null mutants at E9.0. However, one day later, several of these markers presented altered domains of expression in the otocysts of these mutant embryos, suggesting that *Tbx1* is not required for the establishment of spatial patterns in the otocyst, but rather for their maintenance. The inability of the *Tbx1*$^{-/-}$ embryos to keep properly segregated functional domains in the otocyst is likely the cause of the strong inner ear phenotypes observed in these mutants.

INTRODUCTION

The mammalian hearing apparatus consists of three main compartments, the outer, middle and inner ears. The outer ear receives acoustic waves from the air, which are amplified and transmitted by the middle ear elements into the inner ear to generate vibrations in the endolymph. These vibrations excite the hair cells of the organ of Corti, located in the cochlear part of the inner ear, to generate neural impulses that are transmitted to the brain through the acoustic nerve. While the outer and middle ears are exclusively implicated in hearing, the inner ear is also involved in the process of balance, centered in the vestibular area. Specific sensory receptors located in the cristae and maculae detect, respectively, movements of the liquid in the semicircular channels and the position of the otoliths in the utricle and saccule.

In recent decades, impressive advances have been made in our understanding of the embryological, molecular and genetic bases of the development of the different ear compartments (Mallo, 1998; Torres and Giraldez, 1998; Mallo, 2001; Riley and Phillips, 2003). The outer and middle ears derive from the first and second branchial arches. Their development is closely linked to general patterning and morphogenetic processes in this area, which require cells of the cranial neural crest and their interactions with the ectodermal and endodermal compartments of the developing branchial arches (Mallo, 1998; Mallo, 2001). The origin of the inner ear is completely different. It derives from the otic placode, an ectodermal thickening adjacent to the hindbrain. The placode invaginates and forms first the otic cup and then the otic vesicle (also known as the otocyst), which undergoes a complex series of morphogenetic and differentiation processes, eventually giving rise to a variety of structures and cell types (Torres and Giraldez, 1998; Riley and Phillips, 2003). As the otic epithelium differentiates, it interacts with the surrounding mesenchyme to induce formation of a skeletal case for the inner ear.

The otic vesicle develops in a sequential fashion. In an early stage, a group of cells in the rostro-ventral part becomes committed to a neural fate and delaminates to give rise to the neurons of the VIIIth cranial ganglion (also called the cochleo-vestibular ganglion, cvg) (Torres and Giraldez, 1998). The endolymphatic duct also starts its morphogenesis at a very early stage, as an outgrowth in the dorsal part of the otic vesicle (Brigande et al., 2000). Later on, differential gene expression within the otocyst results in the formation of the cochlea, semicircular channels, utricle and saccule from specific areas of the otic epithelium (Torres and Giraldez, 1998; Riley and Phillips, 2003). Several of the genes responsible for these differentiation processes have been identified, mostly by using mutational approaches. Different groups of genes, including transcription factors, secreted molecules and their receptors, have been implicated in these processes, and some of the networks connecting these molecules are beginning to be understood (Torres et al., 1996; Hadrys et al., 1998; Ma et al., 1998; Wang et al., 1998; Acampora et al., 1999; Depew et al., 1999; Xu et al., 1999; Liu et al., 2000; Riccomagno et al., 2002; Bachiller et al., 2003; Laclef et al., 2003; Zheng et al., 2003).

Tbx1 is a member of the T-box-containing family of transcription factors (Bollag et al., 1994). In humans, *TBX1* gene is located within the microdeletion on chromosome 22 associated with the DiGeorge syndrome (Scambler, 2000), characterized by cardiovascular malformations, hypoplasia or aplasia of the thymus and parathyroid glands, and craniofacial defects (Scambler, 2000). Recent studies indicated that *TBX1* is one of the major players in the etiopathogenesis of the DiGeorge syndrome, which results from haploinsufficiency of this gene (Merscher et al., 2001). In the mouse, mutations in the *Tbx1* gene have been generated and haploinsufficient phenotypes have also been described (Jerome and Papaioannou, 2001; Lindsay and Baldini, 2001; Merscher et al., 2001). These phenotypes are mostly milder than in the human DiGeorge syndrome, with low penetrance and dependence on the genetic background. In the homozygous state, the *Tbx1* null mutation produces a lethal

phenotype with complete penetrance that affects the thymus, the heart outflow tract, the craniofacial area and the ear (Jerome and Papaioannou, 2001; Lindsay and Baldini, 2001; Merscher et al., 2001). Recent studies have shown that *Tbx1* plays multiple roles in the development of the pharyngeal region and in the remodelling of the aortic arches (Vitelli et al., 2002a). In addition, it has been suggested that some of these activities may be mediated through the control of *Fgf* expression in the branchial arches (Vitelli et al., 2002b). A role for *Tbx1* in inner ear development has also been reported (Funke et al., 2001; Vitelli et al., 2003; Raft et al., 2004). Analysis of *Tbx1* null mutant embryos revealed that the inner ear is strongly affected. However, while Vitelli et al. (2003) suggest that this gene is required for expansion of a subpopulation of cells in the otic vesicle responsible for development of both the cochlear and vestibular areas, Raft et al. (2004) recently proposed that *Tbx1* gene function suppresses neural fate specification in the otocyst.

Here we show that *Tbx1* is required for the development of all the ear compartments. In the middle ear, deficiencies in the mutant were found associated with other malformations in the branchial arch-derived skeleton, indicating that they may represent one aspect of a more general effect of the *Tbx1* null mutation on the development of the pharyngeal region. The defects in the skeleton derived from the second and more caudal branchial arches can be explained by the strong deficiencies in these arches observed in the *Tbx1* mutants (Jerome and Papaioannou, 2001). In addition, we found that some of the prospective second arch neural crest cells migrate anomalously into the first arch, thus providing an explanation for the phenotype observed in the first arch derivatives. The inner ear was strongly affected in the *Tbx1* mutants. Only the endolymphatic duct and the cochleo-vestibular ganglion, together with rudimentary sensory patches, could be identified associated with a residual small otic capsule. Our molecular studies show that, while patterning of *Tbx1* mutant otocysts is strongly affected at E10.5, it looks largely undisturbed at E9.0-E9.5. On the basis of our results we suggest an alternative explanation for the inner ear

phenotype as resulting from the absence of new morphogenetic processes after the loss of appropriate spatial patterning in the otocyst.

MATERIAL AND METHODS

Mice and embryos

Mice carrying the *Tbx1*^{tm1Pa} null mutation have been described previously (Jerome and Papaioannou, 2001). For simplicity, we refer to the mice carrying one or two *Tbx1*^{tm1Pa} alleles as *Tbx1*$^{+/-}$ and *Tbx1*$^{-/-}$, respectively. For the experiments described in this manuscript, mice in a C57BL/6/129 mixed background were used. Embryos were collected at the specified stages from *Tbx1*$^{+/-}$ intercrosses, and genotyped as previously described (Jerome and Papaioannou, 2001).

Phenotypic analyses

Skeletal staining of newborns was performed using the alcian blue/alizarin red method as described in (Mallo and Brandlin, 1997). Four embryos of each genotype were analysed.

In situ hybridization both in whole embryos and on tissue sections was performed as described in Kanzler et al. (1998), using digoxygenin-labelled riboprobes for *Pax2, Gata3, Nkx5.1, Gbx2, Dlx5, NeuroD, Tbx1, CrabpI, Bmp4, Lfng, Brn3c, Six1, Hoxa2* and *Sox10*. Three to five embryos of each genotype were analysed for each probe. After whole-mount staining, representative embryos were postfixed in 4% paraformaldehyde/0.2% glutaraldehyde, rinsed in PBS, embedded in gelatin, and sectioned with a vibratome at 30-40 μm.

RESULTS

Middle ear defects in *Tbx1*$^{-/-}$ embryos

Preliminary analyses of *Tbx1* null mutants revealed strong malformations in the three ear compartments. The outer ears, particularly the ear pinnae, have been described to be typically absent or small and positioned low (Jerome and Papaioannou, 2001). This may be a consequence of the total or partial absence of the second branchial arch in the mutants (see below), as this arch is the major contributor to the pinna (Carlson, 1999; Mallo, 2003). The middle ear has also been reported to be affected in the *Tbx1* mutants (Jerome and Papaioannou, 2001), but no detailed analysis was performed. Analysis of stained skeletons of *Tbx1*$^{-/-}$ newborns revealed that, of the three middle ear ossicles, the malleus was the least affected (Fig. 2.1A,B). It was still present and all the basic elements of its anatomy were recognizable, but it was slightly hypoplastic. In particular the ossicle's neck was thinner than that of wild-type embryos. The incus of *Tbx1* mutant newborns was reduced to a small cartilaginous nodule articulated with the head of the malleus (Fig. 2.1B). No traces of the third ossicle, the stapes, could be found either in the skeletal preparations or in histological sections (n=7). Other skeletal elements derived from the caudal branchial arches, like the hyoid bone and the thyroid cartilage, were also strongly affected by the *Tbx1* mutation (Fig. 2.1C,D), suggesting that the middle ear malformations are part of a general deficiency in branchial arch development.

The tympanic membrane can be regarded as the connection between the middle and outer ears. Histological analysis revealed that, while its anatomy was slightly affected in newborn mutant mice, all the relevant components (i.e. tympanic ring, external acoustic meatus, malleal manubrium and middle ear endoderm) appeared to be induced and properly arranged (Fig. 2.1E,F). The tympanic ring, which provides support to the membrane, was reduced in length and somewhat

thicker than that of wild-type littermates but still presented the characteristic semicircular morphology (Fig. 2.1B). The external acoustic meatus (EAM) was also induced and had invaginated toward the tympanic ring (Fig. 2.1F). However, it showed a slightly abnormal trajectory, possibly related to the abnormal positioning of the residual ear pinna. At the level of the tympanic ring, the EAM was found to be flattened in the plane defined by the ring and, together with the lateral epithelium of the middle ear cavity and the malleal manubrium, a clearly recognizable eardrum (Fig. 2.1F).

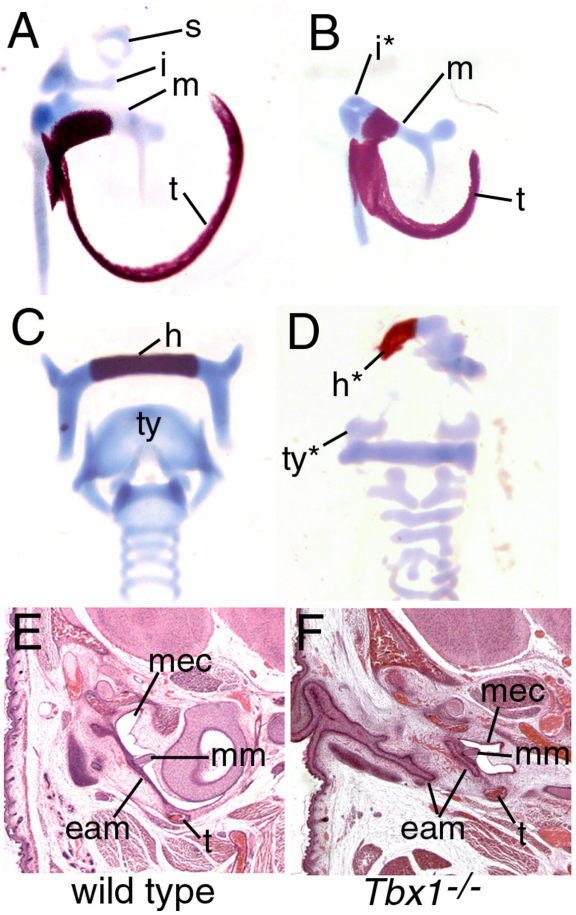

Figure 2.1 Middle ear phenotype of *Tbx1* mutants.
A,B: Dissection of stained middle ear skeleton of wild-type (A) and *Tbx1*$^{-/-}$ (B) newborns. In the wild-type, the three ossicles, malleus (m), incus (i) and stapes (s), together with the tympanic ring (t) are shown. In the *Tbx1*$^{-/-}$ mutants (B), the malleus and tympanic ring are still recognizable, but the stapes is not present and the incus is reduced to a small cartillaginous nodule (i*).
C: The typical wild-type neck skeleton is shown, including the hyoid bone (h) and thyroid cartilage (ty). **D:** In the *Tbx1*$^{-/-}$ mutants, the neck skeleton is very affected and contains only malformed remnants of the hyoid (h*) and thyroid cartilage (ty*). **E:** In frontal sections, the tympanic membrane of wild-type newborns contains two epithelia, the external acoustic meatus (eam) and that of the middle ear cavity (mec), which entrap a skeletal element, the manubrium of the malleus (mm). The membrane is supported in the tympanic ring (t). **F:** All the elements of the tympanic membrane can be seen correctly organized in *Tbx1*$^{-/-}$ mutants, although on a smaller scale. The pictures shown in E and F correspond to frontal sections, oriented to position lateral on the left and rostral at the top.

To further understand the middle ear phenotype, we analysed the branchial area of *Tbx1* mutant embryos at earlier developmental stages. Morphological analyses of the mutant embryos revealed that, while the first branchial arch was clearly recognizable and seemingly normal looking, the second and more caudal arches were absent or strongly hypoplastic (Fig. 2.2B,F) as already previously reported (Jerome and Papaioannou, 2001). This would explain the strong malformations observed in the skeletal derivatives of the affected arches, like the stapes and the hyoid bone. However, it cannot explain the anomalies observed in the first arch derivatives. Previous studies revealed that neural crest cells normally populating the second and more caudal arches are generated in the *Tbx1* mutants, but that their migration into the corresponding branchial arches is seriously compromised (Vitelli et al., 2002a). Analysis of *Crabp1* expression in *Tbx1* mutant embryos confirmed these observations and revealed the existence of an additional stream of neural crest cells that migrate into the first arch from rhombomere (r) 4 (Fig. 2.2B,H). A similar observation was made using *Sox10* (Fig. 2.2D) as a marker of neural crest cells fated to become the glia of the cranial nerves and ganglia (Britsch et al., 2001). The abnormal invasion of the first branchial arch by r4-derived neural crest cells (which eventually mix with those derived from r2), provides an explanation for the fusion of the Vth and the VII/VIIIth cranial nerves in *Tbx1*$^{-/-}$ mutant embryos (Vitelli et al., 2002a).

To further ascertain the abnormal migration of r4 neural crest cells, which normally populate the second arch (Serbedzija et al., 1992), we did *in situ* analysis of *Hoxa2*, which is expressed in the second arch neural crest cells and never in the first arch (Prince and Lumsden, 1994; Mallo, 1997). In *Tbx1* null mutant embryos, a stream of *Hoxa2*-positive cells could be observed arising from r4 and entering the first branchial arch (Fig. 2.2F,J). This result confirms the abnormal migratory pathway of some neural crest cells in the absence of *Tbx1* and provides an explanation for the skeletal deficiencies in the first arch derivatives (see Discussion).

It has been shown that the mesoderm adjacent to the hindbrain is patterned by

signals from the neuroectoderm and surface ectoderm to maintain the segregation of neural crest cells arising at different rostro-caudal areas of the hindbrain (Golding et al., 2000). Anomalies in neural crest cell migration have also been found in association with alterations in the patterning of the aortic arches (Trokovic et al., 2003). To ask whether the abnormal neural crest migration in *Tbx1* mutant embryos was associated with mesodermal tissue or with altered branching of the embryonic aortic tree, we sectioned stained whole-mounted embryos to localize the neural crest cells within the arch mesenchyme. Both *Crabp1* and *Hoxa2*-positive neural crest cells that migrated from r4 into the first branchial arches in the *Tbx1* mutants followed a subepidermal trajectory adjacent to the mesodermal core, and both were far from the abnormal blood vessels linking the heart with the dorsal aorta of these mutant embryos (Fig. 2.2H,J). These results suggest that the anomalies of neural crest cell migration in *Tbx1*$^{-/-}$ embryos could result from the inability of the mesoderm adjacent to the hindbrain to restrict migration of the neural crest cells to specific streams.

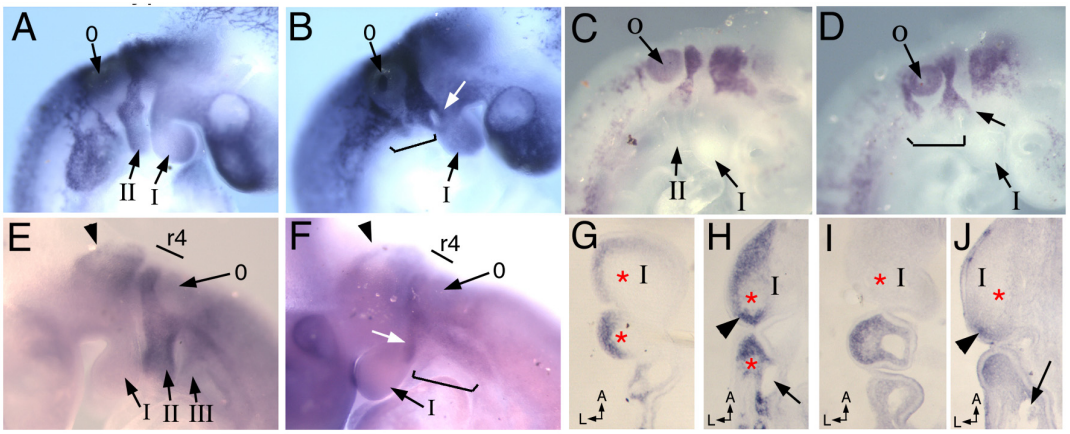

Figure 2.2 Analysis of the neural crest of *Tbx1*$^{-/-}$ mutant embryos.
Wild-type (A,C,E,G,I) and *Tbx1*$^{-/-}$ (B,D,F,H,J) E9.5 embryos were analysed by *in situ* hybridization with probes for *Crabp1* (A,B,G,H), *Sox10* (C,D) and *Hoxa2* (E,F,I,J).
A,B: The *Crabp1* staining shows that migration of neural crest cells normally populating the branchial arches caudal to the first (I) is strongly compromised. In the *Tbx1*$^{-/-}$ mutants, a group of neural crest cells migrates anomalously into the first arch (white arrow).
C,D: The *Sox10* staining shows neural crest cells contributing to the cranial nerves and ganglia. In the *Tbx1*$^{-/-}$ mutants, a group of neural crest cells migrates anomalously into the first arch (arrow). **E:** In wild-type embryos *Hoxa2* labels neural crest cells migrating from rhombomere 4 (r4) into the second branchial arch (II). **F:** In *Tbx1*$^{-/-}$ embryos, *Hoxa2*-positive cells are seen migrating into the first arch (white arrow). *Tbx1* mutant embryos show a seemingly normal first branchial arch, but the second and more caudal branchial arches are strongly affected (brackets in B,D,F). The arrowheads in E and F indicate the border between rhombomeres 2 and 1. **G,H:** Frontal section through the branchial arch region of *Crabp1*-stained wild-type (G) and *Tbx1*$^{-/-}$ (H) embryos. The labelled neural crest cells are adjacent to the mesodermal core (red asterisk), and not to the vessels (arrow). The arrowhead shows the neural crest stream invading the first arch (I) from r4.
I,J: Frontal section through the branchial arch region of *Hoxa2*-stained wild-type (I) and *Tbx1*$^{-/-}$ (J) embryos. The labelled neural crest cells are adjacent to the mesodermal core (red asterisk), and not close to the vessels (arrow). The arrowhead shows the neural crest stream invading the first arch (I) from r4. Sections are oriented with rostral at the top. Only the left side is shown, being lateral on the left. o, otic vesicle.

The inner ears of *Tbx1*$^{-/-}$ newborns are strongly hypoplastic

When examined in whole mount-stained skeletons, the otic capsules of *Tbx1*$^{-/-}$ newborns were barely distinguishable from surrounding cartilaginous structures and were visible as small vesicles of variable shape (Fig. 2.3D).

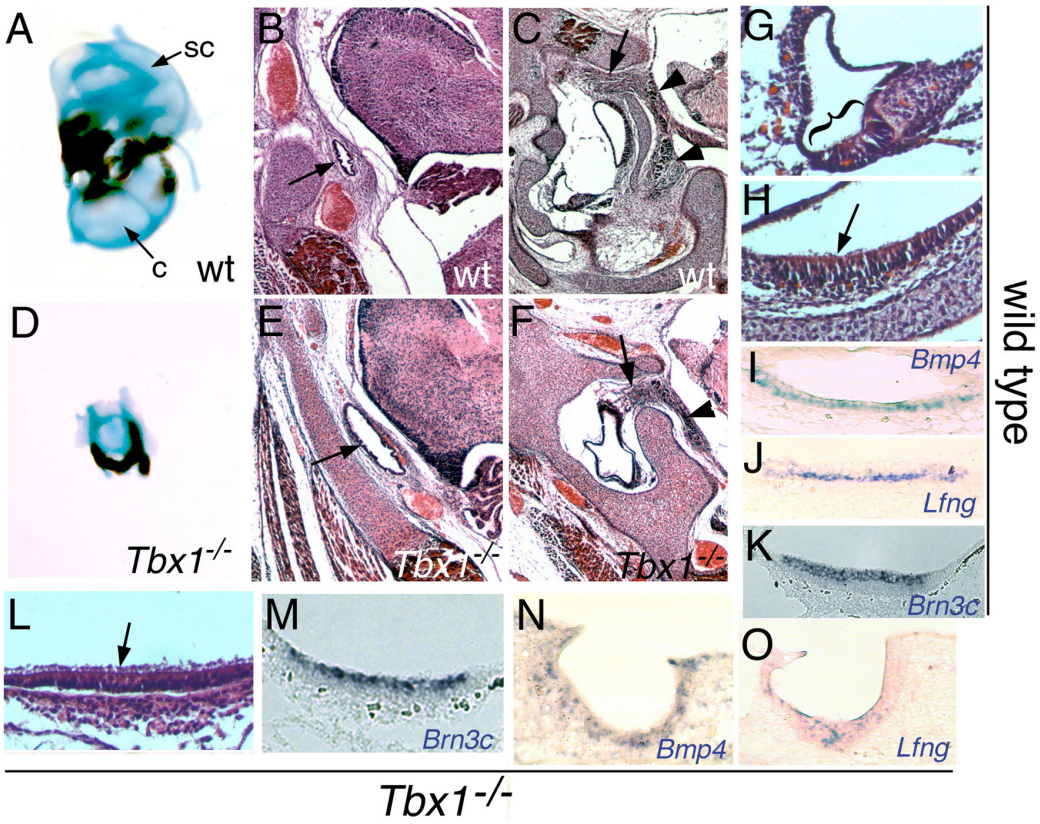

Figure 2.3 Phenotypic analysis of the inner ears of *Tbx1*$^{-/-}$ animals.
A: In wild-type newborns, the inner ear shows all the compartments, including the cochlea (c) and the semicircular canals (sc). **B,C:** In frontal sections, the endolymphatic duct (arrow in B), the cochleo-vestibular ganglion (arrowheads in C) and nerve fibers connecting the sensory epithelium with the ganglion (arrow in C) are visible. D: In *Tbx1*$^{-/-}$ animals, the inner ear is very hypoplastic. **E,F:** In frontal sections, the endolymphatic duct (arrow in E), the cochleo-vestibular ganglion (arrowhead in F) and nerve fibres connecting the sensory epithelium with the ganglion (arrow in F) are also visible. The pictures in D, E and F were taken at the same magnification as those in A, B and C, respectively.
G: Histological section through the organ of Corti of a wild-type newborn. The brackets show the area containing the inner and outer hair cells. **H:** Section through a macula of a wild-type newborn. The arrow indicates hair cells. **I,J:** *In situ* hybridization analysis of a developing sensory patch of a wild-type E15.5 embryo with *Bmp4* (I) and *Lfng* (J). **K:** *In situ* hybridization analysis of a macula of a wild-type newborn with *Brn3c*. **L:** Section through a sensory patch of a *Tbx1*$^{-/-}$ newborn. The arrow indicates hair cells. **M:** *In situ* hybridization analysis of a sensory patch of a *Tbx1*$^{-/-}$ newborn, with *Brn3c*. *In situ* hybridization analysis of a developing patch of a E15.5 *Tbx1*$^{-/-}$ embryo with *Bmp4* (N) and *Lfng* (O).

None of the typical structural compartments of the inner ear could be recognized (compare Figs. 2.3A and D). These observed defects were confirmed on histological sections through the inner ear region of *Tbx1*$^{-/-}$ newborns. Such preparations revealed the presence of a small cartilaginous capsule surrounding a simple cavity where a residual epithelium could still be found (Fig. 2.3F). While there was no discernible indication for the presence of cochlear or vestibular structures, the endolymphatic duct, which at this stage is normally located outside of the cartilaginous capsule (Fig. 2.3B), was readily identified in *Tbx1* mutant newborns (Fig. 2.3E). It is noteworthy that in every mutant embryo analysed the endolymphatic duct looked bigger than in wild-type littermates (compare Fig. 2.3B and E). In addition, the residual otic capsules of *Tbx1*$^{-/-}$ newborns contained epithelia with a degree of differentiation. In particular, some areas within these epithelia presented structures resembling hair cell-containing sensory patches (Fig. 2.3F,L). Their morphology varied among the different specimens, but their histological characteristics were always closer to those of the cristae and maculae than to the distinct cellular arrangement present in the organ of Corti (Fig. 2.3G,H,L). Signs of innervation were seen in some of these patches, namely fibers connecting these sensory structures with the cvg, which was also present in mutants mice, although reduced in size compared to wild-type littermates (Fig. 2.3C,F). These patch-like structures observed in the inner ears of *Tbx1* mutant embryos were positive for *Brn3c* (Fig. 2.3K,M), which labels auditory hair cells (Erkman et al., 1996), further substantiating the notion that they represent inner ear sensory structures. To further characterize these areas, we performed *in situ* hybridization with probes for *Lfng* and *Bmp4*, which are expressed specifically in the sensory organs of the inner ear with somewhat specific patterns for particular structures (Morsli et al., 1998). Both genes are normally expressed in the supporting cells of the three vestibular cristae and *Lfng* is also expressed in the utricular and saccular maculae (Morsli et al., 1998; Fig. 2.3I,J). In the cochlea, they display distinct expression patterns, *Lfng* being expressed in the supporting cells beneath the inner and outer hair cells and *Bmp4* in a more lateral domain

that corresponds to the future Hensen's and/or Claudius' cells (Morsli et al., 1998). For *Tbx1*$^{-/-}$ the areas of otic epithelium resembling sensory patches were positive for expression of both genes (Fig. 2.3N,O), further supporting our histological identification of those epithelial areas as sensory patch-related structures. Their expression domains did not follow any of the patterns described for the maculae, cristae or the organ of Corti (Morsli et al., 1998; Fig. 2.3I,J,N,O) making it difficult to label the patches observed in the *Tbx1* null mutant embryos as equivalent to a specific wild type inner ear sensory structure. However, the finding that the mutant patches express both *Bmp4* and *Lfng* indicates that they may derive from the *Bmp4*-positive anterior stripe of the otocyst destined to become cristae (Morsli et al., 1998).

These results indicate that in *Tbx1*$^{-/-}$ embryos some well organized morphogenesis still occurred in the inner ear primordia even though the inner ear was globally very strongly affected.

Early differentiation arrest of otocyst development

It has been recently proposed that Tbx1 acts to control neural and sensory organ specification in the otocyst (Raft et al., 2004). However, this alone cannot explain the global patterning defects observed in the *Tbx1* mutant. Also, even in these strongly affected inner ears, there was some degree of differentiation. To obtain a more complete view of inner ear development in *Tbx1* mutant embryos, we further characterized early events in otocyst differentiation. At E9.0 the otocysts of *Tbx1*$^{-/-}$ embryos looked morphologically normal in shape, size and position relative to the hindbrain (Figs 2.2 and 2.4). However, at E10.5 the otic vesicles were clearly abnormal (Fig. 2.5). At this stage, the otocysts of *Tbx1*$^{-/-}$ embryos were smaller than those of their wild-type littermates and their shape was abnormal. While the vesicles of E10.5 wild-type embryos presented an elongated shape in the dorso-ventral axis (Fig. 2.5G,J), those of their *Tbx1*$^{-/-}$ littermates were consistently rounder in the ventral area (Fig. 2.5H,L). The endolymphatic tube primordium, the

only morphologically identifiable structure at this stage, was clearly present in the otic vesicles of *Tbx1*$^{-/-}$ E10.5 embryos but looked larger than those of wild-type littermates (e.g. Fig. 2.5E,F). These results indicate that the inner ear phenotype observed in *Tbx1*$^{-/-}$ fetuses and newborns derives from a critical role of this gene at some time prior to E10.5 that first becomes phenotypically evident at E9.5 to E10.5.

Global strong inner ear phenotypes have also been observed in other mouse mutants. *Chrd* mutants show a similar phenotype to that of *Tbx1*$^{-/-}$ embryos (Bachiller et al., 2003). However, *Chrd* is probably upstream of *Tbx1*, because *Chrd* expression is detected earlier than *Tbx1* in wild-type development and *Tbx1* is downregulated in the *Chrd* mutants (Bachiller et al., 2003). *Six1* mutants show, in addition to inner ear phenotypes, middle ear malformations reminiscent of those in the *Tbx1* mutant (Zheng et al., 2003; Ozaki et al., 2004) suggesting that this gene could be a mediator of *Tbx1* activity. *In situ* expression analysis revealed no major differences in *Six1* expression in *Tbx1*$^{-/-}$ embryos (Fig. 2.4A,B), indicating that the *Tbx1* mutant phenotype does not result from downregulation of Six1.

Further analyses of spatial patterning of *Tbx1* mutant otocysts at E9.5 revealed a quite normal distribution of the molecular markers investigated (Fig. 2.4). *Sox10* expression, which is seen in the lateral wall of the otocyst (Fig. 2.4C), was largely unaffected in *Tbx1* mutant embryos (Fig. 2.4D). *Pax2* and *Nkx5.1* show complementary expression patterns in the otic vesicle, *Pax2* labelling the ventro-medial wall and *Nkx5.1* labelling the latero-dorsal areas; these areas correspond to prospective cochlear and vestibular regions respectively (Rinkwitz-Brandt et al., 1996 and Fig. 2.4F,J). Expression of both markers appeared grossly unaffected in *Tbx1* mutant otic vesicles at E9.5 (Fig. 2.4E-L), except that the *Pax2* expression domain appeared weaker in caudal areas of the mutant vesicles (Fig. 2.4E,G). Typical dorsal markers, like *Dlx5* (Acampora et al., 1999; Depew et al., 1999) and *Gbx2* (Bouillet et al., 1995), also showed a normal distribution in *Tbx1* mutant otic vesicles at E9.5 (Fig. 2.4M-P).

It has been reported that expression of *NeuroD*, which marks a group of cells at the anterior part of the vesicle undergoing differentiation and delamination to contribute to the cvg (Liu et al., 2000), is affected in *Tbx1*$^{-/-}$ embryos at E10.0 (Raft et al., 2004). In contrast, at E9.0 we found a fairly normal distribution of *NeuroD* transcripts in the otocysts of *Tbx1* mutant embryos (Fig. 2.4Q,R). Similarly, *Lfng* transcripts, which mark some of the cvg neuroblasts and a subset of the primordial sensory organs in the ventral area of the otocysts (Morsli et al., 1998), and were affected by the *Tbx1* mutation at E10.0 (Raft et al., 2004), looked fairly normal in their distribution at earlier developmental stages (Fig. 2.4S,T). These results indicate that the early phases of otic placode/vesicle patterning and morphogenesis remain largely undisturbed in the absence of *Tbx1*.

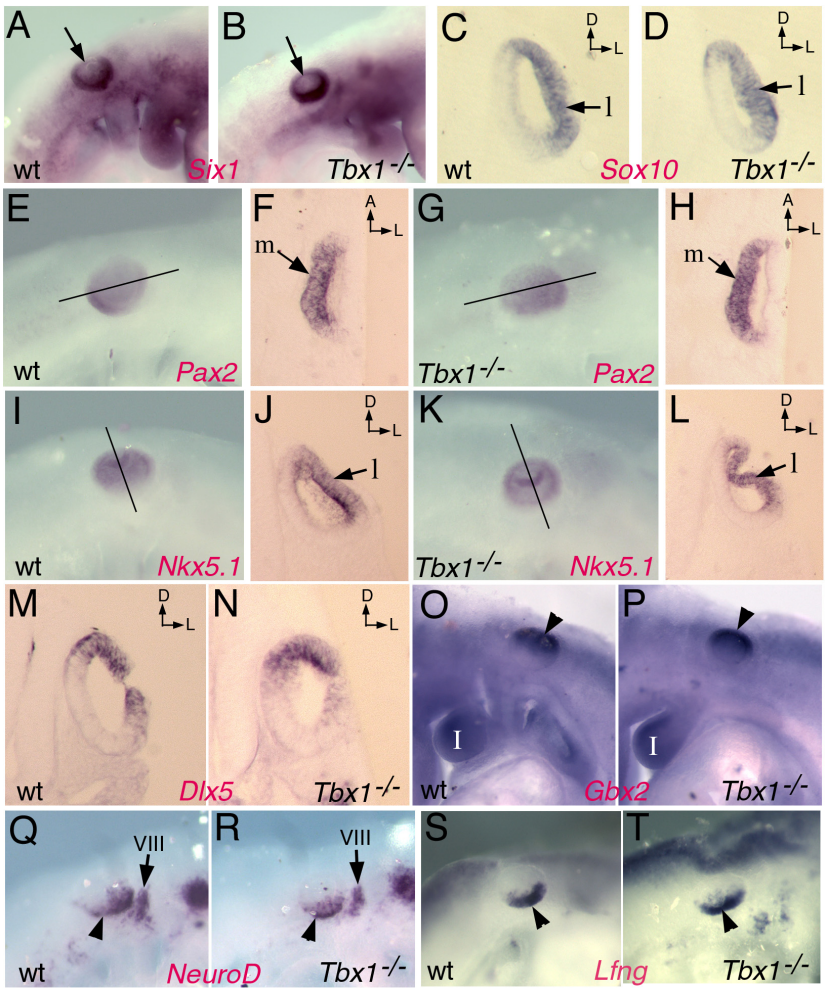

Figure 2.4 Analysis of otocyst patterning in *Tbx1*$^{-/-}$ embryos at E9.0-E9.5.
A,B: At E9.5 *Six1* expression in the otocysts (arrow) is not affected by the *Tbx1* mutation (B). **C,D:** *Sox10* is expressed in the lateral (l) wall of the otocyst both in wild-type (C) and *Tbx1*$^{-/-}$ embryos (D). **E,F:** In wild-type embryos, *Pax2* is expressed in the medial (m) wall of the otocyst. **F** shows a section through the area indicated in **E**. **G,H**: In *Tbx1*$^{-/-}$ embryos, *Pax2* expression is also restricted to the medial wall of the otocyst (m). **I,J:** In wild-type embryos, *Nkx5.1* is expressed in the dorsal and lateral (l) areas of the otocyst. **J** shows a section through the area indicated in **I**. **K,L**: In *Tbx1*$^{-/-}$ embryos, *Nkx5.1* expression is also restricted to the dorsal and lateral (l) areas of the otocyst. **M,N:** *Dlx5* expression is detected in the dorso-lateral areas of the otic vesicle both in wild-type (M) and in *Tbx1*$^{-/-}$ embryos (N). **O,P:** *Gbx2* expression is detected in the dorsal area of the otic vesicle (arrowhead) both in wild-type (O) and in *Tbx1*$^{-/-}$ embryos (P). **Q,R:** *NeuroD* expression is detected in the ventral area of the otic vesicle (arrowhead) and in the VIII cranial ganglion (VIII) both in wild-type (Q) and in Tbx1$^{-/-}$ embryos (R). **S,T:** *Lfng* expression is detected in

the ventral area of the otic vesicle (arrowhead) both in wild-type (S) and in *Tbx1*$^{-/-}$ embryos (T). (I) first branchial arch. All the pictures show stainings by *in situ* hybridization. The specimens are oriented with dorsal at the top of the figure, with the exception of F and H, where anterior is at the top. In all sections, medial is on the left. The whole mounted embryos are shown with the head to the right, except for O,P where the head is to the left.

Abnormal patterning in E10.5 *Tbx1* mutant otocysts

It has been shown that in *Tbx1*$^{-/-}$ embryos the spatial distributions of *NeuroD* and *Lfng*, which look seemingly normal at E9.0-E9.5, are both extended caudally in the otocysts at E10.0 relative to wild-type littermates (Raft et al., 2004). This indicates that, In contrast to what we observed at earlier stages, patterning of the otic vesicle could be affected at later stages, when clear morphological alterations were seen in *Tbx1* mutant embryos. To evaluate this possibility further, we looked at the spatial distribution of other molecular markers at E10.5. The distribution of some transcripts, like *Pax2*, which showed a normal spatial patterning at E9.5, displayed a strongly affected distribution in otocysts of E10.5 *Tbx1*$^{-/-}$ embryos. In normal embryos, its expression at this stage was restricted to specific areas within the medio-ventral regions of the otic vesicles, with a clear border in the anterior-posterior axis (Fig. 2.5A,B). In the mutant, expression was extended to other areas (Fig. 2.5C,D). Differential expression in the medio-lateral axis was lost, as was the anterior limit in the lateral domain, resulting in an extended expression throughout the whole circumference of the vesicle (Fig. 2.5D). Expression of *Sox10* in the otic vesicles was also affected in *Tbx1*$^{-/-}$. In wild-type E10.5 embryos, *Sox10* was detected in the lateral wall of the otic vesicle, with an anterior-posterior polarity, being excluded from antero-ventral areas (Fig. 2.5E), a pattern that resembles that of *Tbx1* (see below). In the *Tbx1* mutant, Sox10 expression was extended to more anterior areas of the otocyst lateral wall (Fig. 2.5F). The abnormalities in the expression of these two genes are interesting, in that they seem to follow a posterior-anterior extension, which is opposite to the anterior-posterior extension described for *NeuroD* (Raft et al., 2004). An extended expression domain at E10.5 was also observed for *Gbx2* in *Tbx1*$^{-/-}$ mutants. In this

case, transcripts seemed to extend across the dorsal border into the lateral wall of the otocyst (Fig. 2.5G,H). *Nkx5.1* expression in the otic vesicles was also slightly affected at E10.5 in *Tbx1*$^{-/-}$ embryos (Fig. 2.5I,L). In particular, while in wild-type embryos it was restricted to a localized area in the dorsal part of the lateral otic vesicle (Fig. 2.5J), in *Tbx1* mutants *Nkx5.1* expression lost intensity and seemed to extend ventrally in the lateral wall (Fig. 2.5L). These results indicate that at E10.5, in contrast to what was seen at E9.5, patterning of the otocyst was affected by the *Tbx1* mutation.

We also studied the distribution of *Bmp4* transcripts at E10.5 in *Tbx1* mutant otic vesicles. This was important because the sensory patches we found in the inner ears of *Tbx1* mutant embryos, displayed molecular characteristics compatible with their having originated in an area equivalent to the antero-lateral stripe of Bmp4-expressing cells that normally originate the cristae (Morsli et al., 1998). In wild-type embryos *Bmp4* was expressed in two areas, in the lateral and posterior walls of the otocyst (Fig. 2.5M,N). The posterior domain was downregulated in most (but not all) *Tbx1*$^{-/-}$ mutant embryos, whereas the lateral domain was still consistently identifiable (Fig. 2.5O,P). Its position in the mutant vesicles was different from that in the controls and clearly wider in the dorso-ventral axis than in wild-type embryos (compare Fig. 2.5N and P). These results indicate that *Bmp4* expression was induced in *Tbx1*$^{-/-}$ otocysts, but that like other molecular markers, its spatial distribution was not correctly maintained in the absence of *Tbx1*.

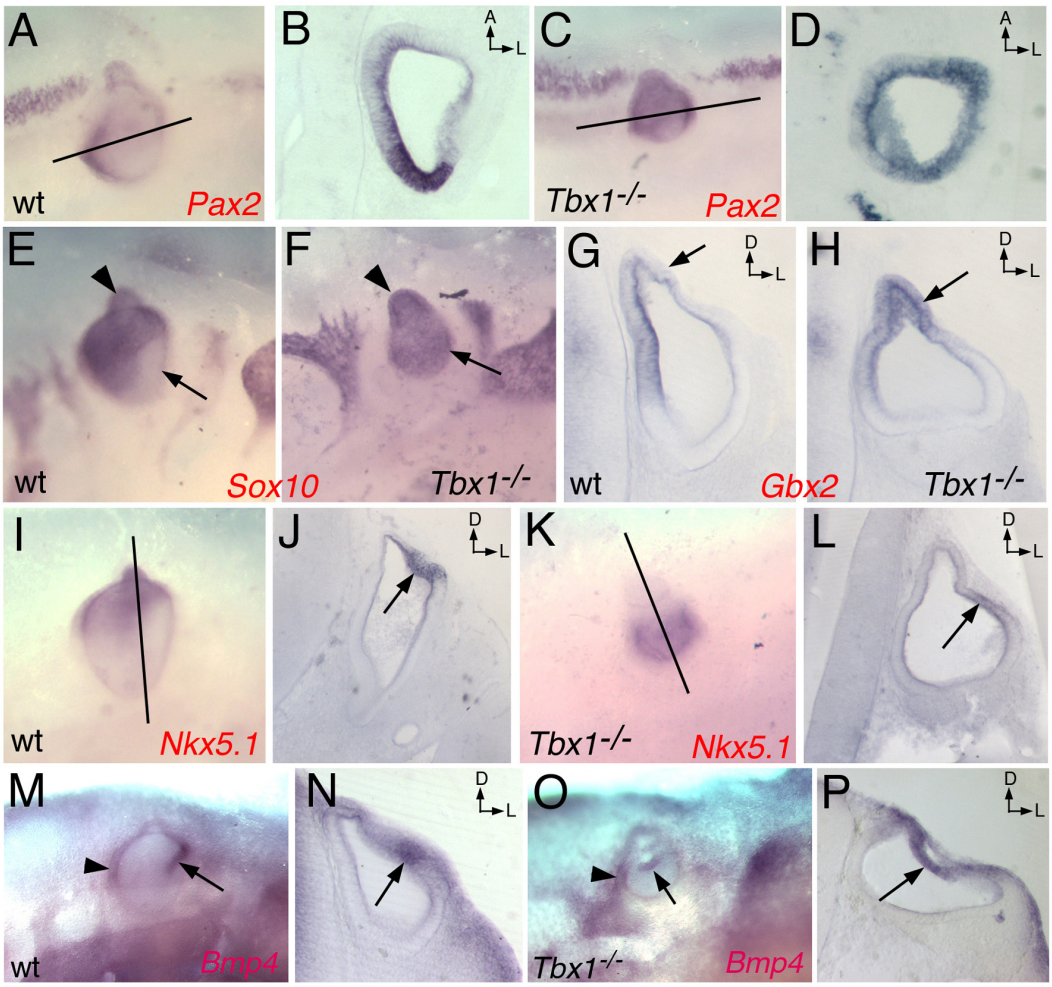

Figure 2.5 Analysis of otocyst patterning in *Tbx1*$^{-/-}$ embryos at E10.5.
A,B. In wild-type embryos *Pax2* is expressed in the ventro-medial and caudal areas of the otic vesicle. **B** shows a section through the plane indicated in A, oriented lateral on the right and anterior at the top. **C,D:** In *Tbx1*$^{-/-}$ embryos, *Pax2* expression is extended to a wider area of the otic vesicle, including the lateral and rostral walls. **D** shows a section through the plane indicated in C, oriented lateral on the right and anterior at the top. **E:** In wild-type embryos, *Sox10* is expressed in the lateral otocyst wall, and is excluded from its anterio-ventral area (arrow). The arrowhead indicates the developing endolymphatic duct. **F:** In *Tbx1*$^{-/-}$ embryos *Sox10* expression is extended to the whole lateral wall of the otocyst. The arrowhead indicates the enlarged developing endolymphatic duct. **G**: In wild-type embryos, *Gbx2* expression is detected in the dorsal half of the medial otocyst wall. **H:** In *Tbx1*$^{-/-}$ embryos *Gbx2* expression is extended through the dorsal tip into the dorsal part of the lateral otocyst wall (arrow). **I,J:** In wild-type embryos *Nkx5.1* is expressed in the lateral and dorsal areas of the otic vesicle. **J** shows a section through the plane indicated in I. **K,L:** In *Tbx1*$^{-/-}$ embryos, *Nkx5.1* expression is extended to a wider area of the lateral wall of the otocyst (arrow). **M,N**. In wild-type embryos, *Bmp4* expression in the otocyst is

localized in two domains, one in the posterior wall (arrowhead) and another in the lateral wall (arrow). **N** shows a section through the otocyst of the embryo shown in M. **O,P.** In *Tbx1*$^{-/-}$ embryos, *Bmp4* expression can still be detected in the posterior (arrowhead) and lateral (arrow) areas of the otocyst, although with a slightly different disposition and expanding over a wider area of the lateral wall of the otocyst (arrow in P). **P** shows a section through the otocyst of the embryo shown in O. The whole mount specimens are all shown with the head to the right and dorsal on top. All sections are all shown with lateral to the right and dorsal on top, except for panels B and D where anterior is at the top.

Expression of *Tbx1* in the ear compartments

In order to understand how *Tbx1* influences formation of the ear compartments, we analysed its expression in wild-type embryos in the branchial arches and otic vesicle. In the branchial area, this gene was expressed throughout the prechordal mesenchyme even before neural crest cells migrate into the arches (Chapman et al., 1996; Fig. 2.6A). Expression became more restricted to the mesodermal core of the arches at E9.5 (Chapman et al., 1996; Fig. 2.6C), and was then gradually downregulated in the first and second arches (Fig. 2.6F). In this area, *Tbx1* was not expressed in the neural crest-derived mesenchyme. In the otic epithelium, *Tbx1* expression could already be observed at E8.5 in the otic placode stage (Fig. 2.6B). Its expression in this structure was not uniform, appearing slightly stronger in the caudal half. At E9.5, *Tbx1* expression was very strong in the otocyst (Fig. 2.6C-E). It was restricted to the latero-posterior areas of the vesicle (Fig. 2.6D). Along the dorso-ventral axis, *Tbx1* expression was clearly detected in the dorsal areas, the most ventral domain of expression being devoid of *Tbx1* transcripts (Fig. 2.6E). At E10.5, expression of this gene was still detected in the lateral and posterior areas of the vesicle (Fig. 2.6F-H). In addition, a dorsal shift was now evident. The borders of *Tbx1* expression in the otic vesicle in the anterio-posterior and dorso-ventral axes were very sharp (Fig. 2.6G,H).

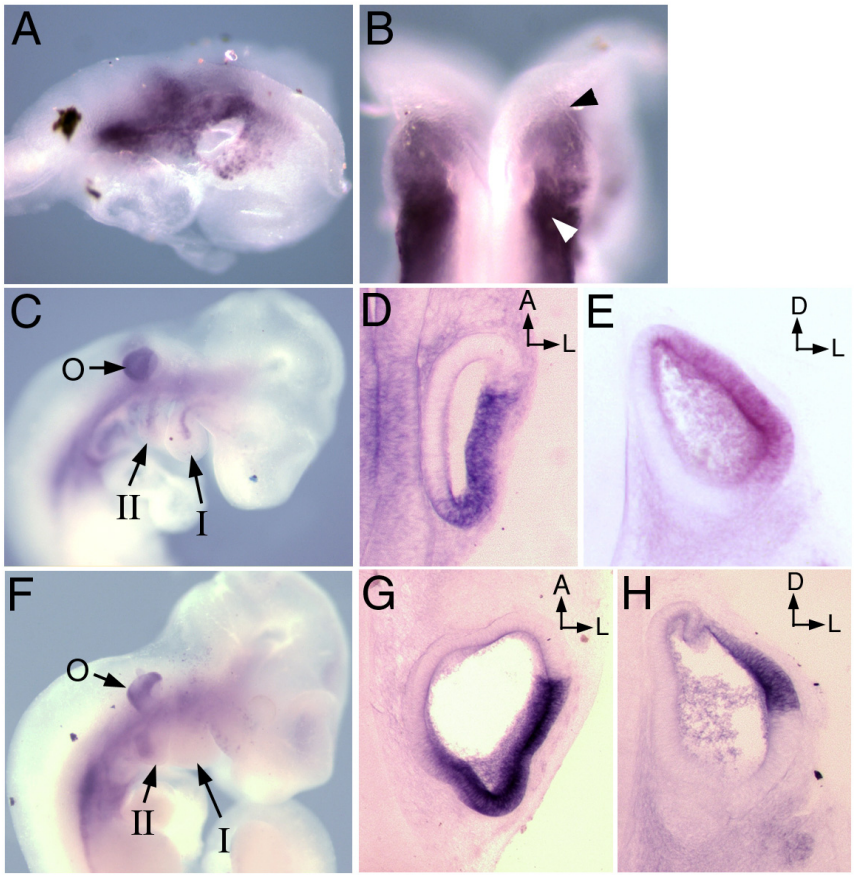

Figure 2.6 Expression of *Tbx1* during early development.
Expression was analysed by whole mount *in situ* hybridization on E8.5 (A,B), E9.5 (C-E) and E10.5 (F-H) embryos**. A:** At E8.5. *Tbx1* is expressed in the mesenchyme beneath the hindbrain and midbrain. **B:** In the otic placode, it is slightly more concentrated in caudal than in rostral areas. The picture shows a dorsal view of the embryo oriented with the anterior part to the top. The arrowheads indicate the rostral (black) and caudal (white) limits of the right placode. **C:** At E9.5, *Tbx1* expression is seen in the mesodermal core of the branchial arches and in the otic vesicle. **D:** Frontal section showing expression in the lateral and posterior areas of the otocyst**. E:** Transverse section showing expression in the lateral and dorsal areas of the otocyst. **F:** At E10.5, *Tbx1* expression is still seen in the mesodermal core of the second branchial arch (II), in the area of the third and fourth arches and in the otic vesicle (o). **G:** Frontal section showing expression in the lateral and posterior areas of the otocyst. The anterior border of expression in the lateral wall is very sharp. **H:** Transverse section showing expression in the lateral and dorsal areas of the otocyst. The ventral border of expression in the lateral wall is also sharp. In all sections, lateral is on the right. The frontal sections (D,G) are shown with anterior to the top. The transverse sections (E,H) are shown with dorsal to the top. I, first branchial arch.

DISCUSSION

In this study we showed that *Tbx1* is essential for development of the mammalian ear. Although all three ear compartments are affected in the *Tbx1*$^{-/-}$ mutants, the origin of the malformations seems not to be the same in all areas.

Middle ear development is affected in *Tbx1*$^{-/-}$ embryos

Development of various middle ear structures is compromised by the absence of *Tbx1* to different degrees. The most clearly affected part of the middle ear is the skeleton. As other branchial arch skeletal elements are also affected in the *Tbx1* mutants, it seems that the middle ear phenotype is the consequence of a more general patterning or morphogenetic defect in the branchial area. Interestingly, the residual elements seem to be able to direct coordinated morphogenesis similar to the wild-type structures. For instance, a normal-looking tympanic membrane is formed, which requires interactions between the tympanic ring, the ectoderm of the EAM and the pharyngeal endoderm (Mallo and Gridley, 1996; Mallo et al., 2000).

The skeletal elements of the branchial arches are neural crest-derived (Couly et al., 1993). Since *Tbx1* is expressed in the mesodermal component of the branchial arches and not in the neural crest-derived mesenchyme, the effect of this gene in the neural crest must be indirect. This interference is in keeping with a recent report indicating that *Tbx1* acts non-cell autonomously in the branchial area (Vitelli et al., 2003). It is possible that *Tbx1* is required for proper migration of the neural crest cells into the branchial arches. In the *Tbx1* mutants most of the neural crest cells originating caudal to r3 are not able to populate prospective second and more caudal branchial arches, which are missing or strongly hypoplastic in the mutant (Jerome and Papaioannou, 2001; Vitelli et al., 2002a; and this study). The absence of these branchial arches and of associated neural crest cells provides an explanation for the strong skeletal phenotypes observed in the derivatives from these areas. For the malleus, incus and tympanic ring, all first

arch derivatives (Mallo, 1998), a likely explanation for their phenotype in *Tbx1 mutants* is the misrouting of *Hoxa2*-positive cells into the first arch. *Hoxa2* is essential for determining the skeletal identity of second arch derivatives (Rijli et al., 1993; Gendron-Maguire et al., 1993) and misexpression of this gene in the first arch has been shown to produce strong hypoplastic phenotypes in the skeleton derived from this area (Mallo and Brandlin, 1997; Creuzet et al., 2002). Thus, the presence of *Hoxa2*-positive cells in the first arch of the *Tbx1* mutant may interfere with normal skeletal development in this arch.

The role of *Tbx1* in neural crest cell migration is still unclear. Two effects have been observed, an inability to migrate into the caudal arches and misrouting. Whether these two effects are related or result from independent mechanisms cannot be discerned from existing data. It has been postulated that segregation of cranial neural crest cell migratory pathways into distinct streams is controlled by some kind of molecular segmentation in the mesoderm adjacent to the hindbrain. The neural crest cell misrouting observed in *Tbx1* mutant embryos suggests that *Tbx1* may play a role in this mesodermal patterning. A variety of experimental data indicates that this mesodermal patterning is provided by signals from the adjacent neural tube and surface ectoderm (Farlie et al., 1999; Golding et al., 2002). As *Tbx1* is not expressed in the neuroectoderm or in the surface ectoderm, it is very probable that this gene plays a role in the mesodermal interpretation of these signals. The nature of the patterning signals is beginning to be elucidated (Golding et al., 2000) but nothing is yet known about the mesodermal component of this patterning interaction, making it difficult to test experimentally the role of *Tbx1* in this process. Recent data suggest that interference with FGF signalling may play a role in the genesis of this *Tbx1*$^{-/-}$ branchial arch phenotype. *Fgfr1* mutant embryos show defects in this area somewhat similar to those observed in the *Tbx1* mutant (Trokovic et al., 2003). In *Fgfr1*$^{-/-}$ embryos, the migration of neural crest cells into the second arch is also compromised. Interestingly, *Fgfr1* is not required in the neural crest, but rather in the branchial arch mesoderm. As expression of several Fgf genes seems to be downregulated in *Tbx1* mutant

embryos (Vitelli et al., 2002b) a possible scenario is that the branchial arch phenotype of these mutants results from the absence of Fgfr1 stimulation in the mesodermal component of the branchial arches. At least two Fgf genes have been reported to be down-regulated in the absence of *Tbx1*. One of them, *Fgf8*, is essential for the development of the branchial arches (Trumpp et al., 1999). However, *Fgf8* seems to be required for correct patterning and survival of postmigratory crest cells and not for their migration into the branchial arches (Trumpp et al., 1999; Bobola et al., 2003). In the case of *Fgf10*, also downregulated in *Tbx1*$^{-/-}$ embryos, no branchial arch phenotype was reported when it is inactivated (Min et al., 1998). This indicates that, if this molecule plays a role in mediating *Tbx1* activity, other molecules can substitute for it in this process. Further work will be required to determine the roles FGFs play as downstream mediators of *Tbx1* activity in the branchial arches, and to identify the still missing factors (FGFs or others) involved in this process.

Morphogenesis of the otocyst is impaired in *Tbx1*$^{-/-}$ embryos

The inner ears of *Tbx1* mutant embryos were reduced to a pair of small hollow cartilaginous vesicles without any structure that could be assigned to the cochlear or vestibular compartments. Quite surprisingly, however, some signs of morphological and histological differentiation were observed within these strongly affected structures. In particular, the endolymphatic duct was clearly discernible, displaying a normal histology, although it was larger than in wild-type littermates. Also, some areas clearly resembling sensory patches were present in the residual inner ear epithelium of the *Tbx1* mutant embryos. Although their morphological and molecular characteristics did not correspond exactly to any of the sensory patches present in normal inner ears, they contained hair cells and were even connected to the cochleo-vestibular ganglion (cvg), also present in the mutant embryos.

Global inner ear phenotypes were also found in *Six1* and *Eya1* mutants (Xu et al.,

1999; Laclef et al., 2003; Zheng et al., 2003; Ozaki et al., 2004). However, contrary to what has been described for those mutants, the *Tbx1* mutant phenotype seems not to derive from global effects on early proliferation and survival processes within the otocyst, because the patterns of apoptosis and cell proliferation were fairly normal in *Tbx1*$^{-/-}$ otocysts (Vitelli et al., 2003). Moreover, these global effects would not explain the conservation of specific inner ear characteristics in the *Tbx1* mutant. The global *Tbx1* mutant phenotype in the inner ear is also not directly obvious from the *Tbx1* expression pattern. In other mutants affecting inner ear development, the affected area typically mirrors the gene's expression domain (Torres et al., 1996; Hadrys et al., 1998; Ma et al., 1998; Torres and Giraldez, 1998; Wang et al., 1998; Acampora et al., 1999; Depew et al., 1999; Liu et al., 2000; Riley and Phillips, 2003). In the case of *Tbx1*, while its expression domain clearly overlaps with the prospective vestibular area, it is transcribed only in a rather small area of the cochlear anlage, thus making it difficult to justify the complete absence of this later structure in the *Tbx1* null mutants. Analysis of the inner ear phenotype at earlier developmental stages suggests a possible explanation for this apparent paradox. When analysed early enough, ear patterning and differentiation processes look fairly normal in *Tbx1*$^{-/-}$ embryos. This indicates that *Tbx1* plays no role in placode induction or in the early morphogenetic events to create a hollow vesicle from a flat epithelial thickening. Also, the establishment of early molecular patterns in the otocyst seems to occur normally in the absence of *Tbx1*, as estimated by the fairly normal distribution of a variety of relevant transcripts in the otic vesicles of E9.0-E9.5 *Tbx1* mutant embryos. It is only after E9.5 that clear morphological and molecular alterations can be observed in *Tbx1* mutant otocysts. The ventral area of the otocysts does not present the elongation that represents the initial cochlear anlage (Li et al., 1978), and show a round-shaped morphology. In addition, the primordium of the endolymphatic duct is still present but is clearly bigger in *Tbx1* mutant embryos than in their wild-type littermates. Also evident at this stage are alterations in the spatial distribution of transcripts for some relevant genes, which

are not restricted to a particular type of process, but seemed to affect the otic vesicle globally. For instance, in mutant otocysts *NeuroD* and *Lfng* expression domains extended posteriorly (Raft et al., 2004), *Pax2* expression extends anteriorly and laterally, the *Sox10* positive area is expanded anteriorly, *Gbx2* expression diffuses latero-ventrally and the *Bmp4* and *Nkx5.1* domains present a dorso-ventral broadening. It has been shown that, while initial patterns in the otocyst are established by signals provided by surrounding tissues (Baker and Bronner-Fraser, 2001), after certain stage otocysts seem to be largely independent of external cues (Swanson et al., 1990; Torres and Giraldez, 1998). As the pattern of *Tbx1* mutant otic vesicles changes from normal to altered, it is possible that *Tbx1* is required for the autonomous conservation of patterns after they have been generated by environmental signals. The highly regionalized expression of *Tbx1* and, most particularly, the sharp borders of its expression domain, which become stronger around E10.5, are nicely consistent with this hypothesis and suggest that control of cell segregation may be part of this mechanism.

A comparison of the early and late stages of inner ear formation in the *Tbx1* mutant reveals an interesting feature. There is a clear correlation between the conserved/lost features observed in the inner ears of newborns and the stage at which they start to be formed. The clearly conserved characteristics, namely the endolymphatic duct, sensory patches and cvg ganglion, represent very early differentiation processes in the otic primordium, which occur before alterations can be observed in *Tbx1* mutant otocysts. Conversely, morphologically organized cochlear and vestibular compartments, which are lost from *Tbx1* mutant animals, start formation later than E10.5, when the otocyst had already lost normal patterning references. This suggests that the strong global phenotypes in *Tbx1* inner ears derive from the inability of the otic vesicle to start morphogenetic processes, probably as a consequence of the lack of segregation of the gene regulatory information responsible for those processes. This hypothesis provides a likely explanation for the failure of structures that develop from an area mostly

negative for *Tbx1*, like the cochlea, to develop in the *Tbx1* null mutants.

An additional implication of the correlation between early and late phenotypic features of *Tbx1* mutant individuals is that the absence of *Tbx1* seems not to hinder progression of differentiation processes once they are started. The *NeuroD*-positive areas produce a cvg ganglion, the primordium of the endolymphatic duct develops further to produce a recognizable structure in the newborns, and the sensory patches observed in the newborns are likely derived from the expanded *Bmp4* lateral domain, as estimated by their molecular characteristics. Not only do these processes proceed further, they also seem to extend to include adjacent areas of the otocyst: already at E10.5, the neurogenic domain incorporates more caudal areas, as described by Raft et al. (2004); the endolymphatic duct enlarges, suggesting the incorporation of adjacent epithelium, and the *Bmp4* lateral domain broadens, indicating the expansion of the sensory anlage.

While we were preparing this manuscript, the inner ear phenotype of *Tbx1* mutants was analysed by other groups (Vitelli et al., 2003; Raft et al., 2004). According to Vitelli et al. (2003) *Tbx1* is required cell autonomously for the expansion of a subpopulation of cells in the otic vesicle required for development of both the cochlear and vestibular areas. However, they did not find differences in cell proliferation or survival in *Tbx1* mutant otocysts. Also, the vestibular and cochlear areas do not seem to derive from complementary areas of the otic vesicle, which are clearly segregated at E9.0 in *Tbx1* mutant embryos, and are under different genetic controls (Torres and Giraldez, 1998). In addition, *Tbx1* expression has only a very small overlap with the prospective cochlear domain (*Pax2*-positive). Therefore, either *Tbx1* has different transcriptional activities in different areas of the otocyst or it is involved in more general functions in the otic epithelium. Raft et al. (2004) propose that *Tbx1* restricts neuogenic potential within the otocyst. We also found an extension of the neurogenic area in the otic vesicles of *Tbx1* mutant embryos after E10.0, in agreement with their results. However, we also found broadening of other domains at the same stage of inner

ear development, which suggests to us that the effect of *Tbx1* on the restriction of the neurogenic area is part of the more global role of *Tbx1* in keeping normal patterns within the otic vesicle.

A mouse model for inner ear disfunction in DiGeorge syndrome patients?

It has been reported that some patients with the DiGeorge syndrome suffer from hearing and balance problems, some of which could be attributable to cochlear and vestibular dysfunction (Digilio et al., 1999; Swillen et al., 1999). As *Tbx1* plays an essential role in inner ear development, it is possible that partial loss of *Tbx1* function could indeed perturb ear development in DiGeorge syndrome patients and be the cause of these clinical manifestations. In mice, inner ear phenotypes associated with *Tbx1* haploinsufficiency have not been reported. It is possible that, like the vascular phenotype in *Tbx1*$^{+/-}$ mice (Jerome and Papaioannou, 2001; Lindsay and Baldini, 2001; Merscher et al., 2001), the extent of expressivity of an ear phenotype in the presence of only one copy of the *Tbx1* gene is also strain-dependent. Therefore, it would be important to introduce the *Tbx1* mutation into different genetic backgrounds and observe the effects on cochlear and vestibular function. Interestingly, hearing and balance deficiencies were observed in mice carrying a transgenic BAC containing the human *TBX1* gene, but only when the mice had a mixed B6/FVB background and not after three generations of backcrossing into C57BL/6 (Funke et al., 2001). This suggests that the FVB strain may be more sensitive to alterations in the *Tbx1* dosage and could be the strain of choice when trying to obtain *Tbx1* haploinsufficient phenotypes in the ear. The existence of such a mouse would provide a useful animal model for the ear defects observed in human DiGeorge syndrome patients.

ACKNOWLEDGEMENTS

We thank E. Bober, T. Gridley, P. Gruss, B. Hogan, A. Kispert, J. Lee, A. P. McMahon, A. Simeone and M. Wegner for kindly sharing cDNA probes with us, and M. Carapuço, F. Giráldez, A. Jacinto, D. Pimentel, J. Rodríguez-León and R. Cassada for useful discussions. This work was supported by FCT/FEDER grant POCTI/MGI/43466/2001 to MM and NIH grant DH33082 to VEP.

Chapter 3:

Bmp2 is required for migration but not for induction of neural crest cells in the mouse

Developmental Dynamics **236**, 2493-501
(2007)

Bmp2 is required for migration but not for induction of neural crest cells in the mouse

Ana Catarina Correia[1] Marta Costa[1] Filipa Moraes[1] Joana Bom, Ana Nóvoa, and Moisés Mallo*

Instituto Gulbenkian de Ciência, Oeiras, Portugal

(1) A. C. Correia, M. Costa, and F. Moraes contributed equally to this work.

CC, MC, FM and MM performed experiments and analysed data. FM made the construct and JB carried out the pronuclear injection to produce *HtPA-RFP* transgenic mouse line. JB and AN gave technical support. MM conceived and directed the project and wrote the published manuscript.

ABSTRACT

Bone morphogenetic protein (BMP) signalling is essential for neural crest development in several vertebrates. Genetic experiments in the mouse have shown that *Bmp2* is essential for the genesis of migratory neural crest cells. Using several markers and a transgenic reporter approach, we now show that neural crest cells are induced in *Bmp2* null mutant embryos, but that these cells fail to migrate out of the neural tube. The absence of migratory neural crest cells in these mutants is not due to their elimination by cell death. The neuroectoderm of *Bmp2*$^{-/-}$ embryos fail to close and create abnormal folds both along the anterior–posterior and medio–lateral axes, which are associated with an apparent medio–lateral expansion of the neural tube. Finally, our data suggest that the molecular cascade downstream of BMP signalling in early neural crest development may be different in mouse and avian embryos.

INTRODUCTION

The neural crest is a group of migratory cells induced at the dorsal tip of the neural tube as a consequence of interactions between the neural and non-neural ectoderm (Barembaum and Bronner-Fraser, 2005). After induction, these cells undergo an epithelial to mesenchymal transition, delaminate from the neuroectoderm and migrate profusely to populate a wide variety of embryonic structures, where they contribute to many different tissues (Le Douarin and Kalcheim, 1999). During the past years, considerable effort has been directed toward understanding the different aspects of neural crest biology, including its induction and delamination from the neuroectoderm, the control of the migratory properties, and the mechanisms of differentiation into specific tissues (Le Douarin and Dupin, 2003; Meulemans and Bronner-Fraser, 2004; Morales et al., 2005). The emerging picture is quite complex and is further complicated by the apparent differences among different model organisms (Aybar and Mayor, 2002). While

many experimental analyses have been performed in chicken, zebrafish, and *Xenopus* embryos, information relating to the early processes of neural crest biology in the mouse is scarce and it is not clear if the mechanisms that are thought to be relevant in other species also apply to mammals. An additional level of difficulty is that often a function that has been associated to a specific member of a gene family in the chicken is performed by a different member of the family in the mouse. For instance, based on expression analyses, it has been suggested that the function of *Snail2* (previously known as *Slug*) in the chicken neural crest is performed by *Snail1* in the mouse (Sefton et al., 1998). However, when this idea was challenged using genetic tools, the results were surprising as they indicated that neither *Snail1* nor *Snail2* seemed to be involved in neural crest production in the mouse (Murray and Gridley, 2006). This finding suggests that some of the mechanisms of neural crest development are not conserved among vertebrates.

The bone morphogenetic proteins (BMPs) were among the first factors implicated in the earliest processes of neural crest cell development. Early experiments performed in chicken embryos suggested that BMP4 and BMP7 were implicated in neural crest cell induction (Liem et al., 1995). This view was challenged by later results, which showed that the ability of these factors to induce neural crest cells *in vitro* depends on the concomitant activity of other still not identified factors present in the serum of the culture medium (Garcia-Castro et al., 2002). A different set of studies performed in chicken embryos suggested that BMPs are required for the migration rather than the induction of neural crest (Sela-Donenfeld and Kalcheim, 1999). In addition, it has been proposed that BMP activity is further modulated by noggin and that the graded inactivation of the expression of this gene controls the onset of neural crest migration (Sela-Donenfeld and Kalcheim, 1999). The molecular mechanisms that mediate BMP signalling in neural crest cell delamination have also been studied. In the initial studies, it was proposed that BMP activity was mediated by induction of *Cad6B* and the GTPase RhoB (Sela-Donenfeld and Kalcheim, 1999). Recent data

implicate BMP signalling in modulating progression through the cell cycle, an effect that could be mediated, at least in part, by Wnt1 (Burstyn-Cohen et al., 2004). It has also been proposed that the activity of BMP signalling is mediated by the cleavage of N-cadherin into a soluble cytoplasmic form, which would participate, together with the canonical Wnt pathway, in the control of neural crest cell emigration (Shoval et al., 2007).

In the mouse, a variety of genetic studies indicate that BMP signalling is essential at different stages of neural crest development. *Bmp5* and *Bmp7* have been reported to be required in a partially redundant manner for the survival of postmigratory crest cells, as demonstrated by their increased death in *Bmp5;Bmp7* double mutant embryos (Solloway and Robertson, 1999). In addition, *Bmp2* is essential for the formation of migratory neural crest cells (Kanzler et al., 2000; Ohnemus et al., 2002). Expression analyses in the mouse indicate that *Bmp2* is expressed in the surface ectoderm adjacent to the neuroectoderm with a spatiotemporal dynamics that correlates with neural crest cell production (Kanzler et al., 2000). Blocking *Bmp2* signalling *in vivo* in the dorsal neural tube through expression of noggin in transgenic mice, resulted in the absence of migratory neural crest cells and in the lack of the corresponding derivatives (Kanzler et al., 2000; Ohnemus et al., 2002). In addition, preliminary analysis of *Bmp2* mutant embryos failed to detect the streams of *Crabp1* reactivity associated with the hindbrain characteristic of neural crest cells, which was correlated with an absence of branchial arches (Kanzler et al., 2000). What is not clear from these studies is whether *Bmp2* is required for the induction of neural crest cells or for their delamination/migration from the neural tube. In this study, we show that neural crest cells are induced in the *Bmp2* mutants. We also show that the absence of migratory neural crest cells in these mutants does not derive from increased death of the premigratory neural crest cells, and thus it is probable that *Bmp2* is required for triggering migration of these progenitors. The absence of migration of these cells seems to result in an extra accumulation of cells in the neuroepithelium, which produces abnormal foldings in the anterior–posterior and

medial–lateral axes. Our results also suggest that, although BMP signalling is required for neural crest cell migration in chicken and mouse embryos, the molecular mediators may differ among vertebrates.

MATERIAL AND METHODS

Mice

The *Bmp2* mutant mice were described previously (Zhang and Bradley, 1996). To generate the *HtPA-RFP* transgenic mice, the *RFP* cDNA was cloned downstream of the *HtPA* enhancer that drives expression in the neural crest (Pietri, et al, 2003). The SV40 polyadenylation signal was cloned downstream of the *RFP* cDNA. The purified construct was used to generate transgenic mice by pronuclear injection according to standard protocols. The *HtPA-RFP* transgenic animals and embryos were identified by polymerase chain reaction (PCR) using the primers 5'-TCCGAGGACGTCATCAGGGAG-3' and 5'-ATGGTGTAGTCCTCGTTGTGG-3'.

In situ Hybridization and Apoptosis

In situ hybridization was performed as previously described (Kanzler et al., 1998). At least three embryos for each genotype were analysed per probe. The probes used were *Ap2*α (Mitchell et al., 1991), *Snail1* (Sefton et al., 1998), *Cad6B* (Inoue et al., 1997), *Wnt1* (Wilkinson et al., 1987), *En2* (Joyner and Martin, 1987), and *Otx2* (Simeone et al., 1992). The *Hoxb1* probe was obtained as a 1.1-kb fragment containing the whole open reading frame by reverse transcriptase-PCR, cloned into the *EcoRI* and *BamHI* sites of pKS Bluescript. The probe for *Id2* was obtained from IMAGE clone 6515664. Stained embryos were embedded in gelatin/sucrose, sectioned to 30 μm with a Vibratome and photographed under Nomarski optics.
Apoptosis was determined by TUNEL as described in Kanzler et al. (2000) except for the use of an alkaline phosphatase-conjugated instead of horseradish peroxidase-conjugated antifluorescein antibody and subsequent detection of the

activity with NBT and BCIP (nitroblue tetrazolium/5-bromo-4-chloro-3-indolyl phosphate) as performed in the *in situ* hybridization protocol. The RFP fluorescence was acquired by confocal microscopy using a Leica TCS SP2 system, and Z-projections of the confocal stacks were processed and colored using Imaris (v5.0.3) and ImageJ (v1.37).

RESULTS

As reported earlier, *Bmp2* mutant embryos do not survive past embryonic day (E) 9.0, which hampers analysis of the formation of neural crest derivatives (Zhang and Bradley, 1996; Kanzler et al., 2000). However, living embryos can be recovered at this stage, thus allowing analysis of early stages of neural crest cell development. A morphological analysis of these "late" *Bmp2* mutants showed several malformations, in addition to those previously reported (Zhang and Bradley, 1996). In particular, the rostral neural tube always failed to close and displayed abnormal foldings both in the anterior–posterior and medial–lateral axes, without a fixed pattern (Fig. 3.1). In addition, the surface of the neural tube seemed extended medial–laterally in the mutant embryos when compared with their wild-type littermates. As the neural tube fails to close, there are no real dorsal and ventral domains, but rather medial and lateral areas in the neuroectoderm, which is the nomenclature that we will use throughout the text.

Neural crest cells are induced in the absence of *Bmp2*

Previous work indicated that *Bmp2* mutant mice have no migratory neural crest cells, but whether this deficiency resulted from a lack of neural crest cell induction or from the inability of these cells to migrate from the neural tube was not investigated (Kanzler et al., 2000). To answer this question, we characterized early events of neural crest biology in *Bmp2* mutant mice. *Ap2*α is a neural crest marker in the mouse (Mitchell et al., 1991) that can be detected in the premigratory neural crest cells at the dorsal tip of the neural tube and in the

migratory neural crest cells, most particularly in the cranial area (Fig. 3.1A,B). Examination of *Ap2*α expression in *Bmp2* mutant embryos revealed no obvious streams of migratory neural crest cells, confirming that no migratory neural crest cells are produced in the absence of *Bmp2* (Fig. 3.1C,D). However, *Bmp2* mutant embryos showed a clear *Ap2*α signal associated with the lateral border of the neural folds. Interestingly, the spatial distribution of the *Ap2*α transcripts in this area along the rostral–caudal axis was very similar to that observed in wild-type embryos, as it combined areas of strong and weak expression, the latter corresponding in wild-type embryos to rhombomeres (r) 3 and 5 (Fig. 3.1A,C).

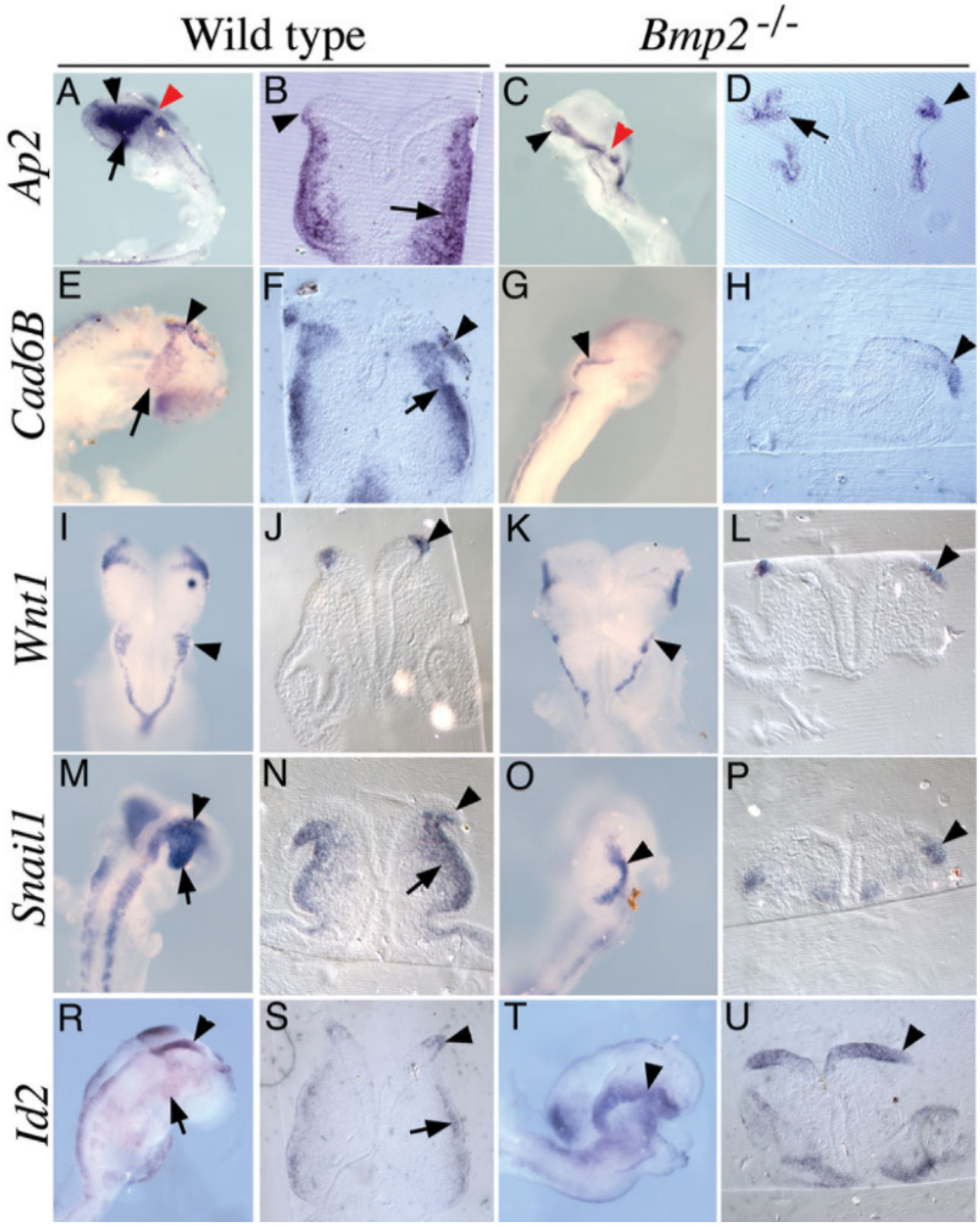

Figure 3.1 Neural crest cell production in *Bmp2*$^{-/-}$ embryos.
Wild-type (A,B,E,F,I,J,M,N,R,S) and *Bmp2* mutant (C,D,G,H,K,L,O,P,T,U) embryos were analysed by whole-mount *in situ* hybridization using probes for *Ap2*α (A–D), *Cad6B* (E–H), *Wnt1* (I–L), *Snail1* (M–P), and *Id2* (R–U). The black arrowheads indicate the dorsal (lateral) edges of the neural tube, the black arrows indicate the migratory neural crest cells, and the red arrowheads in A and C indicate areas of the hindbrain poor in neural crest cell production

Analysis of sections of these embryos confirmed that *Ap2α* expression in *Bmp2* mutant embryos, is indeed associated with the dorsal part of the neural tube (Fig. 3.1D). A careful analysis of the sections revealed that the expression in this area expands medially farther than in wild-type embryos. Indeed, in wild-type embryos, very few cells in the dorsal neural tube were positive for *Ap2α*, possibly as a result of the migration of cells when expression of this transcription factor is activated. In *Bmp2* mutant embryos, *Ap2α* expression was clearly localized to the lateral borders of the neuroectoderm, which could represent an accumulation of induced neural crest cells. In addition, examination of serial sections covering the whole anterior–posterior axis revealed some *Ap2α*-positive cells in the mesenchyme adjacent to the neuroectoderm–surface ectoderm interface. These patches of cells were very rare and involved just a few cells (the picture in the embryo shown in Fig. 3.1D is the best image observed in that particular embryo). This finding suggests that, while the production of migratory neural crest cells is very reduced, some cells do manage to start migration. These results suggest that neural crest cells are induced but fail to migrate in the absence of *Bmp2*.

In chicken embryos, early neural crest biology has been extensively characterized and the role that BMP signalling plays in this process has been addressed by several groups (Selleck et al., 1998; Burstyn-Cohen et al., 2004; Shoval et al., 2007). In those studies, several genes have been reported to be downstream of the BMP signalling pathway during early stages of neural crest cell biology (Burstyn-Cohen et al., 2004). Among these, *Cad6B* and *Wnt1* are also neural crest cell markers in the mouse. As in chicken embryos, *Cad6B* is expressed in the premigratory neural crest of the mouse. However, contrary to what has been reported in chicken (Taneyhill et al., 2007), mouse migratory neural crest is also positive for *Cad6B*, at least in the cranial region (Fig. 3.1E,F). In *Bmp2* mutant embryos, *Cad6B* expression was readily detected in the lateral edges of the neuroectoderm (Fig. 3.1G,H). However, it could not be detected in the domain

where migratory neural crest should be present, further supporting the inference of the absence of this cell population. The other potential BMP target in the neural crest, *Wnt1*, shows an equivalent expression pattern in chicken and mouse embryos, being restricted to the dorsal neural tube but absent from the migratory neural crest population (Wilkinson et al., 1987; Bally-Cuif et al., 1992; Fig. 3.1I,J). In the mouse, a variety of cell tracing and mutagenesis experiments indicates that, while migratory neural crest cells do not contain transcripts for *Wnt1*, the premigratory neural crest cells are included within the expression domain of this gene in the dorsal neural tube (Echelard et al., 1994; Jiang et al., 2000). In *Bmp2* mutant embryos, the expression domain of *Wnt1* in the lateral borders of the neuroectoderm was largely unaffected, including its spatial distribution along the anterior– posterior axis (Fig. 3.1K,L). These results indicate that, contrary to what has been reported for the chicken system (Burstyn-Cohen et al., 2004), in the mouse neither *Cad6B* nor *Wnt1* activity seems to be downstream of BMP signalling in early neural crest biology, at least relating to activity that is dependent on *Bmp2*.

The Snail gene family has been implicated in the delamination of neural crest cells in chicken and *Xenopus* embryos (Nieto et al., 1994; Aybar et al., 2003) and, while some reports consider these genes BMP-independent (Burstyn-Cohen et al., 2004), others place them downstream of BMP signalling (Selleck et al., 1998). In the mouse, *Snail1*, instead of *Snail2*, has been reported to be associated with the neural crest (Sefton et al., 1998). In wild-type embryos, expression of this gene is turned on in cells delaminating from the dorsal neural tube. At least in our hands, it is rarely observed in the premigratory neural crest cells (Fig. 3.1N), probably because of the immediate delamination of the *Snail1*-positive neural crest cells, but gives a strong signal in the streams of migratory neural crest cells (Fig. 3.1M,N). In *Bmp2* mutant embryos, no *Snail1* expression was observed in the mesenchyme adjacent to the cranial neural tube, which is consistent with the absence of migratory neural crest cells (Fig. 3.1O,P). However, a clear signal was observed adjacent to the lateral tip of the neural folds, which is also consistent

with the presence of neural crest cell progenitors that failed to migrate away of the neural tube. Analysis of sections revealed that, in addition to this signal, cells in the lateral tip of the neuroectoderm are often positive for *Snail1* (Fig. 3.1P), a signal that, as mentioned above, was not observed in wild-type embryos (Fig. 3.1O). This result is also consistent with the existence of neural crest progenitors in *Bmp2* mutant embryos, lending further support for a role for *Bmp2* in neural crest migration, rather than induction, in the mouse. Also, these results indicate that expression of the Snail family genes in the neural crest is independent of *Bmp2* signalling.

The Id family genes have also been reported to be downstream of the BMP pathway (Hollnagel et al., 1999) and to play a role in neural crest formation, at least in chicken and *Xenopus* embryos (Kee and Bronner-Fraser, 2005; Martinsen and Bronner-Fraser, 1998). Of the four Id genes that exist in mice, we present only data from the one that seemed to give the clearest expression pattern in the neural crest, the *Id2*. From stages E8.0-E9.0 its expression was detected in the lateral edges of the neuroectoderm and also in the migratory neural crest cells, being stronger in the mesencephalic crest domain (Fig. 3.1R,S). This pattern of expression is compatible with the dynamics of neural crest cell production, although the levels of *Id2* expression in migratory neural crest cells were always very reduced and disappeared after E9.0 (Fig. 3.1R,S). In *Bmp2* mutant embryos, *Id2* expression in the lateral neural folds was very strong, indicating that, at least in this area, *Id2* expression is not under the positive control of *Bmp2*. Actually, in all *Bmp2* mutant embryos analysed (n = 3), expression of *Id2* extended medially to a considerable degree (Fig. 3.1T,U). Nevertheless, if *Id2* also labels the premigratory neural crest population in mouse embryos, the expression of this gene in the *Bmp2* mutant embryos is also consistent with the conclusion that production of neural crest cells is not affected by the absence of *Bmp2*.

To further analyse whether neural crest cells are formed in the absence of *Bmp2*, we used a transgenic approach. It has been described that the *HtPA* gene contains an enhancer that labels specifically the neural crest cells (Pietri et al.,

2003). We used this enhancer to express the *RFP* gene in transgenic mice *(HtPA:RFP mice)*, thus labelling the neural crest cells with red fluorescent protein (RFP). Analysis of transgenic embryos revealed RFP fluorescence in migratory neural crest cells in the cranial region (Fig. 3.2A). In keeping with previous reports, only a few RFP-positive premigratory neural crest cells were observed, arguably because these cells delaminate shortly after activation of the enhancer (Pietri et al., 2003). In the *Bmp2* mutant, background *RFP*-positive cells were also readily detected but remained mostly associated with the dorsal neural tube (Fig. 3.2B). It is possible that a few *RFP*-positive cells were located in the adjacent mesenchyme rather than in the neuroepithelium, which could indicate the existence of a residual migratory ability of the neural crest cells in the absence of *Bmp2*. These results are consistent with the data obtained with molecular markers and further support the conclusion that *Bmp2* does not have an effect on neural crest cell production.

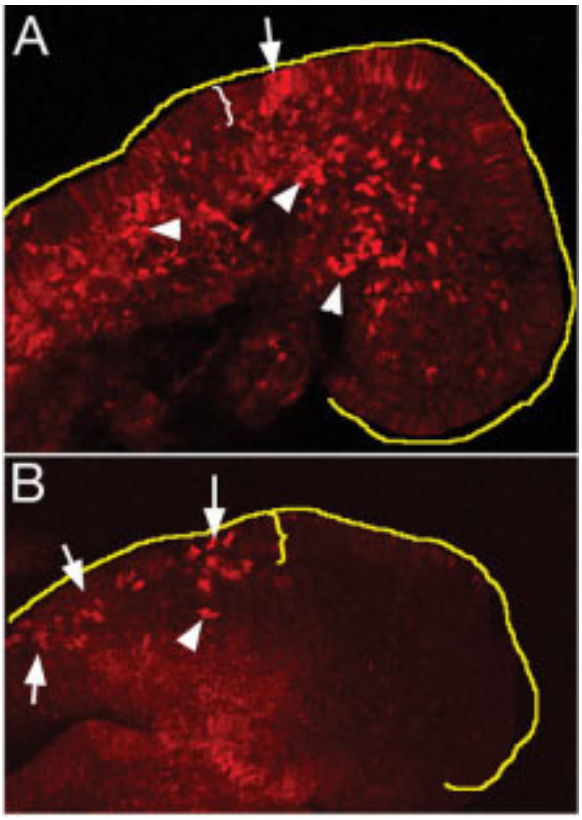

Figure 3.2 Transgenic analysis of neural crest cell production in *Bmp2*$^{-/-}$ embryos.
A,B: *HtPA-RFP* transgenic animals were analysed for red fluorescent protein (RFP) expression in the wild type (A) and *Bmp2*$^{-/-}$ background (B). The yellow line outlines the dorsal part of the head of a wild-type embryo (A) and the lateral border of the head of a *Bmp2*$^{-/-}$ embryo (B). The arrows show some cells that did not leave the neural tube, and the arrowheads, migratory neural crest cells. The brackets show the area where labeled cells are in the neuroectoderm.

Apoptosis in the neural tube of *Bmp2* mutant embryos

To understand whether the absence of migratory neural crest cells in *Bmp2* mutant embryos resulted from the death of the induced progenitors, we performed terminal deoxynucleotidyl transferase–mediated deoxyuridinetriphosphate nick end-Labelling (TUNEL) assays. At E8.5, some TUNEL-positive cells were observed in the dorsal neural tube, with a focal concentration of apoptotic cells in the anterior hindbrain (Fig. 3.3A,B). Considerable cell death was also evident in the forebrain region. In *Bmp2* mutant embryos, no obvious increase of TUNEL-

positive cells was detected associated with the lateral borders of the neural tube (Fig. 3.3C,D), indicating that increased cell death is probably not responsible for the absence of migratory neural crest cells. It should be noted that, in these embryos, focal areas of TUNEL-positive cells were observed in the most anterior part of the neuroepithelium, which corresponds to the forebrain region. In addition, an extra area of increased cell death was observed in *Bmp2* mutant embryos in the region that would correspond to the anterior hindbrain–posterior mesencephalon (Fig. 3.3D), an area where we never observed cell death in control littermates (Fig. 3.3B). The possible relevance of this observation will be discussed later.

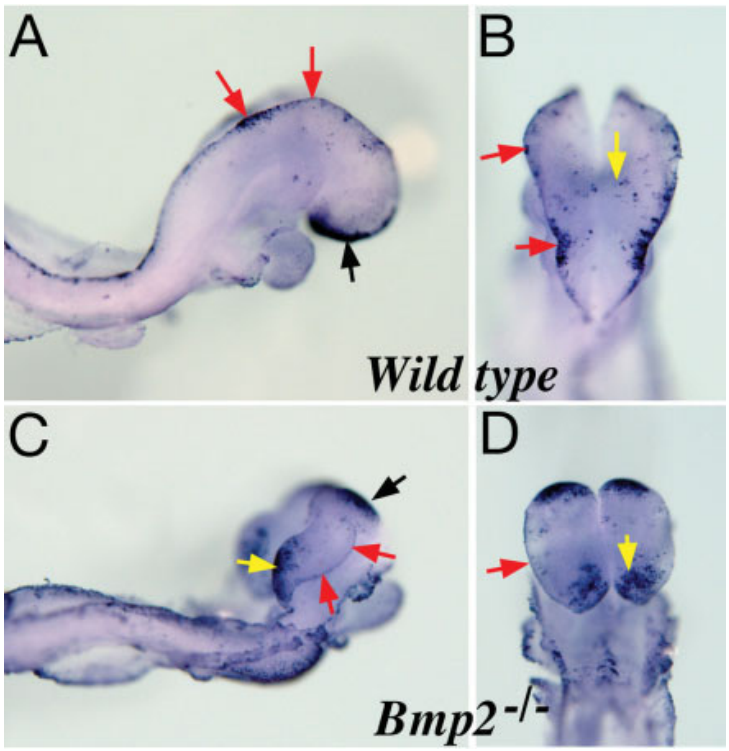

Figure 3.3 TUNEL analysis of *Bmp2*$^{-/-}$ embryos.
A–D: The analysis was performed on E8.5 wild-type (A,B) and *Bmp2*$^{-/-}$ mutant (**C,D**) embryos. The red arrows indicate different areas of the dorsal (lateral) neural tube, which is where the neural crest cells are produced. The black arrows indicate areas of strong cell death in the forebrain. The yellow arrows indicate areas of the neural tube showing increased apoptosis in mutant embryos compared with wild-type littermates.

Anterior–Posterior patterning in the neural tube of *Bmp2* mutant mice

When we analysed expression of *Wnt1* in *Bmp2* mutant embryos, we observed that, while expression in the dorsal tip of the neural tube was not compromised, expression in the midbrain–hindbrain boundary could not be detected (Fig. 3.1K). As the neuroectoderm in the *Bmp2* mutant embryos is abnormally folded, the absence of *Wnt1* expression in this area could indicate abnormal anterior–posterior patterning of the neural tube in *Bmp2* mutant embryos. Therefore, we analysed expression of a few molecular markers for specific areas of the neural tube in *Bmp2* mutant embryos. Engrailed genes are specifically expressed in the midbrain, next to the midbrain–hindbrain boundary, in an area adjacent to the Wnt1 expression domain (Fig. 3.4A; Joyner and Martin, 1987). *En2* was expressed in equivalent patterns in control embryos and the *Bmp2* mutants (Fig. 3.4B), indicating that the midbrain–hindbrain border was not globally disturbed. Importantly, the *En2* domain was restricted to a specific area of the neural tube and did not extend its most anterior border, suggesting that this area was also correctly patterned. We confirmed this finding with the analysis of *Otx2* expression, which is detected in the forebrain and midbrain down to the border with the hindbrain (Fig. 3.4C,D; Simeone et al., 1992). In addition, the hindbrain also seemed to keep a normal anterior–posterior pattern, as indicated by the restricted expression of hindbrain markers like *Hoxb1*, which is expressed in r4 (Fig. 3.4E,F; Frohman et al.,1990) results indicate that, globally, the neuroectoderm of the *Bmp2* mutant embryos is correctly patterned along the anterior posterior axis, although expression of specific markers, most particularly *Wnt1*, seemed affected.

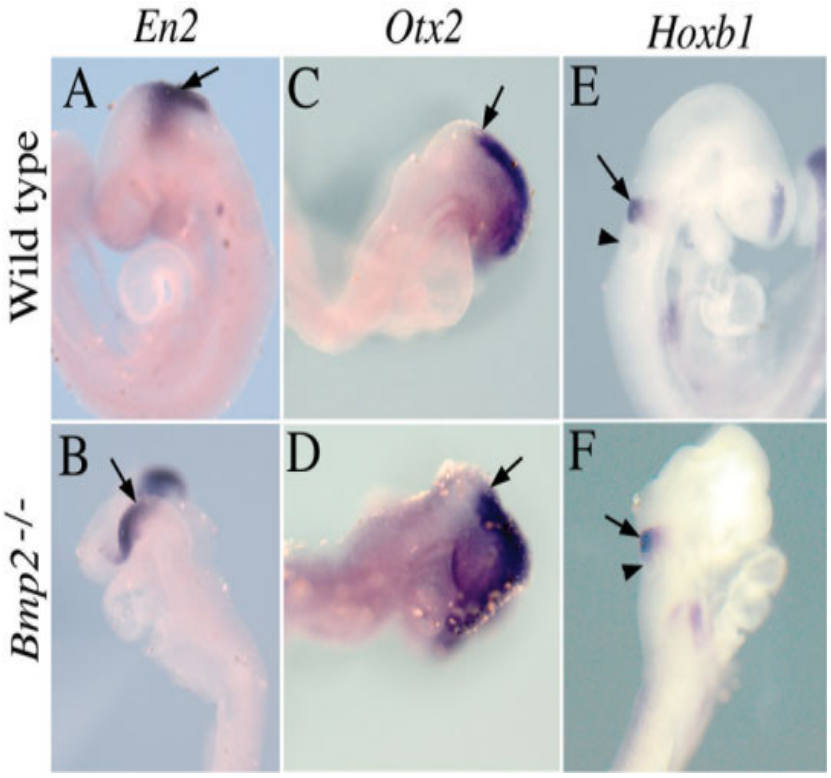

Figure 3.4 Analysis of anterior–posterior patterning in the neural tube of *Bmp2* mutant embryos.
A–F: Wild-type (**A,C,E**) and *Bmp2*$^{-/-}$ embryos (**B,D,F**) were analysed by whole-mount *in situ* hybridization using *En2* (**A,B**), *Otx2* (**C,D**), and *Hoxb1* (**E,F**). The arrows in A and B indicate the domain of *En2* expression, in C and D the posterior limit of *Otx2* expression, and in E and F the domain of *Hoxb1* expression. The arrowheads in E and F indicate the otic vesicle.

DISCUSSION

In this manuscript, we showed that, in the mouse, *Bmp2* is not required for the induction of neural crest cells, but it is essential for their migration from the neural tube. It is clear that migratory neural crest production is strongly compromised in the absence of *Bmp2*, which is in keeping with our previous data using biochemical blockage of BMP signalling in transgenic embryos (Kanzler et al., 2000; Ohnemus et al., 2002). However, all tests for neural crest cell induction, either using a variety of molecular markers or a transgenic approach, turned out positive in the *Bmp2* mutant embryos, indicating that *Bmp2* is not essential for the induction of this cell population, but rather for its migration from the neural tube. Interestingly, with the limitations inherent to the abnormal neural tube morphology of *Bmp2* mutant embryos, the spatial distribution of transcripts for the neural crest cell markers along the anterior–posterior axis was very similar to that observed in wild-type embryos. Thus, there were areas of strong expression, which corresponded to the neural crest-producing domains, and areas with very little or no expression, which corresponded to the neural crest-free areas of the hindbrain (Lumsden et al., 1991). This finding suggests that not only neural crest cell induction occurs in the absence of *Bmp2*, but also that the basic mechanisms are still in place in *Bmp2* mutant embryos. It should be noted that we cannot rule out that specific subsets of neural crest cells fail to be induced in *Bmp2* mutant embryos. The absence of migratory neural crest cells seems not to be a consequence of increased cell death, as no increase in TUNEL-positive cells was detected associated with the lateral borders of the neuroectoderm in *Bmp2* null mutant embryos. It is still possible that the elimination of migratory cells occurs at a rate below the levels of detection of our assay. However, apoptotic cells were readily detected in embryos carrying mutations in other genes essential for survival of postmigratory neural crest cells (Solloway and Robertson, 1999; Trumpp et al., 1999). Therefore, given the large numbers of neural crest cells

produced during the early stages of embryogenesis, an extent of cell death that could account for the absence of this migratory population should most probably be above the level of detection by TUNEL. An alternative hypothesis for the absence of migratory neural crest cells in *Bmp2* mutants is that *Bmp2* is involved in triggering the migratory competence of the induced neural crest cells. A role for BMP (Dpp) signalling in the promotion of cell movement has already been reported in other systems (Vincent et al., 1997). Moreover, some of our data can be interpreted according to this hypothesis. In particular, we have observed that cells positive for some neural crest markers, like *Ap2*α, *Snail1*, or the RFP in *Tg(HtPA-RFP)* transgenics, which are rarely detected in the dorsal neural tube but rather in migratory neural crest population, seem to accumulate in the lateral edges of the neuroectoderm, remaining as premigratory neural crest cells. It will be important to address this problem directly and determine the underlying mechanism.

It could be expected that, in the absence of migration, neural crest cells accumulate in the lateral neural tube of *Bmp2* mutant embryos. Although the domain positive for neural crest cell markers in *Bmp2* mutants may be slightly extended compared with wild-type embryos, it is clear that there is no overt accumulation of premigratory neural crest cells. Experiments in chicken and amphibian embryos indicate that neural crest cell induction requires interactions between the surface ectoderm and the neuroectoderm (Moury and Jacobson, 1990; Selleck and Bronner-Fraser, 1995). If the same is true for mouse embryos, the signals involved in this process could have a limited range of activity and, therefore, could not act much further than a few cells in distance. In this context, the induced neural crest cells that fail to migrate could act as a barrier for further neural crest induction in more medial cells within the neuroectoderm, thus maintaining the size of the neural crest compartment within normal limits. Another consequence of the absence of neural crest cell migration and their lack of elimination by death could be an abnormal accumulation of cells in the neuroepithelium. This explanation is consistent with the observation that

neuroepithelium of *Bmp2* mutant embryos is clearly wider than those of control embryos and is abnormally folded. It should be noted, however, that increased apoptosis was also detected in specific areas of the neuroepithelium, which could contribute (at least partially) to the elimination of the extra cells accumulating as a result of the absence of migration of the induced crest cells. This cell death, of unclear origin, could also account for the lack of *Wnt1* expression in the midbrain/hindbrain boundary that we observed in the *Bmp2* mutants. Indeed, the observed domain of cell death contains the area of *Wnt1* expression in the neuroepithelium.

An important implication of our results is that the role of *Bmp2* in mouse neural crest development seems to be different to what has been reported for BMP signalling in other vertebrates. In chicken embryos, *Cad6B* and *Wnt1* are both downstream of BMPs in the signalling cascades that generate migratory neural crest cells (Sela-Donenfeld and Kalcheim, 1999; Burstyn-Cohen et al., 2004). Most particularly, it was proposed that *Wnt1* was an essential mediator of BMP signalling in the induction of migratory properties to neural crest cells (Burstyn-Cohen et al., 2004). In our case, it is clear that neither of the two genes was affected by the absence of *Bmp2*, but neural crest cells were still unable to migrate. There are several possible explanations for these inconsistencies. This may reflect another basic difference in the mechanisms that modulate production of migratory neural crest cells in the two vertebrates. The existence of such divergences has been clearly documented for the Snail family of transcription factors. It has been reported that *Snail2* (previously known as *Slug*) is required for the epidermal to mesenchymal transitions involved in the genesis of migratory neural crest cells in chicken embryos (Nieto et al., 1994). However, a recent report has clearly shown that mouse embryos carrying null mutations for both *Snail1* and *Snail2* still produce migratory neural crest cells, indicating that neither of these two genes is essential for this process in the mouse (Murray and Gridley, 2006). In this context, it is important to note that *Snail2* expression is maintained in the *Bmp2* mutants and neural crest cell delamination is still blocked. It is also

clear that canonical Wnt signalling in the mouse cannot play the essential role in neural crest cell delamination reported for chicken embryos, as both *Wnt1;Wnt3A* double mutants and conditional mutants for *β-catenin* in the neural crest seem to have no problems in neural crest cell delamination (Ikeya et al., 1997; Brault et al., 2001). In the case of BMP signalling in the neural crest cells, additional differences have already been reported between mouse and chicken embryos. For instance, BMP4 seems to be the relevant molecule for the induction/ migration of chicken neural crest cells (although an activity for BMP7 has also been reported), while *Bmp2* seemed irrelevant in this process (Liem et al., 1995). Conversely, inactivation of *Bmp2* alone is enough to block production of migratory neural crest cells in the mouse, while *Bmp4* does not seem to play a major role in the process in this species (Kanzler et al., 2000). *Bmp5* and *Bmp7* also seem to play a role in the development of neural crest cells, but their function seems to be required at later stages (Solloway and Robertson, 1999). Another apparent BMP signalling-related difference between mouse and chicken neural crest is that mutant data in the mouse are not consistent with a role for the BMP inhibitor Noggin in the spatial and temporal control of neural crest cell delamination that has been proposed according to experiments performed in chicken embryos (McMahon et al., 1998; Sela-Donenfeld and Kalcheim, 1999).

Another possible explanation for the inconsistency of our results with those obtained for BMP signalling in chicken and *Xenopus* embryos is that, while most of our analyses have been performed in the cranial region, which is where our phenotypes were most easily scored, experiments performed to evaluate the relevance of BMP signalling in chicken neural crest delamination have been typically performed in the caudal neural tube. This finding would suggest that induction/delamination of cranial and caudal neural crest cells is controlled by different mechanisms.

In conclusion, while BMP signalling seems to be required for neural crest cell migration in various vertebrates, the molecular mechanisms for this process evidently diverge among species.

ACKNOWLEDGEMENTS

We thank Trish Labosky and Allan Bradley for the *Bmp2* mutant mice, Silvye Dufour for the *HtPA* enhancer, Angela Nieto for the *Snail1* probe, Andy McMahon for the *Wnt1* probe, Hubert Schorle for the *Ap1*α probe, Andreas Kispert for the *Cad6B* probe, José Belo for the *En2* and *Otx2* probes, Randy Cassada for reading the manuscript, and all members of the Mallo laboratory for support and discussion. This work was funded by the Centro de Biologia do Desenvolvimento and by FCT.

Chapter 4:
Imaging methods to study aortic arch development in mouse embryos

Imaging methods to study aortic arch development in mouse embryos

Filipa Moraes [1,2], Joana Bom[1], Moisés Mallo[1,5]

(1) Instituto Gulbenkian de Ciência, Oeiras, Portugal.
(2) Centro de Biologia do Desenvolvimento, Oeiras, Portugal
(5) Departmento de Histologia e Embriologia, Facultade de Medicina, Lisboa, Portugal

The work presented here was carried out in collaboration between all authors.
FM performed the research, JB carried out the pronuclear injections to make *Tg(HtPA-RFP)* transgenic mice and gave technical support screening mouse lines. FM and MM designed the research, analysed data and wrote the manuscript.

ABSTRACT

In this chapter I developed new imaging tools to study vascular development, in particular to analyse the embryonic arteries passing through pharyngeal arches in mammalian embryos. Firstly, double transgenic reporter mouse lines were produced with endothelial cells and neural crest cells expressing the fluorescent GFP and RFP proteins, respectively. The transgenic mouse lines produced during this work allow observation of endothelial and neural crest simultaneously in fresh embryos. This imaging tool establishes a basis for the future challenge of culturing live mammalian embryos in order to observe their development. In addition, this chapter reports the development and optimization of a staining technique that enables the analyses of the vasculature of the entire embryo in three dimensions. The embryonic arteries were immunostained with the endothelial specific marker PECAM and simultaneously with the vascular smooth muscle marker SMA to observe the coverage of these large vessels by vascular smooth muscle cells (VSMC). This technique was applied to analyse defects in vascular smooth muscle cells in the embryonic arteries of some mouse mutants, such as *Tbx1* and *Gbx2* KO embryos. We were also able to show that the impaired development of embryonic arch arteries was more severe in $Tbx1^{+/-};Gbx2^{-/-}$ mutants than in $Gbx2^{-/-}$ embryos. These observations suggested that the decreased dosage of *Tbx1* in *Gbx2* mutant background leads to a cumulative effect in the development of the aortic arteries.

INTRODUCTION

Microscopic imaging represents one of the major analytical techniques utilized in the field of developmental biology. As such, technical advances are continuously adapted, typically using confocal microscopy and fluorescent protein technology (Conchello and Lichtman, 2005; Nowotschin et al., 2009), to determine the normal course of events in embryonic development and to characterize experimental

perturbations (Suchting et al., 2007; Jones et al., 2008). The cardiovascular system of vertebrate embryos has been extensively studied using this technology (Waldo et al., 2005; Anderson et al., 2008) and has contributed to the improvement of several imaging techniques (Fraser, 2005; Kulesa et al., 2005; Walls et al., 2008). The study of the mammalian vasculature has been hampered by the difficulties associated with visualizing the embryo and its entire vascular network. Moreover, there have been major challenges in interpreting some phenotypes from mouse mutants due to the thickness and opacity of the mouse embryo after the earliest stages of development. Several research groups are attempting to achieve a number of principal technical goals including: a) the ability to study vascular development in mouse embryos with high resolution; b) the ability to visualize specimens *in toto* to obtain a 3D perspective (Hiruma et al., 2002; Walls et al., 2008); c) the development of methods to maintain live mouse embryos under the confocal microscope to allow visualization of developmental processes in living embryos (Jones et al., 2002). Indeed, the ability to perform time-lapse movies has been a major quest for many groups in mouse development biology (Jones et al., 2002; Hadjantonakis and Papaioannou, 2004; Yamanaka et al., 2007).

This chapter reviews an attempt to overcome some limitations in the analysis of vascular phenotypes in entire embryos, firstly by utilizing fluorescent reporter mouse lines and secondly by optimizing immunostaining techniques that enable the analyses of the vasculature in whole mount fixed specimens.

As the main focus of this thesis is to study the key players involved in development of the branchial arches and their corresponding arteries, we analysed wild type and a variety of mutant model embryos where the development of these structures is compromised. This approach permitted observation of the cells involved in this process, namely the endothelial cells that contribute to the formation of the embryonic arch arteries, the migratory neural crest cells populating the branchial arches and the neural crest-derived vascular smooth muscle cells that surround these arteries. It was possible to produce

double transgenic mouse embryos expressing GFP (green fluorescent protein) in endothelial cells and RFP (red fluorescent protein) in migratory neural crest cells, which were analysed in a wild-type and also in a *Tbx1* mutant background. This permitted the examination of the mis-patterned vasculature of *Tbx1* null embryos as described previously (Jerome and Papaioannou, 2001; Lindsay et al., 2001) as well as the observation of misrouting of neural crest in these mutant embryos, thus confirming what we had observed by *in situ* hybridization in chapter 2.

Another important challenge in the analysis of fixed specimens is the visualization of the entire structure of the branchial arch area and interpretation of vascular phenotypes, because of the opacity and relative inaccessibility of the mouse embryo. In general, some of the major drawbacks have been overcome using techniques like scanning electron microscopy of vascular casts (Hiruma et al., 2002) or applying a refined protocol for optical projection tomography (Sharpe et al., 2002; Walls et al., 2008). Confocal microscopy is commonly used to study small samples or transparent embryos such as zebrafish (Motoike et al., 2000). Until now confocal microscopy was not sufficient to visualize in detail the vasculature of mouse embryos after E8.5. However, a staining technique described herein was developed and optimized based on simple confocal microscopy that enables the complete coverage of the mouse embryo until E11.5. This technique allowed a detailed analysis of the remodelling of the embryonic arteries by immunostaining with the endothelial specific marker PECAM. In addition, it permitted the simultaneous observation of the coverage of these large vessels by vascular smooth muscle cells (VSMCs) stained with the vascular smooth muscle marker SMA.

Thus, this section reviews 1) the use of confocal microscopy on fresh transgenic specimens to analyse their vasculature; and 2) the development of a staining technique to better visualize the formation and remodelling of the embryonic aortic arches. These techniques were applied to analyse defects in vascular smooth muscle cells in the embryonic arteries of some mouse mutants which are associated with aberrant remodelling of the embryonic arch arteries, as described

in the next chapter.

RESULTS AND DISCUSSION

Imaging developing vessels of wild type and *Tbx1* mutant mouse embryos using transgenic *Tie2-GFP* mouse line

Abnormalities in the growth and development of the cardiovascular system are among the most common congenital birth defects (Sandler, 2004), sometimes affecting formation and remodelling of the pharyngeal arch artery apparatus during vertebrate embryo development (Bergwerff et al., 1999; Jerome and Papaioannou, 2001; Baldini, 2002). This structure develops sequentially, in a cranial-to-caudal order, as the pharynx undergoes segmentation into a series of arches and pouches. Mammals have five pharyngeal arches (also called branchial arches), each of which contains an embryonic arch artery (EAA numbered 1–4 and 6) surrounded by a layer of mesoderm and neural crest cells (NCCs) (Graham, 2001). These arteries are the primary vessels that allow blood flow from the heart into the embryonic vasculature (Hiruma et al., 2002).

We analysed the development of the embryonic arch arteries using a transgenic mouse line (*Tie2-GFP*) expressing the green fluorescent protein (GFP) specifically in vascular endothelial cells under the control of the Tie2 promoter/enhancer (Motoike et al., 2000). These embryos were imaged under a confocal microscope at E8.5-E9.5 to observe the developing aortic arch area. In hemizygous transgenics the endothelial cells of the arch arteries gave a weak GFP signal. Therefore, in order to increase the fluorescence intensity of these cells, homozygous transgenic mice were generated and analysed.

The general pattern of the vascular network was obtained by z-projection of serial confocal stacks. This enabled us to acquire images that represent the entire vasculature of the mouse embryo (Fig. 4.1 A-C) as well the vascular pattern of the head (Fig. 4.1E), heart (Fig. 4.1F) and hindbrain (Fig. 4.1G and H). Observing

different transgenic embryos at early E9.5, one could distinguish the first, second and third aortic arches already formed (Fig. 4.1C, I, K and M). The 4th aortic arch, at this stage (E9.5) is not completely formed. It seems to arise when endothelial cells elongate and sprout from the heart, growing from the aortic area to join in the middle in order to form this vessel (Fig. 4.1I', K' and M').

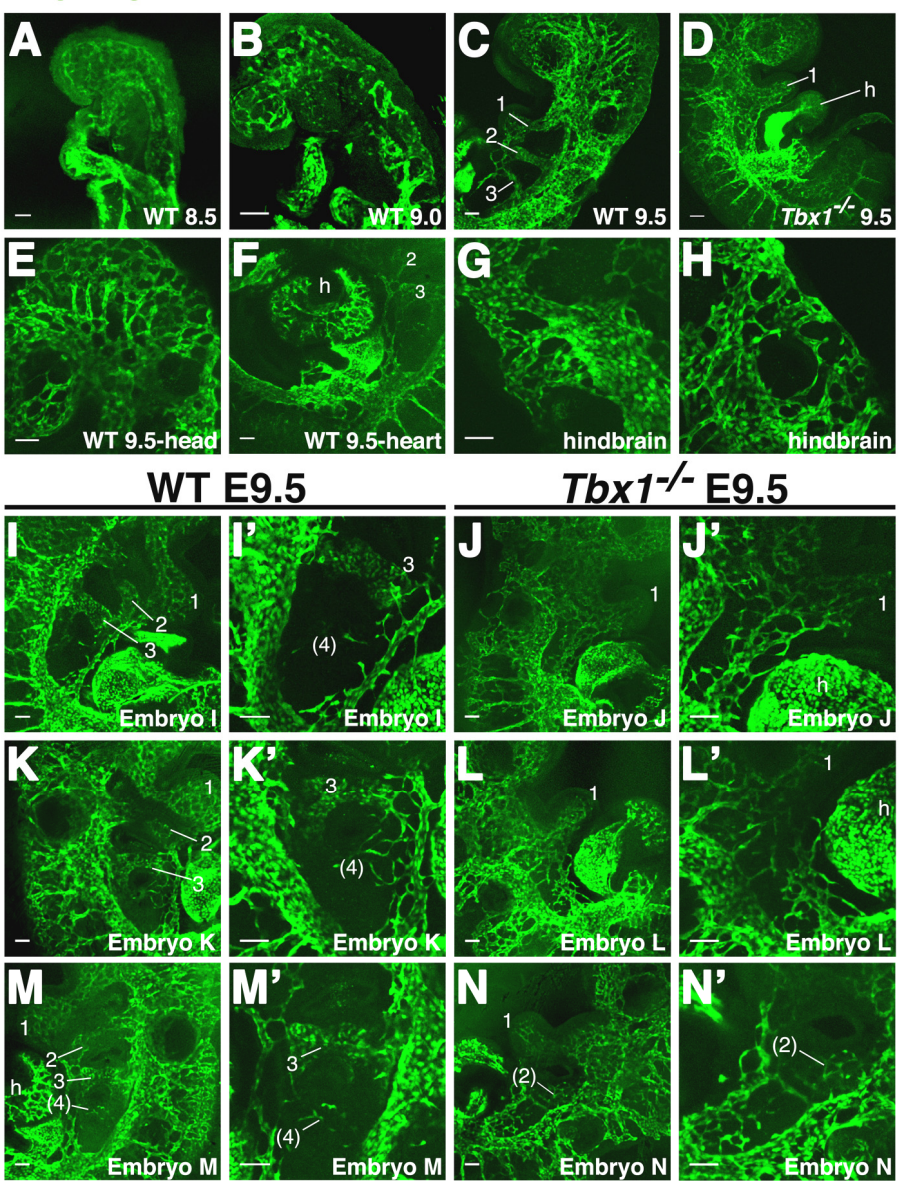

Figure 4.1 Imaging of GFP vessels of wt and *Tbx1* mutant mouse embryos.

Images of E8.5 (A), E9.0 (B) and E9.5 (C-N) are shown. Whole embryos wild type (A-C, E-H, I,I', K,K', M, M') and *Tbx1*$^{-/-}$ (D, J,J', L,L', N,N´'). Vasculature of the head (E); heart region (F); hindbrain-right side (G) and hindbrain-left side (H). C, I, K, M At E9.5 three embryonic arch arteries are seen (1, 2, 3) connected to the dorsal aorta, while in *Tbx1* null embryos (D, J, L, N) only the 1st aortic arch (1) seems to be completely formed, rarely it is possible to see a 2nd aortic arch not completely separated from the 1st aortic arch (N, N´). Magnification of the 3rd aortic arch region (I´, K', M') in wild type shows a completely formed 3rd aortic arch and the initiation of the 4th arch formation. Magnification of the corresponding region in the *Tbx1* null mutant embryos (J', L', N') shows only a plexus of endothelial cells without any type of vessel segmentation. EAA, embryonic arch arteries. 1, 2, 3, 4: first, second, third and fourth arch arteries. h, heart. Scale bar: 100μm

Taking advantage of this reporter mouse line we then used this imaging tool to analyse the development of the embryonic arch arteries (EAA) in *Tbx1* mutants. Mutations in the *Tbx1* gene have been identified as the major cause responsible for the human DiGeorge syndrome, which is characterized by aortic arch patterning defects, cardiac outflow tract anomalies, thymus and parathyroid hypoplasia, cleft palate and facial dysmorphogenesis (Jerome and Papaioannou, 2001; Lindsay et al., 2001). *Tbx1* is required for aortic arch patterning in earlier stages of development and for cardiac outflow tract morphogenesis at later stages (Xu et al., 2004). Therefore *Tg(Tie2-GFP)* mice were crossed with *Tbx1*$^{+/-}$ animals to generate *Tbx1*$^{+/-}$ mice carrying the Tie2-GFP transgene. Intercrosses between animals with this genotype were used as the source of *Tbx1*$^{-/-}$ embryos expressing GFP in the endothelia. With these embryos, we could confirm our previous data, which had shown that *Tbx1*$^{-/-}$ embryos have abnormal development of the aortic arches, resulting in the formation of a single aortic arch artery (Fig. 4.1D). Analysis of *Tbx1*$^{-/-}$*;Tg(Tie2-GFP)* embryos from the right side (Fig. 4.1J, J and L, L'), revealed a disorganized vasculature, in the aortic arch region, when compared with the segmented aortic arches from their wild type littermates (Fig. 4.1I, I' and K, K' respectively). Furthermore, it was not possible to distinguish a lumen corresponding to the first aortic arch in these mutant embryos (Fig. 4.1J' and L'). Observation from the left side revealed a completely formed 1st aortic arch in *Tbx1* mutant embryos, together with a hypoplastic 2nd aortic arch, which was not completely separated from the 1st aortic arch (Fig. 4.1N and N').

An additional benefit of using this GFP reporter mouse line is the possibility to perform non-invasive examinations of vascular development in mice, allowing observation of the entire vasculature with cell level resolution. Traditional imaging methods only permit visualization of the vasculature when vessels are perfused. (Hiruma et al., 2002). In contrast, this transgenic mouse line allows the visualization of vessels that do not have a flow yet, as well as those that regress before or after making a complete functional vessel.

While we were in the final phase of this work, additional fluorescent reporter lines were created and described by other groups with better results. The signal produced by the *Tg(Tie2-GFP)* transgenics is weak in the aortic arch area, while those recently produced transgenic mouse lines present higher expression levels. Examples of these are the *Tg(Flk1::H2B-EYFP)* mouse line, where a human histone H2B fusion was tagged with the enhanced yellow fluorescent protein (EYFP) and expressed under the control of an *Flk1* (also known as vascular endothelial growth factor receptor-2 or *Kdr*) promoter (Fraser, 2005). This endothelial-specific transgenic mouse line enables the imaging of endothelial cells at subcellular resolution. Another useful new reporter transgenic mouse line is the *Tg*(*Flk1-myr::mCherry*), in which endothelial cell membranes are brightly labelled with mCherry, a red fluorescent protein (Larina et al., 2009; Poche et al., 2009). Both of these transgenic lines (*Flk1::H2B-EYFP* and *Flk1-myr::mCherry*) were combined recently enabling the quantification of endothelial cells and analysis of the contribution of individual endothelial cells to the structure of each vessel (Larina et al., 2009).

In the future, further analysis of *Tbx1*$^{-/-}$ embryos would benefit from the analysis of these novel transgenic mice in the *Tbx1* mutant background.

Production of reporter mice to image migratory neural crest in wild type and *Tbx1* null embryos

In addition to endothelial cells, development of the heart outflow tract requires the

contribution of cardiac neural crest cells (Bockman et al., 1987; Bockman et al., 1989; Jiang et al., 2000). Indeed, a number of cardiovascular malformations are associated with alterations in cardiac neural crest cells (Creazzo et al., 1998). Until recently no reliable cell markers were available in mouse embryos and the vital dye staining commonly used in chick had limited success in mammalian embryos in culture because under *in vitro* culture conditions normal development cannot be maintained for more than twenty-four hours. Some researchers have overcome these problems by using vital dye labelling with *exo utero* embryological techniques (Serbedzija et al., 1992). In addition, fate-mapping studies with gene expression markers for neural crest have been used to identify the migration patterns of neural crest cells in mammalian species (Jiang et al., 2000). In particular, genetic strategies that included neural crest specific promoters (like P0, Pax3, Wnt1, Ht-PA) allowed lineage tracing of neural crest cells *in vivo* (Yamauchi et al., 1999; Jiang et al., 2000; Li et al., 2000; Pietri et al., 2003).

The relationship between aortic arch formation and migration of the neural crest cells into the branchial arches is an important topic to address. The promoter of human tissue plasminogen activator (Ht-PA), which has been shown to be active specifically in all NCCs throughout embryonic development and in the adult (Pietri et al., 2003), was used to express *RFP* specifically in migratory neural crest cells of transgenic mice.

Seven transgenic lines were obtained by pronuclear microinjection and the ones with stronger expression of RFP in neural crest cells were selected for further breeding to generate the *HtPA-RFP* transgenic line. Analysis of *HtPA-RFP*$^{+/0}$-embryos under a confocal microscope showed RFP expression in migratory neural crest cells delaminating from the neural tube and populating the presumptive first pharyngeal arch already as early as E8.5 (Fig. 4.2A). At later stages (E9-E9.5) RFP-positive cells were observed in the fronto-nasal region and in the first and second branchial arches (Fig. 4.2B and C).

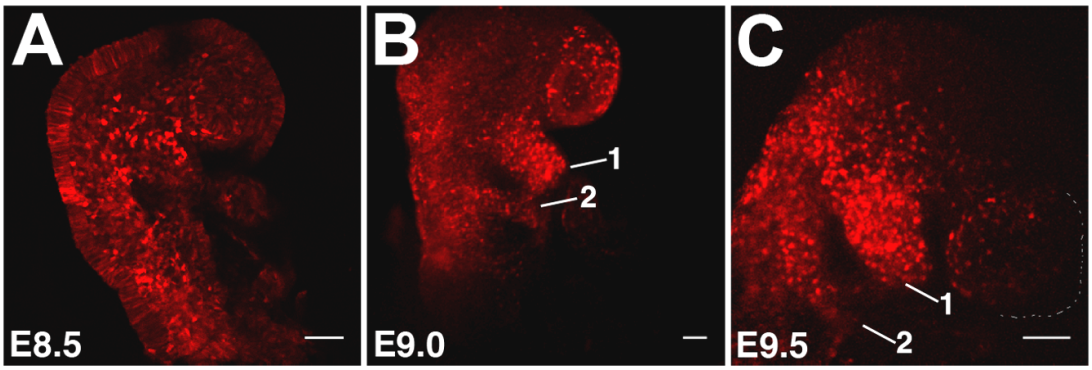

Figure 4.2 Production of a fluorescent reporter mouse line for migratory neural crest cells.
RFP expressing cells in the *HtPA-RFP* mouse embryos at E8.5 (A), E9.0 (B), E9.5 (C) are shown in the forebrain and in the first and second branchial arches (1,2). Scale bar: 100μm

Considering that RFP has an emission peak at 607 nm, it is easily distinguished from blue, green, or yellow fluorescent proteins. For this, *Tg(HtPA-RFP)* mice can be used in combination with other transgenics in which other relevant structures are labelled with a different fluorescent protein. In this work we crossed it with the *Tg(Tie2-GFP)* line to visualize simultaneously the formation of the aortic arches and neural crest cell migration streams into the embryonic aortic arch area (Fig. 4.3A''' and D''). These trangenics were used to validate this imaging tool for future analysis of different mutant mouse lines. Additionally, these *Tie2-GFP;HtPA-RFP* double transgenics were introduced into the *Tbx1* null background in order to confirm the phenotype of these mutants already described by other methods.

Wide field images and magnifications of the cranial region of E9.5 embryos revealed GFP expression in the head vasculature, heart and first aortic arches of *Tg(Tie2-GFP; HtPA-RFP)* embryos, both in wild type (Fig. 4.3A and A') and in *Tbx1* mutant backgrounds (Fig. 4.3B and B'). In addition, neural crest cells were seen in the first branchial arch and in the frontonasal prominence (Fig. 4.3A'' and B''). At this stage the second aortic arch was already present in wild type embryos (Fig. 4.3A') but it was absent or hypoplastic in *Tbx1*$^{-/-}$ embryos (Fig. 4.3B'). The amount of NCCs migrating into the second branchial arch was less in *Tbx1*

mutants (Fig. 4.3E and F) than in control embryos (Fig. 4.3C, D' and G), which was associated with a smaller number of endothelial cells in the second branchial arch of these embryos (Fig. 4.3F) compared with their wild type littermates (Fig. 4.3D). Interestingly, in *Tbx1* mutants, the stream of NCCs that would migrate into the second arch seemed to join the NCC stream that migrates into the first branchial arch (Fig. 4.3E). This misrouting of neural crest cells was already described in chapter 2 using other methods.

It should be noted that endothelial and neural crest cells are in close contact with each other during the critical stages of development (Fig. 4.3 A''', B''',D'' and F''). Therefore it would be interesting to see how the dynamics of these two cell populations influence each other. This would involve culturing the transgenic embryos on the microscope stage under conditions that allow both normal development and observation for long periods. As the yolk sac is required for correct blood flow circulation during development, the embryo should be cultured and imaged inside the yolk sac. Under these conditions it is possible to see the vasculature of the yolk sac from E8.5 embryo (Fig. 4.3H). By adjusting the focus to a deeper focal plane it is also possible to visualize *RFP* expression in the neural crest cells present in the fronto-nasal prominence and in the first branchial arch (Fig. 4.3H', H''). Since these conditions seemed to allow visual accessibility to the embryo, we could eventually culture and time-lapse image these embryos in order to observe how these two cell populations behave in wild type and in *Tbx1* mutant mice. This requires appropriate environmental conditions (temperature, media, CO2) and also optical adjustments, such as reducing phototoxic effects of higher laser power or reducing exposure time (Jones et al., 2002).

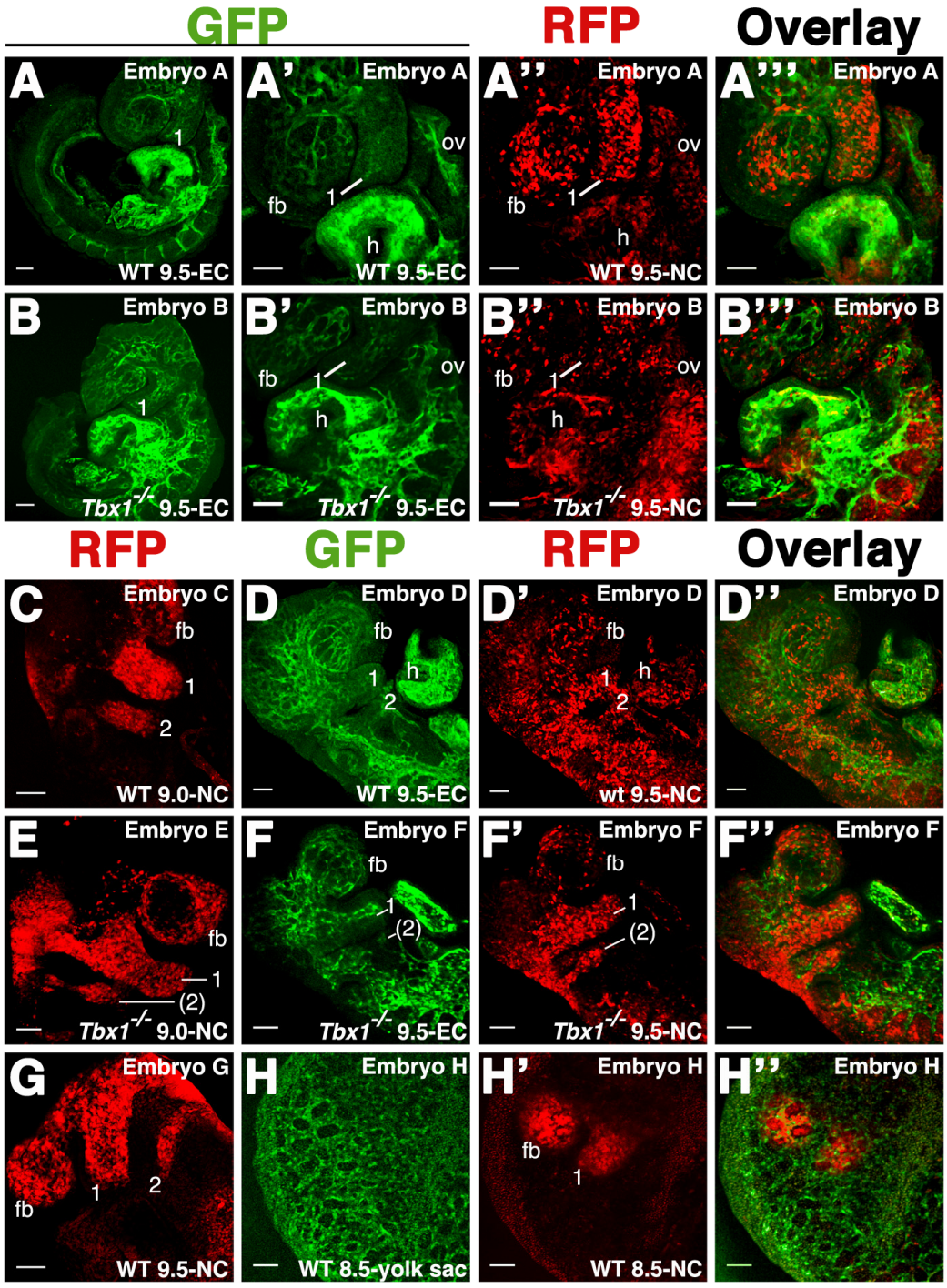

Figure 4.3 Imaging of endothelial cells and neural crest cells in transgenic mouse embryos

GFP vessels and RFP neural crest of whole embryos wild type (A, C, D, G, H) and *Tbx1*$^{-/-}$ (B, E, F) from E8.5 (H), E9.0 (C, E) and E9.5 (A,C,D,F-H). Endothelial cells expressing GFP are shown in green channel images (A, A',B,B',D,F and H). Neural crest expressing RFP are shown in the red channel images (A'', B'', C,D', E,F', G, H'). Merge of green and red channel show both cell populations (A´´´,B''',D'',F'',H''). At early E9.5 there is no considerable differences between the vasculature of wt (A) and *Tbx1*$^{-/-}$ (B) but the stream of neural crest populating the second branchial arch is thinner in the mutants (B'',E,F',) comparing with the corresponding controls wt (A'',C, D'), due to hypoplastic 2nd branchial arch. On panels H, H´, H''' is shown E8.5 wt embryo inside the yolk sac. H: vasculature of the yolk sac. H', H'': The embryo with RFP expressing cells is seen through the yolk sac (H´, H''). Scale bar: 100μm.

Ideally, one would be able to image a single living mouse embryo over an extended period of time in order to visualize the complete development of the vasculature. 3D time lapse of the live mouse embryo however is still a challenge, mainly due to the *in utero* development of mouse embryos and the light spreading caused by living tissue. Although we tried to set up this technique in our laboratory we were not successful in maintaining embryos alive for the adequate time needed to perform time-lapse analysis. Nevertheless, the *Tg(Tie2-GFP;HtPA-RFP)* transgenic mouse line permits observation of endothelial and neural crest populations simultaneously in fresh embryos. This imaging tool establishes a basis for the future challenge, shared by many groups, of culturing live mammalian embryos in order to observe their development. Alternatively, the *in vivo* time course can be approximated by static imaging of multiple mouse embryos collected at different stages throughout gestation. To this end, we further developed a whole mount staining technique to study the early embryonic vasculature, as described in the next section.

Immunostaining for smooth muscle cells and endothelial cells from the embryonic arch area of wt and mutant embryos

Analysis of aortic arch development in the mouse and subsequent interpretation of mutant vascular phenotypes has proven challenging due to an inability to observe the vasculature of mouse embryos as a whole. Most published characterizations of the aortic arches have been performed using a variety of staining techniques on histological sections (Bergwerff et al., 1999; Oh et al., 2005; Gittenberger-de Groot et al., 2006). This data is often difficult to interpret and to combine into a global view, thus making it difficult to reach clear-cut conclusions. For this reason, I developed a technique to enable three-dimensional analysis of the entire embryo, focusing on the pharyngeal arch area. The embryonic arch arteries were observed by confocal microscopy using immunostaining with anti-PECAM and anti-Smooth Muscle Actin (SMA) antibodies to identify endothelial cells and smooth muscle cells, respectively. This technique allowed observation of the entire vasculature of mouse embryos up to around E11.5.

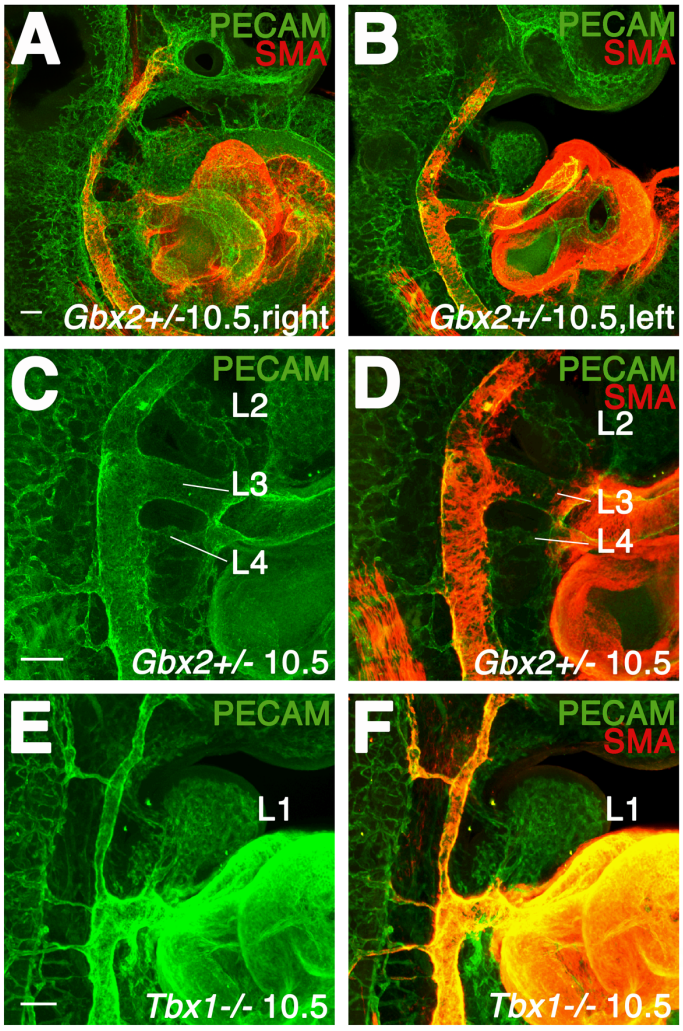

Figure 4.4 Imaging recruitment of vascular smooth muscle cells to the embryonic arch arteries (EAA) in whole mouse embryos.
Immunostaining showing the endothelial network (PECAM, green) and vascular smooth muscle cells (SMA, red) of control *Gbx2*$^{+/-}$ embryos at E10.5 (A-C), *Tbx1*$^{-/-}$ embryos at E9.5 (E) and E10.5 (F-G). **A:** At E10.5 the right side of the embryo is seen where SMA positive cells cover the dorsal aorta and the heart**. B:** Deepen the focus medially is possible to see the left side of the embryo with four embryonic arteries already formed and VSMCs surrounding the third EAA, the heart and the dorsal aorta. **C,D:** Magnification of image B show in more detail the VSMCs covering the third embryonic arch artery. **E:** At E10.5 *Tbx1*$^{-/-}$ embryos show impaired development of the EAA, the lumen of the first embryonic aortic arch is absent and it is only observed a vascular bed in the remaining area. **F:** In *Tbx1*$^{-/-}$ embryos the heart is connected to the dorsal aorta through the aortic sac also covered by VSMCs, the EAAs are not formed in these mutant embryos(E,F) compared with segmented EAAs in control embryos *Gbx2*$^{+/-}$(C,D). Scale bar: 100μm.

In early E10.25 control embryos, the first, second and third embryonic arch arteries, the dorsal aorta and the heart were clearly stained with PECAM and SMA positive cells, both in the right (Fig. 4.4A) and left sides (Fig. 4.4B). Figure 4.4C allowed a closer observation of the left side of the embryo. At this stage, formation of the third EAA was complete and the fourth aortic arch was undergoing morphogenesis, while the second aortic arch has already started to regress. Vascular smooth muscle cells covered the dorsal aorta and the third embryonic arch artery completely (Fig. 4.4D).

Observation of late E10.5 embryos showed that the two most rostral arteries had regressed and only a vascular bed was seen in the region of the first and second EAAs (Fig. 4.5A). At this developmental stage, the third, fourth and sixth EAAs (R3-6) were present on the right side of the embryo (Fig. 4.5A' magnification of image 5A) and the 3th and 4th EAA were covered by VSMCs (Fig. 4.5A'' and A'''). These observations are different from what was previously described by Byrd and colleagues (2005), where at E10.5 embryos, the smooth muscle actin (α-SMA) is only detectable in third EAAs (not fourth EAAs) even though a fourth aortic arch lumen is present. However, according to our data, VSMCs can already be seen around the 4th EAA at E10.5 (Fig. 4.5A''). It is worth considering that these conflicting results could be associated with the different techniques used. Byrd and colleagues (2005) used staining of VSMCs in sections where the probability to miss SMA positive cells is higher, while in this work the whole embryo was analysed, supporting the observation that whole mount staining is more reliable than staining in sections. An alternative explanation could be that the control embryos used in the previous study from Byrd and co-workers (2005) were at earlier developmental stages and the recruitment of VSMC to 4th EAA had not been initiated.

As a proof of principle we used this technique to evaluate the phenotype of specific mutants with abnormal aortic arch development. In particular we analysed mutants for the transcription factors *Tbx1* and *Gbx2* as they allowed comparison with previously published data using other methods (Vitelli et al., 2002a; Hu et al.,

2004; Byrd and Meyers, 2005). Firstly, the developmental defects from *Tbx1* null mutant embryos have already been mentioned in a previous section (Chapter 2). In this Chapter, using this whole mount staining technique, we could confirm what has been previously described (Lindsay et al., 2001; Vitelli et al., 2002a). At E10.5, the caudal EAA of *Tbx1*$^{-/-}$ embryos were not formed (Fig. 4.4E and F). As a result these embryos presented an impaired development of the aortic arches in comparison with segmented embryonic aortic arches (EAA) in control embryos (Fig. 4.4C and D)

Secondly, we addressed the vascular phenotypes of *Gbx2* null mutant embryos (Fig. 4.5B) and compared to the control littermates *Gbx2*$^{+/-}$ (Fig. 4.5A). The cardiovascular phenotype of these embryos has been recently described by other techniques and consists of absence of the fourth arch artery associated with impaired migration and differentiation of neural crest cells (Byrd and Meyers, 2005). We decided to analyse these mutants by whole mount staining to address if any variations to this phenotype might be seen. Indeed at E10.5, analysis of the *Gbx2*$^{-/-}$ embryos revealed the presence of the third EAA, a thinner 4th EAA and a hypoplastic 6th EAA (Fig. 4.5B and B'). Only the third EAA is covered with VSMCs, whilst they are not detected in the 4th or 6th arteries (Fig. 4.5B'' and B'''). Both our results and the ones from Byrd et al show lack of VSMCs in the 4th pharyngeal arch area from *Gbx2*$^{-/-}$ embryos. However, our study revealed a lumenized 4th EAA without VSMCs (Fig. 4.5B) compared with the control (Fig. 4.5A), whilst Byrd et al interpretations were entirely based from observations on the complete absence of the 4th EAA in *Gbx2*$^{-/-}$ embryos. There could be two explanations for these conflicting results: a) the *Gbx2*$^{-/-}$ embryos analysed by Byrd et al were at earlier developmental stage and the formation of the 4th EAA had not been formed yet or b) the different techniques used to visualize endothelial and VSMC cells (sections in Byrd et al; Whole mount in our study) could produce different observations. In order to confirm our analysis, we studied later developmental stages (E11.0) of *Gbx2*$^{-/-}$ embryos. A left side view from *Gbx2*$^{-/-}$ embryos (wild field - Fig. 4.6A and its magnification - Fig. 4.6A') revealed the

completely formed and well-defined 3-6 EAAs all covered by VSMCs (Fig. 4.6A'', and A'''). On the right side of the embryo (Fig. 4.6B-B''') the 3rd and 4th EAA are present (Fig. 4.6B and B') and covered by VSMCs (Fig. 4.6B'' and B'''). Interestingly we find well-formed 4th EAA in *Gbx2* mutant embryos (left-Fig. 4.6A' and right-Fig. 4.6B'), contrary to what was previously shown (Byrd and Meyers, 2005). Moreover the right 6th EAA is absent already at this E11.0 stage, whereas in wt condition the right 6th EAA only regresses at E12.0 (Hiruma, et al, 2002). These observations support what was seen in *Gbx2* mutants at E10.5. There was already a hypoplastic sixth EAA deprived of VSMCs on the right side (Fig. 4.5B') that eventually did not recruit VSMCs and as a consequence disappeared due to lack of stability. This data may suggest that indeed the vessel is formed, although abnormal, and the lack of recruitment of VSMCs leads to its regression.

It has been suggested that *Tbx1* controls *Gbx2* activity in the development of the caudal aortic arteries via Fgf8 signalling. Therefore, we analysed $Tbx1^{+/-};Gbx2^{-/-}$ double mutants in comparison with their control littermates $(Gbx2^{-/-})$ in order to further determine if *Gbx2* might interact with *Tbx1* in the aortic arch development, as previously suggested.

The analysis of the right and left EAAs of $Tbx1^{+/-}Gbx2^{-/-}$ embryos (Fig. 4.5C and D respectively) revealed an almost absent, hypoplastic 4th EAA when compared with the control $Gbx2^{-/-}$ embryos where the 4th EAA is present (Fig. 4.5B). SMA staining revealed VSMCs covering the third EAA in both $Tbx1^{+/-}Gbx2^{-/-}$ embryos (Fig. 4.5C'' and D''). The right 6th appears to be covered by SMA positive cells (Fig. 4.5C'' and C'''), while in the 6th EAA of $Gbx2^{-/-}$ embryos the VSMCs were not present (Fig. 4.5B'',B'''). Observing the right side of the $Tbx1^{+/-}Gbx2^{-/-}$ embryo (Fig. 4.5C'' and C''') we identified an association between the abnormal recruitment of VSMCs to the 6th EAA and the lack of 4th EAA, suggesting that the 6th EAA must be stabilized in order to compensate the absence of the 4th EAA. Indeed, the lack of lumenization of a given vessel (*e.g.*, R4 EAA) could be overcomed by its neighbours (*e.g.*, R6 EAA), thus assuring the continuity of blood flow circulation throughout the embryo. One important observation was that

the 4th EAA was absent in these double mutants whereas it was present in the single *Gbx2* null mutants.

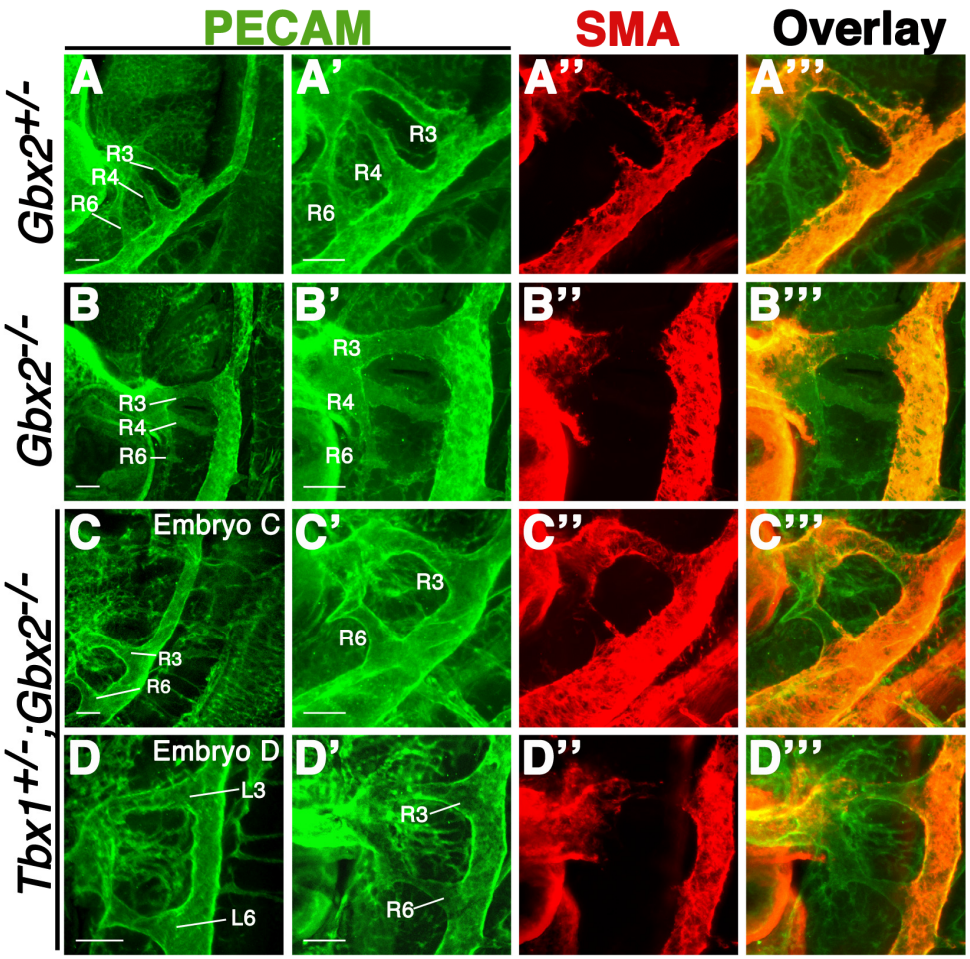

Figure 4.5 Imaging embryonic arteries and vascular smooth muscle cells in whole embryos.
Immunostaining showing the endothelial network (PECAM, green) (A,A', B, B', C, C',D,D') and vascular smooth muscle cells (SMA, red) (A'',B'', C'', D'') of control embryos *Gbx2*$^{+/-}$ (A), *Gbx2* homozygous null mutant-*Gbx2*$^{-/-}$ (B), and two distinct double mutants *Tbx1*$^{+/-}$*;Gbx2*$^{-/-}$ at E10.5 (C,D). A''', B''', C''' and D''' show an overlay of the PECAM and SMA stainings. A', B', C' are magnifications of A, B, C respectively; D and D' are left and right EAA of the same embryo. In the control embryos the third fourth and sixth aortic arteries are seen (A, A') and VSMCs are covering the third and fourth aortic arteries (A''). In the null mutant *Gbx2*$^{-/-}$, the 6th artery is missing or hypoplastic (B) and only the third EAA is covered by VSMCs (B''). In double mutants *Tbx1*$^{+/-}$*;Gbx2*$^{-/-}$ the lack of 4th aortic artery is often observed (C,D). Scale bar: 100μm.

In order to determine if there were indeed differences between the phenotypes of *Tbx1*$^{+/-}$*Gbx2*$^{-/-}$ and *Gbx2*$^{-/-}$ mutants, embryos were analysed at later stages (E11.5).

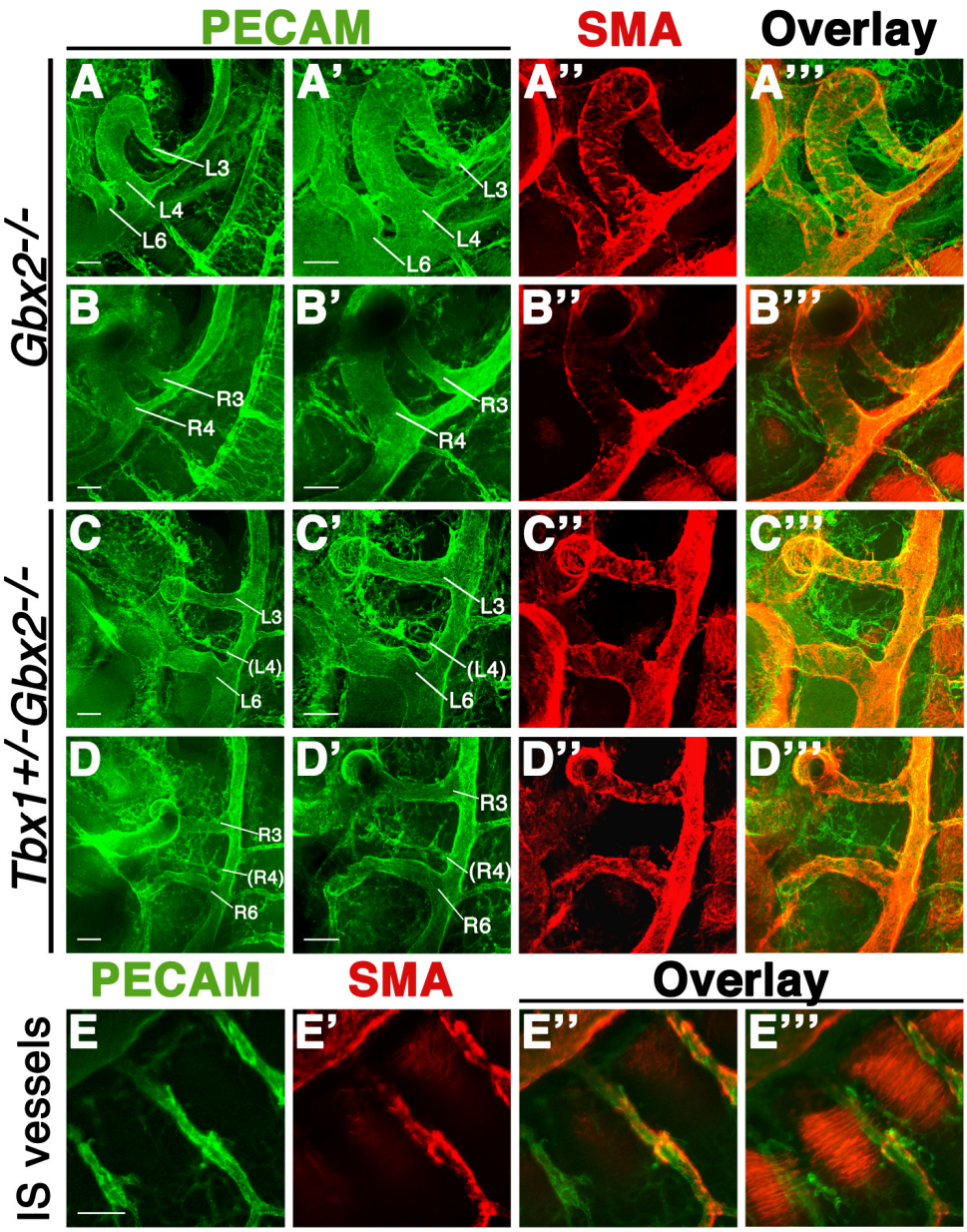

Figure 4.6 Normal embryonic arteries seen in *Gbx2* mutant embryos and absence of the fourth arch artery in *Tbx1*$^{+/-}$*;Gbx2*$^{-/-}$ embryos at E11.5.
Immunostaining showing the endothelial cells (PECAM, green) and vascular smooth

muscle cells (SMA, red) in the aortic arch arteries of E11.5 - 40ss of *Gbx2*$^{-/-}$(A-left, B-right) and double mutants *Tbx1*$^{+/-}$*;Gbx2*$^{-/-}$ (C,left and D,right) and in the intersegmental vessels(E) of whole mouse embryos. In the *Gbx2*$^{-/-}$ embryos (A) the third, fourth and sixth aortic arteries are seen in left side (A) and the third and fourth are seen in the right side (B) whereas the double mutant for *Tbx1*$^{+/-}$*Gbx2*$^{-/-}$ lack the fourth arch artery on both sides (C,D). Images E-E'' display detailed intersegmental vessel endothelial cells (E) covered by SMA positive cells (E''). On E''' a more superficial image showing the somites constituted by SMA positive fibers separated from each other by the intersegmental vessels. Left view, scale bar: 100μm.

We could not find any 4th aortic arch in all double mutants analysed (left side-Fig. 4.6C and C'; right side-Fig. 4.6D and D'). The 3rd and 6th EAAs were present at this stage and completely covered by VSMCs (Fig. 6C'',C''',D'',D'''). We found that the impaired development of embryonic arch arteries was more severe in *Tbx1*$^{+/-}$*;Gbx2*$^{-/-}$ mutants than in *Gbx2*$^{-/-}$ embryos. These observations suggested that the decreased dosage of *Tbx1* in *Gbx2* mutant background leads to a cumulative effect in the development of the aortic arteries. We could explain this effect by impairment in the migration or differentiation of neural crest cells, already described in *Gbx2* null mutants (Byrd and Meyers, 2005), which could be higher with the loss of one copy of *Tbx1*. However an assessment of the neural crest population would be necessary to confirm this hypothesis.

A few studies have identified modifier genetic factors that enhance the phenotype of model organisms lacking *Tbx1* (Vitelli et al., 2002b; Stalmans et al., 2003; Guris et al., 2006). Furthermore, in this Chapter, as well as and in the study performed by Byrd et al., (2005), developmental defects associated with the loss of *Gbx2* and *Tbx1* have been linked to the Fgf8 signalling pathways implicated in the pathogenesis of a DGS-like phenotype. Accordingly, it would be worthwhile examining the effects of a decreased dosage of *Tbx1* in *Gbx2* deficiency on expression of Fgf8 target genes compared to the single *Gbx2*$^{-/-}$ null mutant. However the molecular analysis of Fgf8 signalling was not performed in double mutants as part of this investigation.

In order to address different regions of the embryo where this staining technique could be applied, inter-segmental vessels were analysed at different depths inside

the embryo. Figure 4.6 6E displays a detailed view of a group of inter-segmental vessels in the somite region of the embryo (E11). Figure 4.6 6E'' shows inter-segmental vessels already formed and covered by perycites, which are also stained by SMA. Figures 4.6E-E'' shows a more medial view than Figure 4.6E'''. In the later image we could see the somites and the muscle fibers of somites also stained with SMA. With this technique it is possible to reach and visualize structures localized in deaper regions of the embryo, that previously were only accessible by sectioning the specimen.

In summary, the data reported here has provided insights into the early processes in the remodelling of the embryonic aortic tree towards formation of the mature heart outflow tract. Furthermore, the whole mount staining technique adapted in this study aids clarification of the phenotypes observed in those tissues in animals carrying specific mutant conditions.

In addition to the imaging techniques used to observe mouse embryo phenotypes at early developmental stages (image and culture of fluorescent reporter mouse embryos E8-E9), this chapter covers an improved method of whole mount immunostaining with SMA-PECAM (E10-E11). This work enabled assessment of the three dimensional structure of the embryonic arch area in wild type and mutant embryos, which is typically difficult to characterize due to the intricate phenotypes that are not easy to visualize. Consequently this adapted staining technique can be used in the future for a better interpretation of different vascular phenotypes, thus contributing to increase our knowledge of mammalian vascular development.

ACKNOWLEDGEMENTS

This work was funded by Centro de Biologia do Desenvolvimento (BIOS-LVT-Oeiras-664), Pfizer grant (João Cid dos Santos - 2004) and FCT grant POCTI/BIA-BCM/60420/2004 to M.Mallo and a FCT scholarship SFRH/BD/18620/2004 to F.Moraes. We thank S. Dufour for providing the HtPA

promoter; G.Martins for staining imaging troubleshooting; A.T.Tavares, J.Rowland and M. Costa for helpful discussions and critical reading of the manuscript.

MATERIAL AND METHODS

Mouse Lines

DNA construct to produce the transgenic mouse line *Ht-PA-mRFP*

The plasmid construct to express mRFP in migratory neural crest cells was cloned in a modified pKS-BS vector with a distinct MCS named pKXM. The vector, containing the *HtPA* promoter, was kindly provided by Dr. Sylvie Dufour (Pietri et al., 2003). The mRFP cDNA was inserted in the pKXM-HtPA backbone followed by the insertion of SV40 polyadenylation signal downstream of the *RFP* cDNA. The *HtPA-RFP* transgenic animals (produced in Transgenic Unit according to standard procedures) were identified by PCR using the primers:
5‘-TCCGAGGACGTCATCAGGGAG-3‘ and
5‘-ATGGTGTAGTCCTCGTTGTGG-3’.

Breeding

The transgenic mouse line *Tg(Tie2-GFP)* described in (Motoike et al., 2000) was obtained, from Jackson laboratories and the mice were bred to establish homozygosity for the transgene *Tie2-GFP*; the homozygosity was confirmed by amplification of the transgene with LightCycler (Desligneres and Larroche, 1970) using the Quantitect SYBR green PCR kit. The amplification of the gene *IL2* was used for normalization. The *Tg(Tie2-GFP)* mouse line was crossed with the mutant mouse line *Tbx1* (Jerome and Papaioannou, 2001), kindly provided by Virginia Papaioannou, also used in the study presented in Chapter 2 (Moraes et al., 2005). After bringing again the transgene *Tie2-GFP* to homozygosity the mouse line *Tbx1*$^{+/-}$*; Tg(Tie2-GFP)* was established.

In parallel, the *HtPA-RFP* transgenic animals were crossed with *Tg(Tie2-GFP)* to obtain *Tg(Tie2-GFP; Ht-PA-mRFP)* mice. These last mouse line was crossed with Tbx1$^{+/-}$; *Tg(Tie2-GFP)* in order to finally obtain the *Tbx1$^{+/-}$; Tg(Tie2-GFP; Ht-PA-mRFP)* mice. *Tbx1$^{-/-}$* embryos carrying the *Tg(Tie2-GFP;Ht-PA-mRFP)* transgenes were obtained by intercrosses between *Tbx1$^{+/-}$; Tg(Tie2-GFP; Ht-PA-mRFP)* mice. These mouse lines were maintained in a mixed FVB/C57Bl6 genetic backgrounds.

The mutant mouse line *Gbx2KO* was described previously (Wassarman et al., 1997) and provided by Antonio Simeone. The *Gbx2$^{+/-}$* line was crossed with the mutant mouse line *Tbx1* (Jerome and Papaioannou, 2001) and maintained in a C57Bl6 genetic background.

Embryo collection and culture

This technique was taught by Elizabeth Jones, adapted from *Jones et. al 2002*

Dissection

Embryos were obtained from time matings and the presence of vaginal plug was taken as 0.5dpc. Embryos were collected on the morning of day 8 (E8.5) or day nine (E9.5).

In order to take snapshots images the embryos were dissected at 4ºC and imaged under a confocal microscope.

For culture experiments the embryos were dissected over a Plexiglas hood heated to 37°C in the prewarmed dissecting media prepared by mixing 45 ml of D-MEM/F-12 with 4.5 ml of heat-inactivated fetal bovine serum, 0.5 ml of Pen-Strep solution and 0.5 mL of HEPES 1M solution. Females were euthanized with CO2 followed by cervical dislocation. The uterine horns were dissected out and placed in warmed dissecting medium and the embryos isolated. Yolk sacs were left intact on E8.5 embryos but were removed for E9.5 embryos.

Rat Serum

At the time of the work presented in this Chapter it was recommended, by people in the field (Alexander Aulehla, Yoshiro Yamanaka, Christina Pyrgaki, Liz Jones) not to use commercial rat serum but produce homemade rat serum using ether as the anesthetic (Jones et al., 2002). This anesthetic is easily eliminated by aeration, which was thought to be essential. Rat serum was prepared from blood collected from the dorsal aorta of male rats described in (Nagy et al., 2003) with the following modifications. Blood was collected into vacutainer tubes (Becton-Dickinson No. SSTII Advance 8.5ml No. 367953) using a butterfly needle (Becton-Dickinson, No. 367284). After collection, the blood was centrifuged at 2,500 rpm for 20 min. The plasma was isolated and supernatant from multiple rats were pooled. The serum was then centrifuged again at 2,500 rpm for 10 min to remove remaining cells. The supernatant was heat-inactivated at 56°C for 30 min with the lid removed to allow the ether to evaporate. The serum was then filtered using a 0.45 um filter and aliquoted into 1-mL samples. These samples were stored in a –80°C freezer.

Incubation, culturing and imaging whole mouse embryos

The culturing medium was prepared by mixing D-MEM/F-12 (40-30%) with heat-inactivated rat serum (60-70%) and 1:50 of Pen-Strep, and 1:50 HEPES buffer solution 1M. The medium was filtered with a 0.2 um filter and allowed to equilibrate, with the lid off, in a CO2 incubator for 1 h. During dissection three embryos were being transferred to each culture vial with 2ml of culture media. Each vial was closed and placed in a roller culture apparatus, at 37ºC with constant gas supply (5% CO2, 95% air). The embryos were cultured in the roller unit for at least one hour and afterwards were transferred to culture chambers (LabTek #155380) with fresh culture media. The culture chambers were covered with a thin layer of 1% agarose (dissolved in DMEM/F:12) with little holes where the embryos were placed directly sitting on glass and stabilized by the

surrounding agarose. Three embryos were placed per chamber and 2 mL of the culturing media was added. The embryos were placed on a SP5 confocal stage covered by a chamber for temperature (37ºC) and atmosphere control (5% CO2, 95% air). The embryos were imaged for 2-6 hours, with time intervals of 5 min. The development was assessed by ability to turn, somite number and formation of the branchial arches. The embryos were imaged with either bright-field or confocal microscopy taken on two distinct inverted microscopes (Zeiss, LSM 510 META; Leica SP5). Images were taken at 10x and 20x magnification.

Whole-Mount Staining PECAM/SMA

(Modified from protocols by R. Adams' lab, and Sato's lab)
The protocol was developed during the course of this thesis, and is as described:

- Mouse embryos were collected and fixed o/n at 4°C in 4% Paraformaldehyde (PFA made in PBS: dissolve by heating to 65°C and let it cool down to room temperature. It should be used fresh or stored at –20°C).
- Wash embryos for 2x 10 min each in PBS at 4° C (for big embryos or large pieces of tissue, extend the washing times). Wash at 4° C, for 15 min each, with 50%, 75% methanol in PBS, then twice in methanol. The embryos can be stored at this stage at –20°C.
- Alternative to step1) and 2) Other fixation procedure was used: Fixation o/n at 4°C DMSO/MetOH (1:4). Wash twice in MetOH and store at -20ºC.
- Rehydrate by washing at 4° C, 15 min each, in 75%, 50%, 25% methanol in PBS, then twice in PBS, at RT.
- If the embryos are older than E9.0, introduce a sharp incision along the dorsal midline of the hindbrain using a pulled injection needle. Wash 5min with PBS.
- Permeabilise/Block for 4 hours at RT or O/N at 4% solution in

PERM./BLOCK solution (1% BSA + 0.5% TWEEN-20 in PBS)

- Wash 3 x 5 min in PBT.
- Incubate with primary antibody rat anti-mouse PECAM CD31 (Pharmingen 557355) 1:100 - O/N at 4°C (in PERM./BLOCK solution 1:1 diluted with PBS)
- Wash thoroughly with PBT (4 x 45min) at RT.
- Incubate with secondary antibody Goat anti-rat Alexa488 1:100 (Molecular Probes A-11006) together with cy3 conjugated mouse monoclonal anti-smooth muscle actin antiSMA (clone 1A4 SIGMA C6198) 1:400 O/N at 4°C (in PERM./BLOCK solution 1:1 diluted with PBS) Cy3 conjugated mouse monoclonal anti-Smooth Muscle Actin (clone 1A4 SIGMA C6198) 1:400 O/N at 4°C (in PERM./BLOCK SOLUTION 1:1 diluted with PBS).
- Wash thoroughly with PBT (4 x 45min) at RT
- Wash the embryos twice in PBT and dehydrate the embryos as in step 2).
- Wash several times through Methyl Salicylate 25% 50% 75% in MetOH and then wash twice with 100% of Methyl Salicylate to clear the embryo. Do these steps very carefully and take enough time to avoid damaging the embryo!
- Mount in Methyl Salicylate (SIGMA #M6752) seal it and analyse under confocal microscope.
- Factors that improve result: Usage of fresh embryos immediately after dissection Fresh 4% PFA. Intense washing after Ab incubation to reduce background. Add small volumes (200μl) of Methyl Salicylate to the embryos in MetOH to avoid damaging the embryos.
- 16) Analyse under the SP5 LEICA confocal microscope, with a 10x (NA 0.4) or 20x (NA 0.7) dry objectives. Acquire using the Leica software and use ImageJ and Adobe photoshop for image processing.

Chapter 4: Imaging methods to study aortic arch development

Chapter 5:
A role for the absence of vascular smooth muscle cells in the regression of the first and second embryonic arch arteries

A role for the absence of vascular smooth muscle cells in the regression of the first and second embryonic arch arteries

Filipa Moraes[1,2], Ana Nóvoa[1,2], Joana Bom[1], Karen Handschuh[3], Shelley Dixon[4], Masashi Yanagisawa[4,5], Licia Selleri[3], Moisés Mallo[1,2,6,]

(1) Instituto Gulbenkian de Ciência, Oeiras, Portugal.
(2) Centro de Biologia do Desenvolvimento, Oeiras, Portugal
(3) Department of Cell and Developmental Biology, Cornell University Medical School, New York, USA
(4) Department of Molecular Genetics, University of Texas Southwestern Medical Center, Dallas, USA
(5) Howard Hughes Medical Institute, University of Texas Southwestern Medical Center, Dallas, USA
(6) Departmento de Histologia e Embriologia, Facultade de Medicina, Lisboa, Portugal

The work presented here was carried out in collaboration between all authors.
FM performed the research and made the construct. JB and AN carried out the pronuclear injections to make *HtpA-Myoc::Mkl2* transgenic embryos. FM and MM designed experiments, analysed data and wrote the paper, KH, SD, MY and LS contributed biological samples.

ABSTRACT

Formation of the mature heart outflow tract is initiated with the remodelling of five paired embryonic vessels. We studied their recruitment and explored whether the potential of the endothelial embryonic arch arteries to recruit vascular smooth muscle cells (VSMCs) plays a role in their stabilization or regression.

In wild type embryos the first and second arch arteries, which undergo a physiological process of regression and never form part of the mature aortic tree, never become associated with smooth muscle cells. Conversely, the third, fourth and sixth arch arteries recruit smooth muscle cells to their walls shortly after their formation as endothelial vessels and generate a symmetric arterial tree. We also analysed the aortic arches of two mutant strains that have abnormal development in this area to find a correlation between the presence or absence of VSMCs and the stabilization or regression of the arch arteries. In particular, we show that the persistent second arch artery found in mutants for the endothelin receptor A is associated with the presence of VSMCs and that the prematurely regressing fourth arch artery of *Pbx1* mutants fails to recruit vascular smooth muscle cells before its regression. Finally, we show that forced differentiation of VSMCs in the rostral arches is sufficient to stabilize their normally regressing arteries. Our data indicates that the physiological regression of the first and second arch arteries results from their failure to recruit VSMCs, most likely because these arches are not populated by cardiac neural crest cells, which are the source of VSMCs in this area of the embryo.

INTRODUCTION

The mature heart outflow tract derives from complex remodelling of the embryonic arch arteries (EAAs) and the aortic sac. The EAAs are five bilaterally symmetric arteries that run through the branchial arches to connect the embryonic heart with the paired dorsal aortae allowing blood circulation throughout the embryo. The development of the EAAs follows a rostro-caudal sequence, beginning around embryonic day (E) 8.5 with formation of the most cranial (first) EAAs, which traverses the first branchial arch (Waldo and Kirby, 1998; Hiruma et al., 2002). Within the next two days, the second, third, fourth and sixth (none of the arteries is named as fifth) will appear sequentially following the formation of the branchial arches through which they run. To complete the morphogenesis of the heart outflow tract, the embryonic arch artery tree undergoes a complex remodelling process, which starts even before formation of the most caudal EAAs is completed (Waldo and Kirby, 1998; Hiruma et al., 2002). This process includes the regression of the first two EAAs to form capillary beds, which eventually disappear. Regression of these arteries occurs at the same time the third and fourth EAAs are being formed (Hiruma et al., 2002). In addition, the caudal EAAs (third, fourth, and sixth) undergo a complex asymmetric remodelling, which includes coordinated fusion and regression of specific portions of these vessels, ultimately leading to the formation of the mature heart outflow tract with newborn characteristics.

Ablation experiments performed in avian embryos revealed that proper development of the aortic arches requires the presence of cardiac neural crest cells (Kirby et al., 1983; Bockman et al., 1987; Bockman et al., 1989; Waldo et al., 1996; Waldo et al., 1998), a subpopulation of the neural crest that migrates into the third, fourth and sixth pharyngeal and contributes to the walls of the great arteries at the exit of the heart (Le Lievre and Le Douarin, 1975; Miyagawa-Tomita et al., 1991; Waldo et al., 1998; Jiang et al., 2000). In those experiments, it

was shown that removal of the cardiac neural crest from early chick embryos results in a number of cardiovascular defects including persistent truncus arteriosus, outflow misalignment and abnormal patterning of the great arteries (Kirby et al., 1983; Bockman et al., 1987; Bockman et al., 1989). The contribution of cardiac neural crest cells to the development of the heart outflow tract is also supported by the analysis of mouse mutants with impaired production or differentiation of neural crest cells in general or its cardiac subpopulation in particular (Epstein et al., 1991; Feiner et al., 2001; Yanagisawa et al., 1998; Abu-Issa et al., 2002; Brewer et al., 2002; Ohnemus et al., 2002; Vitelli et al., 2002; Varadkar et al., 2008; Wang et al., 2006;). The mechanisms by which the cardiac neural crest cells control development of the heart outflow tract are not clear. Several studies indicate that the ability of this neural crest cell population to generate the vascular smooth muscle cells (VSMCs) that associate with the EAAs is among the most important factors contributing to this process (Waldo et al., 1996; High et al., 2007; Mancini et al., 2007). Indeed, mutations that affect differentiation of VSMCs from the cardiac neural crest cells resulted in cardiovascular malformations in the structures derived from the EAAs (Conway et al., 1997; Kochilas et al., 2002; Tallquist et al., 2003; Oh et al., 2005; Wei et al., 2007; Huang et al., 2008; Varadkar et al., 2008;).

Whilst most studies addressing heart outflow tract development have focused on the mechanisms guiding remodelling of the caudal EAAs, little attention has been given to the mechanisms responsible for the physiological regression of the two most rostral EAAs. Considering that VSMCs associated to vessels in the arch region are neural crest derived (Jiang et al., 2000; Le Lievre and Le Douarin, 1975; Snider et al., 2007) and that the first two branchial arches are not populated by cardiac neural crest cells (Le Lievre and Le Douarin, 1975; Couly and Le Douarin, 1990; Miyagawa-Tomita et al., 1991; Kanzler et al., 1998), we hypothesized that the regression of the first and second EAAs could be linked to their inability to recruit smooth muscle cells from surrounding mesenchyme. Here, we show that, while VSMCs are readily identified in the third, fourth and sixth

EAAs shortly after their initial formation, the two most rostral EAAs never become associated to VSMCs. Additionally, we analyse the EAAs in mutant embryos with persistent second EAAs (Yanagisawa et al., 1998) or with abnormally regressing EAAs (Manley et al., 2004; Chang et al., 2008) to find a direct correlation between the presence or absence of VSMCs and the persistence or regression of the EAAs. Finally, using a transgenic approach, we forced VSMC differentiation in neural crest cells of the rostral branchial arches by expression of *Myocardin* (*Myoc*) and *Myocardin-like 2* (*Mkl2*) under the control of a neural crest promoter (Pietri et al., 2003). We observed transgenic embryos containing persistent second arches, which were always associated with VSMCs. Our data is consistent with the hypothesis that regression of the first two EAAs results from their inability to recruit VSMCs, possibly because of the absence of cardiac neural crest cells migrating into the first and second branchial arches.

RESULTS

Cranial EAAs are not associated with vascular smooth muscle cells.

The two most rostral EAAs are first formed during embryonic development but eventually regress and do not contribute to the formation of the outflow tract of newborn animals. To understand how this regression is regulated we analysed formation of the EAAs in mouse embryos and the presence of vascular smooth muscle cells associated to these blood vessels. At E9.0-E9.5 the most rostral EAAs could be observed by confocal microscopy using immunostaining with anti-PECAM antibodies (Fig. 5.1A), which is similar to what has been previously described using other methods (Hiruma et al., 2002; Walls et al., 2008). At E10.5, a well-formed third EAA was evident, which connected the truncus arteriosus with the dorsal aorta, and formation of the fourth EAA was almost completed (Fig. 5.1D). At this stage, PECAM staining revealed a capillary bed in the first and second branchial arches instead of the arteries observed in younger embryos,

which is part of the regression processes of these arch arteries. Half a day later, the third, fourth and sixth EAAs could be observed by PECAM staining and regression of the two rostral most arch arteries was already completed (Fig. 5.1G).

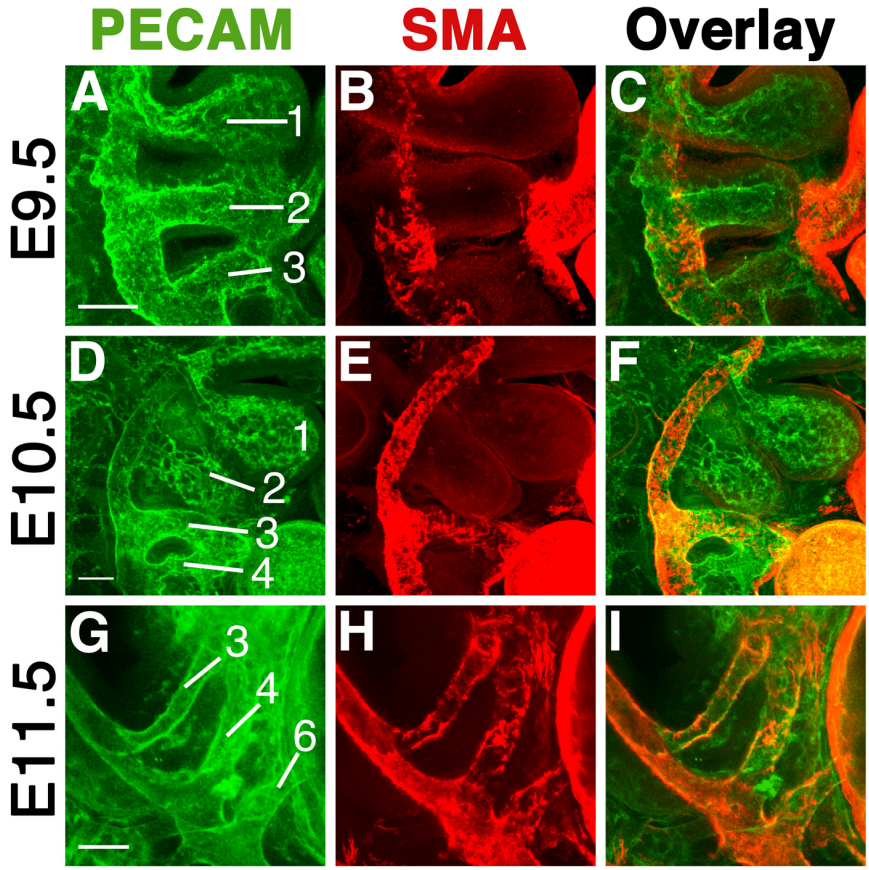

Figure 5.1 Recruitment of vascular smooth muscle cells to the embryonic arch arteries.
Whole mount immunostaining showing the endothelial network (PECAM, green) (A,D,G) and vascular smooth muscle cells (SMA, red) (B.E, H) of wild type embryos at E9.5 (A-C), E10.5 (D-F) and E11.5 (G-I). C, F and I show an overlay of the PECAM and SMA stainings. **A-C:** At E9.5 three embryonic arch arteries are seen (1, 2, 3) connected to the dorsal aorta. SMA positive cells were detected in dorsal aorta and heart but were not detected in the walls of EAA. **D-F**: At E10.5 the first and second aortic arches (1 and 2) started to regress while the third (3) were fully formed. SMA positive cells were seen associated to the dorsal aorta and third arch artery but were absent from the capillary beds of the first and second arches. **G-I:** At E11.5 formation of the 3rd 4th and 6th arch arteries was complete, and they were covered by SMA-positive cells. Right view, scale bar: 100μm.

These results indicate that in their initial stages of development, all EAAs form an endothelial vessel, with a lumen, connected to the heart and dorsal aorta, but that at this initial stage they are not associated with VSMCs. In addition, while the three most caudal EAAs recruit VSMCs to their walls in a rosto-caudal progression, the first and second EAAs never become associated with VSMCs. The embryo shown in Fig. 5.1A-C is particularly informative in this respect because it shows a transition stage. In particular, the first EAA is still a recognizable vessel, with a lumen that opens into the dorsal aorta, but it might already have started physiological regression; the second EAA is a well-formed vessel with a lumen that connects the truncus arteriosus with the dorsal aorta; and formation of the third EAA is almost completed. Therefore, it shows a first arch artery starting regression and a second EAA shortly before the start of this process and no signs of VSMCs were found associated to any of these arteries even at these stages.

These results show an association between the presence or the absence of VSMCs and the persistence or regression of the EAAs. This is consistent with a requirement of VSMCs for stabilization of these arteries, supporting the hypothesis that regression of the two most rostral EAAs could result from their inability to recruit these cells to their walls.

Analysis of VSMCs in abnormally behaving arch arteries of mutant embryos

To further analyse if regression of the embryonic arch arteries could result from the lack of VSMCs we studied the EAAs of two mutant mouse strains, which present abnormal development of these embryonic arteries in a somewhat complementary fashion.

One of these strains is the mutant for the Endothelin receptor A (*ET-A*), which presents abnormal persistence of the second arch arteries in about 25% of the embryos (Yanagisawa et al., 1998). Analysis of *ET-A* null mutants with persistent

second EAAs at E10.5 (Fig. 5.2D) (three embryos) revealed the presence of VSMCs associated to the persistent second arch artery (Fig. 5.2E,F). The size of this artery was consistently smaller than those of wild type E9.5 embryos (Fig. 5.1A), but it remained connected to the dorsal aorta. This result is consistent with the idea that regression of the rostral arches results from their failure to recruit VSMCs to their walls.

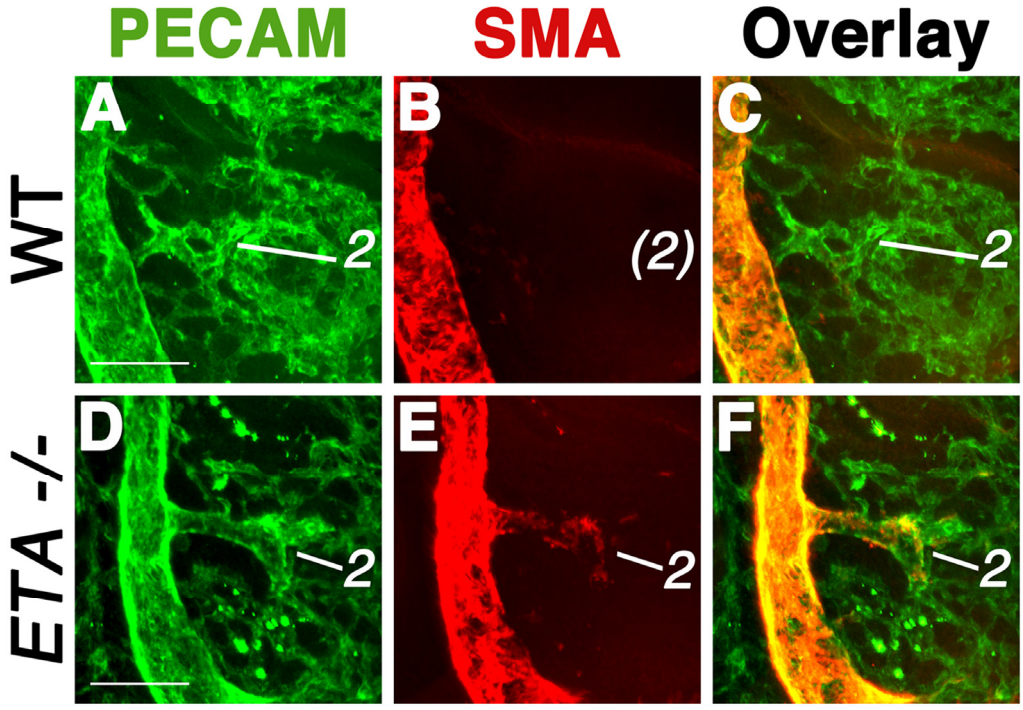

Figure 5.2 Persistent second arch artery in *ET-A* null mutants is covered by VSMCs. Immunostaining for PECAM (A, D) and SMA (B, E) in wild type (A-C) and *ET-A*$^{-/-}$ (D-F) embryos at E10.5 (33ss). C and F show an overlay of the PECAM and SMA stainings. A-C: In wild type embryos, the second arch artery has already regressed (A) and shows no SMA positive cells (B,C). D-F: In *ET-A*$^{-/-}$ embryos a persistent second arch artery (2) can be observed (D), which is is associated with SMA-positive cells (E). Right view, scale bar: 100μm.

Null mutants for the *Pbx1* gene, which codes for a TALE-class homeodomain transcription factor (Burglin, 1997), offered a suitable complementary system to analyse this problem, because in these embryos development of the caudal EAAs is compromised (Manley et al., 2004; Chang et al., 2008). The sixth EAA fails to

form and the fourth arch artery is present in a proportion of mutant embryos at E11.5 but seems to disappear at later stages (Chang et al., 2008). Our analysis of *Pbx1* mutant embryos at E11.0 using anti PECAM antibodies revealed the presence of a third EAA, which was larger than the same artery in wild type control embryos (Fig. 5.3A,D), as previously described in E11.5 embryos (Chang et al., 2008). Additionally, and similar to what has been previously described (Chang et al., 2008), we could not find the sixth aortic arch artery. At this stage, in the four mutant embryos that we analysed, we could observe the presence of the fourth EAA (Fig. 5.3D), which was considerably thinner than its counterpart on wild type embryos (Fig. 5.3A). Staining with anti-SMA antibodies revealed the presence of VSMCs in the third EAA but no traces of these cells could be found in the fourth arch artery (Fig. 5.3E,F). Although it is not possible to determine the fate of the fourth EAAs of these specific E11.0 *Pbx1*$^{-/-}$ embryos, published data indicates that they regress at later stages (Chang et al., 2008). Therefore, our data indicates that in *Pbx1* mutants, only the arch arteries that become associated with VSMCs are maintained from the two caudal EAA that are initially formed, and that those that fail to recruit VSMCs regress prematurely.

Altogether, these results reveal that the correlation between presence or absence of VSMCs and persistence or regression of EAAs is also observed in caudal arch arteries that deviate from their normal development in these mutant mouse models.

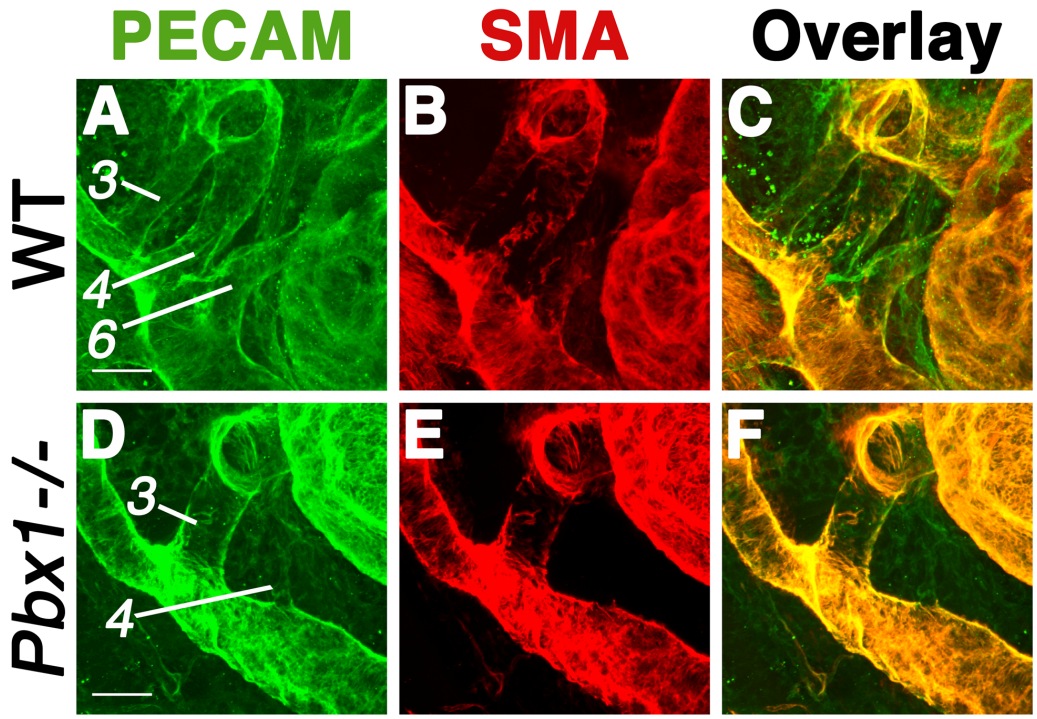

Figure 5.3 Absence of VSMCs in the fourth arch artery of *Pbx1* null embryos. Whole-mount immunostaining with antibodies against PECAM (A, D) or SMA (B, D) of wild type (A-C) and *Pbx1* mutant (D-F) embryos at E11.0 (35-37ss). C and F show an overlay of the PECAM and SMA stainings. **A-C:** At E11.0 all three pairs of caudal arch arteries are observed (3, 4, 6), associated with SMA-positive cells. **D-F:** In *Pbx1*$^{-/-}$ embryos the third arch artery (3) is larger than in wild type littermates and a small fourth arch artery (4) is observed (D). SMA-positive cells are associated to the third but not to the fourth arch artery (E,F). Right view, scale bar: 100μm.

Forced VSMC differentiation produces stabilization of the second arch artery.

The above results reveal a correlation between the VSMCs and stability of EAAs both under normal and mutant conditions. To understand if recruitment of VSMCs is instrumental in the stabilization of these arch arteries, we designed an experiment to force VSMC differentiation from neural crest cells anterior to the third branchial arch to see if this would be enough to stabilize the most rostral EAAs. For this, we created transgenic embryos expressing *Myoc* and *Mkl2*, two transcription factors known to be coactivators of smooth muscle cell differentiation

(Wang et al., 2001; Wang and Olson, 2004; Li et al., 2005; Pipes et al., 2006), under the control of the neural crest enhancer of the *HtPA* gene (Pietri et al., 2003). We observed persistent second EAAs at E10.5 (Fig. 5.4G, compare with littermate control Fig. 5.4D) in a fraction of *HtpA-Myoc::Mkl2* embryos (3/13). Despite the low number of transgenic embryos showing this phenotype, it should be noted that all of these persistent second arch arteries were associated with VSMCs (Fig. 5.4H,I, compare with littermate control Fig. 5.4E,F). In contrast, all other transgenic embryos in which the first two arch arteries regressed as in wild type (Fig. 5.4D-F) embryos had no signs of VSMC differentiation in these arches.

The low number of transgenics with this phenotype could result from a variety of experimental problems, including low activity of the promoter or inefficiency of *Myoc* and *Mkl2* to dominantly promote VSMC differentiation in this cellular context. To make sure that persistence of the anterior EAAs was associated with transgene expression, we cut the transgenic embryos in half sagitally and analysed expression of *Myoc* in one side of the embryo and stained the other half with PECAM/SMA antibodies. In most embryos, *Myoc* expression was similar to wild type embryos (Fig. 5.4 J,K), and when overexpression in the cranial arches was observed its levels were rather low (Fig. 5.4L), indicating that either the activity of this promoter was not very strong or that the stability of the *Myoc* mRNA was low. However, and importantly, only those embryos in which *Myoc* overexpression was observed presented SMA positive cells together with a persistent second aortic artery.

These results indicate that forced VSMC differentiation in the branchial arches is associated with persistence of EAAs that regress under normal conditions, which is consistent with the hypothesis that the absence of VSMC recruitment to the wall of the EAAs is a major determinant of the physiological regression of the rostral embryonic arch arteries.

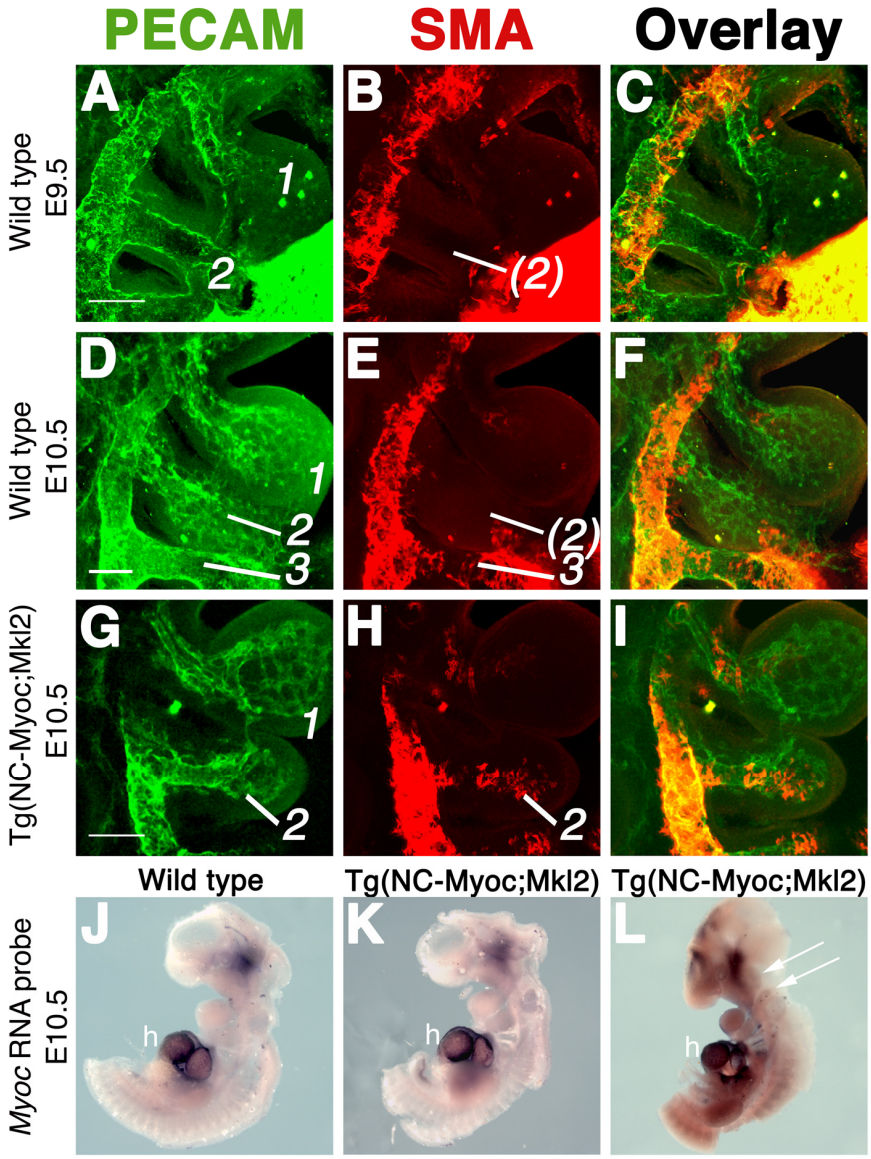

Figure 5.4 *HtpA-Myoc::Mkl2* transgenic embryos contain a persistent second arch artery covered by VSMCs.
Whole-mount immunostaining with antibodies against PECAM (A, D, G) or SMA (B, E, H) of wild type embryos at E9.5 (A-C) or E10.5 (D-F) and in *HtpA-Myoc::Mkl2* transgenic embryos at E10.5 (G-I). C, F and I show an overlay of the PECAM and SMA stainings. A persistent second arch artery can be observed in *HtpA-Myoc::Mkl2* transgenic embryos (G) at a stage in which this artery is already regressing in wild type embryos (D). The persistent second arch artery of *HtpA-Myoc::Mkl2* transgenics is associated with SMA-positive cells (H, I), a situation not seen in the second arch artery of wild type controls at any stage (B, C, E, F). 1, 2, 3: first, second and third embryonic arch arteries. Right view,

scale bar: 100μm. J-L: *In situ* hybridization of the left side of the wild type (J) and *HtpA-Myoc::Mkl2* transgenic (K, L) embryos using a *Myoc* antisense probe. Wild type embryos and a fraction of *HtpA-Myoc::Mkl2* transgenic embryos (J, K) only show *Myoc* expression in the heart. L: A few *HtpA-Myoc::Mkl2* transgenic embryos also show *Myoc* expression in migratory neural crest cells that populate the branchial arches (arrows). h, heart.

DISCUSSION

While formation of the heart outflow tract starts with the sequential formation of five pairs of embryonic arch arteries, only the three most caudal contribute to the mature arterial tree. The two rostral pairs undergo physiological regression (Hiruma et al., 2002). The data we present in this manuscript suggest that regression of the first and second arch arteries results from their failure to recruit vascular smooth muscle cells (VSMCs) from the surrounding mesenchyme. Several lines of evidence support this hypothesis. In normal embryos, while the three caudal EAAs become associated with VSMCs after they formed an endothelial vessel, we were unable to find those cells in the walls of the first and second EAAs at any stage of their development. In addition, analysis of a few mutant conditions was also consistent with this hypothesis. Perhaps, the most compelling evidence was provided by the stabilization of the second EAAs when formation of VSMCs was experimentally promoted by the expression of *Myoc* and *Mkl2* in the neural crest migrating into the branchial arches. In these embryos, stabilization was always associated with VSMC recruitment to the vessel. We also observed an association between EAA persistence or regression and the presence or absence of VSMCs in two other mutant conditions. In particular, we found that persistent second embryonic arch arteries of *ET-A* mutant embryos (Yanagisawa et al., 1998) were always associated with VSMCs and that the fourth EAAs of *Pbx1* mutant embryos, which regress around E11.5 (Chang et al., 2008), were not associated with VSMCs at E11.0. A role for the absence of VSMCs in the regression of the first and second EAAs is also consistent with published data showing strong vascular phenotypes resulting from blocking recruitment of mural cells, which seemed to derived from a failure in vessel stabilization (Benjamin et

al., 1998; Oh et al., 2005).

Although intrinsic factors in the endothelia of the first and second arch arteries cannot be excluded, the most probable cause for the failure of these EAAs to recruit VSMCs is the absence of cardiac neural crest cells in the corresponding branchial arches. The VSMCs of the aortic tree derive from the cardiac neural crest cells (Le Lievre and Le Douarin, 1975; Jiang et al., 2000; Snider et al., 2007) and not from the mesoderm, which is the origin of these cells in most of the embryo (Mikawa and Gourdie, 1996; Vrancken Peeters et al., 1999; Pouget et al., 2006). As the cardiac neural crest cells populate only the third and more caudal branchial arches, the first two EAAs never come in contact with this neural crest subpopulation and thus cannot recruit VSMCs from them. Clearly, the mesoderm also fails to contribute VSMCs to the first and second aortic arteries.

The role of cardiac neural crest cells in the stabilization and remodelling of the EAAs has been recognized for already more than two decades. Classical experiments with avian embryos showed that ablation of these cells produces strong vascular phenotypes in the area derived from the EAAs (Kirby et al., 1983; Bockman et al., 1987; Bockman et al., 1989). Interestingly, in a study centered on the third arch artery, it was shown that cardiac neural crest cells are not required for the formation of the endothelial EAA but for its maintenance after the artery was formed and allowed blood flow (Waldo et al., 1996). As the destabilization of the artery was previous to the formation of the tunica media, it is very probable that it was a consequence of the lack of neural crest-derived VSMCs. The situation we have described for the first two EAAs is very similar to the phenotype resulting from these neural crest ablation experiments. In the initial stages of development the presence of the first two arches is essential to allow blood circulation from the heart into the dorsa aorta. However, the blood flow will also act as a destabilizing factor for these endothelial arteries, as it happened in the neural crest-depleted third EAAs described in Waldo et al., 1996. While in normal third (and probably more caudal) EAAs the endothelial artery becomes stabilized by recruitment of neural crest-derived VSMCs, the first and second EAAs cannot

reverse the destabilization process because of their failure to recruit VSMCs to their walls, eventually leading to physiological regression. As a consequence of the differential remodelling process, the third, fourth and sixth EAAs form a symmetric aortic tree composed of stabilized EAAs, which will provide the substrate on which processes like apoptosis (Molin et al., 2002; Poelmann and Gittenberger-de Groot, 2005) or differential blood flow (Yashiro et al., 2007) will produce asymmetric remodelling.

In this context, it should be noted that the vascular phenotype of *Pbx1* mutants may also originate from compromised VSMC production. While the absence of the sixth EAA in *Pbx1* mutant embryos might derive from their failure to form caudal branchial arches, which prevents separation of individual vessels (Manley et al., 2004; Chang et al., 2008), their alterations in the fourth EAA must have a different origin, as this artery can be detected initially (Chang et al., 2008; our data in this manuscript). We have shown that these fourth EAAs fail to recruit VSMCs after the endothelial artery was formed. Therefore, it is very probable that regression of this artery could be linked to the absence of smooth muscle cells, which could be a consequence of alterations in cardiac neural crest development resulting from the transient downregulation of *Pax3* observed in the hindbrain of these embryos (Chang et al., 2008).

Concomitantly, we have also shown recruitment of smooth muscle cells to the second arch artery of *ET-A* mutant embryos. This was surprising because previous reports have indicated that the absence of endothelin signalling compromises development of the smooth muscle cells associated to the caudal EAAs, eventually leading to a variety of malformations in the heart outflow tract (Clouthier et al., 1998; Yanagisawa et al., 1998). This apparent contradiction, which was also observed in mutants for the endothelin converting enzyme 1 (*ECE-1*) (Morishima et al., 2003), might be due to the fact that endothelin signalling in the rostral and caudal EAAs acts on different cell substrates. The mutant phenotype in the caudal EAAs could derive from a requirement of endothelin signalling for the differentiation of cardiac neural crest cells into smooth

muscle cells. In the rostral arches endothelin signalling cannot activate this process as no cardiac neural crest cells are available and the absence of VSMCs indicates that the mesoderm is also unable to contribute these cells to the EAAs in this area. Intriguingly, the second EAA succeeds in recruiting VSMCs in the absence of endothelin signalling. Whilst we do not know the origin of these cells, it is possible that they could originate from mesodermal cells regaining their differentiation potential into VSMCs or from non-cardiac neural crest cells. If this is the case, it would mean that one of the functions of endothelin signalling in the branchial arches is to prevent mesenchymal cells of an origin other than the cardiac neural crest from contributing to the vascular tunica in this area, whilst also promoting their recruitment from the cardiac neural crest cell population.
Although it is not well known how the smooth muscle cells stabilize the endothelial tubes and prevent them from regressing, apart from providing structural support, our data contribute to deepen the knowledge in the etiology of developmental defects caused by impaired remodelling of the embryonic arteries as regulation of vascular integrity is a key process for human physiology and pathology.

MATERIAL AND METHODS

Mice

The *Pbx1* and *ET-A* mutant mice were described previously (Yanagisawa et al., 1998; Selleri et al., 2001). *Pbx1* null mutants and wt littermates were analysed at the 35-37 somite stage and the *ET-A* mutants that we had analysed had 33-34 somites. To generate *HtpA-Myoc::Mkl2* transgenic embryos, two individual constructs were produced, one with *Myoc* and one with *Mkl2*. For this, the *Myoc* (Wang et al., 2001) and *Mkl2* (Oh et al., 2005) cDNAs were cloned downstream of the *HtPA* enhancer that drives expression in the neural crest (Pietri et al., 2003), followed by the SV40 polyadenylation signal. The purified constructs were mixed in a 1:1 proportion and used to generate double transgenic mice by pronuclear

injection according to standard protocols. The *HtpA-Myoc::Mkl2* transgenic embryos were identified by PCR on DNA isolated from the yolk sacs using the following primers: Myoc-F: 5´ATGACACTCCTGGGGTCTGAAC-3; Myoc-R:5´-GCGATCTTCTCATTGAGGTC-3; Mkl2-F: 5´-GAAGAGTCCAGCAGCATTCC-3´; Mkl2-R: 5´-ACTCGCCATGAGTGTGAGG-3'.

Immunofluorescence staining and phenotypic analysis

Fluorescent immunostaining on whole mount embryos was adapted from previously described protocols (Foo et al., 2006) with small modifications. In brief, embryos were isolated, fixed overnight at 4ºC in 4% paraformaldehyde (made in phosphate buffered saline, PBS), transferred to 100% methanol, rehydrated and blocked in PBS containing 1% BSA and 0.5% Tween20-100 (PBX) for 4 hours at room temperature. They were then incubated overnight with the primary antibody rat anti-mouse PECAM-1 MEC13.3 (Pharmingen, 1:100) at 4°C with gentle agitation. Embryos were washed five times (45 each) in PBS containing 0.5% Tween 20 (PBT), incubated overnight at 4°C with the primary antibody α-SMA, Cy3-conjugated (Clone1A4, Sigma, 1:400) and the secondary antibody goat anti-rat IgG, Alexa 488-conjugated (Molecular Probes, 1:100). Samples were washed five times 45 min each in PBT at room temperature, dehydrated to methanol and cleared and mounted in Methyl Salicylate. Images were acquired with a Leica TCS SP5 confocal microscope. Z-projections of the confocal stacks were processed using ImageJ (v1.42g) and Adobe Photoshop CS4.
Whole mount *in situ* hybridization was performed as described in (Kanzler et al., 1998) using an antisense riboprobe for *Myoc*.

ACKNOWLEDGEMENTS

This work was funded by Centro de Biologia do Desenvolvimento (BIOS-LVT-Oeiras-664), Pfizer grant (João Cid dos Santos - 2004) and FCT grant POCTI/BIA-BCM/60420/2004 to M. Mallo and a FCT scholarship

SFRH/BD/18620/2004 to F. Moraes. We thank S. Dufour for providing the HtPA promoter, E. Olson for providing pcDNA3.1-Myoc and pcDNA3.0-Mkl2 plasmids, G. Martins for staining imaging troubleshooting; J. Rowland, A.T. Tavares, C. Freitas, R. Carvalho and Marta Costa for critical support and helpfull discussions.

Chapter 6:
General Discussion

GOALS

The main focus of this thesis was to further understand the morphogenetic events of the cell populations and the genetic players involved in the development of craniofacial area and the pharyngeal system. It is important to understand what happens when this development is compromised giving rise to several malformations in mice that model most of the congenital defects in humans.
More specifically some of the goals were to:

- Discover the role of *Tbx1* in the mammalian ear development.
- Discover the function of *Bmp2* in the induction of neural crest during mouse development.
- Determine the function of vascular smooth muscle cells in the remodelling of the embryonic arteries.

CONCLUSIONS

The major conclusions from this thesis are:

- *Tbx1* is essential for inner ear development having a global role in keeping normal patterns within the otic vesicle. In addition, it is also required to maintain the segregation of neural crest streams.
- *Bmp2* is required for the migration of the neural crest but not for its induction.
- The lack of recruitment of vascular smooth muscle cells around the cranial arch arteries appears to be one of the major reasons for the regression of these vessels during development.

DISCUSSION

The findings obtained during the course of this thesis were discussed in the specific results chapters. In this section, I will discuss the most important results incorporating them with relevant and more recently published work.

1. The role of *Tbx1* in mouse embryonic development

The role of *Tbx1* in inner ear development

The work described in **Chapter 2** involved characterization of the ear phenotype of null mutant embryos for the *Tbx1* gene. TBX1 is the major genetic determinant for the pharyngeal arch-derived defects observed in individuals with DiGeorge syndrome, characterized by severe malformations in the derivatives of the pharyngeal system (Scambler, 2000; Yagi et al., 2003). Most patients have ear defects associated with hearing impairment (Greenberg, 1989; Digilio et al., 1999; McDonald-McGinn et al., 1999; Reyes et al., 1999). We showed that *Tbx1* is essential for the development of all three compartments of the mouse ear and the defects seem to be a consequence of different cell populations. Our observations of *Tbx1* mutant mouse embryos showed that inner ears were hypoplastic without any structure that could be designated as cochlear or vestibular compartments. Although the complete sensory organs do not form, some signs of differentiation were observed within these strongly affected structures. We could observe the presence of sensory patches that contained specified hair cells in the residual inner ear epithelium of the *Tbx1* mutant embryos. Also in these mutants the endolymphatic duct was present even though it was bigger than in wild type controls.

Severe inner ear phenotypes involving developmental arrest of otic vesicle, were also found in mice mutant for *Eya1* or *Six1*, two genetically linked genes that seem to act upstream of *Tbx1* (Zheng et al., 2003; Ruf et al., 2004; Friedman et al., 2005). Increased apoptosis in the *Eya1* null mice and a combination of

abnormal cell death and proliferation in the Six1 mutant embryos is the underlying cellular mechanism for the otic vesicle phenotype in *Eya*$^{-/-}$ *and Six1*$^{-/-}$ mice (Xu et al., 1999; Laclef et al., 2003; Zou et al., 2004, Friedman et al., 2005). On the other hand, the phenotypes of *Tbx1* null mutants do not seem to be a consequence of these effects since previous studies did not observe any difference in apoptosis or cell proliferation between *Tbx1* mutants and their littermates (Vitelli et al., 2003). In addition, another important difference is that, in our observations, *Tbx1* mutant inner ears retain some degree of cell differentiation, which has not been reported in these mutants previously. Furthermore, the ear defects in *Eya*$^{-/-}$ *and Six1*$^{-/-}$ mutants correlate with the expression domains of the genes, whereas in *Tbx1* mutants, the global effects observed (e.g. deeply affected vestibular and cochlear regions) are not directly associated with the *Tbx1* expression pattern. Although expression of *Tbx1* in the otic vesicle correlates with the future vestibular area, it is transcribed only in a small area overlapping with the prospective cochlear domain (*Pax2*-positive). Therefore, either *Tbx1* has different activities across different areas of the otic epithelium or it is involved in more general functions in the otocyst.

Several lines of evidence support the existence of compartmental boundaries of gene expression within the otic vesicle leading to the divergence of epithelial cell lineages (Fekete and Wu, 2002). Our data shows that the establishment of early molecular patterns in the otocyst seems to occur normally in the absence of *Tbx1*, as estimated by the normal distribution of several relevant markers in the otic vesicles of E9.5 *Tbx1* mutant embryos (*Pax2*, *Nkx5.1*, *Gbx2*, *Lfng*, *NeuroD*, *Sox10*). However, one day later, obvious molecular alterations can be observed in the spatial distribution of transcripts for some relevant genes, which are not restricted to a particular type of process, but seemed to affect the otic vesicle globally. As the expression patterns in *Tbx1* mutant otic vesicles changes from normal (around E9.5) to altered (at E10.5), it is possible that *Tbx1* is required for the autonomous conservation of patterns after they have been generated by environmental signals. Consistent with this hypothesis is the highly regionalized

expression of *Tbx1* suggesting that control of cell segregation may be part of this mechanism. Our data suggests that *Tbx1* is required for regional specification within the otocyst and this role is cell autonomous in the otic epithelium.

Since *Tbx1* is expressed dynamically in a variety of surrounding tissues apart from the otic vesicle (such as pharyngeal arch endoderm and periotic mesoderm) tissue-specific gene inactivation strategies are required to dissect the specific contributions of *Tbx1* activity during inner ear development. In fact, recent studies have addressed this issue and are partly in agreement with our data that indicate a cell autonomous role of *Tbx1* in the otic vesicle (Arnold et al., 2006a). In particular, conditional inactivation of *Tbx1* using different Cre lines that specifically ablate *Tbx1* in the otic epithelium lead to severe hypoplasia of the sensory organs and expanded neurogenesis (Arnold et al., 2006a). These effects are similar to what we and others have observed in *Tbx1* global null embryos (Raft et al., 2004). These authors (Raft et al., 2004; Arnold et al., 2006a) suggest that *Tbx1* specifies a midline boundary between the anterior (neurogenic and sensory) and posterior (sensory) regions of the otic vesicle, restricting the neurogenic potential within the otocyst. Together these studies show that in *Tbx1* null mutants the expression domains of anteriorly-expressed genes (such as *NeuroD1*, *Lfng* and *Fgf3)* lose their normal anterior restriction in the otocyst and expand into more posterior regions. In contrast, the expression domains of posteriorly-expressed genes (such as *Otx1, Otx2)* are abolished (Vitelli et al., 2003; Raft et al., 2004; Arnold et al., 2006a). However, in our work, the down-regulation of posteriorly-expressed genes was not a rule (the posterior expression domains of *Nkx5.1* and *Pax2* were not abolished). Moreover, we argue that the restriction of the neurogenic area is part of the more global role of *Tbx1* in keeping normal patterns within the otic vesicle, because we also observe expansion of other domains apart from sensory/neurogenic at the same stage of inner ear development in *Tbx1* null mutants. This role of *Tbx1* in maintaining compartmentalized expression patterns is mediated by its expression within the otic epithelium rather than by its expression in the surrounding mesenchyme (Arnold et al., 2006a). This is in

agreement with previous observations showing that after a certain stage, development of the otic vesicle is independent of external cues (Swanson et al., 1990; Torres and Giraldez, 1998). Nevertheless, surrounding tissues provide the extrinsic factors that are responsible for setting of the initial patterns in the otocyst (Baker and Bronner-Fraser, 2001). As shown by our data at E9.5, this process seems to be independent of *Tbx1.*

It will be important to identify the neighbouring cellular environments that could regulate this process. As already mentioned in the introduction, the developing hindbrain could provide at least part of this regulation. For example *kreisler* mutant mice, which have a complete absence of r5 and r6, display severe malformations of the semicircular canals and cochlea in the absence of expression of this gene in the developing ear (McKay et al., 1994; Choo et al., 2006). Similar to this phenotype, *Gbx2* mutants show that the hindbrain abnormalities also perturb the otic patterning leading to an expansion of the ventral *Otx2* domain (Lin et al., 2005; Choo et al., 2006). In the context of a compartment boundary model of the developing otocyst, expansion of expression domain of relevant genes, such as *Otx2*, disrupts the normal cochlear compartment boundary and could be linked to the cochlear phenotype observed in both mouse mutants.

In an attempt to reconcile theories of hindbrain effects on the developing otic vesicle and a compartment model of otocyst patterning it would be important to determine whether loss of hindbrain genes (*Gbx2* or *Kreisler*) affects *Tbx1* activity in the otic vesicle and how this molecular pathway could mediate the abnormal patterning events observed in *kreisler* and *Gbx2* mutant otocysts. Although *Tbx1* has been proposed as a key suppressor of the neurogenic fate in otic epithelial cells (Raft et al., 2004; Arnold et al., 2006a), recent studies in *kreisler* null mutants did not observe any effect on *Tbx1* expression, even in areas that show ectopic neuroblast specification (Vazquez-Echeverria et al., 2008). This recent study is in agreement with our results favouring the idea that *Tbx1* is a key factor in maintaining compartmentalized expression domains to guarantee correct cell fate

rather than setting early expression patterns for neurogenic cell specification (Vazquez-Echeverria et al., 2008). Therefore, the notion that *Tbx1* is a key player in antagonizing the neuronal fate (Raft et al., 2004, Arnold et al., 2006a) is not supported by our data and could not be confirmed by this recent work (Vazquez-Echeverria et al., 2008). The extrinsic signals that could directly regulate *Tbx1* expression in otic epithelium remain to be discovered.

Impaired neural crest migration in *Tbx1*$^{-/-}$ embryos.

The middle ear skeleton components were strongly affected in *Tbx1* null embryos due to a combination of underdeveloped branchial arches and misrouting of neural crest cells. In the *Tbx1* mutants most of the neural crest cells arising caudally to r3 are not able to populate second and more caudal branchial arches, which are missing or underdeveloped in the mutant (Jerome and Papaioannou, 2001; Vitelli et al., 2002a; and this study). The strong deficiencies in these arches and corresponding neural crest population could explain the skeletal phenotypes observed in the derivatives from these areas. For the malleus, incus and tympanic ring, all first arch derivatives (Mallo, 1998), an expected explanation for their phenotype is the misrouting of *Hoxa2*-positive cells into the first arch in the *Tbx1* mutants. *Hoxa2* is a key player in the determination of the skeletal identity of second arch derivatives (Gendron-Maguire et al., 1993; Rijli et al., 1993) and misexpression of this gene in the first arch has been shown to produce strong hypoplastic phenotypes in the skeleton derived from this area (Mallo and Brandlin, 1997; Creuzet et al., 2002). As a result, the aberrant migration of *Hoxa2* expressing neural crest cells originating from r4 into the first branchial arch may interfere with normal skeletal development in this arch. It seems *Tbx1* is required for proper migration of the neural crest cells into the branchial arches. However *Tbx1* is not expressed in neural crest cells suggesting that *Tbx1* may be acting non-cell autonomously in directing the migration pathways of cranial neural crest cells. Neural crest defects observed in *Tbx1* null mutants are likely to be secondary to the lack of *Tbx1* activity in surrounding tissues. The primary defect

possibly lies in the mesoderm or endoderm, which are the main regions of *Tbx1* expression. In fact FGF and retinoid signalling from the ectoderm and endoderm are key regulators of neural crest cell migration, survival and differentiation (Pratt et al., 1987; Lee et al., 1995; Trumpp et al., 1999; Kubota and Ito, 2000; Trokovic et al., 2003). For example treatments of mouse embryos with retinoic acid in culture results in the ectopic migration of second arch neural crest cells into the first arch (Trainor and Krumlauf, 2000), which interestingly mimics the *Tbx1* mutant neural crest cell migration phenotype that we observe. Moreover these FGF and retinoid pathways have been shown to interact with *Tbx1* (Vitelli et al., 2002b; Guris et al., 2006; Moon et al., 2006;).

Our work, together with recent studies highlights the importance of studying essential interactions between neural crest cells and the endoderm, mesoderm and ectoderm for proper craniofacial development. Previous studies already had shown abnormal neural crest cell (NCC) distribution in *Tbx1* homozygous mutants (Vitelli et al., 2002a). These NCCs were able to migrate but they appear to lack appropriate directional cues consistent with a disorganization of the pharyngeal system in *Tbx1*. In fact in the null mutants for *Tbx1* all the caudal pharyngeal arches were extensively disorganized leading to major cardiovascular defects (Jerome and Papaioannou, 2001).

Considering that major cardiovascular phenotypes are related with defects in neural crest development it is possible that cardiovascular anomalies such as those seen in DiGeorge syndrome in which *Tbx1* mutations are implicated, may occur as a secondary consequence of defects in neural crest migration, which is affected in the absence of this gene. However the interactions between neural crest and surrounding tissues are so varied that it would be important to understand at which stage and on which process are these cells important. In order to achieve this goal, we produced transgenic reporter mouse lines with endothelial and neural crest cells expressing the fluorescent GFP and RFP proteins, respectively (**Chapter 4**). These transgenic mouse lines, *Tie2-GFP;HtPA-RFP,* when introduced into the *Tbx1* null background, confirmed the

phenotype of these mutants already described by other methods in **Chapter 2**. It would be interesting for future work to use these promising genetic tools to study the dynamics of these cell populations over time in cultured mammalian embryos. Recent studies in mice have determined that the major cause leading to DiGeorge syndrome phenotype is the cell autonomous role *Tbx1* exerts in the endoderm (Arnold et al., 2006b). This work has shown that complete inactivation of *Tbx1* in the pharyngeal endoderm mimics the phenotype of *Tbx1* null mutants in the pharyngeal area and demonstrated an early role for the gene in the patterning and outgrowth of the pharyngeal pouches (Arnold et al., 2006b). The lack of segmentation of the pharyngeal arches in these conditional mutants, affects neural crest-mesenchyme and ultimately, cause malformations in the derivatives of the pharyngeal system. These results support the notion that pharyngeal endoderm is an essential source of inductive signals, which are necessary for proper development of the pharyngeal apparatus and its derivatives. In agreement with this idea other studies have shown that retinoid acid signalling is essential for patterning the endoderm of the posterior pharyngeal arches and affects neural crest cells and angioblasts only secondarily (Wendling et al., 2000). Therefore, these studies argue against our suggestion above that neural crest is the primary cause of the DiGeorge phenotype. However, as it will be discussed below the neural crest might have a role in the later stages of development, during morphogenesis of pharyngeal arch derivatives.

2. The role of BMP signalling in neural crest

We have taken advantage of the tool we have produced, described in **Chapters 3** and **4**, the reporter mouse line for migratory neural crest *Tg(HtPA-RFP)*, to complete several investigations. Firstly to study *Tbx1* null phenotype, and simultaneously we have started to analyse with more detail, the neural crest development of *Bmp2* null mutants described in **Chapter 3.** Briefly, the fluorescent reporter mouse line for neural crest cells was introduced into the

Bmp2 null background and this transgenic approach together with molecular analysis showed that neural crest cells are induced in *Bmp2* null mutant embryos, but are not able to migrate out of the neural tube.

The role of BMP signalling in neural crest induction and migration has been extensively anaylsed in several model organisms and most of the times, the results have been conflicting across species.

Studies in *Xenopus* and zebrafish suggested that neural crest induction could be explained by a response of the ectoderm to a precise threshold concentration gradient of BMP signalling, considered to be crucial for this process (Mayor et al., 1995; Marchant et al., 1998; Barth et al., 1999). However, other studies in frogs showed that BMP signalling alone is not sufficient for neural crest induction *in vivo* and there is a direct requirement for a Wnt signal for this process to occur (LaBonne and Bronner-Fraser, 1998). Initial studies in chicken embryos showed that *Bmp4* and *Bmp7,* expressed in the dorsal epidermis, were implicated in neural crest induction (Liem et al., 1995; Selleck et al., 1998), although *Bmp2* did not appear to be relevant in this process (Liem et al., 1995). By contrast, in mouse embryos, mutations in *Bmp4* or *Bmp7* do not produce any obvious deficiencies in cranial neural crest development (Dudley et al., 1995; Luo et al., 1995; Winnier et al., 1995). Furthermore, the idea that *Bmp4* and *Bmp7* were sufficient to induce neural crest cells was confronted later by work from Garcia-Castro and colleagues (2002) showing that induction of neural crest cells *in vitro* was not only dependent of BMP signals but also depends on the simultaneous activity of other factors (Garcia-Castro et al., 2002). Functional redundancy could explain the lack of an effect. However, even mouse embryos mutant for both *Bmp7* and *Bmp5* also present normal patterns of neural crest cell formation and migration (Solloway and Robertson, 1999).

In mammalian embryos, the strongest evidence for a role of BMP signalling in neural crest cell production derives from previous work from Mallo and co-workers (Kanzler et al., 2000). In order to disrupt BMP signalling in neural crest cells, without the misleading interpretations caused by functional redundancy, *Xenopus*

noggin was expressed in areas of the neural tube corresponding to the origin of neural crest that migrates to the second and more caudal branchial arches. The results from this biochemical block of BMP signalling are in agreement with the work presented in **Chapter 3** using *Bmp2* mutants, in the sense that in both studies the migration of cranial neural crest cells was almost completely abolished. However, in this previous work (Kanzler et al., 2000), the existence of neural crest cells was assayed by the expression of the neural crest cell marker *Crabp1*, which labels the migratory population, and markers of neural crest cell formation, such as *Snail2,* were not used. Therefore, it was not possible to rule out the hypothesis that neural crest cells formed but failed to migrate. Our results using molecular markers such as *Snail2*, showed that neural crest induction indeed occurs in *Bmp2* mutant embryos, indicating that *Bmp2* is not essential for the induction of neural crest but rather for its migration from the neural tube. An important implication of these results is that the role of *Bmp2* in mouse neural crest development might be somewhat different to chick, frog and zebrafish embryos, where the emphasis lies with Wnt signalling. For example in avian embryos, it has been proposed that *Cad6b* and *Wnt1* were downstream mediators of BMP signalling in the induction of migratory properties in neural crest cells (Sela-Donenfeld and Kalcheim, 1999; Burstyn-Cohen et al., 2004). Instead, our results do not show any downregulation of these genes in the absence of *Bmp2*, even though the neural crest cells could not migrate in these mutants.

Since there were no detectable differences in apoptosis and at the same time the neural crest migration was abolished, we could think that the specified neural crest would accumulate in the neuroepithelium. Interestingly, we observed the neuroepithelium of *Bmp2* mutant embryos is undoubtedly larger than wildtype and is abnormally folded. Recent studies, using *Bmp2* chimeras from *Bmp2* null ES cells and wildtype blastocysts, have shown that *Bmp2* is required for neural tube closure (Castranio and Mishina, 2009). According to this recent work, the defects in neural crest migration in *Bmp2* mutants may be consequence of anomalies during neural tube closure. An alternative or complementary explanation for the

lack of migratory cells would be that *Bmp2* is involved in triggering cell delamination and/or movement away from the neural tube, and in these mutants the neural crest cells that cannot migrate accumulate in the neuroectoderm. Segregation of neural crest from dorsal neuroepithelium, is mediated by early neural crest specifiers, such as *Pax3* (Le Douarin and Kalcheim, 1999). Interestingly in this recent study, the authors also used a *Bmp2* mouse line maintained in a mixed genetic background once these lines are generally less vulnerable to genetic defects. Therefore, they could survive at later stages, enabling analysis of *Bmp2* during neural tube closure. In these embryos *Pax3* expression is absent in the unclosed neural tube regions in *Bmp2* mutants, supporting a possible mechanism that prevent neural crest migration in these mutant embryos mediated by the *Pax3* gene (Castranio and Mishina, 2009).

One of the crucial steps in neural crest development is the migration of neural crest cells from the neural tube to their final destinations throughout the body. The formation of neural crest cells is associated with their delamination and emigration from the neural tube and it has been difficult to distinguish between a failure of neural crest cell induction versus a complete failure of neural crest migration largely because the latter depends on the former. Prior to our work described in **Chapter 3** most of the analysis of the induction and specification of neural crest cell in mammalian embryos were intimately related to aberrant streams of neural crest cells observed *in vivo* and *in vitro*. Our work describes for the first time a mouse model where neural crest cells were induced to form but failed to migrate. Additionally our work supports the idea that the molecular mechanisms required for neural crest development have diverged across species.

3. Neural crest role in the remodelling of the embryonic arch arteries

During the course of this thesis, we analysed *Tbx1* and *Bmp2* mutant mouse embryos and observed that either *Bmp2* or *Tbx1* absence cause neural crest migration defects to different extents. Several studies have shown that both

mutant embryos have compromised aortic arch development associated with neural crest abnormalities (Ohnemus et al., 2002; Vitelli et al., 2002a). Indeed, fate mapping experiments in the mouse revealed a strong contribution of neural crest cells to structures derived from the embryonic arch arteries (Jiang et al., 2000). These results were also shown in chicken embryos where it was revealed that a subpopulation of neural crest cells, called cardiac neural crest, migrate to caudal pharyngeal arches and differentiate into smooth muscle cells contributing to the walls of the arteries that exit the heart (Kirby et al., 1983; Le Douarin and Kalcheim, 1999). Ablation of these cells in avian embryos produces strong vascular phenotypes in the area derived from the embryonic arteries (Kirby et al., 1983; Bockman et al., 1987; Bockman et al., 1989). Therefore, proper development of the aortic arches requires the presence of cardiac neural crest cells (Kirby et al., 1983; Bockman et al., 1987; Bockman et al., 1989; Waldo et al., 1996; Waldo et al., 1998).

BMP signalling seems to have a role in the biology of this neural crest population. Inactivation of BMP signalling in the mouse neural tube resulted in heart outflow tract phenotypes resembling the DiGeorge syndrome (Ohnemus et al., 2002), most probably due to its effects on neural crest migration. Studies in mice involving Bmp receptors have shown that when BMP receptor IA is ablated from neural crest before their migration, these embryos present a shortened outflow tract and defective septation, and die before birth due to acute heart failure (Stottmann et al., 2004). In addition, tissue-specific inactivation of BMP receptor-Alk2 in neural crest, also causes persistent truncus arteriosus because not enough cells reach the outflow tract to effect normal septation. Moreover these mice present abnormal maturation of the arch arteries due to deficient differentiation of neural crest to smooth muscle around these vessels (Kaartinen et al., 2004).

Along with these observations related to BMP signalling, the transcription factor *Tbx1* plays a vital role in aortic arch development and is a major contributor to cardiovascular disease associated with DiGeorge syndrome, as mentioned in the

introduction. Heterozygous inactivation of *Tbx1* causes anomalies in heart outflow tract development and impairment of neural crest-derived smooth muscle cell differentiation (Lindsay et al., 2001; Merscher et al., 2001; Kochilas et al., 2002). Considering these *Tbx1* and *Bmp2* studies as examples, these findings are likely to be applicable to a broad range of smooth muscle related disorders, specifically those involving neural crest derived smooth muscle (Epstein et al., 1991; Feiner et al., 2001; Yanagisawa et al., 1998; Abu-Issa et al., 2002; Brewer et al., 2002; Ohnemus et al., 2002; Vitelli et al., 2002a; Wang et al., 2006; Varadkar et al., 2008). It is important to acknowledge that a common mechanism for impaired stabilization and remodelling of the embryonic arch arteries has been clearly shown to be related to cardiac neural crest defects, and more specifically with the ability of neural crest to differentiate into smooth muscle. Nevertheless, a detailed analysis of neural crest-derived smooth muscle recruitment around the pharyngeal arch arteries and subsequent interpretation of mutant vascular phenotypes has proven challenging due to the inability to observe the vasculature of mouse embryos as a whole. Most published characterizations of the aortic arches have been performed using a variety of staining techniques on histological sections (Bergwerff et al., 1999; Oh et al., 2005; Gittenberger-de Groot et al., 2006; High et al., 2007; Varadkar et al., 2008). This data is often difficult to interpret and to combine into a global view, thus making it challenging to reach clear-cut conclusions. For this reason, I developed a technique that enables three-dimensional analysis of the entire embryo, focusing on the pharyngeal arch area (**Chapter 4)**. Taking advantage of this imaging tool, in **Chapter 5,** I described the study of smooth muscle recruitment around the embryonic arch arteries in wild type mouse embryos, in two mutant strains (*ETA*$^{-/-}$ and *Pbx1*$^{-/-}$) and in transgenic embryos (*HtpA-Myoc::Mkl2)* produced for this project. The data we presented in this chapter suggested that regression of the first and second arch arteries results from their failure to recruit vascular smooth muscle cells (VSMCs) most likely because these arches are not populated by cardiac neural crest cells, which are the source of VSMCs in this area of the embryo. Possibly, the most

obvious evidence was provided by the stabilization of the second aortic arch, when formation of VSMCs was experimentally promoted by the expression of *Myoc* and *Mkl2* in the neural crest migrating into the branchial arches. In these embryos, stabilization was always associated with VSMC recruitment to the vessel. Nevertheless, it would be interesting to analyse transgenic embryos older than E10.5 in order to show if the second embryonic arch persists until a later stage.

Myocardin and Mkl2 are potent transcriptional coactivators that bind to serum response factor (SRF) and synergistically activate transcription of a subset of genes involved in smooth muscle cell differentiation (Wang et al., 2002; Li et al., 2003; Wang and Olson, 2004; Pipes et al., 2006). In agreement with our work, recent studies have demonstrated that these genes play specific and crucial roles in differentiation of neural crest–derived smooth muscle cells populating the cardiac outflow tract and great arteries (Oh et al., 2005; Wei et al., 2007; Huang et al., 2008).

Extrapolating from our results we suggest that cardiac neural crest cells are not required for the initial formation of the endothelial channels that form the arch arteries, since the first and second aortic arches are formed in earlier stages of development. Instead, this cell population seems to be required for the correct final patterning and stabilization of these vessels. Previous studies in avian embryos confirm this line of thought (Bockman et al., 1987; Waldo et al., 1996). These studies also suggested that there is a time interval after vessel formation, which requires the presence of the cardiac neural crest (Waldo et al., 1996). It would be worthwhile to study, with further detail, the dynamics of neural crest migration and vascular smooth muscle cell differentiation around embryonic arteries during mouse embryonic development. Since we had already produced the transgenic mouse lines expressing GFP and RFP in endothelial and neural crest cells respectively, it may be worth introducing the SM22::myr-YFP transgene in order to produce a reporter mouse line that enables visualization of these three cell populations simultaneously (Moessler et al., 1996; Shaner et al., 2004). RFP

and GFP are easily distinguished (RFP emission peak at 607 nm and GFP at 509nm), however GFP and YFP have partially overlapping spectra (YFP emission 530nm). To minimize this problem we could use YFP fused with an engineered myristoylation sequence (myr) that specifically labels cell membranes, allowing a better distinction between GFP and YFP (Larina et al 2009).

Eventually, in the near future, time lapse imaging of cultured mouse embryos would allow the assessment of what would be the crucial time interval in which neural crest derived-smooth muscle cells are necessary for the remodelling of the arch arteries. In addition these fluorescent mouse lines could be used in mutant backgrounds to study in detail the cell biology of these malformations.

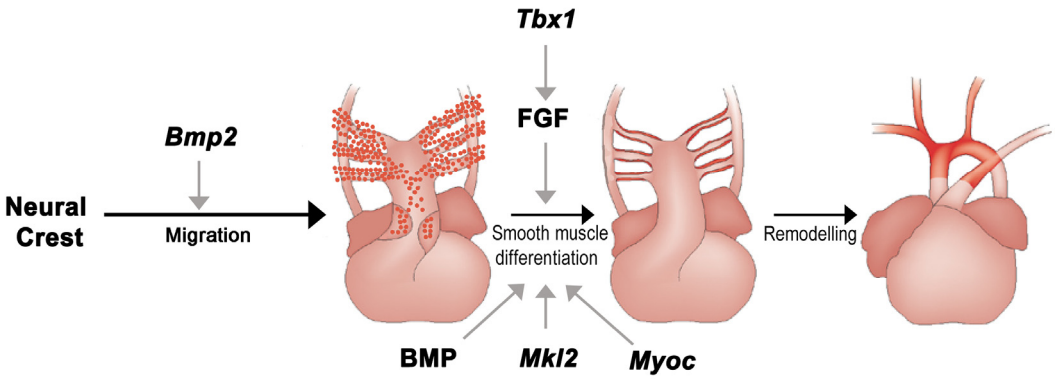

Figure 6.1 Schematic representation of cardiac neural crest migration and differentiation into vascular smooth muscle.
Some of the genes discussed herein are indicated (adapted from High et al, 2008).

Many examples of cardiac outflow tract defects in animal models, as well as in humans relate to deficient smooth muscle differentiation of cardiac neural crest, and there has been an increasing amount of data describing molecules that play specific roles in neural crest smooth muscle differentiation (Fig 6.1). These observations provide numerous candidate genes for involvement in congenital heart disease and detailed interactions between neural crest, vascular smooth muscle and endothelium, the study of which has become an exciting area of active investigation.

Together the results of this thesis have contributed to the understanding of cellular and genetic players involved in the development of the craniofacial area and in the morphogenesis of the pharyngeal arches and their associated embryonic arteries.

References

References

Abu-Issa, R., Smyth, G., Smoak, I., Yamamura, K. and Meyers, E. N. (2002). Fgf8 is required for pharyngeal arch and cardiovascular development in the mouse. *Development* **129**, 4613-25.

Acampora, D., Merlo, G. R., Paleari, L., Zerega, B., Postiglione, M. P., Mantero, S., Bober, E., Barbieri, O., Simeone, A. and Levi, G. (1999). Craniofacial, vestibular and bone defects in mice lacking the Distal-less-related gene Dlx5. *Development* **126**, 3795-809.

Akhurst, R. J., Lehnert, S. A., Faissner, A. and Duffie, E. (1990). TGF beta in murine morphogenetic processes: the early embryo and cardiogenesis. *Development* **108**, 645-56.

Akitaya, T. and Bronner-Fraser, M. (1992). Expression of cell adhesion molecules during initiation and cessation of neural crest cell migration. *Dev Dyn* **194**, 12-20.

Akiyama, H., Chaboissier, M. C., Behringer, R. R., Rowitch, D. H., Schedl, A., Epstein, J. A. and de Crombrugghe, B. (2004). Essential role of Sox9 in the pathway that controls formation of cardiac valves and septa. *Proc Natl Acad Sci U S A* **101**, 6502-7.

Arnold, J. S., Braunstein, E. M., Ohyama, T., Groves, A. K., Adams, J. C., Brown, M. C. and Morrow, B. E. (2006a). Tissue-specific roles of Tbx1 in the development of the outer, middle and inner ear, defective in 22q11DS patients. *Hum Mol Genet* **15**, 1629-39.

Arnold, J. S., Werling, U., Braunstein, E. M., Liao, J., Nowotschin, S., Edelmann, W., Hebert, J. M. and Morrow, B. E. (2006b). Inactivation of Tbx1 in the pharyngeal endoderm results in 22q11DS malformations. *Development* **133**, 977-87

Aybar, M. J. and Mayor, R. (2002). Early induction of neural crest cells: lessons learned from frog, fish and chick. *Curr Opin Genet Dev* **12**, 452-8.

Aybar, M. J., Nieto, M. A. and Mayor, R. (2003). Snail precedes slug in the genetic cascade required for the specification and migration of the Xenopus neural crest. *Development* **130**, 483-94.

Anderson, M. J., Pham, V. N., Vogel, A. M., Weinstein, B. M. and Roman, B. L. (2008). Loss of unc45a precipitates arteriovenous shunting in the aortic arches. *Dev Biol* **318**, 258-67.

Anniko, M. and Wikstrom, S. O. (1984). Pattern formation of the otic placode and morphogenesis of the otocyst. *Am J Otolaryngol* **5**, 373-81.

Arnold, J. S., Werling, U., Braunstein, E. M., Liao, J., Nowotschin, S., Edelmann, W., Hebert, J. M. and Morrow, B. E. (2006). Inactivation of Tbx1 in the pharyngeal endoderm results in 22q11DS malformations. *Development* **133**, 977-87.

Bachiller, D., Klingensmith, J., Shneyder, N., Tran, U., Anderson, R., Rossant, J. and De Robertis, E. M. (2003). The role of chordin/Bmp signals in mammalian pharyngeal development and DiGeorge syndrome. *Development* **130**, 3567-78.

Baker, C. V. and Bronner-Fraser, M. (2001). Vertebrate cranial placodes I. Embryonic

induction. *Dev Biol* **232**, 1-61.

Baldini, A. (2002). DiGeorge syndrome: the use of model organisms to dissect complex genetics. *Hum Mol Genet* **11**, 2363-9.

Bally-Cuif, L., Alvarado-Mallart, R. M., Darnell, D. K. and Wassef, M. (1992). Relationship between Wnt-1 and En-2 expression domains during early development of normal and ectopic met-mesencephalon. *Development* **115**, 999-1009.

Barembaum, M. and Bronner-Fraser, M. (2005). Early steps in neural crest specification. *Semin Cell Dev Biol* **16**, 642-6.

Barth, K. A., Kishimoto, Y., Rohr, K. B., Seydler, C., Schulte-Merker, S. and Wilson, S. W. (1999). Bmp activity establishes a gradient of positional information throughout the entire neural plate. *Development* **126**, 4977-87.

Bastidas, F., De Calisto, J. and Mayor, R. (2004). Identification of neural crest competence territory: role of Wnt signaling. *Dev Dyn* **229**, 109-17.

Beghetti, M., Black, S. M. and Fineman, J. R. (2005). Endothelin-1 in congenital heart disease. *Pediatr Res* **57**, 16R-20R.

Belloni, E., Muenke, M., Roessler, E., Traverso, G., Siegel-Bartelt, J., Frumkin, A., Mitchell, H. F., Donis-Keller, H., Helms, C., Hing, A. V. et al. (1996). Identification of Sonic hedgehog as a candidate gene responsible for holoprosencephaly. *Nat Genet* **14**, 353-6.

Benjamin, L., Hemo, E. I. and Keshet, E. (1998). A plasticity window for blood vessel remodelling is defined by pericyte coverage of the preformed endothelial network and is regulated by PDGF-B and VEGF. *Development* **125**, 1591-1598.

Bergwerff, M., DeRuiter, M. C., Hall, S., Poelmann, R. E. and Gittenberger-de Groot, A. C. (1999). Unique vascular morphology of the fourth aortic arches: possible implications for pathogenesis of type-B aortic arch interruption and anomalous right subclavian artery. *Cardiovasc Res* **44**, 185-96.

Birgbauer, E., Sechrist, J., Bronner-Fraser, M. and Fraser, S. (1995). Rhombomeric origin and rostrocaudal reassortment of neural crest cells revealed by intravital microscopy. *Development* **121**, 935-45.

Bobola, N., Carapuco, M., Ohnemus, S., Kanzler, B., Leibbrandt, A., Neubuser, A., Drouin, J. and Mallo, M. (2003). Mesenchymal patterning by Hoxa2 requires blocking Fgf-dependent activation of Ptx1. *Development* **130**, 3403-14.

Bok, J., Bronner-Fraser, M. and Wu, D. K. (2005). Role of the hindbrain in dorsoventral but not anteroposterior axial specification of the inner ear. *Development* **132**, 2115-24.

Bok, J., Chang, W. and Wu, D. K. (2007). Patterning and morphogenesis of the vertebrate inner ear. *Int J Dev Biol* **51**, 521-33.

Bockman, D. E., Redmond, M. E. and Kirby, M. L. (1989). Alteration of early vascular development after ablation of cranial neural crest. *Anat Rec* **225**, 209-17.

Bockman, D. E., Redmond, M. E., Waldo, K., Davis, H. and Kirby, M. L. (1987). Effect of neural crest ablation on development of the heart and arch arteries in the chick. *Am J Anat* **180**, 332-41.

Bollag, R. J., Siegfried, Z., Cebra-Thomas, J. A., Garvey, N., Davison, E. M. and Silver, L. M. (1994). An ancient family of embryonically expressed mouse genes sharing a conserved protein motif with the T locus. *Nat Genet* **7**, 383-9.

Bouillet, P., Chazaud, C., Oulad-Abdelghani, M., Dolle, P. and Chambon, P. (1995). Sequence and expression pattern of the Stra7 (Gbx-2) homeobox-containing gene induced by retinoic acid in P19 embryonal carcinoma cells. *Dev Dyn* **204**, 372-82.

Brault, V., Moore, R., Kutsch, S., Ishibashi, M., Rowitch, D. H., McMahon, A. P., Sommer, L., Boussadia, O. and Kemler, R. (2001). Inactivation of the beta-catenin gene by Wnt1-Cre-mediated deletion results in dramatic brain malformation and failure of craniofacial development. *Development* **128**, 1253-64.

Breier, G., Albrecht, U., Sterrer, S. and Risau, W. (1992). Expression of vascular endothelial growth factor during embryonic angiogenesis and endothelial cell differentiation. *Development* **114**, 521-32.

Brewer, S., Jiang, X., Donaldson, S., Williams, T. and Sucov, H. M. (2002). Requirement for AP-2alpha in cardiac outflow tract morphogenesis. *Mech Dev* **110**, 139-49.

Brigande, J. V., Iten, L. E. and Fekete, D. M. (2000a). A fate map of chick otic cup closure reveals lineage boundaries in the dorsal otocyst. *Dev Biol* **227**, 256-70.

Brigande, J. V., Kiernan, A. E., Gao, X., Iten, L. E. and Fekete, D. M. (2000b). Molecular genetics of pattern formation in the inner ear: do compartment boundaries play a role? *Proc Natl Acad Sci U S A* **97**, 11700-6.

Brito, J. M., Teillet, M. A. and Le Douarin, N. M. (2006). An early role for sonic hedgehog from foregut endoderm in jaw development: ensuring neural crest cell survival. *Proc Natl Acad Sci U S A* **103**, 11607-12.

Britsch, S., Goerich, D. E., Riethmacher, D., Peirano, R. I., Rossner, M., Nave, K. A., Birchmeier, C. and Wegner, M. (2001). The transcription factor Sox10 is a key regulator of peripheral glial development. *Genes Dev* **15**, 66-78.

Brown, C. B., Feiner, L., Lu, M. M., Li, J., Ma, X., Webber, A. L., Jia, L., Raper, J. A. and Epstein, J. A. (2001). PlexinA2 and semaphorin signaling during cardiac neural crest development. *Development* **128**, 3071-80.

Brown, C. B., Wenning, J. M., Lu, M. M., Epstein, D. J., Meyers, E. N. and Epstein, J. A. (2004). Cre-mediated excision of Fgf8 in the Tbx1 expression domain reveals a critical role for Fgf8 in cardiovascular development in the mouse. *Dev Biol* **267**, 190-202.

Burglin, T. R. (1997). Analysis of TALE superclass homeobox genes (MEIS, PBC, KNOX, Iroquois, TGIF) reveals a novel domain conserved between plants and animals. *Nucleic Acids Res* **25**, 4173-80.

Burstyn-Cohen, T., Stanleigh, J., Sela-Donenfeld, D. and Kalcheim, C. (2004). Canonical Wnt activity regulates trunk neural crest delamination linking BMP/noggin signaling with G1/S transition. *Development* **131**, 5327-39.

Burton, Q., Cole, L. K., Mulheisen, M., Chang, W. and Wu, D. K. (2004). The role of Pax2 in mouse inner ear development. *Dev Biol* **272**, 161-75.

Byrd, N. A. and Meyers, E. N. (2005). Loss of Gbx2 results in neural crest cell patterning and pharyngeal arch artery defects in the mouse embryo. *Dev Biol* **284**, 233-45.

Cano, A., Perez-Moreno, M. A., Rodrigo, I., Locascio, A., Blanco, M. J., del Barrio, M. G., Portillo, F. and Nieto, M. A. (2000). The transcription factor snail controls epithelial-mesenchymal transitions by repressing E-cadherin expression. *Nat Cell Biol* **2**, 76-83.

Carlson, B. M. (1999). Human embryology and developmental biology. 2nd ed. Mosby, Inc., St. Louis.

Carmeliet, P. and Jain, R. K. (2000). Angiogenesis in cancer and other diseases. *Nature* **407**, 249-57.

Carmeliet, P., Ng, Y. S., Nuyens, D., Theilmeier, G., Brusselmans, K., Cornelissen, I., Ehler, E., Kakkar, V. V., Stalmans, I., Mattot, V. et al. (1999). Impaired myocardial angiogenesis and ischemic cardiomyopathy in mice lacking the vascular endothelial growth factor isoforms VEGF164 and VEGF188. *Nat Med* **5**, 495-502.

Carmeliet, P. and Tessier-Lavigne, M. (2005). Common mechanisms of nerve and blood vessel wiring. *Nature* **436**, 193-200.

Cassels, D. E. (1973). The ductus arteriosus. *Thomas, Springfield, Illinois*.

Castranio, T. and Mishina, Y. (2009). Bmp2 is required for cephalic neural tube closure in the mouse. *Dev Dyn* **238**, 110-22.

Cerny, R., Meulemans, D., Berger, J., Wilsch-Brauninger, M., Kurth, T., Bronner-Fraser, M. and Epperlein, H. H. (2004). Combined intrinsic and extrinsic influences pattern cranial neural crest migration and pharyngeal arch morphogenesis in axolotl. *Dev Biol* **266**, 252-69.

Chan, S. K., Jaffe, L., Capovilla, M., Botas, J. and Mann, R. S. (1994). The DNA binding specificity of Ultrabithorax is modulated by cooperative interactions with extradenticle, another homeoprotein. *Cell* **78**, 603-15.

Chan, S. K., Ryoo, H. D., Gould, A., Krumlauf, R. and Mann, R. S. (1997). Switching the in vivo specificity of a minimal Hox-responsive element. *Development* **124**, 2007-14.

Chang, C. P., Shen, W. F., Rozenfeld, S., Lawrence, H. J., Largman, C. and Cleary, M. L. (1995). Pbx proteins display hexapeptide-dependent cooperative DNA binding with a subset of Hox proteins. *Genes Dev* **9**, 663-74.

Chang, C. P., Stankunas, K., Shang, C., Kao, S. C., Twu, K. Y. and Cleary, M. L. (2008). Pbx1 functions in distinct regulatory networks to pattern the great arteries and cardiac outflow tract. *Development* **135**, 3577-86.

Chapman, D. L., Garvey, N., Hancock, S., Alexiou, M., Agulnik, S. I., Gibson-Brown, J. J., Cebra-Thomas, J., Bollag, R. J., Silver, L. M. and Papaioannou, V. E. (1996). Expression of the T-box family genes, Tbx1-Tbx5, during early mouse development. *Dev Dyn* **206**, 379-90.

Chen, J., Kitchen, C. M., Streb, J. W. and Miano, J. M. (2002). Myocardin: a component of a molecular switch for smooth muscle differentiation. *J Mol Cell Cardiol* **34**, 1345-56.

Chisaka, O. and Capecchi, M. R. (1991). Regionally restricted developmental defects resulting from targeted disruption of the mouse homeobox gene hox-1.5. *Nature* **350**, 473-9.

Choo, D., Ward, J., Reece, A., Dou, H., Lin, Z. and Greinwald, J. (2006). Molecular mechanisms underlying inner ear patterning defects in kreisler mutants. *Dev Biol* **289**, 308-17.

Choudhary, B., Ito, Y., Makita, T., Sasaki, T., Chai, Y. and Sucov, H. M. (2006). Cardiovascular malformations with normal smooth muscle differentiation in neural crest-specific type II TGFbeta receptor (Tgfbr2) mutant mice. *Dev Biol* **289**, 420-9.

Clouthier, D. E., Hosoda, K., Richardson, J. A., Williams, S. C., Yanagisawa, H., Kuwaki, T., Kumada, M., Hammer, R. E. and Yanagisawa, M. (1998). Cranial and cardiac neural crest defects in endothelin-A receptor-deficient mice. *Development* **125**, 813-24.

Conchello, J. A. and Lichtman, J. W. (2005). Optical sectioning microscopy. *Nat Methods* **2**, 920-31.

Condie, B. G. and Capecchi, M. R. (1994). Mice with targeted disruptions in the paralogous genes hoxa-3 and hoxd-3 reveal synergistic interactions. *Nature* **370**, 304-7.

Conway, S. J., Godt, R. E., Hatcher, C. J., Leatherbury, L., Zolotouchnikov, V. V., Brotto, M. A., Copp, A. J., Kirby, M. L. and Creazzo, T. L. (1997a). Neural crest is involved in development of abnormal myocardial function. *J Mol Cell Cardiol* **29**, 2675-85.

Conway, S. J., Henderson, D. J. and Copp, A. J. (1997b). Pax3 is required for cardiac neural crest migration in the mouse: evidence from the splotch (Sp2H) mutant. *Development* **124**, 505-14.

Conway, S. J., Henderson, D. J., Kirby, M. L., Anderson, R. H. and Copp, A. J. (1997c). Development of a lethal congenital heart defect in the splotch (Pax3) mutant mouse. *Cardiovasc Res* **36**, 163-73.

Couly, G., Coltey, P., Eichmann, A. and Le Douarin, N. M. (1995). The angiogenic potentials of the cephalic mesoderm and the origin of brain and head blood vessels. *Mech Dev* **53**, 97-112.

Couly, G., Creuzet, S., Bennaceur, S., Vincent, C. and Le Douarin, N. M. (2002). Interactions between Hox-negative cephalic neural crest cells and the foregut endoderm in patterning the facial skeleton in the vertebrate head. *Development* **129**, 1061-73.

Couly, G. and Le Douarin, N. M. (1990). Head morphogenesis in embryonic avian chimeras: evidence for a segmental pattern in the ectoderm corresponding to the neuromeres. *Development* **108**, 543-58.

Couly, G. F., Coltey, P. M. and Le Douarin, N. M. (1992). The developmental fate of the cephalic mesoderm in quail-chick chimeras. *Development* **114**, 1-15.

Couly, G. F., Coltey, P. M. and Le Douarin, N. M. (1993). The triple origin of skull in higher vertebrates: a study in quail-chick chimeras. *Development* **117**, 409-29.

Cox, C. M. and Poole, T. J. (2000). Angioblast differentiation is influenced by the local environment: FGF-2 induces angioblasts and patterns vessel formation in the quail

embryo. *Dev Dyn* **218**, 371-82.

Creazzo, T. L., Godt, R. E., Leatherbury, L., Conway, S. J. and Kirby, M. L. (1998). Role of cardiac neural crest cells in cardiovascular development. *Annu Rev Physiol* **60**, 267-86.

Creuzet, S., Couly, G., Vincent, C. and Le Douarin, N. M. (2002). Negative effect of Hox gene expression on the development of the neural crest-derived facial skeleton. *Development* **129**, 4301-13

Crump, J. G., Maves, L., Lawson, N. D., Weinstein, B. M. and Kimmel, C. B. (2004). An essential role for Fgfs in endodermal pouch formation influences later craniofacial skeletal patterning. *Development* **131**, 5703-16.

D'Amico-Martel, A. and Noden, D. M. (1983). Contributions of placodal and neural crest cells to avian cranial peripheral ganglia. *Am J Anat* **166**, 445-68.

David, N. B., Saint-Etienne, L., Tsang, M., Schilling, T. F. and Rosa, F. M. (2002). Requirement for endoderm and FGF3 in ventral head skeleton formation. *Development* **129**, 4457-68.

Davy, A., Aubin, J. and Soriano, P. (2004). Ephrin-B1 forward and reverse signaling are required during mouse development. *Genes Dev* **18**, 572-83.

Depew, M. J., Liu, J. K., Long, J. E., Presley, R., Meneses, J. J., Pedersen, R. A. and Rubenstein, J. L. (1999). Dlx5 regulates regional development of the branchial arches and sensory capsules. *Development* **126**, 3831-46.

Depew, M. J., Lufkin, T. and Rubenstein, J. L. (2002). Specification of jaw subdivisions by Dlx genes. *Science* **298**, 381-5.

Depew, M. J. and Simpson, C. A. (2006). 21st century neontology and the comparative development of the vertebrate skull. *Dev Dyn* **235**, 1256-91.

Desligneres, S. and Larroche, J. C. (1970). Ductus arteriosus. I. Anatomical and histological study of its development during the second half of gestation and its closure after birth. II. Histological study of a few cases of patent ductus arteriosus in infancy. *Biol Neonate* **16**, 278-96

Digilio, M. C., Pacifico, C., Tieri, L., Marino, B., Giannotti, A. and Dallapiccola, B. (1999). Audiological findings in patients with microdeletion 22q11 (di George/velocardiofacial syndrome). *Br J Audiol* **33**, 329-33.

Dryden, R. (2004). **http://www.bionalogy.com/eye_and_ear.htm**.

Du, K. L., Ip, H. S., Li, J., Chen, M., Dandre, F., Yu, W., Lu, M. M., Owens, G. K. and Parmacek, M. S. (2003). Myocardin is a critical serum response factor cofactor in the transcriptional program regulating smooth muscle cell differentiation. *Mol Cell Biol* **23**, 2425-37.

Dudley, A. T., Lyons, K. M. and Robertson, E. J. (1995). A requirement for bone morphogenetic protein-7 during development of the mammalian kidney and eye. *Genes Dev* **9**, 2795-807.

Duester, G. (2000). Families of retinoid dehydrogenases regulating vitamin A function: production of visual pigment and retinoic acid. *Eur J Biochem* **267**, 4315-24.

Dupin, E., Calloni, G., Real, C., Goncalves-Trentin, A. and Le Douarin, N. M. (2007). Neural crest progenitors and stem cells. *C R Biol* **330**, 521-9.

Echelard, Y., Vassileva, G. and McMahon, A. P. (1994). Cis-acting regulatory sequences governing Wnt-1 expression in the developing mouse CNS. *Development* **120**, 2213-24.

Eickholt, B. J., Mackenzie, S. L., Graham, A., Walsh, F. S. and Doherty, P. (1999). Evidence for collapsin-1 functioning in the control of neural crest migration in both trunk and hindbrain regions. *Development* **126**, 2181-9.

Eichmann, A., Makinen, T. and Alitalo, K. (2005). Neural guidance molecules regulate vascular remodelling and vessel navigation. *Genes Dev* **19**, 1013-21.

Endo, Y., Osumi, N. and Wakamatsu, Y. (2002). Bimodal functions of Notch-mediated signaling are involved in neural crest formation during avian ectoderm development. *Development* **129**, 863-73.

Engleka, K. A., Gitler, A. D., Zhang, M., Zhou, D. D., High, F. A. and Epstein, J. A. (2005). Insertion of Cre into the Pax3 locus creates a new allele of Splotch and identifies unexpected Pax3 derivatives. *Developmental Biology* **280**, 396-406.

Epstein, D. J., Malo, D., Vekemans, M. and Gros, P. (1991). Molecular characterization of a deletion encompassing the splotch mutation on mouse chromosome 1. *Genomics* **10**, 89-93.

Epstein, D. J., Vekemans, M. and Gros, P. (1991). Splotch (Sp2H), a mutation affecting development of the mouse neural tube, shows a deletion within the paired homeodomain of Pax-3. *Cell* **67**, 767-74.

Epstein, J. A., Li, J., Lang, D., Chen, F., Brown, C. B., Jin, F., Lu, M. M., Thomas, M., Liu, E., Wessels, A. et al. (2000). Migration of cardiac neural crest cells in Splotch embryos. *Development* **127**, 1869-78.

Erkman, L., McEvilly, R. J., Luo, L., Ryan, A. K., Hooshmand, F., O'Connell, S. M., Keithley, E. M., Rapaport, D. H., Ryan, A. F. and Rosenfeld, M. G. (1996). Role of transcription factors Brn-3.1 and Brn-3.2 in auditory and visual system development. *Nature* **381**, 603-6.

Etchevers, H. C., Vincent, C., Le Douarin, N. M. and Couly, G. F. (2001). The cephalic neural crest provides pericytes and smooth muscle cells to all blood vessels of the face and forebrain. *Development* **128**, 1059-68.

Farlie, P. G., Kerr, R., Thomas, P., Symes, T., Minichiello, J., Hearn, C. J. and Newgreen, D. (1999). A paraxial exclusion zone creates patterned cranial neural crest cell outgrowth adjacent to rhombomeres 3 and 5. *Dev Biol* **213**, 70-84.

Feiner, L., Webber, A. L., Brown, C. B., Lu, M. M., Jia, L., Feinstein, P., Mombaerts, P., Epstein, J. A. and Raper, J. A. (2001). Targeted disruption of semaphorin 3C leads to persistent truncus arteriosus and aortic arch interruption. *Development* **128**, 3061-70.

Fekete, D. M. and Wu, D. K. (2002). Revisiting cell fate specification in the inner ear. *Curr Opin Neurobiol* **12**, 35-42.

Ferguson, C. A. and Graham, A. (2004). Redefining the head-trunk interface for the

neural crest. *Dev Biol* **269**, 70-80.

Ferrara, N., Carver-Moore, K., Chen, H., Dowd, M., Lu, L., O'Shea, K. S., Powell-Braxton, L., Hillan, K. J. and Moore, M. W. (1996). Heterozygous embryonic lethality induced by targeted inactivation of the VEGF gene. *Nature* **380**, 439-42.

Flamme, I., Frolich, T. and Risau, W. (1997). Molecular mechanisms of vasculogenesis and embryonic angiogenesis. *J Cell Physiol* **173**, 206-10.

Foo, S. S., Turner, C. J., Adams, S., Compagni, A., Aubyn, D., Kogata, N., Lindblom, P., Shani, M., Zicha, D. and Adams, R. H. (2006). Ephrin-B2 controls cell motility and adhesion during blood-vessel-wall assembly. *Cell* **124**, 161-73

Frank, D. U., Fotheringham, L. K., Brewer, J. A., Muglia, L. J., Tristani-Firouzi, M., Capecchi, M. R. and Moon, A. M. (2002). An Fgf8 mouse mutant phenocopies human 22q11 deletion syndrome. *Development* **129**, 4591-603.

Franz, T. (1989). Persistent truncus arteriosus in the Splotch mutant mouse. *Anat Embryol (Berl)* **180**, 457-64.

Fraser, S. D. e. a. (2005). Using a Histone Yellow Fluorescent Protein Fusion for Tagging and Tracking Endothelial Cells in ES Cells and Mice. *Genesis* **42**, 162-171.

Friedman, R. A., Makmura, L., Biesiada, E., Wang, X. and Keithley, E. M. (2005). Eya1 acts upstream of Tbx1, Neurogenin 1, NeuroD and the neurotrophins BDNF and NT-3 during inner ear development. *Mech Dev* **122**, 625-34.

Frohman, M. A., Boyle, M. and Martin, G. R. (1990). Isolation of the mouse Hox-2.9 gene; analysis of embryonic expression suggests that positional information along the anterior-posterior axis is specified by mesoderm. *Development* **110**, 589-607.

Frohman, M. A., Martin, G. R., Cordes, S. P., Halamek, L. P. and Barsh, G. S. (1993). Altered rhombomere-specific gene expression and hyoid bone differentiation in the mouse segmentation mutant, kreisler (kr). *Development* **117**, 925-36.

Fujii, H., Sato, T., Kaneko, S., Gotoh, O., Fujii-Kuriyama, Y., Osawa, K., Kato, S. and Hamada, H. (1997). Metabolic inactivation of retinoic acid by a novel P450 differentially expressed in developing mouse embryos. *EMBO J* **16**, 4163-73

Funke, B., Epstein, J. A., Kochilas, L. K., Lu, M. M., Pandita, R. K., Liao, J., Bauerndistel, R., Schuler, T., Schorle, H., Brown, M. C. et al. (2001). Mice overexpressing genes from the 22q11 region deleted in velo-cardio-facial syndrome/DiGeorge syndrome have middle and inner ear defects. *Hum Mol Genet* **10**, 2549-56.

Gans, C. and Northcutt, R. G. (1983). Neural Crest and the Origin of Vertebrates: A New Head. *Science* **220**, 268-273.

Garcia-Castro, M. I., Marcelle, C. and Bronner-Fraser, M. (2002). Ectodermal Wnt function as a neural crest inducer. *Science* **297**, 848-51.

Gavalas, A., Trainor, P., Ariza-McNaughton, L. and Krumlauf, R. (2001). Synergy between Hoxa1 and Hoxb1: the relationship between arch patterning and the generation of cranial neural crest. *Development* **128**, 3017-27.

Gendron-Maguire, M., Mallo, M., Zhang, M. and Gridley, T. (1993). Hoxa-2 mutant mice

exhibit homeotic transformation of skeletal elements derived from cranial neural crest. *Cell* **75**, 1317-31.

Gilbert, S. F. (2003). Developmental Biology. Sunderland: Sinauer Associates, Inc.

Gitler, A. D., Lu, M. M. and Epstein, J. A. (2004). PlexinD1 and semaphorin signaling are required in endothelial cells for cardiovascular development. *Dev Cell* **7**, 107-16.

Gittenberger-de Groot, A. C., Azhar, M. and Molin, D. G. (2006). Transforming growth factor beta-SMAD2 signaling and aortic arch development. *Trends Cardiovasc Med* **16**, 1-6.

Glavic, A., Silva, F., Aybar, M. J., Bastidas, F. and Mayor, R. (2004). Interplay between Notch signaling and the homeoprotein Xiro1 is required for neural crest induction in Xenopus embryos. *Development* **131**, 347-59.

Golding, J. P., Dixon, M. and Gassmann, M. (2002). Cues from neuroepithelium and surface ectoderm maintain neural crest-free regions within cranial mesenchyme of the developing chick. *Development* **129**, 1095-105.

Golding, J. P., Trainor, P., Krumlauf, R. and Gassmann, M. (2000). Defects in pathfinding by cranial neural crest cells in mice lacking the neuregulin receptor ErbB4. *Nat Cell Biol* **2**, 103-9.

Goulding, M., Sterrer, S., Fleming, J., Balling, R., Nadeau, J., Moore, K. J., Brown, S. D., Steel, K. P. and Gruss, P. (1993). Analysis of the Pax-3 gene in the mouse mutant splotch. *Genomics* **17**, 355-63.

Graham, A. (2001). The development and evolution of the pharyngeal arches. *J Anat* **199**, 133-41.

Graham, A. and Smith, A. (2001). Patterning the pharyngeal arches. *Bioessays* **23**, 54-61.

Graham, A. (2008). Deconstructing the pharyngeal metamere. *J Exp Zool B Mol Dev Evol* **310**, 336-44.

Graham, A., Begbie, J. and McGonnell, I. (2004). Significance of the cranial neural crest. *Dev Dyn* **229**, 5-13.

Graham, A., Heyman, I. and Lumsden, A. (1993). Even-numbered rhombomeres control the apoptotic elimination of neural crest cells from odd-numbered rhombomeres in the chick hindbrain. *Development* **119**, 233-45.

Greenberg, F. (1989). What defines DiGeorge anomaly? *J Pediatr* **115**, 412-3.

Gu, Z., Reynolds, E. M., Song, J., Lei, H., Feijen, A., Yu, L., He, W., MacLaughlin, D. T., van den Eijnden-van Raaij, J., Donahoe, P. K. et al. (1999). The type I serine/threonine kinase receptor ActRIA (ALK2) is required for gastrulation of the mouse embryo. *Development* **126**, 2551-61.

Guris, D. L., Duester, G., Papaioannou, V. E. and Imamoto, A. (2006). Dose-dependent interaction of Tbx1 and Crkl and locally aberrant RA signaling in a model of del22q11 syndrome. *Dev Cell* **10**, 81-92.

Guris, D. L., Fantes, J., Tara, D., Druker, B. J. and Imamoto, A. (2001). Mice lacking

the homologue of the human 22q11.2 gene CRKL phenocopy neurocristopathies of DiGeorge syndrome. *Nat Genet* **27**, 293-8.

Haddon, C., Mowbray, C., Whitfield, T., Jones, D., Gschmeissner, S. and Lewis, J. (1999). Hair cells without supporting cells: further studies in the ear of the zebrafish mind bomb mutant. *J Neurocytol* **28**, 837-50.

Hadjantonakis, A. K. and Papaioannou, V. E. (2004). Dynamic in vivo imaging and cell tracking using a histone fluorescent protein fusion in mice. *BMC Biotechnol* **4**, 33.

Hadrys, T., Braun, T., Rinkwitz-Brandt, S., Arnold, H. H. and Bober, E. (1998). Nkx5-1 controls semicircular canal formation in the mouse inner ear. *Development* **125**, 33-9.

Hain, T. (2008). www.american-hearing.org/images/master-ear.jpg.

Hall, B. K. (1999). The Neural Crest in Development and Evolution,. *New York, NY: Springer-Verlag*.

Harrison, R. G. (1936). Relations of Symmetry in the Developing Ear of Amblystoma Punctatum. *Proc Natl Acad Sci U S A* **22**, 238-47.

Hensey, C. and Gautier, J. (1998). Programmed cell death during Xenopus development: a spatio-temporal analysis. *Dev Biol* **203**, 36-48.

Hensey, C. and Gautier, J. (1999). Developmental regulation of induced and programmed cell death in Xenopus embryos. *Ann N Y Acad Sci* **887**, 105-19.

Hertzano, R., Montcouquiol, M., Rashi-Elkeles, S., Elkon, R., Yucel, R., Frankel, W. N., Rechavi, G., Moroy, T., Friedman, T. B., Kelley, M. W. et al. (2004). Transcription profiling of inner ears from Pou4f3(ddl/ddl) identifies Gfi1 as a target of the Pou4f3 deafness gene. *Hum Mol Genet* **13**, 2143-53.

High, F. A. and Epstein, J. A. (2008). The multifaceted role of Notch in cardiac development and disease. *Nat Rev Genet* **9**, 49-61.

High, F. A., Zhang, M., Proweller, A., Tu, L., Parmacek, M. S., Pear, W. S. and Epstein, J. A. (2007). An essential role for Notch in neural crest during cardiovascular development and smooth muscle differentiation. *J Clin Invest* **117**, 353-63.

Hiruma, T., Nakajima, Y. and Nakamura, H. (2002). Development of pharyngeal arch arteries in early mouse embryo. *J Anat* **201**, 15-29.

Ho, S. Y. and Anderson, R. H. (1979). Anatomical closure of the ductus arteriosus: a study in 35 specimens. *J Anat* **128**, 829-36.

Holderfield, M. T. and Hughes, C. C. (2008). Crosstalk between vascular endothelial growth factor, notch, and transforming growth factor-beta in vascular morphogenesis. *Circ Res* **102**, 637-52.

Hollnagel, A., Oehlmann, V., Heymer, J., Ruther, U. and Nordheim, A. (1999). Id genes are direct targets of bone morphogenetic protein induction in embryonic stem cells. *J Biol Chem* **274**, 19838-45.

Hu, D., Marcucio, R. S. and Helms, J. A. (2003). A zone of frontonasal ectoderm regulates patterning and growth in the face. *Development* **130**, 1749-58.

Hu, T., Yamagishi, H., Maeda, J., McAnally, J., Yamagishi, C. and Srivastava, D.

(2004). Tbx1 regulates fibroblast growth factors in the anterior heart field through a reinforcing autoregulatory loop involving forkhead transcription factors. *Development* **131**, 5491-502.

Huang, J., Cheng, L., Li, J., Chen, M., Zhou, D., Lu, M. M., Proweller, A., Epstein, J. A. and Parmacek, M. S. (2008). Myocardin regulates expression of contractile genes in smooth muscle cells and is required for closure of the ductus arteriosus in mice. *J Clin Invest* **118**, 515-25.

Hunt, P., Gulisano, M., Cook, M., Sham, M. H., Faiella, A., Wilkinson, D., Boncinelli, E. and Krumlauf, R. (1991). A distinct Hox code for the branchial region of the vertebrate head. *Nature* **353**, 861-4.

Hunter, M. P. and Prince, V. E. (2002). Zebrafish hox paralogue group 2 genes function redundantly as selector genes to pattern the second pharyngeal arch. *Dev Biol* **247**, 367-89.

Hutson, M. R. and Kirby, M. L. (2007). Model systems for the study of heart development and disease. Cardiac neural crest and conotruncal malformations. *Semin Cell Dev Biol* **18**, 101-10.

Ikeya, M., Lee, S. M., Johnson, J. E., McMahon, A. P. and Takada, S. (1997). Wnt signalling required for expansion of neural crest and CNS progenitors. *Nature* **389**, 966-70.

Inoue, T., Chisaka, O., Matsunami, H. and Takeichi, M. (1997). Cadherin-6 expression transiently delineates specific rhombomeres, other neural tube subdivisions, and neural crest subpopulations in mouse embryos. *Dev Biol* **183**, 183-94.

Jeong, J., Mao, J., Tenzen, T., Kottmann, A. H. and McMahon, A. P. (2004). Hedgehog signaling in the neural crest cells regulates the patterning and growth of facial primordia. *Genes Dev* **18**, 937-51.

Jacobson, A. G. (1963). The Determination and Positioning of the Nose, Lens and Ear. Iii. Effects of Reversing the Antero-Posterior Axis of Epidermis, Neural Plate and Neural Fold. *J Exp Zool* **154**, 293-303.

Jacobson, A. G. (1966). Inductive processes in embryonic development. *Science* **152**, 25-34.

Jerome, L. A. and Papaioannou, V. E. (2001). DiGeorge syndrome phenotype in mice mutant for the T-box gene, Tbx1. *Nat Genet* **27**, 286-91.

Jiang, X., Rowitch, D. H., Soriano, P., McMahon, A. P. and Sucov, H. M. (2000). Fate of the mammalian cardiac neural crest. *Development* **127**, 1607-16.

Jones, E. A., Yuan, L., Breant, C., Watts, R. J. and Eichmann, A. (2008). Separating genetic and hemodynamic defects in neuropilin 1 knockout embryos. *Development* **135**, 2479-88.

Joyner, A. L. and Martin, G. R. (1987). En-1 and En-2, two mouse genes with sequence homology to the Drosophila engrailed gene: expression during embryogenesis. *Genes Dev* **1**, 29-38.

Kaartinen, V., Dudas, M., Nagy, A., Sridurongrit, S., Lu, M. M. and Epstein, J. A.

(2004). Cardiac outflow tract defects in mice lacking ALK2 in neural crest cells. *Development* **131**, 3481-90.

Kameda, Y., Nishimaki, T., Takeichi, M. and Chisaka, O. (2002). Homeobox gene hoxa3 is essential for the formation of the carotid body in the mouse embryos. *Dev Biol* **247**, 197-209.

Kameda, Y., Watari-Goshima, N., Nishimaki, T. and Chisaka, O. (2003). Disruption of the Hoxa3 homeobox gene results in anomalies of the carotid artery system and the arterial baroreceptors. *Cell Tissue Res* **311**, 343-52.

Kanzler, B., Foreman, R. K., Labosky, P. A. and Mallo, M. (2000). BMP signaling is essential for development of skeletogenic and neurogenic cranial neural crest. *Development* **127**, 1095-104.

Kanzler, B., Kuschert, S. J., Liu, Y. H. and Mallo, M. (1998). Hoxa-2 restricts the chondrogenic domain and inhibits bone formation during development of the branchial area. *Development* **125**, 2587-97.

Kawasaki, T., Kitsukawa, T., Bekku, Y., Matsuda, Y., Sanbo, M., Yagi, T. and Fujisawa, H. (1999). A requirement for neuropilin-1 in embryonic vessel formation. *Development* **126**, 4895-902.

Kee, Y. and Bronner-Fraser, M. (2005). To proliferate or to die: role of Id3 in cell cycle progression and survival of neural crest progenitors. *Genes Dev* **19**, 744-55.

Kelly, R. G., Jerome-Majewska, L. A. and Papaioannou, V. E. (2004). The del22q11.2 candidate gene Tbx1 regulates branchiomeric myogenesis. *Hum Mol Genet* **13**, 2829-40.

Kempf, H., Linares, C., Corvol, P. and Gasc, J. M. (1998). Pharmacological inactivation of the endothelin type A receptor in the early chick embryo: a model of mispatterning of the branchial arch derivatives. *Development* **125**, 4931-41.

Kingsley, D. M., Bland, A. E., Grubber, J. M., Marker, P. C., Russell, L. B., Copeland, N. G. and Jenkins, N. A. (1992). The mouse short ear skeletal morphogenesis locus is associated with defects in a bone morphogenetic member of the TGF beta superfamily. *Cell* **71**, 399-410.

Kirby, M. L., Gale, T. F. and Stewart, D. E. (1983). Neural crest cells contribute to normal aorticopulmonary septation. *Science* **220**, 1059-61.

Kitamura, K., Miura, H., Miyagawa-Tomita, S., Yanazawa, M., Katoh-Fukui, Y., Suzuki, R., Ohuchi, H., Suehiro, A., Motegi, Y., Nakahara, Y. et al. (1999). Mouse Pitx2 deficiency leads to anomalies of the ventral body wall, heart, extra- and periocular mesoderm and right pulmonary isomerism. *Development* **126**, 5749-58.

Kochilas, L., Merscher-Gomez, S., Lu, M. M., Potluri, V., Liao, J., Kucherlapati, R., Morrow, B. and Epstein, J. A. (2002). The role of neural crest during cardiac development in a mouse model of DiGeorge syndrome. *Dev Biol* **251**, 157-66.

Kontges, G. and Lumsden, A. (1996). Rhombencephalic neural crest segmentation is preserved throughout craniofacial ontogeny. *Development* **122**, 3229-42.

Kubota, Y. and Ito, K. (2000). Chemotactic migration of mesencephalic neural crest cells in the mouse. *Dev Dyn* **217**, 170-9.

Kulesa, P. M., Lu, C. C. and Fraser, S. E. (2005). Time-lapse analysis reveals a series of events by which cranial neural crest cells reroute around physical barriers. *Brain Behav Evol* **66**, 255-65.

Kurihara, Y., Kurihara, H., Oda, H., Maemura, K., Nagai, R., Ishikawa, T. and Yazaki, Y. (1995). Aortic arch malformations and ventricular septal defect in mice deficient in endothelin-1. *J Clin Invest* **96**, 293-300.

Kurihara, Y., Kurihara, H., Suzuki, H., Kodama, T., Maemura, K., Nagai, R., Oda, H., Kuwaki, T., Cao, W. H., Kamada, N. et al. (1994). Elevated blood pressure and craniofacial abnormalities in mice deficient in endothelin-1. *Nature* **368**, 703-10.

Kwang, S. J., Brugger, S. M., Lazik, A., Merrill, A. E., Wu, L. Y., Liu, Y. H., Ishii, M., Sangiorgi, F. O., Rauchman, M., Sucov, H. M. et al. (2002). Msx2 is an immediate downstream effector of Pax3 in the development of the murine cardiac neural crest. *Development* **129**, 527-38.

LaBonne, C. and Bronner-Fraser, M. (1998). Neural crest induction in Xenopus: evidence for a two-signal model. *Development* **125**, 2403-14.

Laclef, C., Souil, E., Demignon, J. and Maire, P. (2003). Thymus, kidney and craniofacial abnormalities in Six 1 deficient mice. *Mech Dev* **120**, 669-79.

Ladher, R. K., Anakwe, K. U., Gurney, A. L., Schoenwolf, G. C. and Francis-West, P. H. (2000). Identification of synergistic signals initiating inner ear development. *Science* **290**, 1965-7.

Ladher, R. K., Wright, T. J., Moon, A. M., Mansour, S. L. and Schoenwolf, G. C. (2005). FGF8 initiates inner ear induction in chick and mouse. *Genes Dev* **19**, 603-13.

Lampe, X., Samad, O. A., Guiguen, A., Matis, C., Remacle, S., Picard, J. J., Rijli, F. M. and Rezsohazy, R. (2008). An ultraconserved Hox-Pbx responsive element resides in the coding sequence of Hoxa2 and is active in rhombomere 4. *Nucleic Acids Res* **36**, 3214-25.

Larina, I. V., Shen, W., Kelly, O. G., Hadjantonakis, A. K., Baron, M. H. and Dickinson, M. E. (2009). A membrane associated mCherry fluorescent reporter line for studying vascular remodelling and cardiac function during murine embryonic development. *Anat Rec (Hoboken)* **292**, 333-41.

Le Douarin, N. M., Creuzet, S., Couly, G. and Dupin, E. (2004). Neural crest cell plasticity and its limits. *Development* **131**, 4637-50.

Le Douarin, N. M. and Dupin, E. (2003). Multipotentiality of the neural crest. *Curr Opin Genet Dev* **13**, 529-36.

Le Douarin, N. M. and Jotereau, F. V. (1975). Tracing of cells of the avian thymus through embryonic life in interspecific chimeras. *J Exp Med* **142**, 17-40.

Le Douarin, N. M. and Kalcheim, C. (1999). The neural crest. 2nd edition Cambridge, UK: Cambridge University Press.

Le Douarin, N. M., Ziller, C. and Couly, G. F. (1993). Patterning of neural crest derivatives in the avian embryo: in vivo and in vitro studies. *Dev Biol* **159**, 24-49.

Leger, S. and Brand, M. (2002). Fgf8 and Fgf3 are required for zebrafish ear placode

induction, maintenance and inner ear patterning. *Mech Dev* **119**, 91-108.

Lepore, J. J., Mericko, P. A., Cheng, L., Lu, M. M., Morrisey, E. E. and Parmacek, M. S. (2006). GATA-6 regulates semaphorin 3C and is required in cardiac neural crest for cardiovascular morphogenesis. *J Clin Invest* **116**, 929-39.

Le Lievre, C. S. and Le Douarin, N. M. (1975). Mesenchymal derivatives of the neural crest: analysis of chimaeric quail and chick embryos. *J Embryol Exp Morphol* **34**, 125-54.

Lee, Y. M., Osumi-Yamashita, N., Ninomiya, Y., Moon, C. K., Eriksson, U. and Eto, K. (1995). Retinoic acid stage-dependently alters the migration pattern and identity of hindbrain neural crest cells. *Development* **121**, 825-37.

Lewis, J. L., Bonner, J., Modrell, M., Ragland, J. W., Moon, R. T., Dorsky, R. I. and Raible, D. W. (2004). Reiterated Wnt signaling during zebrafish neural crest development. *Development* **131**, 1299-308.

Li, J., Chen, F. and Epstein, J. A. (2000). Neural crest expression of Cre recombinase directed by the proximal Pax3 promoter in transgenic mice. *Genesis* **26**, 162-4.

Li, C. W., Van De Water, T. R. and Ruben, R. J. (1978). The fate mapping of the eleventh and twelfth day mouse otocyst: an in vitro study of the sites of origin of the embryonic inner ear sensory structures. *J Morphol* **157**, 249-67.

Li, J., Zhu, X., Chen, M., Cheng, L., Zhou, D., Lu, M. M., Du, K., Epstein, J. A. and Parmacek, M. S. (2005). Myocardin-related transcription factor B is required in cardiac neural crest for smooth muscle differentiation and cardiovascular development. *Proc Natl Acad Sci U S A* **102**, 8916-21.

Li, S., Wang, D. Z., Wang, Z., Richardson, J. A. and Olson, E. N. (2003). The serum response factor coactivator myocardin is required for vascular smooth muscle development. *Proc Natl Acad Sci U S A* **100**, 9366-70.

Li, C. W., Van De Water, T. R. and Ruben, R. J. (1978). The fate mapping of the eleventh and twelfth day mouse otocyst: an in vitro study of the sites of origin of the embryonic inner ear sensory structures. *J Morphol* **157**, 249-67.

Liem, K. F., Jr., Tremml, G., Roelink, H. and Jessell, T. M. (1995). Dorsal differentiation of neural plate cells induced by BMP-mediated signals from epidermal ectoderm. *Cell* **82**, 969-79.

Lin, Z., Cantos, R., Patente, M. and Wu, D. K. (2005). Gbx2 is required for the morphogenesis of the mouse inner ear: a downstream candidate of hindbrain signaling. *Development* **132**, 2309-18

Lindsay, E. A. and Baldini, A. (2001). Recovery from arterial growth delay reduces penetrance of cardiovascular defects in mice deleted for the DiGeorge syndrome region. *Hum Mol Genet* **10**, 997-1002.

Lindsay, E. A., Vitelli, F., Su, H., Morishima, M., Huynh, T., Pramparo, T., Jurecic, V., Ogunrinu, G., Sutherland, H. F., Scambler, P. J. et al. (2001). Tbx1 haploinsufficieny in the DiGeorge syndrome region causes aortic arch defects in mice. *Nature* **410**, 3 97-101.

Liu, D., Chu, H., Maves, L., Yan, Y. L., Morcos, P. A., Postlethwait, J. H. and Westerfield, M. (2003). Fgf3 and Fgf8 dependent and independent transcription factors

are required for otic placode specification. *Development* **130**, 2213-24.

Liu, M., Pereira, F. A., Price, S. D., Chu, M. J., Shope, C., Himes, D., Eatock, R. A., Brownell, W. E., Lysakowski, A. and Tsai, M. J. (2000). Essential role of BETA2/NeuroD1 in development of the vestibular and auditory systems. *Genes Dev* **14**, 2839-54.

Liem, K. F., Jr., Tremml, G., Roelink, H. and Jessell, T. M. (1995). Dorsal differentiation of neural plate cells induced by BMP-mediated signals from epidermal ectoderm. *Cell* **82**, 969-79.

Lindsay, E. A., Vitelli, F., Su, H., Morishima, M., Huynh, T., Pramparo, T., Jurecic, V., Ogunrinu, G., Sutherland, H. F., Scambler, P. J. et al. (2001). Tbx1 haploinsufficieny in the DiGeorge syndrome region causes aortic arch defects in mice. *Nature* **410**, 3 97-101.

Liu, W., Selever, J., Wang, D., Lu, M. F., Moses, K. A., Schwartz, R. J. and Martin, J. F. (2004). Bmp4 signaling is required for outflow-tract septation and branchial-arch artery remodelling. *Proc Natl Acad Sci U S A* **101**, 4489-94.

Lo, C. W., Cohen, M. F., Huang, G. Y., Lazatin, B. O., Patel, N., Sullivan, R., Pauken, C. and Park, S. M. (1997). Cx43 gap junction gene expression and gap junctional communication in mouse neural crest cells. *Dev Genet* **20**, 119-32.

Lumsden, A., Sprawson, N. and Graham, A. (1991). Segmental origin and migration of neural crest cells in the hindbrain region of the chick embryo. *Development* **113**, 1281-91.

Lumsden, A. G. (1988). Spatial organization of the epithelium and the role of neural crest cells in the initiation of the mammalian tooth germ. *Development* **103 Suppl**, 155-69.

Luo, G., Hofmann, C., Bronckers, A. L., Sohocki, M., Bradley, A. and Karsenty, G. (1995). BMP-7 is an inducer of nephrogenesis, and is also required for eye development and skeletal patterning. *Genes Dev* **9**, 2808-20.

Luo, Y., High, F. A., Epstein, J. A. and Radice, G. L. (2006). N-cadherin is required for neural crest remodelling of the cardiac outflow tract. *Dev Biol* **299**, 517-28.

Ma, Q., Chen, Z., del Barco Barrantes, I., de la Pompa, J. L. and Anderson, D. J. (1998). neurogenin1 is essential for the determination of neuronal precursors for proximal cranial sensory ganglia. *Neuron* **20**, 469-82.

Macatee, T. L., Hammond, B. P., Arenkiel, B. R., Francis, L., Frank, D. U. and Moon, A. M. (2003). Ablation of specific expression domains reveals discrete functions of ectoderm- and endoderm-derived FGF8 during cardiovascular and pharyngeal development. *Development* **130**, 6361-74.

Maconochie, M. K., Nonchev, S., Studer, M., Chan, S. K., Popperl, H., Sham, M. H., Mann, R. S. and Krumlauf, R. (1997). Cross-regulation in the mouse HoxB complex: the expression of Hoxb2 in rhombomere 4 is regulated by Hoxb1. *Genes Dev* **11**, 1885-95.

Mallo, M. (1997). Retinoic acid disturbs mouse middle ear development in a stage-dependent fashion. *Dev Biol* **184**, 175-86.

Mallo, M. (1998). Embryological and genetic aspects of middle ear development. *Int J Dev Biol* **42**, 11-22.

Mallo, M. (2001). Formation of the middle ear: recent progress on the developmental and

molecular mechanisms. *Dev Biol* **231**, 410-9.

Mallo, M. (2003). Formation of the outer and middle ear, molecular mechanisms. *Curr Top Dev Biol* **57**, 85-113.

Mallo, M. and Brandlin, I. (1997). Segmental identity can change independently in the hindbrain and rhombencephalic neural crest. *Dev Dyn* **210**, 146-56

Mallo, M. and Gridley, T. (1996). Development of the mammalian ear: coordinate regulation of formation of the tympanic ring and the external acoustic meatus. *Development* **122**, 173-9.

Mancilla, A. and Mayor, R. (1996). Neural crest formation in Xenopus laevis: mechanisms of Xslug induction. *Dev Biol* **177**, 580-9.

Mancini, M. L., Verdi, J. M., Conley, B. A., Nicola, T., Spicer, D. B., Oxburgh, L. H. and Vary, C. P. (2007). Endoglin is required for myogenic differentiation potential of neural crest stem cells. *Dev Biol* **308**, 520-33.

Mani, P., Jarrell, A., Myers, J. and Atit, R. (2010). Visualizing canonical Wnt signaling during mouse craniofacial development. *Dev Dyn*, 354-363.

Manley, N. R., Selleri, L., Brendolan, A., Gordon, J. and Cleary, M. L. (2004). Abnormalities of caudal pharyngeal pouch development in Pbx1 knockout mice mimic loss of Hox3 paralogs. *Dev Biol* **276**, 301-12.

Marchant, L., Linker, C., Ruiz, P., Guerrero, N. and Mayor, R. (1998). The inductive properties of mesoderm suggest that the neural crest cells are specified by a BMP gradient. *Dev Biol* **198**, 319-29.

Mark, M., Ghyselinck, N. B. and Chambon, P. (2004). Retinoic acid signalling in the development of branchial arches. *Curr Opin Genet Dev* **14**, 591-8.

Maroon, H., Walshe, J., Mahmood, R., Kiefer, P., Dickson, C. and Mason, I. (2002). Fgf3 and Fgf8 are required together for formation of the otic placode and vesicle. *Development* **129**, 2099-108.

Martinsen, B. J. and Bronner-Fraser, M. (1998). Neural crest specification regulated by the helix-loop-helix repressor Id2. *Science* **281**, 988-91.

Mayor, R., Morgan, R. and Sargent, M. G. (1995). Induction of the prospective neural crest of Xenopus. *Development* **121**, 767-77.

McCright, B., Lozier, J. and Gridley, T. (2002). A mouse model of Alagille syndrome: Notch2 as a genetic modifier of Jag1 haploinsufficiency. *Development* **129**, 1075-82.

McDonald-McGinn, D. M., Kirschner, R., Goldmuntz, E., Sullivan, K., Eicher, P., Gerdes, M., Moss, E., Solot, C., Wang, P., Jacobs, I. et al. (1999). The Philadelphia story: the 22q11.2 deletion: report on 250 patients. *Genet Couns* **10**, 11-24.

McKay, I. J., Muchamore, I., Krumlauf, R., Maden, M., Lumsden, A. and Lewis, J. (1994). The kreisler mouse: a hindbrain segmentation mutant that lacks two rhombomeres. *Development* **120**, 2199-211.

McMahon, J. A., Takada, S., Zimmerman, L. B., Fan, C. M., Harland, R. M. and McMahon, A. P. (1998). Noggin-mediated antagonism of BMP signaling is required for

growth and patterning of the neural tube and somite. *Genes Dev* **12**, 1438-52.

Mendelsohn, C., Lohnes, D., Decimo, D., Lufkin, T., LeMeur, M., Chambon, P. and Mark, M. (1994). Function of the retinoic acid receptors (RARs) during development (II). Multiple abnormalities at various stages of organogenesis in RAR double mutants. *Development* **120**, 2749-71.

Merlo, G. R., Paleari, L., Mantero, S., Zerega, B., Adamska, M., Rinkwitz, S., Bober, E. and Levi, G. (2002). The Dlx5 homeobox gene is essential for vestibular morphogenesis in the mouse embryo through a BMP4-mediated pathway. *Dev Biol* **248**, 157-69.

Merscher, S., Funke, B., Epstein, J. A., Heyer, J., Puech, A., Lu, M. M., Xavier, R. J., Demay, M. B., Russell, R. G., Factor, S. et al. (2001). TBX1 is responsible for cardiovascular defects in velo-cardio-facial/DiGeorge syndrome. *Cell* **104**, 619-29.

Meulemans, D. and Bronner-Fraser, M. (2004). Gene-regulatory interactions in neural crest evolution and development. *Dev Cell* **7**, 291-9.

Min, H., Danilenko, D. M., Scully, S. A., Bolon, B., Ring, B. D., Tarpley, J. E., DeRose, M. and Simonet, W. S. (1998). Fgf-10 is required for both limb and lung development and exhibits striking functional similarity to Drosophila branchless. *Genes Dev* **12**, 3156-61.

Mitchell, P. J., Timmons, P. M., Hebert, J. M., Rigby, P. W. and Tjian, R. (1991). Transcription factor AP-2 is expressed in neural crest cell lineages during mouse embryogenesis. *Genes Dev* **5**, 105-19.

Miyagawa-Tomita, S., Waldo, K., Tomita, H. and Kirby, M. L. (1991). Temporospatial study of the migration and distribution of cardiac neural crest in quail-chick chimeras. *Am J Anat* **192**, 79-88

Moens, C. B., Cordes, S. P., Giorgianni, M. W., Barsh, G. S. and Kimmel, C. B. (1998). Equivalence in the genetic control of hindbrain segmentation in fish and mouse. *Development* **125**, 381-91.

Moessler, H., Mericskay, M., Li, Z., Nagl, S., Paulin, D. and Small, J. V. (1996). The SM 22 promoter directs tissue-specific expression in arterial but not in venous or visceral smooth muscle cells in transgenic mice. *Development* **122**, 2415-25

Moga, M. (2004). Vestibulocochlear Apparatus (Ear). Histology lecture D502. http://anatomy.iupui.edu/courses/histo_D502/D502f04/lecture.f04/Earf04/eardev.jpg.

Molin, D. G., Bartram, U., Van der Heiden, K., Van Iperen, L., Speer, C. P., Hierck, B. P., Poelmann, R. E. and Gittenberger-de-Groot, A. C. (2003). Expression patterns of Tgfbeta1-3 associate with myocardialisation of the outflow tract and the development of the epicardium and the fibrous heart skeleton. *Dev Dyn* **227**, 431-44.

Molin, D. G., DeRuiter, M. C., Wisse, L. J., Azhar, M., Doetschman, T., Poelmann, R. E. and Gittenberger-de Groot, A. C. (2002). Altered apoptosis pattern during pharyngeal arch artery remodelling is associated with aortic arch malformations in Tgfbeta2 knock-out mice. *Cardiovasc Res* **56**, 312-22.

Moon, A. M., Guris, D. L., Seo, J. H., Li, L., Hammond, J., Talbot, A. and Imamoto, A. (2006). Crkl deficiency disrupts Fgf8 signaling in a mouse model of 22q11 deletion syndromes. *Dev Cell* **10**, 71-80.

Moore-Scott, B. A. and Manley, N. R. (2005). Differential expression of Sonic hedgehog along the anterior-posterior axis regulates patterning of pharyngeal pouch endoderm and pharyngeal endoderm-derived organs. *Dev Biol* **278**, 323-35.

Moraes, F., Novoa, A., Jerome-Majewska, L. A., Papaioannou, V. E. and Mallo, M. (2005). Tbx1 is required for proper neural crest migration and to stabilize spatial patterns during middle and inner ear development. *Mech Dev* **122**, 199-212.

Morales, A. V., Barbas, J. A. and Nieto, M. A. (2005). How to become neural crest: from segregation to delamination. *Semin Cell Dev Biol* **16**, 655-62.

Morishima, M., Yanagisawa, H., Yanagisawa, M. and Baldini, A. (2003). Ece1 and Tbx1 define distinct pathways to aortic arch morphogenesis. *Dev Dyn* **228**, 95-104

Morrison-Graham, K., Schatteman, G. C., Bork, T., Bowen-Pope, D. F. and Weston, J. A. (1992). A PDGF receptor mutation in the mouse (Patch) perturbs the development of a non-neuronal subset of neural crest-derived cells. *Development* **115**, 133-42.

Morsli, H., Choo, D., Ryan, A., Johnson, R. and Wu, D. K. (1998). Development of the mouse inner ear and origin of its sensory organs. *J Neurosci* **18**, 3327-35.

Motoike, T., Loughna, S., Perens, E., Roman, B. L., Liao, W., Chau, T. C., Richardson, C. D., Kawate, T., Kuno, J., Weinstein, B. M. et al. (2000). Universal GFP reporter for the study of vascular development. *Genesis* **28**, 75-81.

Moury, J. D. and Jacobson, A. G. (1990). The origins of neural crest cells in the axolotl. *Dev Biol* **141**, 243-53.

Muller, U. and Littlewood-Evans, A. (2001). Mechanisms that regulate mechanosensory hair cell differentiation. *Trends Cell Biol* **11**, 334-42.

Murray, S. A. and Gridley, T. (2006). Snail family genes are required for left-right asymmetry determination, but not neural crest formation, in mice. *Proc Natl Acad Sci U S A* **103**, 10300-4.

Nagy, A., Gertsenstein, M., Vintersten, K. and Behringer, R. (2003). Manipulating the Mouse Embryo. A Laboratory Manual, 3rd Edition.Cold Spring Harbor Laboratory Press 2003

Nakagawa, S. and Takeichi, M. (1998). Neural crest emigration from the neural tube depends on regulated cadherin expression. *Development* **125**, 2963-71.

Niederreither, K., Vermot, J., Le Roux, I., Schuhbaur, B., Chambon, P. and Dolle, P. (2003). The regional pattern of retinoic acid synthesis by RALDH2 is essential for the development of posterior pharyngeal arches and the enteric nervous system. *Development* **130**, 2525-34.

Niederreither, K., Vermot, J., Messaddeq, N., Schuhbaur, B., Chambon, P. and Dolle, P. (2001). Embryonic retinoic acid synthesis is essential for heart morphogenesis in the mouse. *Development* **128**, 1019-31.

Nieto, M. A., Sargent, M. G., Wilkinson, D. G. and Cooke, J. (1994). Control of cell behavior during vertebrate development by Slug, a zinc finger gene. *Science* **264**, 835-9.

Noden, D. M. (1983a). The embryonic origins of avian cephalic and cervical muscles and associated connective tissues. *Am J Anat* **168**, 257-76.

Noden, D. M. (1983b). The role of the neural crest in patterning of avian cranial skeletal, connective, and muscle tissues. *Dev Biol* **96**, 144-65.

Noden, D. M. (1986). Origins and patterning of craniofacial mesenchymal tissues. *J Craniofac Genet Dev Biol Suppl* **2**, 15-31.

Noden, D. M. (1988). Interactions and fates of avian craniofacial mesenchyme. *Development* **103 Suppl**, 121-40.

Noden, D. M. and Trainor, P. A. (2005). Relations and interactions between cranial mesoderm and neural crest populations. *J Anat* **207**, 575-601.

Noramly, S. and Grainger, R. M. (2002). Determination of the embryonic inner ear. *J Neurobiol* **53**, 100-28.

Nowotschin, S., Eakin, G. S. and Hadjantonakis, A. K. (2009). Live-imaging fluorescent proteins in mouse embryos: multi-dimensional, multi-spectral perspectives. *Trends Biotechnol* **27**, 266-76.

Oh, J., Richardson, J. A. and Olson, E. N. (2005). Requirement of myocardin-related transcription factor-B for remodelling of branchial arch arteries and smooth muscle differentiation. *Proc Natl Acad Sci U S A* **102**, 15122-7.

Ohnemus, S., Kanzler, B., Jerome-Majewska, L. A., Papaioannou, V. E., Boehm, T. and Mallo, M. (2002). Aortic arch and pharyngeal phenotype in the absence of BMP-dependent neural crest in the mouse. *Mech Dev* **119**, 127-35.

Ota, M. S., Loebel, D. A., O'Rourke, M. P., Wong, N., Tsoi, B. and Tam, P. P. (2004). Twist is required for patterning the cranial nerves and maintaining the viability of mesodermal cells. *Dev Dyn* **230**, 216-28.

Ozaki, H., Nakamura, K., Funahashi, J., Ikeda, K., Yamada, G., Tokano, H., Okamura, H. O., Kitamura, K., Muto, S., Kotaki, H. et al. (2004). Six1 controls patterning of the mouse otic vesicle. *Development* **131**, 551-62.

Ozeki, H., Kurihara, Y., Tonami, K., Watatani, S. and Kurihara, H. (2004). Endothelin-1 regulates the dorsoventral branchial arch patterning in mice. *Mech Dev* **121**, 387-95.

Parr, B. A., Shea, M. J., Vassileva, G. and McMahon, A. P. (1993). Mouse Wnt genes exhibit discrete domains of expression in the early embryonic CNS and limb buds. *Development* **119**, 247-61.

Pfab, T., Thone-Reineke, C., Theilig, F., Lange, I., Witt, H., Maser-Gluth, C., Bader, M., Stasch, J. P., Ruiz, P., Bachmann, S. et al. (2006). Diabetic endothelin B receptor-deficient rats develop severe hypertension and progressive renal failure. *J Am Soc Nephrol* **17**, 1082-9.

Phillips, B. T., Bolding, K. and Riley, B. B. (2001). Zebrafish fgf3 and fgf8 encode redundant functions required for otic placode induction. *Dev Biol* **235**, 351-65.

Phillips, B. T., Storch, E. M., Lekven, A. C. and Riley, B. B. (2004). A direct role for Fgf but not Wnt in otic placode induction. *Development* **131**, 923-31.

Phippard, D., Lu, L., Lee, D., Saunders, J. C. and Crenshaw, E. B., 3rd. (1999). Targeted mutagenesis of the POU-domain gene Brn4/Pou3f4 causes developmental defects in the inner ear. *J Neurosci* **19**, 5980-9.

Pietri, T., Eder, O., Blanche, M., Thiery, J. P. and Dufour, S. (2003). The human tissue plasminogen activator-Cre mouse: a new tool for targeting specifically neural crest cells and their derivatives in vivo. *Dev Biol* **259**, 176-87.

Piotrowski, T., Ahn, D. G., Schilling, T. F., Nair, S., Ruvinsky, I., Geisler, R., Rauch, G. J., Haffter, P., Zon, L. I., Zhou, Y. et al. (2003). The zebrafish van gogh mutation disrupts tbx1, which is involved in the DiGeorge deletion syndrome in humans. *Development* **130**, 5043-52.

Piotrowski, T. and Nusslein-Volhard, C. (2000). The endoderm plays an important role in patterning the segmented pharyngeal region in zebrafish (Danio rerio). *Dev Biol* **225**, 339-56.

Pipes, G. C., Creemers, E. E. and Olson, E. N. (2006). The myocardin family of transcriptional coactivators: versatile regulators of cell growth, migration, and myogenesis. *Genes Dev* **20**, 1545-56

Poche, R. A., Larina, I. V., Scott, M. L., Saik, J. E., West, J. L. and Dickinson, M. E. (2009). The Flk1-myr::mCherry mouse as a useful reporter to characterize multiple aspects of ocular blood vessel development and disease. *Dev Dyn* **238**, 2318-26

Popperl, H., Bienz, M., Studer, M., Chan, S. K., Aparicio, S., Brenner, S., Mann, R. S. and Krumlauf, R. (1995). Segmental expression of Hoxb-1 is controlled by a highly conserved autoregulatory loop dependent upon exd/pbx. *Cell* **81**, 1031-42.

Poswillo, D. (1988). The aetiology and pathogenesis of craniofacial deformity. *Development* **103 Suppl**, 207-12.

Pouget, C., Gautier, R., Teillet, M. A. and Jaffredo, T. (2006). Somite-derived cells replace ventral aortic hemangioblasts and provide aortic smooth muscle cells of the trunk. *Development* **133**, 1013-22.

Pratt, R. M., Goulding, E. H. and Abbott, B. D. (1987). Retinoic acid inhibits migration of cranial neural crest cells in the cultured mouse embryo. *J Craniofac Genet Dev Biol* **7**, 205-17.

Price, R. L., Thielen, T. E., Borg, T. K. and Terracio, L. (2001). Cardiac Defects Associated with the Absence of the Platelet-derived Growth Factor alpha Receptor in the Patch Mouse. *Microsc Microanal* **7**, 56-65.

Prince, V. and Lumsden, A. (1994). Hoxa-2 expression in normal and transposed rhombomeres: independent regulation in the neural tube and neural crest. *Development* **120**, 911-23.

Qiu, M., Bulfone, A., Ghattas, I., Meneses, J. J., Christensen, L., Sharpe, P. T., Presley, R., Pedersen, R. A. and Rubenstein, J. L. (1997). Role of the Dlx homeobox genes in proximodistal patterning of the branchial arches: mutations of Dlx-1, Dlx-2, and Dlx-1 and -2 alter morphogenesis of proximal skeletal and soft tissue structures derived from the first and second arches. *Dev Biol* **185**, 165-84.

Quinlan, R., Martin, P. and Graham, A. (2004). The role of actin cables in directing the morphogenesis of the pharyngeal pouches. *Development* **131**, 593-9.

Raft, S., Nowotschin, S., Liao, J. and Morrow, B. E. (2004). Suppression of neural fate and control of inner ear morphogenesis by Tbx1. *Development* **131**, 1801-12.

Represa, J., Leon, Y., Miner, C. and Giraldez, F. (1991). The int-2 proto-oncogene is responsible for induction of the inner ear. *Nature* **353**, 561-3.

Restivo, A., Piacentini, G., Placidi, S., Saffirio, C. and Marino, B. (2006). Cardiac outflow tract: a review of some embryogenetic aspects of the conotruncal region of the heart. *Anat Rec A Discov Mol Cell Evol Biol* **288**, 936-43.

Reyes, M. R., LeBlanc, E. M. and Bassila, M. K. (1999). Hearing loss and otitis media in velo-cardio-facial syndrome. *Int J Pediatr Otorhinolaryngol* **47**, 227-33.

Riccomagno, M. M., Martinu, L., Mulheisen, M., Wu, D. K. and Epstein, D. J. (2002). Specification of the mammalian cochlea is dependent on Sonic hedgehog. *Genes Dev* **16**, 2365-78.

Riccomagno, M. M., Takada, S. and Epstein, D. J. (2005). Wnt-dependent regulation of inner ear morphogenesis is balanced by the opposing and supporting roles of Shh. *Genes Dev* **19**, 1612-23.

Rijli, F. M., Mark, M., Lakkaraju, S., Dierich, A., Dolle, P. and Chambon, P. (1993). A homeotic transformation is generated in the rostral branchial region of the head by disruption of Hoxa-2, which acts as a selector gene. *Cell* **75**, 1333-49.

Riley, B. B. and Phillips, B. T. (2003). Ringing in the new ear: resolution of cell interactions in otic development. *Dev Biol* **261**, 289-312.

Rinkwitz, S., Bober, E. and Baker, R. (2001). Development of the vertebrate inner ear. *Ann N Y Acad Sci* **942**, 1-14.

Rinkwitz-Brandt, S., Arnold, H. H. and Bober, E. (1996). Regionalized expression of Nkx5-1, Nkx5-2, Pax2 and sek genes during mouse inner ear development. *Hear Res* **99**, 129-38.

Risau, W. and Flamme, I. (1995). Vasculogenesis. *Annu Rev Cell Dev Biol* **11**, 73-91.

Roberts, C., Ivins, S., Cook, A. C., Baldini, A. and Scambler, P. J. (2006). Cyp26 genes a1, b1 and c1 are down-regulated in Tbx1 null mice and inhibition of Cyp26 enzyme function produces a phenocopy of DiGeorge Syndrome in the chick. *Hum Mol Genet* **15**, 3394-410.

Robledo, R. F. and Lufkin, T. (2006). Dlx5 and Dlx6 homeobox genes are required for specification of the mammalian vestibular apparatus. *Genesis* **44**, 425-37.

Roessler, E., Belloni, E., Gaudenz, K., Vargas, F., Scherer, S. W., Tsui, L. C. and Muenke, M. (1997). Mutations in the C-terminal domain of Sonic Hedgehog cause holoprosencephaly. *Hum Mol Genet* **6**, 1847-53.

Ruf, R. G., Xu, P. X., Silvius, D., Otto, E. A., Beekmann, F., Muerb, U. T., Kumar, S., Neuhaus, T. J., Kemper, M. J., Raymond, R. M., Jr. et al. (2004). SIX1 mutations cause branchio-oto-renal syndrome by disruption of EYA1-SIX1-DNA complexes. *Proc Natl Acad Sci U S A* **101**, 8090-5.

Sandler, T. (2004). *Langman's Medical Embryology*, Philadelphia, PA: Lippincott,Williams & Wilkins.

Saint-Jeannet, J. P., He, X., Varmus, H. E. and Dawid, I. B. (1997). Regulation of dorsal fate in the neuraxis by Wnt-1 and Wnt-3a. *Proc Natl Acad Sci U S A* **94**, 13713-8.

References

Sanyanusin, P., Schimmenti, L. A., McNoe, L. A., Ward, T. A., Pierpont, M. E., Sullivan, M. J., Dobyns, W. B. and Eccles, M. R. (1995). Mutation of the PAX2 gene in a family with optic nerve colobomas, renal anomalies and vesicoureteral reflux. *Nat Genet* **9**, 358-64.

Sato, T., Sasai, N. and Sasai, Y. (2005). Neural crest determination by co-activation of Pax3 and Zic1 genes in Xenopus ectoderm. *Development* **132**, 2355-63.

Sauka-Spengler, T. and Bronner-Fraser, M. (2008). A gene regulatory network orchestrates neural crest formation. *Nat Rev Mol Cell Biol* **9**, 557-68.

Scambler, P. J. (2000). The 22q11 deletion syndromes. *Hum Mol Genet* **9**, 2421-6.

Schatteman, G. C., Morrison-Graham, K., van Koppen, A., Weston, J. A. and Bowen-Pope, D. F. (1992). Regulation and role of PDGF receptor alpha-subunit expression during embryogenesis. *Development* **115**, 123-31.

Schilling, T. F. and Kimmel, C. B. (1994). Segment and cell type lineage restrictions during pharyngeal arch development in the zebrafish embryo. *Development* **120**, 483-94.

Schlosser, G. (2006). Induction and specification of cranial placodes. *Dev Biol* **294**, 303-51.

Schoenwolf, G. C., Francis-West, P. H., Brauer, P. R. and Bleyl, S. B. (2008). Larsen'S Human Embryology: Philadelphia : Churchill Livingstone/Elsevier.

Sechrist, J., Serbedzija, G. N., Scherson, T., Fraser, S. E. and Bronner-Fraser, M. (1993). Segmental migration of the hindbrain neural crest does not arise from its segmental generation. *Development* **118**, 691-703.

Sefton, M., Sanchez, S. and Nieto, M. A. (1998). Conserved and divergent roles for members of the Snail family of transcription factors in the chick and mouse embryo. *Development* **125**, 3111-21.

Sela-Donenfeld, D. and Kalcheim, C. (1999). Regulation of the onset of neural crest migration by coordinated activity of BMP4 and Noggin in the dorsal neural tube. *Development* **126**, 4749-62.

Selleck, M. A. and Bronner-Fraser, M. (1995). Origins of the avian neural crest: the role of neural plate-epidermal interactions. *Development* **121**, 525-38.

Selleck, M. A. and Bronner-Fraser, M. (1996). The genesis of avian neural crest cells: a classic embryonic induction. *Proc Natl Acad Sci U S A* **93**, 9352-7.

Selleck, M. A., Garcia-Castro, M. I., Artinger, K. B. and Bronner-Fraser, M. (1998). Effects of Shh and Noggin on neural crest formation demonstrate that BMP is required in the neural tube but not ectoderm. *Development* **125**, 4919-30.

Selleri, L., Depew, M. J., Jacobs, Y., Chanda, S. K., Tsang, K. Y., Cheah, K. S., Rubenstein, J. L., O'Gorman, S. and Cleary, M. L. (2001). Requirement for Pbx1 in skeletal patterning and programming chondrocyte proliferation and differentiation. *Development* **128**, 3543-57.

Serbedzija, G. N., Bronner-Fraser, M. and Fraser, S. E. (1992). Vital dye analysis of cranial neural crest cell migration in the mouse embryo. *Development* **116**, 297-307.

Shalaby, F., Rossant, J., Yamaguchi, T. P., Gertsenstein, M., Wu, X. F., Breitman, M. L. and Schuh, A. C. (1995). Failure of blood-island formation and vasculogenesis in Flk-1-deficient mice. *Nature* **376**, 62-6.

Shamim, H. and Mason, I. (1998). Expression of Gbx-2 during early development of the chick embryo. *Mech Dev* **76**, 157-9.

Sharpe, J., Ahlgren, U., Perry, P., Hill, B., Ross, A., Hecksher-Sorensen, J., Baldock, R. and Davidson, D. (2002). Optical projection tomography as a tool for 3D microscopy and gene expression studies. *Science* **296**, 541-5.

Shaner, N. C., Campbell, R. E., Steinbach, P. A., Giepmans, B. N., Palmer, A. E. and Tsien, R. Y. (2004). Improved monomeric red, orange and yellow fluorescent proteins derived from Discosoma sp. red fluorescent protein. *Nat Biotechnol* **22**, 1567-72.

Shoval, I., Ludwig, A. and Kalcheim, C. (2007). Antagonistic roles of full-length N-cadherin and its soluble BMP cleavage product in neural crest delamination. *Development* **134**, 491-501.

Simeone, A., Acampora, D., Gulisano, M., Stornaiuolo, A. and Boncinelli, E. (1992). Nested expression domains of four homeobox genes in developing rostral brain. *Nature* **358**, 687-90.

Smith, A. and Graham, A. (2001). Restricting Bmp-4 mediated apoptosis in hindbrain neural crest. *Dev Dyn* **220**, 276-83.

Smith, A., Robinson, V., Patel, K. and Wilkinson, D. G. (1997). The EphA4 and EphB1 receptor tyrosine kinases and ephrin-B2 ligand regulate targeted migration of branchial neural crest cells. *Curr Biol* **7**, 561-70.

Snider, P., Olaopa, M., Firulli, A. B. and Conway, S. J. (2007). Cardiovascular development and the colonizing cardiac neural crest lineage. *ScientificWorldJournal* **7**, 1090-113

Solloway, M. J. and Robertson, E. J. (1999). Early embryonic lethality in Bmp5;Bmp7 double mutant mice suggests functional redundancy within the 60A subgroup. *Development* **126**, 1753-68.

Soo, K., O'Rourke, M. P., Khoo, P. L., Steiner, K. A., Wong, N., Behringer, R. R. and Tam, P. P. (2002). Twist function is required for the morphogenesis of the cephalic neural tube and the differentiation of the cranial neural crest cells in the mouse embryo. *Dev Biol* **247**, 251-70.

Soriano, P. (1997). The PDGF alpha receptor is required for neural crest cell development and for normal patterning of the somites. *Development* **124**, 2691-700.

Stalmans, I., Lambrechts, D., De Smet, F., Jansen, S., Wang, J., Maity, S., Kneer, P., von der Ohe, M., Swillen, A., Maes, C. et al. (2003). VEGF: a modifier of the del22q11 (DiGeorge) syndrome? *Nat Med* **9**, 173-82.

Steel, K. P. (1995). Inherited hearing defects in mice. *Annu Rev Genet* **29**, 675-701.

Steventon, B., Carmona-Fontaine, C. and Mayor, R. (2005). Genetic network during neural crest induction: from cell specification to cell survival. *Semin Cell Dev Biol* **16**, 647-54.

References

Stottmann, R. W., Choi, M., Mishina, Y., Meyers, E. N. and Klingensmith, J. (2004). BMP receptor IA is required in mammalian neural crest cells for development of the cardiac outflow tract and ventricular myocardium. *Development* **131**, 2205-18.

Streit, A. (2001). Origin of the vertebrate inner ear: evolution and induction of the otic placode. *J Anat* **199**, 99-103.

Streit, A., Lee, K. J., Woo, I., Roberts, C., Jessell, T. M. and Stern, C. D. (1998). Chordin regulates primitive streak development and the stability of induced neural cells, but is not sufficient for neural induction in the chick embryo. *Development* **125**, 507-19.

Su, Y. and Meng, A. (2002). The expression of gbx-2 during zebrafish embryogenesis. *Mech Dev* **113**, 107-10.

Sulik, K. and Bream, P. R. (1995). *Langman's Medical Embryology*, 7th Edition. T.W. Sadler. Lippincott, Williams & Wilkins. http://www.med.unc.edu/embryo_images

Suchting, S., Freitas, C., le Noble, F., Benedito, R., Breant, C., Duarte, A. and Eichmann, A. (2007). The Notch ligand Delta-like 4 negatively regulates endothelial tip cell formation and vessel branching. *Proc Natl Acad Sci U S A*.

Swanson, G. J., Howard, M. and Lewis, J. (1990). Epithelial autonomy in the development of the inner ear of a bird embryo. *Dev Biol* **137**, 243-57.

Swillen, A., Devriendt, K., Legius, E., Prinzie, P., Vogels, A., Ghesquiere, P. and Fryns, J. P. (1999). The behavioural phenotype in velo-cardio-facial syndrome (VCFS): from infancy to adolescence. *Genet Couns* **10**, 79-88.

Tallquist, M. D., French, W. J. and Soriano, P. (2003). Additive effects of PDGF receptor beta signaling pathways in vascular smooth muscle cell development. *PLoS Biol* **1**, E52.

Tallquist, M. D. and Soriano, P. (2003). Cell autonomous requirement for PDGFRalpha in populations of cranial and cardiac neural crest cells. *Development* **130**, 507-18.

Taneyhill, L. A., Coles, E. G. and Bronner-Fraser, M. (2007). Snail2 directly represses cadherin6B during epithelial-to-mesenchymal transitions of the neural crest. *Development* **134**, 1481-90.

Torres, M. and Giraldez, F. (1998). The development of the vertebrate inner ear. *Mech Dev* **71**, 5-21.

Torres, M., Gomez-Pardo, E. and Gruss, P. (1996). Pax2 contributes to inner ear patterning and optic nerve trajectory. *Development* **122**, 3381-91.

Toyofuku, T., Yoshida, J., Sugimoto, T., Yamamoto, M., Makino, N., Takamatsu, H., Takegahara, N., Suto, F., Hori, M., Fujisawa, H. et al. (2008). Repulsive and attractive semaphorins cooperate to direct the navigation of cardiac neural crest cells. *Dev Biol* **321**, 251-62.

Trainor, P. and Krumlauf, R. (2000). Plasticity in mouse neural crest cells reveals a new patterning role for cranial mesoderm. *Nat Cell Biol* **2**, 96-102.

Trainor, P. A., Sobieszczuk, D., Wilkinson, D. and Krumlauf, R. (2002). Signalling between the hindbrain and paraxial tissues dictates neural crest migration pathways. *Development* **129**, 433-42.

Trainor, P. A. and Tam, P. P. (1995). Cranial paraxial mesoderm and neural crest cells of the mouse embryo: co-distribution in the craniofacial mesenchyme but distinct segregation in branchial arches. *Development* **121**, 2569-82.

Trainor, P. A., Tan, S. S. and Tam, P. P. (1994). Cranial paraxial mesoderm: regionalisation of cell fate and impact on craniofacial development in mouse embryos. *Development* **120**, 2397-408.

Trokovic, N., Trokovic, R., Mai, P. and Partanen, J. (2003). Fgfr1 regulates patterning of the pharyngeal region. *Genes Dev* **17**, 141-53.

Trokovic, N., Trokovic, R. and Partanen, J. (2005). Fibroblast growth factor signalling and regional specification of the pharyngeal ectoderm. *Int J Dev Biol* **49**, 797-805.

Trumpp, A., Depew, M. J., Rubenstein, J. L., Bishop, J. M. and Martin, G. R. (1999). Cre-mediated gene inactivation demonstrates that FGF8 is required for cell survival and patterning of the first branchial arch. *Genes Dev* **13**, 3136-48.

Varadkar, P., Kraman, M., Despres, D., Ma, G., Lozier, J. and McCright, B. (2008). Notch2 is required for the proliferation of cardiac neural crest-derived smooth muscle cells. *Dev Dyn* **237**, 1144-52.

Vazquez-Echeverria, C., Dominguez-Frutos, E., Charnay, P., Schimmang, T. and Pujades, C. (2008). Analysis of mouse kreisler mutants reveals new roles of hindbrain-derived signals in the establishment of the otic neurogenic domain. *Dev Biol* **322**, 167-78.

Veitch, E., Begbie, J., Schilling, T. F., Smith, M. M. and Graham, A. (1999). Pharyngeal arch patterning in the absence of neural crest. *Curr Biol* **9**, 1481-4.

Vincent, S., Ruberte, E., Grieder, N. C., Chen, C. K., Haerry, T., Schuh, R. and Affolter, M. (1997). DPP controls tracheal cell migration along the dorsoventral body axis of the Drosophila embryo. *Development* **124**, 2741-50.

Vitelli, F., Morishima, M., Taddei, I., Lindsay, E. A. and Baldini, A. (2002a). Tbx1 mutation causes multiple cardiovascular defects and disrupts neural crest and cranial nerve migratory pathways. *Hum Mol Genet* **11**, 915-22.

Vitelli, F., Taddei, I., Morishima, M., Meyers, E. N., Lindsay, E. A. and Baldini, A. (2002b). A genetic link between Tbx1 and fibroblast growth factor signaling. *Development* **129**, 4605-11.

Vitelli, F., Viola, A., Morishima, M., Pramparo, T., Baldini, A. and Lindsay, E. (2003). TBX1 is required for inner ear morphogenesis. *Hum Mol Genet* **12**, 2041-8.

Vrancken Peeters, M. P., Gittenberger-de Groot, A. C., Mentink, M. M. and Poelmann, R. E. (1999). Smooth muscle cells and fibroblasts of the coronary arteries derive from epithelial-mesenchymal transformation of the epicardium. *Anat Embryol (Berl)* **199**, 367-78.

Wang, D. Z., Li, S., Hockemeyer, D., Sutherland, L., Wang, Z., Schratt, G., Richardson, J. A., Nordheim, A. and Olson, E. N. (2002). Potentiation of serum response factor activity by a family of myocardin-related transcription factors. *Proc Natl Acad Sci U S A* **99**, 14855-60.

Waldo, K. L., Hutson, M. R., Ward, C. C., Zdanowicz, M., Stadt, H. A., Kumiski, D.,

Abu-Issa, R. and Kirby, M. L. (2005). Secondary heart field contributes myocardium and smooth muscle to the arterial pole of the developing heart. *Dev Biol* **281**, 78-90

Waldo, K. and Kirby, M. L. (1998). Living Morphogenesis of the Heart. Boston, MA: eds de la Cruz, M.& Markwald, R., **Birkhäuser, Boston, MA**.

Waldo, K., Miyagawa-Tomita, S., Kumiski, D. and Kirby, M. L. (1998). Cardiac neural crest cells provide new insight into septation of the cardiac outflow tract: aortic sac to ventricular septal closure. *Dev Biol* **196**, 129-44.

Waldo, K. L., Kumiski, D. and Kirby, M. L. (1996). Cardiac neural crest is essential for the persistence rather than the formation of an arch artery. *Dev Dyn* **205**, 281-92.

Waldo, K. L., Lo, C. W. and Kirby, M. L. (1999). Connexin 43 expression reflects neural crest patterns during cardiovascular development. *Dev Biol* **208**, 307-23.

Walls, J. R., Coultas, L., Rossant, J. and Henkelman, R. M. (2008). Three-dimensional analysis of vascular development in the mouse embryo. *PLoS ONE* **3**, e2853

Wang, D., Chang, P. S., Wang, Z., Sutherland, L., Richardson, J. A., Small, E., Krieg, P. A. and Olson, E. N. (2001). Activation of cardiac gene expression by myocardin, a transcriptional cofactor for serum response factor. *Cell* **105**, 851-62.

Wang, D. Z. and Olson, E. N. (2004). Control of smooth muscle development by the myocardin family of transcriptional coactivators. *Curr Opin Genet Dev* **14**, 558-66

Wang, J., Nagy, A., Larsson, J., Dudas, M., Sucov, H. M. and Kaartinen, V. (2006). Defective ALK5 signaling in the neural crest leads to increased postmigratory neural crest cell apoptosis and severe outflow tract defects. *BMC Dev Biol* **6**, 51.

Wang, W., Van De Water, T. and Lufkin, T. (1998). Inner ear and maternal reproductive defects in mice lacking the Hmx3 homeobox gene. *Development* **125**, 621-34.

Walshe, J. and Mason, I. (2003). Fgf signalling is required for formation of cartilage in the head. *Dev Biol* **264**, 522-36.

Wassarman, K. M., Lewandoski, M., Campbell, K., Joyner, A. L., Rubenstein, J. L., Martinez, S. and Martin, G. R. (1997). Specification of the anterior hindbrain and establishment of a normal mid/hindbrain organizer is dependent on Gbx2 gene function. *Development* **124**, 2923-34.

Watari, N., Kameda, Y., Takeichi, M. and Chisaka, O. (2001). Hoxa3 regulates integration of glossopharyngeal nerve precursor cells. *Dev Biol* **240**, 15-31.

Waters, S. T. and Lewandoski, M. (2006). A threshold requirement for Gbx2 levels in hindbrain development. *Development* **133**, 1991-2000.

Wawersik, S., Evola, C. and Whitman, M. (2005). Conditional BMP inhibition in Xenopus reveals stage-specific roles for BMPs in neural and neural crest induction. *Dev Biol* **277**, 425-42.

Wei, K., Che, N. and Chen, F. (2007). Myocardin-related transcription factor B is required for normal mouse vascular development and smooth muscle gene expression. *Dev Dyn* **236**, 416-25.

Wendling, O., Dennefeld, C., Chambon, P. and Mark, M. (2000). Retinoid signaling is

essential for patterning the endoderm of the third and fourth pharyngeal arches. *Development* **127**, 1553-62.

Weinstein, B. M. (2005). Vessels and nerves: marching to the same tune. *Cell* **120**, 299-302.

Whitfield, T. T., Granato, M., van Eeden, F. J., Schach, U., Brand, M., Furutani-Seiki, M., Haffter, P., Hammerschmidt, M., Heisenberg, C. P., Jiang, Y. J. et al. (1996). Mutations affecting development of the zebrafish inner ear and lateral line. *Development* **123**, 241-54.

Wilkinson, D. G., Bailes, J. A. and McMahon, A. P. (1987). Expression of the proto-oncogene int-1 is restricted to specific neural cells in the developing mouse embryo. *Cell* **50**, 79-88.

Winnier, G., Blessing, M., Labosky, P. A. and Hogan, B. L. (1995). Bone morphogenetic protein-4 is required for mesoderm formation and patterning in the mouse. *Genes Dev* **9**, 2105-16.

Wright, T. J. and Mansour, S. L. (2003). Fgf3 and Fgf10 are required for mouse otic placode induction. *Development* **130**, 3379-90.

Wu, D. K., Nunes, F. D. and Choo, D. (1998). Axial specification for sensory organs versus non-sensory structures of the chicken inner ear. *Development* **125**, 11-20.

Wu, J., Saint-Jeannet, J. P. and Klein, P. S. (2003). Wnt-frizzled signaling in neural crest formation. *Trends Neurosci* **26**, 40-5.

Wurdak, H., Ittner, L. M., Lang, K. S., Leveen, P., Suter, U., Fischer, J. A., Karlsson, S., Born, W. and Sommer, L. (2005). Inactivation of TGFbeta signaling in neural crest stem cells leads to multiple defects reminiscent of DiGeorge syndrome. *Genes Dev* **19**, 530-5.

Xiang, M., Gao, W. Q., Hasson, T. and Shin, J. J. (1998). Requirement for Brn-3c in maturation and survival, but not in fate determination of inner ear hair cells. *Development* **125**, 3935-46.

Xu, H., Morishima, M., Wylie, J. N., Schwartz, R. J., Bruneau, B. G., Lindsay, E. A. and Baldini, A. (2004). Tbx1 has a dual role in the morphogenesis of the cardiac outflow tract. *Development* **131**, 3217-27

Xu, P. X., Adams, J., Peters, H., Brown, M. C., Heaney, S. and Maas, R. (1999). Eya1-deficient mice lack ears and kidneys and show abnormal apoptosis of organ primordia. *Nat Genet* **23**, 113-7.

Xue, Y., Gao, X., Lindsell, C. E., Norton, C. R., Chang, B., Hicks, C., Gendron-Maguire, M., Rand, E. B., Weinmaster, G. and Gridley, T. (1999). Embryonic lethality and vascular defects in mice lacking the Notch ligand Jagged1. *Hum Mol Genet* **8**, 723-30.

Yagi, H., Furutani, Y., Hamada, H., Sasaki, T., Asakawa, S., Minoshima, S., Ichida, F., Joo, K., Kimura, M., Imamura, S. et al. (2003). Role of TBX1 in human del22q11.2 syndrome. *Lancet* **362**, 1366-73.

References

Yamanaka, Y., Tamplin, O. J., Beckers, A., Gossler, A. and Rossant, J. (2007). Live imaging and genetic analysis of mouse notochord formation reveals regional morphogenetic mechanisms. *Dev Cell* **13**, 884-96.

Yamagishi, H., Maeda, J., Hu, T., McAnally, J., Conway, S. J., Kume, T., Meyers, E. N., Yamagishi, C. and Srivastava, D. (2003). Tbx1 is regulated by tissue-specific forkhead proteins through a common Sonic hedgehog-responsive enhancer. *Genes Dev* **17**, 269-81.

Yamauchi, Y., Abe, K., Mantani, A., Hitoshi, Y., Suzuki, M., Osuzu, F., Kuratani, S. and Yamamura, K. (1999). A novel transgenic technique that allows specific marking of the neural crest cell lineage in mice. *Dev Biol* **212**, 191-203.

Yanagisawa, H., Hammer, R. E., Richardson, J. A., Williams, S. C., Clouthier, D. E. and Yanagisawa, M. (1998). Role of Endothelin-1/Endothelin-A receptor-mediated signaling pathway in the aortic arch patterning in mice. *J Clin Invest* **102**, 22-33.

Yashiro, K., Shiratori, H. and Hamada, H. (2007). Haemodynamics determined by a genetic programme govern asymmetric development of the aortic arch. *Nature* **450**, 285-288.

Yoshida, T., Sinha, S., Dandre, F., Wamhoff, B. R., Hoofnagle, M. H., Kremer, B. E., Wang, D. Z., Olson, E. N. and Owens, G. K. (2003). Myocardin is a key regulator of CArG-dependent transcription of multiple smooth muscle marker genes. *Circ Res* **92**, 856-64.

Zhang, Z., Cerrato, F., Xu, H., Vitelli, F., Morishima, M., Vincentz, J., Furuta, Y., Ma, L., Martin, J. F., Baldini, A. et al. (2005). Tbx1 expression in pharyngeal epithelia is necessary for pharyngeal arch artery development. *Development* **132**, 5307-15.

Zhang, H. and Bradley, A. (1996). Mice deficient for BMP2 are nonviable and have defects in amnion/chorion and cardiac development. *Development* **122**, 2977-86.

Zhang, Z., Huynh, T. and Baldini, A. (2006). Mesodermal expression of Tbx1 is necessary and sufficient for pharyngeal arch and cardiac outflow tract development. *Development* **133**, 3587-95.

Zheng, W., Huang, L., Wei, Z. B., Silvius, D., Tang, B. and Xu, P. X. (2003). The role of Six1 in mammalian auditory system development. *Development* **130**, 3989-4000.

Zou, D., Silvius, D., Fritzsch, B. and Xu, P. X. (2004). Eya1 and Six1 are essential for early steps of sensory neurogenesis in mammalian cranial placodes. *Development* **131**, 5561-72.

Curriculum Vitae

Curriculum Vitae

Filipa Moraes was born on the 2nd of June in Lisbon, Portugal. She completed secondary education in Liceu Camões, Lisbon, in 1994 and studied Applied Chemistry/Biotechnology at the Faculdade de Ciências e Tecnologia of the Universidade Nova de Lisboa. She graduated in 2001, completing her undergraduate thesis in the Immunology Department at *Faculdade de Ciências Médicas*, *Universidade Nova de Lisboa*, under the supervision of Prof. Dr. Maria Fernanda Barros. In 2002 she started working as a technician, at the Transgenic Unit run by Prof. Dr. Moisés Mallo, at *Instituto Gulbenkian de Ciência, Oeiras*, Portugal, and continued on in 2004 with her PhD studies investigating the role of *Tbx1* gene in mouse embryonic development and the role of neural crest-derived smooth muscle cells during remodelling of the mammalian vasculature. The research in this thesis was carried out under the supervision of Prof. Dr. Moisés Mallo.

Publications

Publications

Moraes, F., Novoa, A., Jerome-Majewska, L. A., Papaioannou, V. E. and Mallo, M. (2005). Tbx1 is required for proper neural crest migration and to stabilize spatial patterns during middle and inner ear development. Mech Dev 122, 199-212.

Correia, A. C*., Costa, M*., **Moraes, F*.,** Bom, J., Nóvoa, A. and Mallo, M. (2007). *Bmp2* is required for migration but not for induction of neural crest cells in the mouse. Dev Dyn 236, 2493-501 (* joint first author).

Date: 18.March.2010

Appendix

Mechanisms of Development **122**, 199-212
(2005)

Developmental Dynamics **236**, 2493-501
(2007)

ELSEVIER

Mechanisms of Development 122 (2005) 199–212

www.elsevier.com/locate/modo

Tbx1 is required for proper neural crest migration and to stabilize spatial patterns during middle and inner ear development

Filipa Moraes[a,b], Ana Nóvoa[a], Loydie A. Jerome-Majewska[c], Virginia E. Papaioannou[c], Moisés Mallo[a,*]

[a]*Instituto Gulbenkian de Ciência, UT, Rua da Quinta Grande 6, 2780-156 Oeiras, Portugal*
[b]*Centro de Biologia do Desenvolvimento at IGC, Oeiras, Portugal*
[c]*Department of Genetics and Development, College of Physicians and Surgeons of Columbia University, New York, NY, USA*

Received 24 March 2004; received in revised form 29 September 2004; accepted 8 October 2004
Available online 4 November 2004

Abstract

Tbx1 belongs to the family of T-box containing transcription factors. In humans, *TBX1* is implicated in the etiology of the DiGeorge syndrome. Inactivation of the *Tbx1* gene in mice produces a variety of malformations including abnormal branching of the heart outflow tract, deficiencies in the branchial arch derivatives, agenesis of pharyngeal glands and abnormal development of the auditory system. We analyze here the middle and inner ear phenotypes of the *Tbx1* null mice. The middle ear is strongly affected. Its skeletal components are malformed to varying degrees, some being slightly hypoplastic and others completely absent. However, a seemingly normal-looking tympanic membrane can still be recognized. Middle ear anomalies are associated with other skeletal deficiencies in the branchial arch-derived skeleton. These phenotypes derive from a combination of the failure of the posterior branchial arches to develop and the misrouting of neural crest cells. The inner ears of $Tbx1^{-/-}$ animals are hypoplastic. No vestibular or cochlear structures are detectable, but the endolymphatic duct, the cochleovestibular ganglia and residual sensory patches are still identifiable. Molecular analyses revealed a seemingly normal spatial distribution of a variety of patterning markers in the otic vesicles of *Tbx1* null mutants at E9.0. However, 1 day later, several of these markers presented altered domains of expression in the otocysts of these mutant embryos, suggesting that *Tbx1* is not required for the establishment of spatial patterns in the otocyst, but rather for their maintenance. The inability of the $Tbx1^{-/-}$ embryos to keep properly segregated functional domains in the otocyst is likely the cause of the strong inner ear phenotypes observed in these mutants.
© 2005 Elsevier Ireland Ltd. All rights reserved.

Keywords: *Tbx1*; T-box; Middle ear; Inner ear; DiGeorge syndrome

1. Introduction

The mammalian hearing apparatus consists of three main compartments, the outer, middle and inner ears. The outer ear receives acoustic waves from the air, which are amplified and transmitted by the middle ear elements into the inner ear to generate vibrations in the endolymph. These vibrations excite the hair cells of the organ of Corti, located in the cochlear part of the inner ear, to generate neural impulses that are transmitted to the brain through the acoustic nerve. While the outer and middle ears are exclusively implicated in hearing, the inner ear is also involved in the process of balance, centered in the vestibular area. Specific sensory receptors located in the cristae and maculae detect, respectively, movements of the liquid in the semicircular channels and the position of the otoliths in the utricule and sacculus.

In recent decades, impressive advances have been made in our understanding of the embryological, molecular and genetic bases of the development of the different ear compartments (reviewed in Mallo, 1998, 2001, 2003; Torres and Giráldez, 1998; Riley and Phillips, 2003). The outer and middle ears derive from the first and second branchial arches. Their development is closely linked to general patterning and morphogenetic processes in this area, which require cells of the cranial neural crest and their interactions

* Corresponding author. Tel.: +351 21 446 4624; fax: +351 21 440 7970.
E-mail address: mallo@igc.gulbenkian.pt (M. Mallo).

0925-4773/$ - see front matter © 2005 Elsevier Ireland Ltd. All rights reserved.
doi:10.1016/j.mod.2004.10.004

with the ectodermal and endodermal compartments of the developing branchial arches (reviewed in Mallo, 1998, 2001, 2003). The origin of the inner ear is completely different. It derives from the otic placode, an ectodermal thickening adjacent to the hindbrain. The placode invaginates and forms first the otic cup and then the otic vesicle (also known as the otocyst), which undergoes a complex series of morphogenetic and differentiation processes, eventually giving rise to a variety of structures and cell types (Torres and Giráldez, 1998; Riley and Phillips, 2003). As the otic epithelium differentiates, it interacts with the surrounding mesenchyme to induce formation of a skeletal case for the inner ear.

The otic vesicle develops in a sequential fashion. In an early stage, a group of cells in the rostro-ventral part becomes committed to a neural fate and delaminates to give rise to the neurons of the VIIIth cranial ganglion (also called the cochleo-vestibular ganglion, cvg) (Torres and Giráldez, 1998). The endolymphatic duct also starts its morphogenesis at a very early stage, as an outgrowth in the dorsal part of the otic vesicle (Brigande et al., 2000). Later on, differential gene expression within the otocyst results in the formation of the cochlea, semicircular channels, utricule and sacculus from specific areas of the otic epithelium (Torres and Giráldez, 1998; Riley and Phillips, 2003). Several of the genes responsible for these differentiation processes have been identified, mostly by using mutational approaches. Different groups of genes, including transcription factors, secreted molecules and their receptors, have been implicated in these processes, and some of the networks connecting these molecules are beginning to be understood (Torres et al., 1996; Hadrys et al., 1998; Ma et al., 1998; Wang et al., 1998; Acampora et al., 1999; Depew et al., 1999; Xu et al., 1999; Liu et al., 2000; Riccomagno et al., 2002; Bachiller et al., 2003; Laclef et al., 2003; Zheng et al., 2003).

Tbx1 is a member of the T-box-containing family of transcription factors (Bollag et al., 1994). In humans, the *TBX1* gene is located within the microdeletion on chromosome 22 associated with the DiGeorge syndrome (Scambler, 2000), characterized by cardiovascular malformations, hypoplasia or aplasia of the thymus and parathyroid glands, and craniofacial defects (Scambler, 2000). Recent studies indicated that *TBX1* is one of the major players in the etiopathogenesis of the DiGeorge syndrome, which results from haploinsufficiency of this gene (Merscher et al., 2001). In the mouse, mutations in the *Tbx1* gene have been generated and haploinsufficient phenotypes have also been described (Jerome and Papaioannou, 2001; Lindsay et al., 2001; Merscher et al., 2001). These phenotypes are mostly milder than in the human DiGeorge syndrome, with low penetrance and dependence on the genetic background. In the homozygous state, the *Tbx1* null mutation produces a lethal phenotype with complete penetrance that affects the thymus, the heart outflow tract, the craniofacial area and the ear (Jerome and Papaioannou, 2001; Lindsay et al., 2001; Merscher et al., 2001). Recent studies have shown that *Tbx1* plays multiple roles in the development of the pharyngeal region and in the remodelling of the aortic arches (Vitelli et al., 2002a). In addition, it has been suggested that some of these activities may be mediated through the control of *Fgf* expression in the branchial arches (Vitelli et al., 2002b). A role for *Tbx1* in inner ear development has also been reported (Funke et al., 2001; Vitelli et al., 2003; Raft et al., 2004). Analysis of *Tbx1* null mutant embryos revealed that the inner ear is strongly affected. However, while Vitelli et al. (2003) suggested that this gene is required for expansion of a subpopulation of cells in the otic vesicle responsible for development of both the cochlear and vestibular areas, Raft et al. (2004) recently proposed that *Tbx1* gene function suppresses neural fate specification in the otocyst.

Here we show that *Tbx1* is required for the development of all the ear compartments. In the middle ear, deficiencies in the mutant were found associated with other malformations in the branchial arch-derived skeleton, indicating that they may represent one aspect of a more general effect of the *Tbx1* null mutation on the development of the pharyngeal region. The defects in the skeleton derived from the second and more caudal branchial arches can be explained by the strong deficiencies in these arches observed in the *Tbx1* mutants (Jerome and Papaioannou, 2001). In addition, we found that some of the prospective second arch neural crest cells migrate anomalously into the first arch, thus providing an explanation for the phenotype observed in the first arch derivatives. The inner ear was strongly affected in the *Tbx1* mutants. Only the endolymphatic duct and the cochleo-vestibular ganglion, together with rudimentary sensory patches, could be identified associated with a residual small otic capsule. Our molecular studies show that, while patterning of *Tbx1* mutant otocysts is strongly affected at E10.5, it still looks largely undisturbed at E9.0–E9.5. On the basis of our results we suggest an alternative explanation for the inner ear phenotype as resulting from the absence of new morphogenetic processes after the loss of appropriate spatial patterning in the otocyst.

2. Results

2.1. Middle ear defects in *Tbx1*$^{-/-}$ embryos

Preliminary analyses of *Tbx1* null mutants revealed strong malformations in the three ear compartments. The outer ears, particularly the ear pinnae, have been described as being typically absent or small and positioned low (Jerome and Papaioannou, 2001). This may be a consequence of the total or partial absence of the second branchial arch in the mutants (see below), as this arch is the major contributor to the pinna (Carlson, 1999; Mallo, 2003). The middle ear has also been reported to be affected in the *Tbx1*

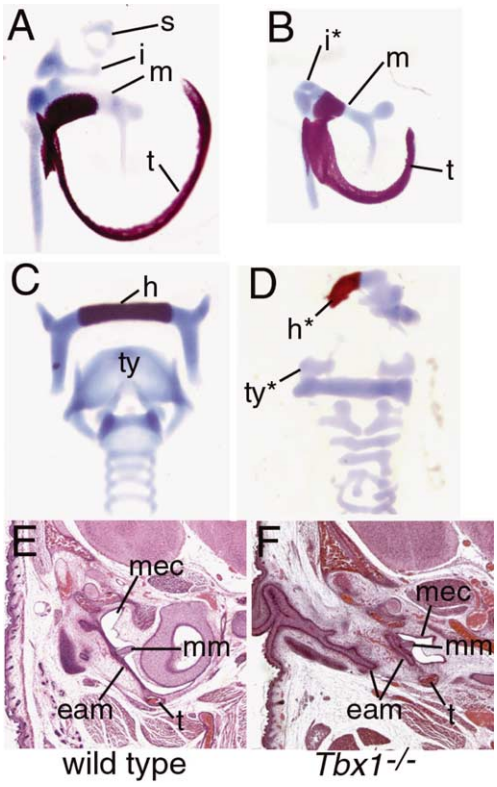

Fig. 1. Middle ear phenotype of *Tbx1* mutants. (A,B) Dissection of stained middle ear skeleton of wild-type (A) and *Tbx1*$^{-/-}$ (B) newborns. In the wild type, the three ossicles, malleus (m), incus (i) and stapes (s), together with the tympanic ring (t) are shown. In the *Tbx1*$^{-/-}$ mutants (B), the malleus and tympanic ring are still recognizable, but the stapes is not present and the incus is reduced to a small cartilaginous nodule (i*). (C) The typical wild-type neck skeleton is shown, including the hyoid bone (h) and thyroid cartilage (ty). (D) In the *Tbx1*$^{-/-}$ mutants, the neck skeleton is very affected and contains only malformed remnants of the hyoid (h*) and thyroid cartilage (ty*). (E) In frontal sections, the tympanic membrane of wild-type newborns contains two epithelia, the external acoustic meatus (eam) and that of the middle ear cavity (mec), which entrap a skeletal element, the manubrium of the malleus (mm). The membrane is supported in the tympanic ring (t). (F) All the elements of the tympanic membrane can be seen correctly organized in *Tbx1*$^{-/-}$ mutants, although on a smaller scale. The pictures shown in (E) and (F) correspond to frontal sections, oriented to position lateral on the left and rostral at the top.

mutants (Jerome and Papaioannou, 2001), but no detailed analysis has been performed. Analysis of stained skeletons of *Tbx1*$^{-/-}$ newborns revealed that, of the three middle ear ossicles, the malleus was the least affected (Fig. 1A,B). It was still present and all the basic elements of its anatomy were recognizable, but it was slightly hypoplastic. In particular the ossicle's neck was thinner than that of wild-type embryos. The incus of *Tbx1* mutant newborns was reduced to a small cartilaginous nodule articulated with the head of the malleus (Fig. 1B). No traces of the third ossicle, the stapes, could be found either in the skeletal preparations or in histological sections ($n=7$). Other skeletal elements derived from the caudal branchial arches, like the hyoid bone and the thyroid cartilage, were also strongly affected by the *Tbx1* mutation (Fig. 1C,D), suggesting that the middle ear malformations are part of a general deficiency in branchial arch development.

The tympanic membrane can be regarded as the connection between the middle and outer ears. Histological analysis revealed that, while its anatomy was slightly affected in newborn mutant mice, all the relevant components (i.e. tympanic ring, external acoustic meatus, malleal manubrium and middle ear endoderm) appeared to be induced and properly arranged (Fig. 1E,F). The tympanic ring, which provides support to the membrane, was reduced in length and somewhat thicker than that of wild-type littermates but still presented the characteristic semicircular morphology (Fig. 1B). The external acoustic meatus (EAM) was also induced and had invaginated toward the tympanic ring (Fig. 1F). However, it showed a slightly abnormal trajectory, possibly related to the abnormal positioning of the residual ear pinna. At the level of the tympanic ring, the EAM was found to be flattened in the plane defined by the ring and, together with the lateral epithelium of the middle ear cavity and the malleal manubrium, formed a clearly recognizable eardrum (Fig. 1F).

To further understand the middle ear phenotype, we analyzed the branchial area of *Tbx1* mutant embryos at earlier developmental stages. Morphological analyses of the mutant embryos revealed that, while the first branchial arch was clearly recognizable and seemingly normal looking, the second and more caudal arches were absent or strongly hypoplastic (Fig. 2B,F), as already previously reported (Jerome and Papaioannou, 2001). This would explain the strong malformations observed in the skeletal derivatives of the affected arches, like the stapes and the hyoid bone. However, it cannot explain the anomalies observed in the first arch derivatives. Previous studies revealed that neural crest cells normally populating the second and more caudal arches are generated in the *Tbx1* mutants, but that their migration into the corresponding branchial arches is seriously compromised (Vitelli et al., 2002a). Analysis of *Crabp1* expression in *Tbx1* mutant embryos confirmed these observations and revealed the existence of an additional stream of neural crest cells that migrate into the first arch from rhombomere (r) 4 (Fig. 2B,H). A similar observation was made using *Sox10* (Fig. 2D) as a marker of neural crest cells fated to become the glia of the cranial nerves and ganglia (Britsch et al., 2001). The abnormal invasion of the first branchial arch by r4-derived neural crest cells (which eventually mix with those derived from r2), provides an explanation for the fusion of the Vth and the VII/VIIIth cranial nerves in *Tbx1*$^{-/-}$ mutant embryos (Vitelli et al., 2002a; and our unpublished results).

To further ascertain the abnormal migration of r4 neural crest cells, which normally populate the second arch (Serbedzija et al., 1992), we did in situ analysis of *Hoxa2*, which is expressed in the second arch neural crest cells and never in the first arch (Prince and Lumsden, 1994; Mallo, 1997). In *Tbx1* null mutant embryos, a stream of *Hoxa2*-positive cells could be observed arising from r4 and entering

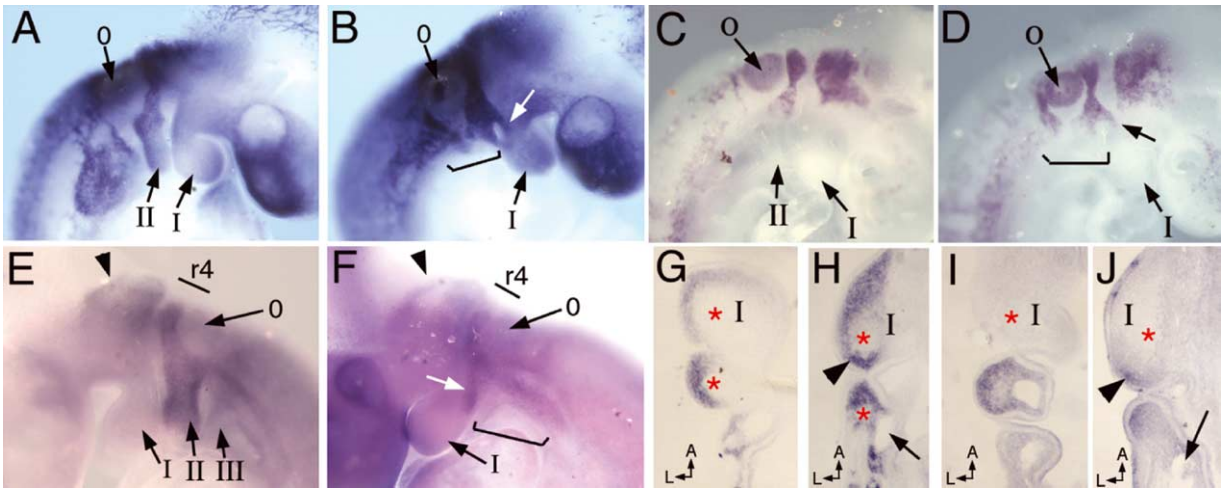

Fig. 2. Analysis of the neural crest of *Tbx1*$^{-/-}$ mutant embryos. Wild-type (A,C,E,G,I) and *Tbx1*$^{-/-}$ (B,D,F,H,J) E9.5 embryos were analyzed by in situ hybridization with probes for *Crabp1* (A,B,G,H), *Sox10* (C,D) and *Hoxa2* (E,F,I,J). (A,B) The *Crabp1* staining shows that migration of neural crest cells normally populating the branchial arches caudal to the first (I) is strongly compromised. In the *Tbx1*$^{-/-}$ mutants, a group of neural crest cells migrates anomalously into the first arch (white arrow). (C,D) The *Sox10* staining shows neural crest cells contributing to the cranial nerves and ganglia. In the *Tbx1*$^{-/-}$ mutants, a group of neural crest cells migrates anomalously into the first arch (arrow). (E) In wild-type embryos *Hoxa2* labels neural crest cells migrating from rhombomere 4 (r4) into the second branchial arch (II). (F) In *Tbx1*$^{-/-}$ embryos, *Hoxa2*-positive cells are seen migrating into the first arch (white arrow). *Tbx1* mutant embryos show a seemingly normal first branchial arch, but the second and more caudal branchial arches are strongly affected (brackets in (B,D,F)). The arrowheads in E and F indicate the border between rhombomeres 2 and 1. (G,H) Frontal section through the branchial arch region of *Crabp1*-stained wild-type (G) and *Tbx1*$^{-/-}$ (H) embryos. The labeled neural crest cells are adjacent to the mesodermal core (red asterisk), and not to the vessels (arrow). The arrowhead shows the neural crest stream invading the first arch (I) from r4. (I,J) Frontal section through the branchial arch region of *Hoxa2*-stained wild-type (I) and *Tbx1*$^{-/-}$ (J) embryos. The labeled neural crest cells are adjacent to the mesodermal core (red asterisk), and not close to the vessels (arrow). The arrowhead shows the neural crest stream invading the first arch (I) from r4. Sections are oriented with rostral at the top. Only the left side is shown, being lateral on the left. o, Otic vesicle.

the first branchial arch (Fig. 2F,J). This result confirms the abnormal migratory pathway of some neural crest cells in the absence of *Tbx1* and provides an explanation for the skeletal deficiencies in the first arch derivatives (see Section 3).

It has been shown that the mesoderm adjacent to the hindbrain is patterned by signals from the neuroectoderm and surface ectoderm to maintain the segregation of neural crest cells arising at different rostro-caudal areas of the hindbrain (Golding et al., 2002). Anomalies in neural crest cell migration have also been found in association with alterations in the patterning of the aortic arches (Trokovic et al., 2003). To ask whether the abnormal neural crest migration in *Tbx1* mutant embryos was associated with mesodermal tissue or with altered branching of the embryonic aortic tree, we sectioned stained whole-mounted embryos to localize the neural crest cells within the arch mesenchyme. Both *Crabp1*- and *Hoxa2*-positive neural crest cells that migrated from r4 into the first branchial arches in the *Tbx1* mutants followed a subepidermal trajectory adjacent to the mesodermal core, and both were far from the abnormal blood vessels linking the the heart with the dorsal aorta of these mutant embryos (Fig. 2H,J). This result suggest that the anomalies of neural crest cell migration in *Tbx1*$^{-/-}$ embryos could result from the inability of the mesoderm adjacent to the hindbrain to restrict migration of the neural crest cells to specific streams.

2.2. The inner ears of *Tbx1*$^{-/-}$ newborns are strongly hypoplastic

When examined in whole mount-stained skeletons, the otic capsules of *Tbx1*$^{-/-}$ newborns were barely distinguishable from surrounding cartilaginous structures and were visible as small vesicles of variable shape (Fig. 3D; and not shown). None of the typical structural compartments of the inner ear could be recognized (compare Fig. 3A,D). These observed defects were confirmed on histological sections through the inner ear region of *Tbx1*$^{-/-}$ newborns. Such preparations revealed the presence of a small cartilaginous capsule surrounding a simple cavity, where a residual epithelium could still be found (Fig. 3F). While there was no discernible indication for the presence of cochlear or vestibular structures, the endolymphatic duct, which at this stage is normally located outside of the cartilaginous capsule (Fig. 3B), was readily identified in *Tbx1* mutant newborns (Fig. 3E). It is noteworthy that in every mutant embryo analyzed the endolymphatic duct looked bigger than in wild-type littermates (compare Fig. 3B,E). In addition, the residual otic capsules of *Tbx1*$^{-/-}$ newborns contained epithelia with a degree of differentiation. In particular, some areas within these epithelia presented structures resembling hair cell-containing sensory patches (Fig. 3F,L). Their morphology varied among the different specimens, but their histological characteristics were always closer to those of the cristae and

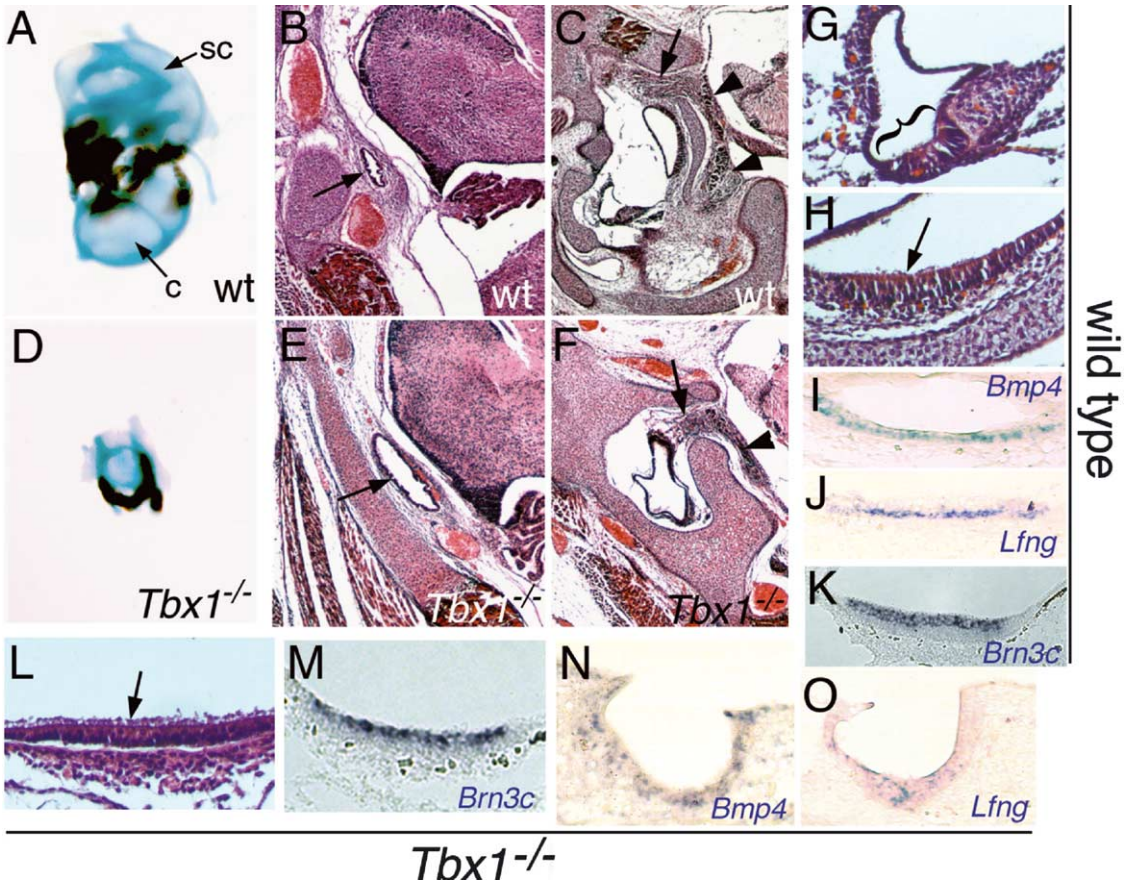

Fig. 3. Phenotypic analysis of the inner ears of *Tbx1*$^{-/-}$ animals. (A) In wild-type newborns, the inner ear shows all the compartments, including the cochlea (c) and the semicircular canals (sc). (B,C) In frontal sections, the endolymphatic duct (arrow in (B)), the cochleo-vestibular ganglion (arrowheads in (C)) and nerve fibers connecting the sensory epithelium with the ganglion (arrow in (C)) are visible. (D) In *Tbx1*$^{-/-}$ animals, the inner ear is very hypoplastic. (E,F) In frontal sections, the endolymphatic duct (arrow in (E)), the cochleo-vestibular ganglion (arrowhead in (F)) and nerve fibers connecting the sensory epithelium with the ganglion (arrow in (F)) are also visible. The pictures in (D–F) were taken at the same magnification as those in (A–C), respectively. (G) Histological section through the organ of Corti of a wild-type newborn. The brackets show the area containing the inner and outer hair cells. (H) Section through a macula of a wild-type newborn. The arrow indicates hair cells. (I,J) In situ hybridization analysis of a developing sensory patch of a wild-type E15.5 embryo with *Bmp4* (I) and *Lfng* (J). (K) In situ hybridization analysis of a macula of a wild-type newborn with *Brn3c*. (L) Section through a sensory patch of a *Tbx1*$^{-/-}$ newborn. The arrow indicates hair cells. (M) In situ hybridization analysis of a sensory patch of a *Tbx1*$^{-/-}$ newborn with *Brn3c*. In situ hybridization analysis of a developing patch of a *Tbx1*$^{-/-}$ E15.5 embryo with *Bmp4* (N) and *Lfng* (O).

maculae than to the distinct cellular arrangement present in the organ of Corti (Fig. 3G,H,L). Signs of innervation were seen in some of these patches, namely fibers connecting these sensory structures with the cvg, which was also present in mutant mice, although reduced in size compared to wild-type littermates (Fig. 3C,F).

These patch-like structures observed in the inner ears of *Tbx1* mutant embryos were positive for *Brn3c* (Fig. 3K,M), which labels auditory hair cells (Erkman et al., 1996), further substantiating the notion that they represent inner ear sensory structures. To further characterize these areas, we performed in situ hybridization with probes for *Lfng* and *Bmp4*, which are expressed specifically in the sensory organs of the inner ear with rather specific patterns for particular structures (Morsli et al., 1998). Both genes are normally expressed in the supporting cells of the three vestibular cristae and *Lfng* is also expressed in the utricular and saccular maculae (Morsli et al., 1998; Fig. 3I,J). In the cochlea, they display distinct expression patterns, *Lfng* being expressed in the supporting cells beneath the inner and outer hair cells and *Bmp4* in a more lateral domain that corresponds to the future Hensen's and/or Claudius' cells (Morsli et al., 1998). For *Tbx1*$^{-/-}$ the areas of otic epithelium resembling sensory patches were positive for expression of both genes (Fig. 3N,O), further supporting our histological identification of those epithelial areas as sensory patch-related structures. Their expression domains did not follow any of the patterns described for the maculae, cristae or the organ of Corti (Morsli et al., 1998; Fig. 3I,J,N,O; and not shown), making it difficult to label the patches observed in the *Tbx1* null mutant embryos as equivalent to a specific wild type inner ear sensory structure. However, the finding that the mutant patches express both *Bmp4* and *Lfng* indicates that they may derive from the *Bmp4*-positive anterior stripe of the otocyst destined to become cristae (Morsli et al., 1998).

These results indicate that in *Tbx1*$^{-/-}$ embryos some well organized morphogenesis still occurred in the inner ear primordia even though the inner ear was globally very strongly affected.

2.3. Early differentiation arrest of otocyst development

It has been recently proposed that *Tbx1* acts to control neural and sensory organ specification in the otocyst (Raft et al., 2004). However, this alone cannot explain the global patterning defects observed in the *Tbx1* mutant. Even in these strongly affected inner ears, there was also some degree of differentiation. To obtain a more complete view of inner ear development in *Tbx1* mutant embryos, we further characterized early events in otocyst differentiation. At E9.0 the otocysts of *Tbx1*$^{-/-}$ embryos looked morphologically normal in shape, size and position relative to the hindbrain (Figs. 2,4). However, at E10.5 the otic vesicles were clearly abnormal (Fig. 5). At this stage, the otocysts of *Tbx1*$^{-/-}$ embryos were smaller than those of their wild-type littermates and their shape was abnormal. While the vesicles of E10.5 wild-type embryos presented an elongated shape in

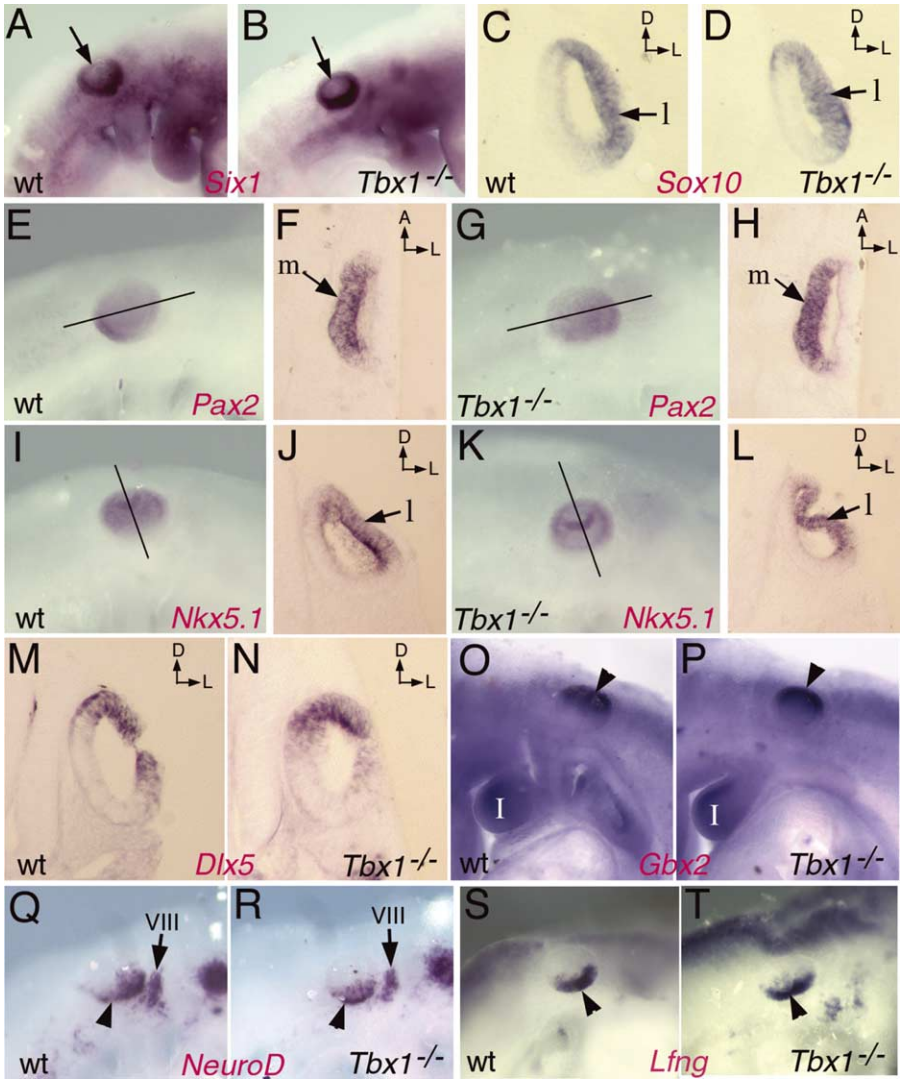

Fig. 4. Analysis of otocyst patterning in *Tbx1*$^{-/-}$ embryos at E9.0–E9.5. (A,B) At E9.5 *Six1* expression in the otocysts (arrow) is not affected by the *Tbx1* mutation (B). (C,D) *Sox10* is expressed in the lateral (l) wall of the otocyst both in wild-type (C) and *Tbx1*$^{-/-}$ embryos (D). (E,F) In wild-type embryos, *Pax2* is expressed in the medial (m) wall of the otocyst. (F) shows a section through the area indicated in (E). (G,H) In *Tbx1*$^{-/-}$ embryos, *Pax2* expression is also restricted to the medial wall of the otocyst (m). (I,J) In wild-type embryos, *Nkx5.1* is expressed in the dorsal and lateral (l) areas of the otocyst. (J) shows a section through the area indicated in (I). (K,L) In *Tbx1*$^{-/-}$ embryos, *Nkx5.1* expression is also restricted to the dorsal and lateral (l) areas of the otocyst. (M,N) *Dlx5* expression is detected in the dorso-lateral areas of the otic vesicle both in wild-type (M) and in *Tbx1*$^{-/-}$ embryos (N). (O,P) *Gbx2* expression is detected in the dorsal area of the otic vesicle (arrowhead) both in wild-type (O) and in *Tbx1*$^{-/-}$ embryos (P). (Q,R) *NeuroD* expression is detected in the ventral area of the otic vesicle (arrowhead) and in the VIII cranial ganglion (VIII) both in wild-type (Q) and in *Tbx1*$^{-/-}$ embryos (R). (S,T) *Lfng* expression is detected in the ventral area of the otic vesicle (arrowhead) both in wild-type (S) and in *Tbx1*$^{-/-}$ embryos (T). (I) First branchial arch. All the pictures show staining by in situ hybridization. The specimens are oriented with dorsal at the top of the figure, with the exception of (F) and (H), where anterior is at the top. In all sections, medial is on the left. The whole-mounted embryos are shown with the head to the right, except for (O,P), where the head is to the left.

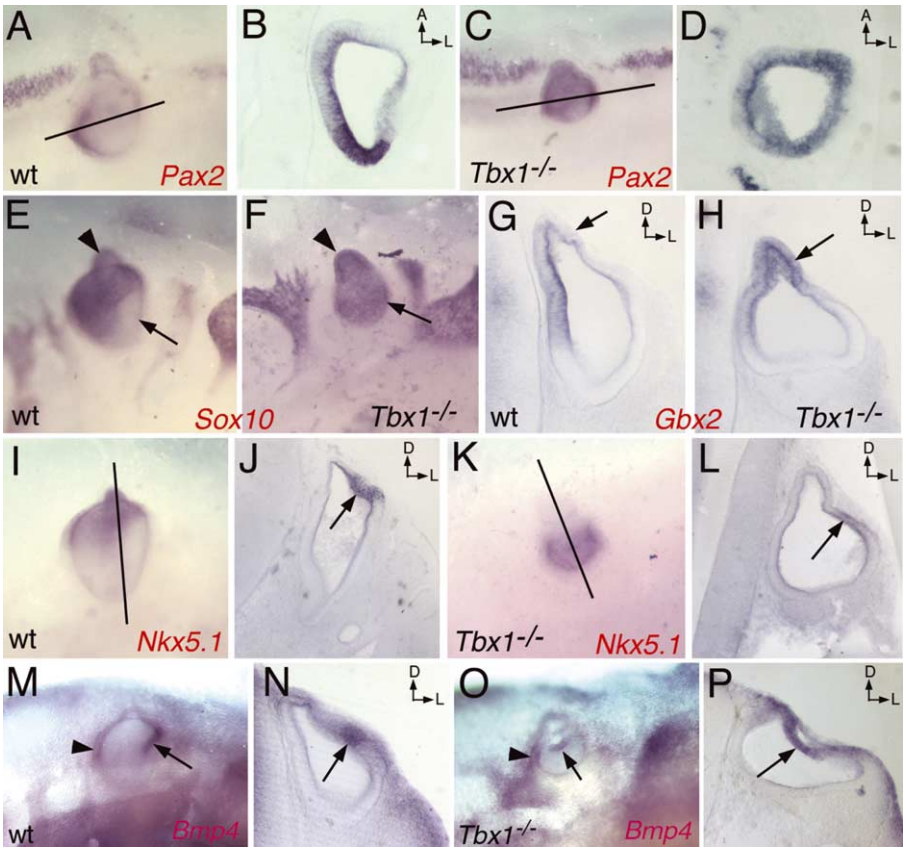

Fig. 5. Analysis of otocyst patterning in *Tbx1*$^{-/-}$ embryos at E10.5. (A,B) In wild-type embryos *Pax2* is expressed in the ventro-medial and caudal areas of the otic vesicle. B shows a section through the plane indicated in (A), oriented lateral on the right and anterior at the top. (C,D) In *Tbx1*$^{-/-}$ embryos, *Pax2* expression is extended to a wider area of the otic vesicle, including the lateral and rostral walls. (D) shows a section through the plane indicated in (C), oriented lateral on the right and anterior at the top. (E) In wild-type embryos, *Sox10* is expressed in the lateral otocyst wall and is excluded from its anterio-ventral area (arrow). The arrowhead indicates the developing endolymphatic duct. (F) In *Tbx1*$^{-/-}$ embryos *Sox10* expression is extended to the whole lateral wall of the otocyst. The arrowhead indicates the enlarged developing endolymphatic duct. (G) In wild-type embryos, *Gbx2* expression is detected in the dorsal half of the medial otocyst wall. (H) In *Tbx1*$^{-/-}$ embryos *Gbx2* expression is extended through the dorsal tip into the dorsal part of the lateral otocyst wall (arrow). (I,J) In wild-type embryos *Nkx5.1* is expressed in the lateral and dorsal areas of the otic vesicle. (J) shows a section through the plane indicated in (I). (K,L) In *Tbx1*$^{-/-}$ embryos, *Nkx5.1* expression is extended to a wider area of the lateral wall of the otocyst (arrow). (M,N) In wild-type embryos, *Bmp4* expression in the otocyst is localized in two domains, one in the posterior wall (arrowhead) and another in the lateral wall (arrow). (N) shows a section through the otocyst of the embryo shown in (M). (O,P) In *Tbx1*$^{-/-}$ embryos, *Bmp4* expression can still be detected in the posterior (arrowhead) and lateral (arrow) areas of the otocyst, although with a slightly different disposition and expanding over a wider area of the lateral wall of the otocyst (arrow in (P)). (P) shows a section through the otocyst of the embryo shown in (O). The whole-mount specimens are all shown with the head to the right and dorsal on top. All sections are shown with lateral to the right and dorsal on top, except for panels (B) and (D), where anterior is at the top.

the dorso-ventral axis (Fig. 5G,J), those of their *Tbx1*$^{-/-}$ littermates were consistently rounder in the ventral area (Fig. 5H,L). The endolymphatic tube primordium, the only morphologically identifiable structure at this stage, was clearly present in the otic vesicles of *Tbx1*$^{-/-}$ E10.5 embryos but looked larger than in E10.5 wild-type littermates (e.g. Fig. 5E,F). A similar lack of morphological differentiation was observed at E11.5 (not shown). These results indicate that the inner ear phenotype observed in *Tbx1*$^{-/-}$ fetuses and newborns derives from a critical role of this gene at some time prior to E10.5 that first becomes phenotypically evident at E9.5–E10.5.

Global strong inner ear phenotypes have also been observed in other mouse mutants. *Chrd* mutants show a similar phenotype to that of *Tbx1*$^{-/-}$ embryos (Bachiller et al., 2003). However, *Chrd* is probably upstream of *Tbx1*, because *Chrd* expression is detected earlier than *Tbx1* in wild-type development and *Tbx1* is downregulated in the *Chrd* mutants (Bachiller et al., 2003). *Six1* mutants show, in addition to inner ear phenotypes, middle ear malformations reminiscent of those in the *Tbx1* mutant (Zheng et al., 2003; Ozaki et al., 2004), suggesting that this gene could be a mediator of *Tbx1* activity. In situ expression analysis revealed no major differences in *Six1* expression in *Tbx1*$^{-/-}$ embryos (Fig. 4A,B), indicating that the *Tbx1* mutant phenotype does not result from downregulation of *Six1*.

Further analyses of spatial patterning of *Tbx1* mutant otocysts at E9.5 revealed a quite normal distribution of the molecular markers investigated (Fig. 4; and not shown). *Sox10* expression, which is seen in the lateral wall of the otocyst (Fig. 4C), was largely unaffected in *Tbx1* mutant

embryos (Fig. 4D). *Pax2* and *Nkx5.1* show complementary expression patterns in the otic vesicle, with *Pax2* labelling the ventro-medial wall and *Nkx5.1* labeling the latero-dorsal areas; these areas correspond to prospective cochlear and vestibular regions, respectively (Rinkwitz-Brandt et al., 1996; and Fig. 4F,J). Expression of both markers appeared grossly unaffected in *Tbx1* mutant otic vesicles at E9.5 (Fig. 4E–L), except that the *Pax2* expression domain appeared weaker in caudal areas of the mutant vesicles (Fig. 4E,G). Typical dorsal markers, like *Dlx5* (Acampora et al., 1999; Depew et al., 1999) and *Gbx2* (Bouillet et al., 1995), also showed a normal distribution at E9.5 in *Tbx1* mutant otic vesicles (Fig. 4M–P; and not shown).

It has been reported that expression of *NeuroD*, which marks a group of cells at the anterior part of the vesicle undergoing differentiation and delamination to contribute to the cvg (Liu et al., 2000), is affected in *Tbx1*$^{-/-}$ embryos at E10.0 (Raft et al., 2004). In contrast, at E9.0 we found a fairly normal distribution of *NeuroD* transcripts in the otocysts of *Tbx1* mutant embryos (Fig. 4Q,R). Similarly, *Lfng* transcripts, which mark some of the cvg neuroblasts and a subset of the primordial sensory organs in the ventral area of the otocysts (Morsli et al., 1998) and were affected by the *Tbx1* mutation at E10.0 (Raft et al., 2004), looked fairly normal in their distribution at earlier developmental stages (Fig. 4S,T). These results indicate that the early phases of otic placode/vesicle patterning and morphogenesis remain largely undisturbed in the absence of *Tbx1*.

2.4. Abnormal patterning in E10.5 Tbx1 mutant otocysts

It has been shown that in *Tbx1*$^{-/-}$ embryos the spatial distributions of *NeuroD* and *Lfng*, which look seemingly normal at E9.0–E9.5, are both extended caudally in the otocysts at E10.0 relative to wild-type littermates (Raft et al., 2004). We could confirm these alterations (not shown), indicating that, differently to what we observed at earlier stages, patterning of the otic vesicle could be affected at later stages, with clear morphological alterations visible in *Tbx1* mutant embryos. To evaluate this possibility further, we looked at the spatial distribution of other molecular markers at E10.5. The distribution of some transcripts, like *Dlx5* and *Gata3*, maintained the normal patterns (not shown), while others presented a clearly abnormal spatial pattern. *Pax2*, which showed normal spatial patterning at E9.5, displayed a strongly affected distribution in otocysts of E10.5 *Tbx1*$^{-/-}$ embryos. In normal embryos, its expression at this stage was restricted to specific areas within the medio-ventral regions of the otic vesicles, with a clear border across the anterior–posterior axis (Fig. 5A,B). In the mutant, expression was extended to other areas (Fig. 5C,D). Differential expression in the medio-lateral axis was lost, as was the anterior limit in the lateral domain, resulting in an extended expression throughout the whole circumference of the vesicle (Fig. 5D). Expression of *Sox10* in the otic vesicles was also affected in *Tbx1*$^{-/-}$. In wild-type E10.5 embryos, *Sox10* was detected in the lateral wall of the otic vesicle, with an anterior–posterior polarity, being excluded from antero-ventral areas (Fig. 5E), a pattern that resembles that of *Tbx1* (see below). In the *Tbx1* mutant, *Sox10* expression was extended to more anterior areas of the otocyst lateral wall (Fig. 5F). The abnormalities in the expression of these two genes are interesting, in that they seem to follow a posterior–anterior extension, which is opposite to the anterior–posterior extension described for *NeuroD* (Raft et al., 2004). An extended expression domain at E10.5 was also observed for *Gbx2* in *Tbx1*$^{-/-}$ mutants. In this case, transcripts seemed to extend across the dorsal border into the lateral wall of the otocyst (Fig. 5G,H). *Nkx5.1* expression in the otic vesicles was also slightly affected at E10.5 in *Tbx1*$^{-/-}$ embryos (Fig. 5I,L). In particular, while in wild-type embryos it was restricted to a localized area in the dorsal part of the lateral otic vesicle (Fig. 5J), in *Tbx1* mutants *Nkx5.1* expression lost intensity and seemed to extend ventrally in the lateral wall (Fig. 5L). These results indicate that at E10.5, in contrast to what was seen at E9.5, patterning of the otocyst was affected by the *Tbx1* mutation.

We also studied the distribution of *Bmp4* transcripts at E10.5 in *Tbx1* mutant otic vesicles. This was important because the sensory patches we found in the inner ears of *Tbx1* mutant embryos displayed molecular characteristics compatible with their having originated in an area equivalent to the antero-lateral stripe of *Bmp4*-expressing cells that normally originate the cristae (Morsli et al., 1998). In wild-type embryos *Bmp4* was expressed in two areas, in the lateral and posterior walls of the otocyst (Fig. 5M,N). The posterior domain was downregulated in most (but not all) *Tbx1*$^{-/-}$ mutant embryos, whereas the lateral domain was still consistently identifiable (Fig. 5O,P). Its position in the mutant vesicles was different from that in the controls and clearly wider along the dorso-ventral axis than in wild-type embryos (compare Fig. 5N,P). These results indicate that *Bmp4* expression was induced in *Tbx1*$^{-/-}$ otocysts, but that like other molecular markers, its spatial distribution was not correctly maintained in the absence of *Tbx1*.

2.5. Expression of Tbx1 in the ear compartments

In order to understand how *Tbx1* influences formation of the ear compartments, we analyzed its expression in wild-type embryos in the branchial arches and otic vesicle. In the branchial area, this gene was expressed throughout the prechordal mesenchyme even before neural crest cells migrated into the arches (Chapman et al., 1996; Fig. 6A; and not shown). Expression became more restricted to the mesodermal core of the arches at E9.5 (Chapman et al., 1996; Fig. 6C), and was then gradually downregulated in the first and second arches (Fig. 6F). In this area, *Tbx1* was not expressed in the neural crest-derived mesenchyme. In the otic epithelium, *Tbx1* expression could already be observed

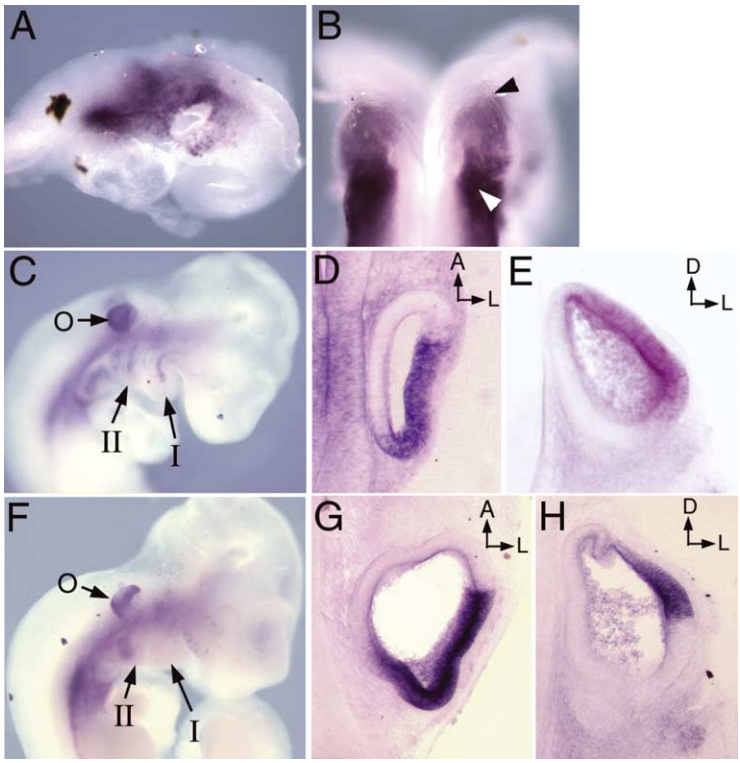

Fig. 6. Expression of *Tbx1* during early development. Expression was analyzed by whole mount in situ hybridization on E8.5 (A,B), E9.5 (C–E) and E10.5 (F–H) embryos. (A) At E8.5. *Tbx1* is expressed in the mesenchyme beneath the hindbrain and midbrain. (B) In the otic placode, it is slightly more concentrated in caudal than in rostral areas. The picture shows a dorsal view of the embryo oriented with the anterior part to the top. The arrowheads indicate the rostral (black) and caudal (white) limits of the right placode. (C) At E9.5, *Tbx1* expression is seen in the mesodermal core of the branchial arches and in the otic vesicle. (D) Frontal section showing expression in the lateral and posterior areas of the otocyst. (E) Transverse section showing expression in the lateral and dorsal areas of the otocyst. (F) At E10.5, *Tbx1* expression is still seen in the mesodermal core of the second branchial arch (II), in the area of the third and fourth arches and in the otic vesicle (o). (G) Frontal section showing expression in the lateral and posterior areas of the otocyst. The anterior border of expression in the lateral wall is very sharp. (H) Transverse section showing expression in the lateral and dorsal areas of the otocyst. The ventral border of expression in the lateral wall is also sharp. In all sections, lateral is on the right. The frontal sections (D,G) are shown with anterior to the top. The transverse sections (E,H) are shown with dorsal to the top. (I) First branchial arch.

at E8.5 in the otic placode (Fig. 6B). Its expression in this structure was not uniform, appearing slightly stronger in the caudal half. At E9.5, *Tbx1* expression was very strong in the otocyst (Fig. 6C–E). It was restricted to the latero-posterior areas of the vesicle (Fig. 6D). Along the dorso-ventral axis, *Tbx1* expression was clearly detected in the dorsal areas, the most ventral domain of expression being devoid of *Tbx1* transcripts (Fig. 6E). At E10.5, expression of this gene was still detected in the lateral and posterior areas of the vesicle (Fig. 6F–H). In addition, a dorsal shift was now evident. The borders of *Tbx1* expression in the otic vesicle in the anterio-posterior and dorso-ventral axes were very sharp (Fig. 6G,H).

3. Discussion

In this study we showed that *Tbx1* is essential for development of the mammalian ear. Although all three ear compartments are affected in the $Tbx1^{-/-}$ mutants, the origin of the malformations seems not to be the same in all areas.

3.1. Middle ear development is affected in $Tbx1^{-/-}$ embryos

Development of various middle ear structures is compromised by the absence of *Tbx1* to different degrees. The most clearly affected part of the middle ear is the skeleton. As other branchial arch skeletal elements are also affected in the *Tbx1* mutants, it seems that the middle ear phenotype is the consequence of a more general patterning or morphogenetic defect in the branchial area. Interestingly, the residual elements seem to be able to direct coordinated morphogenesis similar to the wild-type structures. For instance, a normal-looking tympanic membrane is formed, a process which requires interactions between the tympanic ring, the ectoderm of the EAM and the pharyngeal endoderm (Mallo and Gridley, 1996; Mallo et al., 2000).

The skeletal elements of the branchial arches are neural crest-derived (Couly et al., 1993). Since *Tbx1* is expressed in the mesodermal component of the branchial arches and not in the neural crest-derived mesenchyme, the effect of this gene in the neural crest must be indirect. This inference is in keeping with a recent report indicating that *Tbx1* acts

non-cell autonomously in the branchial area (Vitelli et al., 2003). It is possible that *Tbx1* is required for proper migration of the neural crest cells into the branchial arches. In the *Tbx1* mutants most of the neural crest cells originating caudal to r3 are not able to populate prospective second and more caudal branchial arches, which are missing or strongly hypoplastic in the mutant (Jerome and Papaioannou, 2001; Vitelli et al., 2002a; and this study). The absence of these branchial arches and of associated neural crest cells provides an explanation for the strong skeletal phenotypes observed in the derivatives from these areas. For the malleus, incus and tympanic ring, all first-arch derivatives (Mallo, 1998), a likely explanation for their phenotype in the *Tbx1* mutants is the misrouting of *Hoxa2*-positive cells into the first arch. *Hoxa2* is essential for determining the skeletal identity of second arch derivatives (Gendron-Maguire et al., 1993; Rijli et al., 1993), and misexpression of this gene in the first arch has been shown to produce strong hypoplastic phenotypes in the skeleton derived from this area (Mallo and Brandlin, 1997; Creuzet et al., 2002). Thus, the presence of *Hoxa2*-positive cells in the first arch of the *Tbx1* mutant may interfere with normal skeletal development in this arch.

The role of *Tbx1* in neural crest cell migration is still unclear. Two effects have been observed, an inability to migrate into the caudal arches and misrouting. Whether these two effects are related or result from independent mechanisms cannot be discerned from existing data. It has been postulated that segregation of cranial neural crest cell migratory pathways into distinct streams is controlled by some kind of molecular segmentation in the mesoderm adjacent to the hindbrain. The neural crest cell misrouting observed in *Tbx1* mutant embryos suggests that *Tbx1* may play a role in this mesodermal patterning. A variety of experimental data indicates that this mesodermal patterning is provided by signals from the adjacent neural tube and surface ectoderm (Farlie et al., 1999; Golding et al., 2002). As *Tbx1* is not expressed in the neuroectoderm or in the surface ectoderm, it is very probable that this gene plays a role in the mesodermal interpretation of these signals. The nature of the patterning signals is beginning to be elucidated (Golding et al., 2000) but nothing is yet known about the mesodermal component of this patterning interaction, making it difficult to test experimentally the role of *Tbx1* in this process. Recent data suggest that interference with FGF signaling may play a role in the genesis of this $Tbx1^{-/-}$ branchial arch phenotype. *Fgfr1* mutant embryos show defects in this area somewhat similar to those observed in the *Tbx1* mutant (Trokovic et al., 2003). In $Fgfr1^{-/-}$ embryos, the migration of neural crest cells into the second arch is also compromised. Interestingly, *Fgfr1* is not required in the neural crest, but rather in the branchial arch mesoderm. As expression of several Fgf genes seems to be down-regulated in *Tbx1* mutant embryos (Vitelli et al., 2002b), a possible scenario is that the branchial arch phenotype of these mutants results from the absence of Fgfr1 stimulation in the mesodermal component of the branchial arches. At least two Fgf genes have been reported to be down-regulated in the absence of *Tbx1*. One of them, *Fgf8*, is essential for the development of the branchial arches (Trumpp et al., 1999). However, *Fgf8* seems to be required for correct patterning and survival of postmigratory crest cells and not for their migration into the branchial arches (Trumpp et al., 1999; Bobola et al., 2003). In the case of *Fgf10*, also down-regulated in $Tbx1^{-/-}$ embryos, no branchial arch phenotype was reported when it is inactivated (Min et al., 1998). This indicates that, if this molecule plays a role in mediating *Tbx1* activity, other molecules can substitute for it in this process. Further work will be required to determine the roles FGFs play as downstream mediators of *Tbx1* activity in the branchial arches and to identify the still missing factors (FGFs or not) involved in this process.

3.2. Morphogenesis of the otocyst is impaired in $Tbx1^{-/-}$ embryos

The inner ears of *Tbx1* mutant embryos were reduced to a pair of small hollow cartilaginous vesicles without any structure that could be assigned to the cochlear or vestibular compartments. Quite surprisingly, however, some signs of morphological and histological differentiation were observed within these strongly affected structures. In particular, the endolymphatic duct was clearly discernible, displaying a normal histology, although it was larger than in wild-type littermates. Also, some areas clearly resembling sensory patches were present in the residual inner ear epithelium of the *Tbx1* mutant embryos. Although their morphological and molecular characteristics did not correspond exactly to any of the sensory patches present in normal inner ears, they contained hair cells and were even connected to the cvg, also present in the mutant embryos.

Global inner ear phenotypes were also found in *Six1* and *Eya1* mutants (Xu et al., 1999; Laclef et al., 2003; Zheng et al., 2003; Ozaki et al., 2004). However, in contrast to what has been described for those mutants, the *Tbx1* mutant phenotype seems not to derive from global effects on early proliferation and survival processes within the otocyst, because the patterns of apoptosis and cell proliferation were fairly normal in $Tbx1^{-/-}$ otocysts (Vitelli et al., 2003; our unpublished results). Moreover, these global effects would not explain the conservation of specific inner ear characteristics in the *Tbx1* mutant. The global *Tbx1* mutant phenotype in the inner ear is also not directly obvious from the *Tbx1* expression pattern. In other mutants affecting inner ear development, the affected area typically mirrors the gene's expression domain (Torres et al., 1996; Hadrys et al., 1998; Ma et al., 1998; Torres and Giráldez, 1998; Wang et al., 1998; Acampora et al., 1999; Depew et al., 1999; Liu et al., 2000; Riley and Phillips, 2003). In the case of *Tbx1*, while its expression domain clearly overlaps with

the prospective vestibular area, it is transcribed only in a rather small area of the cochlear anlage, thus making it difficult to justify the complete absence of this later structure in the *Tbx1* null mutants.

Analysis of the inner ear phenotype at earlier developmental stages suggests a possible explanation for this apparent paradox. When analyzed early enough, ear patterning and differentiation processes look fairly normal in $Tbx1^{-/-}$ embryos. This indicates that *Tbx1* plays no role in placode induction or in the early morphogenetic events to create a hollow vesicle from a flat epithelial thickening. Also, the establishment of early molecular patterns in the otocyst seems to occur normally in the absence of *Tbx1*, as estimated by the fairly normal distribution of a variety of relevant transcripts in the otic vesicles of E9.0–E9.5 *Tbx1* mutant embryos. It is only after E9.5 that clear morphological and molecular alterations can be observed in *Tbx1* mutant otocysts. The ventral area of the otocysts does not present the elongation that represents the initial cochlear anlage (Li et al., 1978), and show a round-shaped morphology. In addition, the primordium of the endolymphatic duct is still present but is clearly bigger in *Tbx1* mutant embryos than in their wild-type littermates. Also evident at this stage are alterations in the spatial distribution of transcripts for some relevant genes, which are not restricted to a particular type of process, but seem to affect the otic vesicle globally. For instance, in mutant otocysts *NeuroD* and *Lfng* expression domains are extended posteriorly (Raft et al., 2004; and our unpublished data), *Pax2* expression extends anteriorly and laterally, the *Sox10* positive area is expanded anteriorly, *Gbx2* expression diffuses latero-ventrally and the *Bmp4* and *Nkx5.1* domains present a dorso-ventral broadening. It has been shown that, while initial patterns in the otocyst are established by signals provided by surrounding tissues (Baker and Bronner-Fraser, 2001), after a certain stage otocysts seem to be largely independent of external cues (Swanson et al., 1990; Torres and Giráldez, 1998). As the pattern of *Tbx1* mutant otic vesicles changes from normal to altered, it is possible that *Tbx1* is required for the autonomous conservation of patterns after they have been generated by environmental signals. The highly regionalized expression of *Tbx1* and, most particularly, the sharp borders of its expression domain, which become stronger around E10.5, are nicely consistent with this hypothesis and suggest that control of cell segregation may be part of this mechanism.

A comparison of the early and late stages of inner ear formation in the *Tbx1* mutant reveals an interesting feature. There is a clear correlation between the conserved/lost features observed in the inner ears of newborns and the stage at which they start to be formed. The clearly conserved characteristics, namely the endolymphatic duct, sensory patches and cvg ganglion, represent very early differentiation processes in the otic primordium, which occur before alterations can be observed in *Tbx1* mutant otocysts. Conversely, morphologically organized cochlear and vestibular compartments, which are lost from *Tbx1* mutant animals, start formation later than E10.5, when the otocyst has already lost normal patterning references. This suggests that the strong global phenotypes in *Tbx1* inner ears derive from the inability of the otic vesicle to start morphogenetic processes, probably as a consequence of the lack of segregation of the gene regulatory information responsible for those processes. This hypothesis provides a likely explanation for the failure of structures that develop from an area mostly negative for *Tbx1*, like the cochlea, to develop in the *Tbx1* null mutants.

An additional implication of the correlation between early and late phenotypic features of *Tbx1* mutant individuals is that the absence of *Tbx1* seems not to hinder progression of differentiation processes once they are started. The *NeuroD*-positive areas produce a cvg ganglion, the primordium of the endolymphatic duct develops further to produce a recognizable structure in the newborns, and the sensory patches observed in newborns are likely derived from the expanded *Bmp4* lateral domain, as estimated by their molecular characteristics. Not only do these processes proceed further, they also seem to extend to include adjacent areas of the otocyst; already at E10.5, the neurogenic domain incorporates more caudal areas, as described by Raft et al. (2004); the endolymphatic duct enlarges, suggesting the incorporation of adjacent epithelium; and the *Bmp4* lateral domain broadens, indicating the expansion of the sensory anlage.

While we were preparing this manuscript the inner ear phenotype of *Tbx1* mutants was analyzed by other groups (Vitelli et al., 2003; Raft et al., 2004). According to Vitelli et al. (2003) *Tbx1* is required cell autonomously for the expansion of a subpopulation of cells in the otic vesicle required for development of both the cochlear and vestibular areas. However, like us (unpublished data), they did not find differences in cell proliferation or survival in *Tbx1* mutant otocysts. Also, the vestibular and cochlear areas do not seem to derive from complementary areas of the otic vesicle, which are clearly segregated at E9.0 in *Tbx1* mutant embryos and are under different genetic controls (Torres and Giráldez, 1998). In addition, *Tbx1* expression has only a small overlap with the prospective cochlear domain (*Pax2*-positive). Therefore, either *Tbx1* has different transcriptional activities in different areas of the otocyst or it is involved in more general functions in the otic epithelium. Raft et al. (2004) propose that *Tbx1* restricts neurogenic potential within the otocyst. We also found an extension of the neurogenic area in the otic vesicles of *Tbx1* mutant embryos after E10.0, in accord with their results. However, we also found broadening of other domains at the same stage of inner ear development, which suggests to us that the effect of *Tbx1* on the restriction of the neurogenic area is part of the more global role of *Tbx1* in keeping normal patterns within the otic vesicle.

3.3. A mouse model for inner ear disfunction in DiGeorge syndrome patients?

It has been reported that some patients with the DiGeorge syndrome suffer from hearing and balance problems, some of which could be attributable to cochlear and vestibular dysfunction (Digilio et al., 1999; Swillen et al., 1999). As *Tbx1* plays an essential role in inner ear development, it is possible that partial loss of *TBX1* function could indeed perturb ear development in DiGeorge syndrome patients and be the cause of these clinical manifestations. In mice, inner ear phenotypes associated with *Tbx1* haploinsufficiency have not been reported. It is possible that, like the vascular phenotype in $Tbx1^{+/-}$ mice (Jerome and Papaioannou, 2001; Lindsay et al., 2001; Merscher et al., 2001), the extent of expressivity of an ear phenotype in the presence of only one copy of the *Tbx1* gene is also strain-dependent. Therefore, it would be important to introduce the *Tbx1* mutation into different genetic backgrounds and observe the effects on cochlear and vestibular function. Interestingly, hearing and balance deficiencies were observed in mice carrying a transgenic BAC containing the human *TBX1* gene, but only when the mice had a mixed B6/FVB background and not after three generations of backcrossing into C57BL/6 (Funke et al., 2001). This suggests that the FVB strain may be more sensitive to alterations in the *Tbx1* dosage and could be the strain of choice when trying to obtain *Tbx1* haploinsufficient phenotypes in the ear. The existence of such a mouse would provide a useful animal model for the ear defects observed in human DiGeorge syndrome patients.

4. Experimental procedures

4.1. Mice and embryos

Mice carrying the $Tbx1^{tm1Pa}$ null mutation have been described previously (Jerome and Papaioannou, 2001). For simplicity, we refer to the mice carrying one or two $Tbx1^{tm1Pa}$ alleles as $Tbx1^{+/-}$ and $Tbx1^{-/-}$, respectively. For the experiments described in this manuscript mice in a C57BL/6/129 mixed background were used. Embryos were collected at the specified stages from $Tbx1^{+/-}$ intercrosses, and genotyped as previously described (Jerome and Papaioannou, 2001).

4.2. Phenotypic analyses

Skeletal staining of newborns was performed using the alcian blue/alizarin red method as described in Mallo and Brandlin (1997). Four embryos of each genotype were analyzed.

In situ hybridization both in whole embryos and on tissue sections was performed as described in Kanzler et al. (1998), using digoxygenin-labeled riboprobes for *Pax2*, *Gata3*, *Nkx5.1*, *Gbx2*, *Dlx5*, *NeuroD*, *Tbx1*, *CrabpI*, *Bmp4*, *Lfng*, *Brn3c*, *Six1*, *Hoxa2* and *Sox10*. Three to five embryos of each genotype were analyzed for each probe. After whole-mount staining, representative embryos were post-fixed in 4% paraformaldehyde/0.2% glutaraldehyde, rinsed in PBS, embedded in gelatin, and sectioned with a vibratome at 30–40 μm.

Acknowledgements

We thank E. Bober, T. Gridley, P. Gruss, B. Hogan, A. Kispert, J. Lee, A. P. McMahon, A. Simeone and M. Wegner for kindly sharing cDNA probes with us, and M. Carapuço, F. Giráldez, A. Jacinto, D. Pimentel, J. Rodríguez-León and R. Cassada for useful discussions. This work was supported by FCT/FEDER grant POC-TI/MGI/43466/2001 to MM and NIH grant DH33082 to VEP.

References

Acampora, D., Merlo, G.R., Paleari, L., Zerega, B., Postiglione, M.P., Mantero, S., et al., 1999. Craniofacial, vestibular and bone defects in mice lacking the distal-less-related gene *Dlx5*. Development 126, 3795–3809.

Bachiller, D., Klingensmith, J., Shneyder, N., Tran, U., Anderson, R., Rossant, J., de Robertis, E.M., 2003. The role of chordin/Bmp signals in mammalian pharyngeal development and DiGeorge syndrome. Development 130, 3567–3578.

Baker, C.V., Bronner-Fraser, M., 2001. Vertebrate cranial placodes I. Embryonic induction. Dev. Biol. 232, 1–61.

Bobola, N., Carapuço, M., Ohnemus, S., Kanzler, B., Leibbrandt, A., Neubüser, A., et al., 2003. Mesenchymal patterning by *Hoxa2* requires blocking FGF-dependent activation of *Ptx1*. Development 130, 3403–3414.

Bollag, R.J., Siegfried, Z., Cebra-Thomas, J.A., Garvey, N., Davison, E.M., Silver, L.M., 1994. An ancient family of embryonically expressed mouse genes sharing a conserved protein motif with the T locus. Nat. Genet. 7, 383–389.

Bouillet, P., Chazaud, C., Oulad-Abdelghani, M., Dolle, P., Chambon, P., 1995. Sequence and expression pattern of the *Stra7* (*Gbx-2*) homeobox-containing gene induced by retinoic acid in P19 embryonal carcinoma cells. Dev. Dyn. 204, 372–382.

Brigande, J.V., Kiernan, A.E., Gao, X., Iten, L.E., Fekete, D.M., 2000. Molecular genetics of pattern formation in the inner ear: do compartment boundaries play a role?. Proc. Natl Acad. Sci. USA 97, 11700–11706.

Britsch, S., Goerich, D.E., Riethmacher, D., Peirano, R.I., Rossner, M., Nave, K.A., et al., 2001. The transcription factor Sox10 is a key regulator of peripheral glial development. Genes Dev. 15, 66–78.

Carlson, B.M., 1999. Human Embryology and Developmental Biology, Second ed. Mosby, Inc., St Louis.

Chapman, D.L., Garvey, N., Hancock, S., Alexiou, M., Agulnik, S., Gibson Brown, J.J., et al., 1996. Expression of the T-box family genes, *Tbx1–Tbx5*, during early mouse development. Dev. Dyn. 206, 379–390.

Couly, G.F., Coltey, P.M., le Douarin, N.M., 1993. The triple origin of skull in higher vertebrates: a study in quail-chick chimeras. Development 117, 409–429.

Creuzet, S., Couly, G., Vincent, C., le Douarin, N.M., 2002. Negative effect of *Hox* gene expression on the development of the neural crest-derived facial skeleton. Development 129, 4301–4313.

Depew, M.J., Liu, J.K., Long, J.E., Presley, R., Meneses, J.J., Pedersen, R.A., Rubenstein, J.L., 1999. *Dlx5* regulates regional development of the branchial arches and sensory capsules. Development 126, 3831–3846.

Digilio, M.C., Pacifico, C., Tieri, L., Marino, B., Giannotti, A., Dallapiccola, B., 1999. Audiological findings in patients with microdeletion 22q11 (di George/velocardiofacial syndrome). Br. J. Audiol. 33, 329–333.

Erkman, L., McEvilly, R.J., Luo, L., Ryan, A.K., Hooshmand, F., O'Connell, S.M., et al., 1996. Role of transcription factors Brn-3.1 and Brn-3.2 in auditory and visual system development. Nature 381, 603–606.

Farlie, P.G., Kerr, R., Thomas, P., Symes, T., Minichiello, J., Hearn, C.J., Newgreen, D., 1999. A paraxial exclusion zone creates patterned cranial neural crest cell outgrowth adjacent to rhombomeres 3 and 5. Dev. Biol. 213, 70–84.

Funke, B., Epstein, J.A., Kochilas, L.K., Lu, M.M., Pandita, R.K., Liao, J., et al., 2001. Mice overexpressing genes from the 22q11 region deleted in velo-cardio-facial syndrome/DiGeorge syndrome have middle and inner ear defects. Hum. Mol. Genet. 10, 2549–2556.

Gendron-Maguire, M., Mallo, M., Zhang, M., Gridley, T., 1993. *Hoxa-2* mutant mice exhibit homeotic transformation of skeletal elements derived from cranial neural crest. Cell 75, 1317–1331.

Golding, J.P., Trainor, P., Krumlauf, R., Gassmann, M., 2000. Defects in pathfinding by cranial neural crest cells in mice lacking the neuregulin receptor *ErbB4*. Nature Cell. Biol. 2, 103–109.

Golding, J.P., Dixon, M., Gassmann, M., 2002. Cues from neuroepithelium and surface ectoderm maintain neural crest-free regions within cranial mesenchyme of the developing chick. Development 129, 1095–1105.

Hadrys, T., Braun, T., Rinkwitz-Brandt, S., Arnold, H.H., Bober, E., 1998. *Nkx5-1* controls semicircular canal formation in the mouse inner ear. Development 125, 33–39.

Jerome, L.A., Papaioannou, V.E., 2001. DiGeorge syndrome phenotype in mice mutant for the T-box gene, *Tbx1*. Nat. Genet. 27, 286–291.

Kanzler, B., Kuschert, S.J., Liu, Y.-H., Mallo, M., 1998. *Hoxa2* restricts the chondrogenic domain and inhibits bone formation during development of the branchial area. Development 125, 2587–2597.

Laclef, C., Souil, E., Demignon, J., Maire, P., 2003. Thymus, kidney and craniofacial abnormalities in *Six 1* deficient mice. Mech. Dev. 120, 669–679.

Li, C.W., Van de Water, T.R., Ruben, R.J., 1978. The fate mapping of the eleventh and twelfth day mouse otocyst: an in vitro study of the sites of origin of the embryonic inner ear sensory structures. J. Morphol. 157, 249–267.

Lindsay, E.A., Vitelli, F., Su, H., Morishima, M., Huynh, T., Pramparo, T., et al., 2001. *Tbx1* haploinsufficieny in the DiGeorge syndrome region causes aortic arch defects in mice. Nature 410, 97–101.

Liu, M., Pereira, F.A., Price, S.D., Chu, M.J., Shope, C., Himes, D., et al., 2000. Essential role of BETA2/*NeuroD1* in development of the vestibular and auditory systems. Genes Dev. 14, 2839–2854.

Ma, Q., Chen, Z., del Barco Barrantes, I., de la Pompa, J.L., Anderson, D.J., 1998. *Neurogenin1* is essential for the determination of neuronal precursors for proximal cranial sensory ganglia. Neuron 20, 469–482.

Mallo, M., 1997. Retinoic acid disturbs mouse middle ear development in a stage dependent fashion. Dev. Biol. 184, 175–186.

Mallo, M., 1998. Embryological and genetic aspects of middle ear development. Int. J. Dev. Biol. 42, 11–22.

Mallo, M., 2001. Formation of the middle ear: recent advances on the developmental and molecular mechanisms. Dev. Biol. 231, 410–419.

Mallo, M., 2003. Formation of the outer and middle ear, molecular mechanisms. Curr. Top. Dev. Biol. 57, 83–111.

Mallo, M., Brandlin, I., 1997. Segmental identity can change independently in the hindbrain and rhombencephalic neural crest. Dev. Dyn. 210, 146–156.

Mallo, M., Gridley, T., 1996. Development of the mammalian ear: coordinate regulation of formation of the tympanic ring and the external acoustic meatus. Development 122, 173–179.

Mallo, M., Schrewe, H., Martin, J.F., Olson, E.N., Ohnemus, S., 2000. Assembling a functional tympanic membrane: signals from the external acoustic meatus coordinate development of the malleal manubrium. Development 127, 4127–4136.

Merscher, S., Funke, B., Epstein, J.A., Heyer, J., Puech, A., Lu, M.M., et al., 2001. *TBX1* is responsible for cardiovascular defects in velo-cardio-facial/DiGeorge syndrome. Cell 104, 619–629.

Min, H., Danilenko, D.M., Scully, S.A., Bolon, B., Ring, B.D., Tarpley, J.E., et al., 1998. *Fgf-10* is required for both limb and lung development and exhibits striking functional similarity to Drosophila branchless. Genes Dev. 12, 3156–3161.

Morsli, H., Choo, D., Ryan, A., Johnson, R., Wu, D.K., 1998. Development of the mouse inner ear and origin of its sensory organs. J. Neurosci. 18, 3327–3335.

Ozaki, H., Nakamura, K., Funahashi, J., Ikeda, K., Yamada, G., Tokano, H., et al., 2004. *Six1* controls patterning of the mouse otic vesicle. Development 131, 551–562.

Prince, V., Lumsden, A., 1994. *Hoxa-2* expression in normal and transposed rhombomeres: independent regulation in the neural tube and neural crest. Development 120, 911–923.

Raft, S., Nowotschin, S., Liao, J., Morrow, B.E., 2004. Suppression of neural fate and control of inner ear morphogenesis by *Tbx1*. Development 131, 1801–1812.

Riccomagno, M.M., Martinu, L., Mulheisen, M., Wu, D.K., Epstein, D.J., 2002. Specification of the mammalian cochlea is dependent on Sonic hedgehog. Genes Dev. 16, 2365–2378.

Rijli, F.M., Mark, M., Lakkaraju, S., Dierich, A., Dolle, P., Chambon, P., 1993. A homeotic transformation is generated in the rostral branchial region of the head by disruption of *Hoxa-2*, which acts as a selector gene. Cell 75, 1333–1349.

Riley, B.B., Phillips, B.T., 2003. Ringing in the new ear: resolution of cell interactions in otic development. Dev. Biol. 261, 289–312.

Rinkwitz-Brandt, S., Arnold, H.H., Bober, E., 1996. Regionalized expression of *Nkx5-1*, *Nkx5-2*, *Pax2* and *sek* genes during mouse inner ear development. Hear Res. 99, 129–138.

Scambler, P.J., 2000. The 22q11 deletion syndromes. Hum. Mol. Genet. 9, 2421–2426.

Serbedzija, G.N., Bronner-Fraser, M., Fraser, S.E., 1992. Vital dye analysis of cranial neural crest cell migration in the mouse embryo. Development 116, 297–307.

Swanson, G.J., Howard, M., Lewis, J., 1990. Epithelial autonomy in the development of the inner ear of a bird embryo. Dev. Biol. 137, 243–257.

Swillen, A., Devriendt, K., Legius, E., Prinzie, P., Vogels, A., Ghesquiere, P., Fryns, J.P., 1999. The behavioural phenotype in velo-cardio-facial syndrome (VCFS): from infancy to adolescence. Genet. Couns. 10, 79–88.

Torres, M., Giráldez, F., 1998. The development of the vertebrate inner ear. Mech. Dev. 71, 5–21.

Torres, M., Gómez-Pardo, E., Gruss, P., 1996. *Pax2* contributes to inner ear patterning and optic nerve trajectory. Development 122, 3381–3391.

Trokovic, N., Trokovic, R., Mai, P., Partanen, J., 2003. *Fgfr1* regulates patterning of the pharyngeal region. Genes Dev. 17, 141–153.

Trumpp, A., Depew, M.J., Rubenstein, J.L., Bishop, J.M., Martin, G.R., 1999. Cre-mediated gene inactivation demonstrates that FGF8 is required for cell survival and patterning of the first branchial arch. Genes Dev. 13, 3136–3148.

Vitelli, F., Morishima, M., Taddei, I., Lindsay, E.A., Baldini, A., 2002a. *Tbx1* mutation causes multiple cardiovascular defects and disrupts neural crest and cranial nerve migratory pathways. Hum. Mol. Genet. 11, 915–922.

Vitelli, F., Taddei, I., Morishima, M., Meyers, E.N., Lindsay, E.A., Baldini, A., 2002b. A genetic link between *Tbx1* and fibroblast growth factor signaling. Development 129, 4605–4611.

Vitelli, F., Viola, A., Morishima, M., Pramparo, T., Baldini, A., Lindsay, E., 2003. *TBX1* is required for inner ear morphogenesis. Hum. Mol. Genet. 12, 2041–2048.

Wang, W., Van de Water, T., Lufkin, T., 1998. Inner ear and maternal reproductive defects in mice lacking the *Hmx3* homeobox gene. Development 125, 621–634.

Xu, P.X., Adams, J., Peters, H., Brown, M.C., Heaney, S., Maas, R., 1999. *Eya1*-deficient mice lack ears and kidneys and show abnormal apoptosis of organ primordia. Nat. Genet. 23, 113–117.

Zheng, W., Huang, L., Wei, Z.B., Silvius, D., Tang, B., Xu, P.X., 2003. The role of *Six1* in mammalian auditory system development. Development 130, 3989–4000.

RESEARCH ARTICLE

Bmp2 Is Required for Migration but Not for Induction of Neural Crest Cells in the Mouse

Ana Catarina Correia,[†] Marta Costa,[†] Filipa Moraes,[†‡] Joana Bom, Ana Nóvoa, and Moisés Mallo*

Bone morphogenetic protein (BMP) signaling is essential for neural crest development in several vertebrates. Genetic experiments in the mouse have shown that *Bmp2* is essential for the genesis of migratory neural crest cells. Using several markers and a transgenic reporter approach, we now show that neural crest cells are induced in *Bmp2* null mutant embryos, but that these cells fail to migrate out of the neural tube. The absence of migratory neural crest cells in these mutants is not due to their elimination by cell death. The neuroectoderm of $Bmp2^{-/-}$ embryos fail to close and create abnormal folds both along the anterior–posterior and medio–lateral axes, which are associated with an apparent medio–lateral expansion of the neural tube. Finally, our data suggest that the molecular cascade downstream of BMP signaling in early neural crest development may be different in mouse and avian embryos. *Developmental Dynamics 236: 2493–2501, 2007.* © 2007 Wiley-Liss, Inc.

Key words: neural crest; *Bmp2*; delamination; induction

Accepted 12 June 2007

INTRODUCTION

The neural crest is a group of migratory cells induced at the dorsal tip of the neural tube as a consequence of interactions between the neural and non-neural ectoderm (Barembaum and Bronner-Fraser, 2005). After induction, these cells undergo an epithelial to mesenchymal transition, delaminate from the neuroectoderm and migrate profusely to populate a wide variety of embryonic structures, where they contribute to many different tissues (Le Douarin and Kalcheim, 1999). During the past years, considerable effort has been directed toward understanding the different aspects of neural crest biology, including its induction and delamination from the neuroectoderm, the control of the migratory properties, and the mechanisms of differentiation into specific tissues (Le Douarin and Dupin, 2003; Meulemans and Bronner-Fraser, 2004; Morales et al., 2005). The emerging picture is quite complex and is further complicated by the apparent differences among different model organisms (Aybar and Mayor, 2002).

While many experimental analyses have been performed in chicken, zebrafish, and *Xenopus* embryos, information relating to the early processes of neural crest biology in the mouse is scarce and it is not clear if the mechanisms that are thought to be relevant in other species also apply to mammals. An additional level of difficulty is that often a function that has been associated to a specific member of a gene family in the chicken is performed by a different member of the family in the mouse. For instance, based on expression analyses, it has been suggested that the function of *Snail2* (previously known as *Slug*) in the chicken neural crest is performed by *Snail1* in the mouse (Sefton et al., 1998). However, when this idea was challenged using genetic tools, the results were surprising, as they indicated that neither *Snail1* nor *Snail2* seemed to be involved in neural crest production in the mouse (Murray and Gridley, 2006). This finding suggests that some of the mechanisms of neural

Instituto Gulbenkian de Ciência, Oeiras, Portugal
Grant sponsor: FCT/POCI; Grant number POCI/BIA-BCM/60420/2004; Grant sponsor: Centro de Biologia do Desenvolvimento.
[†]A. C. Correia, M. Costa, and F. Moraes contributed equally to this work.
[‡]M. Costa's present address is Department of Zoology, University of Cambridge, Downing Street, Cambridge CB2 3EJ, UK.
***Correspondence to: Moisés Mallo, Instituto Gulbenkian de Ciência, Rua da Quinta Grande 6, 2780-156 Oeiras, Portugal. E-mail: mallo@igc.gulbenkian.pt**

DOI 10.1002/dvdy.21256
Published online 5 August 2007 in Wiley InterScience (www.interscience.wiley.com).

© 2007 Wiley-Liss, Inc.

crest development are not conserved among vertebrates.

The bone morphogenetic proteins (BMPs) were among the first factors implicated in the earliest processes of neural crest cell development. Early experiments performed in chicken embryos suggested that BMP4 and BMP7 were implicated in neural crest cell induction (Liem et al., 1995). This view was challenged by later results, which showed that the ability of these factors to induce neural crest cells in vitro depends on the concomitant activity of other still not identified factors present in the serum of the culture medium (Garcia-Castro et al., 2002). A different set of studies performed in chicken embryos suggested that BMPs are required for the migration rather than the induction of neural crest cells (Sela-Donenfeld and Kalcheim, 1999). In addition, it has been proposed that BMP activity is further modulated by noggin and that the graded inactivation of the expression of this gene controls the onset of neural crest migration (Sela-Donenfeld and Kalcheim, 1999). The molecular mechanisms that mediate BMP signaling in neural crest cell delamination have also been studied. In the initial studies, it was proposed that BMP activity was mediated by induction of *Cad6B* and the GTPase RhoB (Sela-Donenfeld and Kalcheim, 1999). Recent data implicate BMP signaling in modulating progression through the cell cycle, an effect that could be mediated, at least in part, by *Wnt1* (Burstyn-Cohen et al., 2004). It has also been proposed that the activity of BMP signaling is mediated by the cleavage of N-cadherin into a soluble cytoplasmic form, which would participate, together with the canonical Wnt pathway, in the control of neural crest cell emigration (Shoval et al., 2007).

In the mouse, a variety of genetic studies indicate that BMP signaling is essential at different stages of neural crest development. *Bmp5* and *Bmp7* have been reported to be required in a partially redundant manner for the survival of postmigratory crest cells, as demonstrated by their increased death in *Bmp5;Bmp7* double mutant embryos (Solloway and Robertson, 1999). In addition, *Bmp2* is essential for the formation of migratory neural crest cells (Kanzler et al., 2000; Ohnemus et al., 2002). Expression analyses in the mouse indicate that *Bmp2* is expressed in the surface ectoderm adjacent to the neuroectoderm with a spatiotemporal dynamics that correlates with neural crest cell production (Kanzler et al., 2000). Blocking *Bmp2* signaling in vivo in the dorsal neural tube through expression of noggin in transgenic mice, resulted in the absence of migratory neural crest cells and in the lack of the corresponding derivatives (Kanzler et al., 2000; Ohnemus et al., 2002). In addition, preliminary analysis of *Bmp2* mutant embryos failed to detect the streams of *Crabp1* reactivity associated with the hindbrain characteristic of neural crest cells, which was correlated with an absence of branchial arches (Kanzler et al., 2000). What is not clear from these studies is whether *Bmp2* is required for the induction of neural crest cells or for their delamination/migration from the neural tube. In this study, we show that neural crest cells are induced in the *Bmp2* mutants. We also show that the absence of migratory neural crest cells in these mutants does not derive from increased death of the premigratory neural crest cells, and thus it is probable that *Bmp2* is required for triggering migration of these progenitors. The absence of migration of these cells seems to result in an extra accumulation of cells in the neuroepithelium, which produces abnormal foldings in the anterior–posterior and medial–lateral axes. Our results also suggest that, although BMP signaling is required for neural crest cell migration in chicken and mouse embryos, the molecular mediators may differ among vertebrates.

RESULTS

As reported earlier, *Bmp2* mutant embryos do not survive past embryonic day (E) 9.0, which hampers analysis of the formation of neural crest derivatives (Zhang and Bradley, 1996; Kanzler et al., 2000). However, living embryos can be recovered at this stage, thus allowing analysis of early stages of neural crest cell development. A morphological analysis of these "late" *Bmp2* mutants showed several malformations, in addition to those previously reported (Zhang and Bradley, 1996). In particular, the rostral neural tube always failed to close and displayed abnormal foldings both in the anterior–posterior and medial–lateral axes, without a fixed pattern (Fig. 1). In addition, the surface of the neural tube seemed extended medial–laterally in the mutant embryos when compared with their wild-type littermates. As the neural tube fails to close, there are no real dorsal and ventral domains, but rather medial and lateral areas in the neuroectoderm, which is the nomenclature that we will use throughout the text.

Neural Crest Cells Are Induced in the Absence of *Bmp2*

Previous work indicated that *Bmp2* mutant mice have no migratory neural crest cells, but whether this deficiency resulted from a lack of neural crest cell induction or from the inability of these cells to migrate from the neural tube was not investigated (Kanzler et al., 2000). To answer this question, we characterized early events of neural crest biology in *Bmp2* mutant mice. *Ap2*α is a neural crest marker in the mouse (Mitchell et al., 1991) that can be detected in the premigratory neural crest cells at the dorsal tip of the neural tube and in the migratory neural crest cells, most particularly in the cranial area (Fig. 1A,B). Examination of *Ap2*α expression in *Bmp2* mutant embryos revealed no obvious streams of migratory neural crest cells, confirming that no migratory neural crest cells are produced in the absence of *Bmp2* (Fig. 1C,D). However, *Bmp2* mutant embryos showed a clear *Ap2*α signal associated with the lateral border of the neural folds. Interestingly, the spatial distribution of the *Ap2*α transcripts in this area along the rostral–caudal axis was very similar to that observed in wild-type embryos, as it combined areas of strong and weak expression, the latter corresponding in wild-type embryos to rhombomeres (r) 3 and 5 (Fig. 1A,C). Analysis of sections of these embryos confirmed that *Ap2*α expression in *Bmp2* mutant embryos is indeed associated with the dorsal part of the neural tube (Fig. 1D). A careful analysis of the sections revealed that the expression in this area

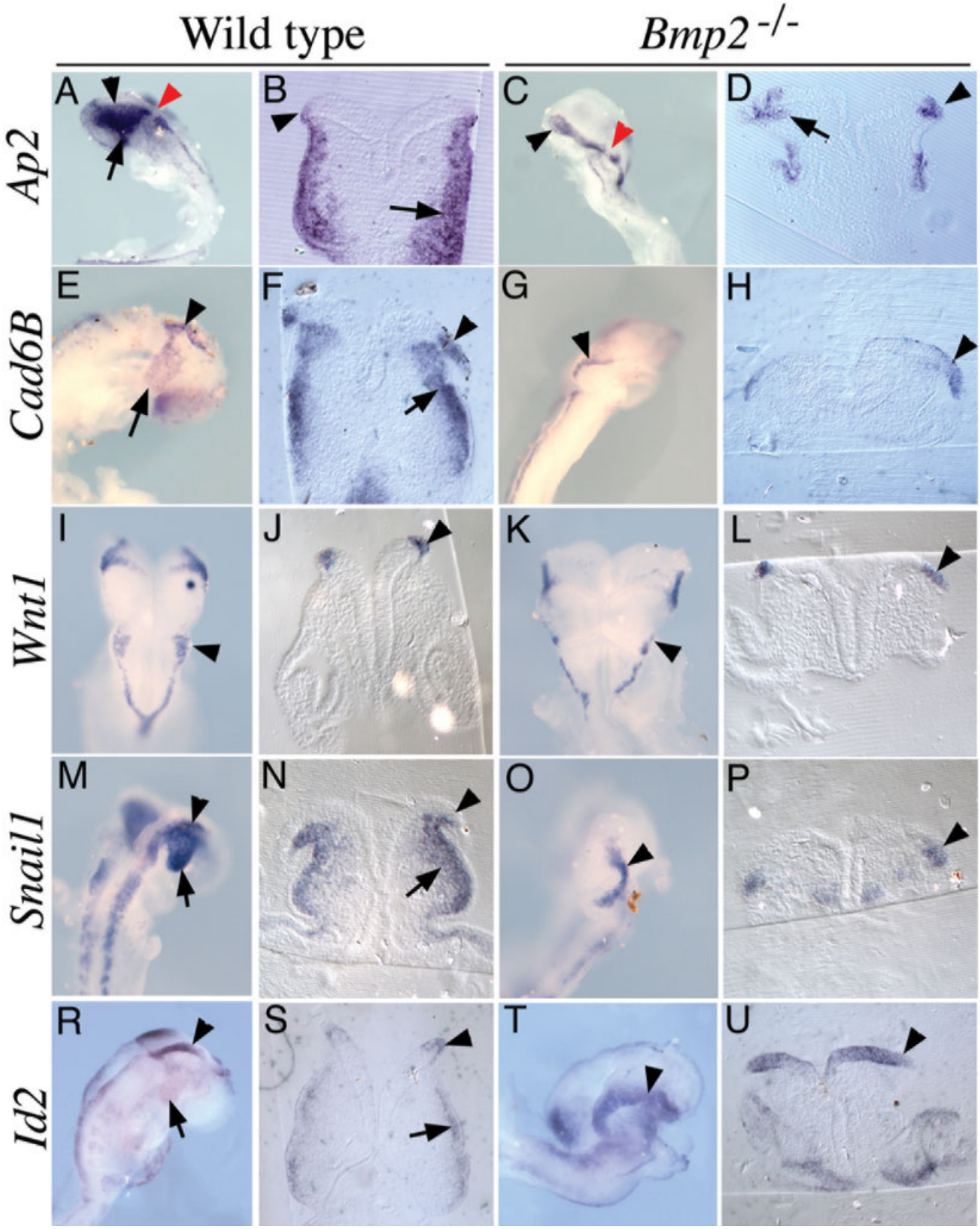

Fig. 1. Neural crest cell production in *Bmp2*$^{-/-}$ embryos. **A–P,R–U:** Wild-type (A,B,E,F,I,J,M,N,R,S) and *Bmp2* mutant (C,D,G,H,K,L,O,P,T,U) embryos were analyzed by whole-mount in situ hybridization using probes for *Ap2*α (A–D), *Cad6B* (**E–H**), *Wnt1* (**I–L**), *Snail1* (**M–P**), and *Id2* (**R–U**). The black arrowheads indicate the dorsal (lateral) edges of the neural tube, the black arrows indicate the migratory neural crest cells, and the red arrowheads in A and C indicate areas of the hindbrain poor in neural crest cell production.

expands medially farther than in wild-type embryos. Indeed, in wild-type embryos, very few cells in the dorsal neural tube were positive for *Ap2*α, possibly as a result of the migration of cells when expression of this transcription factor is activated. In *Bmp2* mutant embryos, *Ap2*α expression was clearly localized to the lateral borders of the neuroectoderm, which could represent an accumulation of induced neural crest cells. In addition, examination of serial sections covering the whole anterior–posterior axis revealed some *Ap2*α-positive cells in the mesenchyme adjacent to the neuroectoderm–surface ectoderm interface. These patches of cells were very rare and involved just a few cells (the picture in the embryo shown in Fig. 1D is the best image observed in that particular embryo). This finding suggests that, while the production of migratory neural crest cells is very reduced, some cells do manage to start migration. These results suggest that neural crest cells are induced but fail to migrate in the absence of *Bmp2*.

In chicken embryos, the early neural crest biology has been extensively characterized and the role that BMP signaling plays in this process has been addressed by several groups (Selleck et al., 1998; Burstyn-Cohen et al., 2004; Shoval et al., 2007). In those studies, several genes have been reported to be downstream of the BMP signaling pathway during early stages of neural crest cell biology (Burstyn-Cohen et al., 2004). Among these, *Cad6B* and *Wnt1* are also neural crest cell markers in the mouse. As in chicken embryos, *Cad6B* is expressed in the premigratory neural crest of the mouse. However, contrary to what has been reported in chicken (Taneyhill et al., 2007), mouse migratory neural crest is also positive for *Cad6B*, at least in the cranial region (Fig. 1E,F). In *Bmp2* mutant embryos, *Cad6B* expression was readily detected in the lateral edges of the neuroectoderm (Fig. 1G,H). However, it could not be detected in the domain where migratory neural crest should be present, further supporting the inference of the absence of this cell population. The other potential BMP target in the neural crest, *Wnt1*, shows an equivalent expression pattern in chicken and mouse embryos, being restricted to the dorsal neural tube but absent from the migratory neural crest population (Wilkinson et al., 1987; Bally-Cuif et al., 1992; Fig. 1I,J). In the mouse, a variety of cell tracing and mutagenesis experiments indicates that, while migratory neural crest cells do not contain transcripts for *Wnt1*, the premigratory neural crest cells are included within the expression domain of this gene in the dorsal neural tube (Echelard et al., 1994; Jiang et al., 2000). In *Bmp2* mutant embryos, the expression domain of *Wnt1* in the lateral borders of the neuroectoderm was largely unaffected, including its spatial distribution along the anterior–posterior axis (Fig. 1K,L). These results indicate that, contrary to what has been reported for the chicken system (Burstyn-Cohen et al., 2004), in the mouse neither *Cad6B* nor *Wnt1* seems to be downstream of BMP signaling in early neural crest biology, at least that dependent on *Bmp2*.

The Snail gene family has been implicated in the delamination of neural crest cells in chicken and *Xenopus* embryos (Nieto et al., 1994; Aybar et al., 2003) and, while some reports consider these genes BMP-independent (Burstyn-Cohen et al., 2004), others place them downstream of BMP signaling (Selleck et al., 1998). In the mouse, *Snail1*, instead of *Snail2*, has been reported to be associated with the neural crest (Sefton et al., 1998). In wild-type embryos, expression of this gene is turned on in cells delaminating from the dorsal neural tube. At least in our hands, it is rarely observed in the premigratory neural crest cells (Fig. 1N), probably because of the immediate delamination of the *Snail1*-positive neural crest cells, but gives a strong signal in the streams of migratory neural crest cells (Fig. 1M,N). In *Bmp2* mutant embryos, no *Snail1* expression was observed in the mesenchyme adjacent to the cranial neural tube, which is consistent with the absence of migratory neural crest cells (Fig. 1O,P). However, a clear signal was observed adjacent to the lateral tip of the neural folds, which is also consistent with the presence of neural crest cell progenitors that failed to migrate away of the neural tube. Analysis of sections revealed that, in addition to this signal, cells in the lateral tip of the neuroectoderm are often positive for *Snail1* (Fig. 1P), a signal that, as mentioned above, was not observed in wild-type embryos (Fig. 1O). This result is also consistent with the existence of neural crest progenitors in *Bmp2* mutant embryos, lending further support for a role for *Bmp2* in neural crest migration, rather than induction, in the mouse. Also, these results indicate that expression of the Snail family genes in the neural crest is independent of *Bmp2* signaling.

The Id family genes have also been reported to be downstream of the BMP pathway (Hollnagel et al., 1999) and to play a role in neural crest formation, at least in chicken and *Xenopus* embryos (Martinsen and Bronner-Fraser, 1998; Kee and Bronner-Fraser, 2005). Of the four Id genes that exist in mice, *Id2* seemed to give the clearest expression pattern in the neural crest (our unpublished data). Its expression was already detected in the lateral edges of the neuroectoderm at E8.0, which is compatible with the dynamics of neural crest cell production (Fig. 1R,S; and not shown). Expression was then detected also in the migratory neural crest cells, being stronger in the mesencephalic crest domain, although the levels of *Id2* expression in migratory neural crest cells were always very reduced and disappeared after E9.0 (Fig. 1R,S; and not shown). In *Bmp2* mutant embryos, *Id2* expression in the lateral neural folds was very strong, indicating that, at least in this area, *Id2* expression is not under the positive control of *Bmp2*. Actually, in all *Bmp2* mutant embryos analyzed (n = 3), expression of *Id2* extended medially to a considerable extent (Fig. 1T,U; and not shown). Nevertheless, if *Id2* also labels the premigratory neural crest population in mouse embryos, the expression of this gene in the *Bmp2* mutant embryos is also consistent with the conclusion that production of neural crest cells is not affected by the absence of *Bmp2*.

To further analyze whether neural crest cells are formed in the absence of *Bmp2*, we used a transgenic approach. It has been described that the *HtPA* gene contains an enhancer that labels specifically the neural crest cells (Pietri et al., 2003). We used this enhancer to express the *RFP* gene in

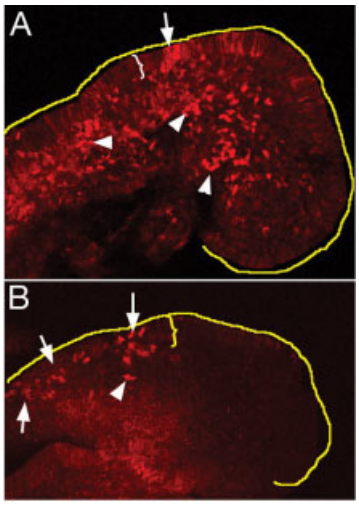

Fig. 2. Transgenic analysis of neural crest cell production in *Bmp2*$^{-/-}$ embryos. **A,B:** HtPA:RFP transgenic animals were analyzed for red fluorescent protein (RFP) expression in the wild type (A) and *Bmp2*$^{-/-}$ background (B). The yellow line outlines the dorsal part of the head of a wild-type embryo (A) and the lateral border of the head of a *Bmp2*$^{-/-}$ embryo (B). The arrows show some cells that did not leave the neural tube, and the arrowheads, migratory neural crest cells. The brackets show the area where labeled cells are in the neuroectoderm.

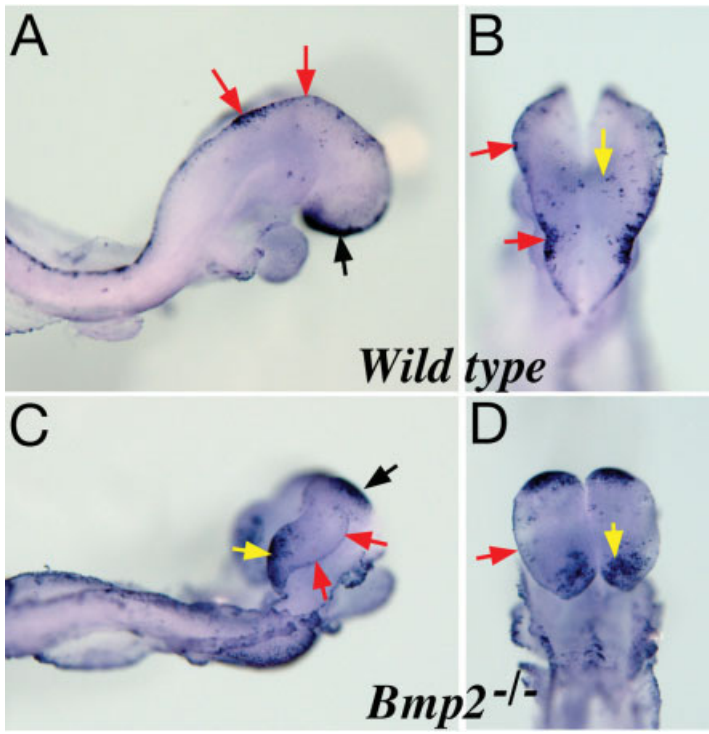

Fig. 3. Terminal deoxynucleotidyl transferase–mediated deoxyuridinetriphosphate nick end-labeling (TUNEL) analysis of *Bmp2*$^{-/-}$ embryos. **A–D:** The analysis was performed on E8.5 wild-type (A,B) and *Bmp2*$^{-/-}$ mutant (C,D) embryos. The red arrows indicate different areas of the dorsal (lateral) neural tube, which is where the neural crest cells are produced. The black arrows indicate areas of strong cell death in the forebrain. The yellow arrows indicate areas of the neural tube showing increased apoptosis in mutant embryos compared with wild-type littermates.

transgenic mice (*HtPA:RFP* mice), thus labeling the neural crest cells with red fluorescent protein (RFP). Analysis of transgenic embryos revealed RFP fluorescence in migratory neural crest cells in the cranial region (Fig. 2A). In keeping with previous reports, only a few RFP-positive premigratory neural crest cells were observed, arguably because these cells delaminate shortly after activation of the enhancer (Pietri et al., 2003). In the *Bmp2* mutant, background RFP-positive cells were also readily detected but remained mostly associated with the dorsal neural tube (Fig. 2B). It is possible that a few RFP-positive cells were located in the adjacent mesenchyme rather than in the neuroepithelium, which could indicate the existence of a residual migratory ability of the neural crest cells in the absence of *Bmp2*. These results are consistent with the data obtained with molecular markers and further support the conclusion that *Bmp2* does not have an effect on neural crest cell production.

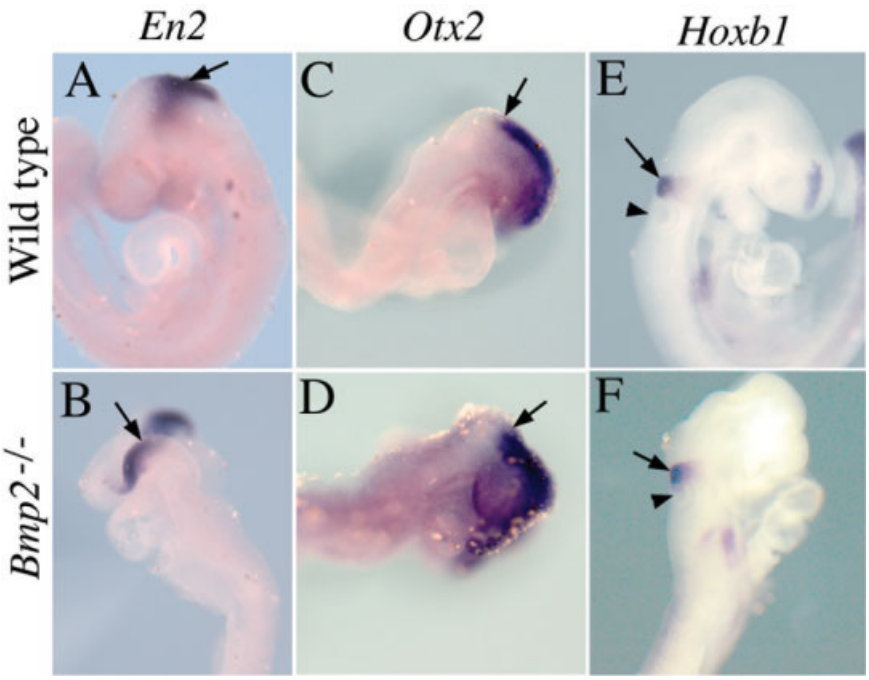

Fig. 4. Analysis of anterior–posterior patterning in the neural tube of *Bmp2* mutant embryos. **A–F:** Wild-type (A,C,E) and *Bmp2*$^{-/-}$ embryos (B,D,F) were analyzed by whole-mount in situ hybridization using *En2* (A,B), *Otx2* (C,D), and *Hoxb1* (E,F). The arrows in A and B indicate the domain of *En2* expression, in C and D the posterior limit of *Otx2* expression, and in E and F the domain of *Hoxb1* expression. The arrowheads in E and F indicate the otic vesicle.

Apoptosis in the Neural Tube of *Bmp2* Mutant Embryos

To understand whether the absence of migratory neural crest cells in *Bmp2* mutant embryos resulted from the death of the induced progenitors, we performed terminal deoxynucleotidyl transferase–mediated deoxyuridinetriphosphate nick end-labeling (TUNEL) assays. At E8.5, some TUNEL-positive cells were observed in the dorsal neural tube, with a focal concentration of apoptotic cells in the anterior hindbrain (Fig. 3A,B). Considerable cell death was also evident in the forebrain region. In *Bmp2* mutant embryos, no obvious increase of TUNEL-positive cells was detected associated with the lateral borders of the neural tube (Fig. 3C,D), indicating that increased cell death is probably not responsible for the absence of migratory neural crest cells. It should be noted that, in these embryos, focal areas of TUNEL-positive cells were observed in the most anterior part of the neuroepithelium, which corresponds to the forebrain region. In addition, an extra area of increased cell death was observed in *Bmp2* mutant embryos in the region that would correspond to the anterior hindbrain–posterior mesencephalon (Fig. 3D), an area where we never observed cell death in control littermates (Fig. 3B). The possible relevance of this observation will be discussed later.

Anterior–Posterior Patterning in the Neural Tube of *Bmp2* Mutant Mice

When we analyzed expression of *Wnt1* in *Bmp2* mutant embryos, we observed that, while expression in the dorsal tip of the neural tube was not compromised, expression in the midbrain–hindbrain boundary could not be detected (Fig. 1K). As the neuroectoderm in the *Bmp2* mutant embryos is abnormally folded, the absence of *Wnt1* expression in this area could indicate abnormal anterior–posterior patterning of the neural tube in *Bmp2* mutant embryos. Therefore, we analyzed expression of a few molecular markers for specific areas of the neural tube in *Bmp2* mutant embryos. Engrailed genes are specifically expressed in the midbrain, next to the midbrain–hindbrain boundary, in an area adjacent to the *Wnt1* expression domain (Fig. 4A; Joyner and Martin, 1987). *En2* was expressed in equivalent patterns in control embryos and the *Bmp2* mutants (Fig. 4B), indicating that the midbrain–hindbrain border was not globally disturbed. Importantly, the *En2* domain was restricted to a specific area of the neural tube and did not extend its most anterior border, suggesting that this area was also correctly patterned. We confirmed this finding with the analysis of *Otx2* expression, which is detected in the forebrain and midbrain down to the border with the hindbrain (Fig. 4C,D; Simeone et al., 1992). In addition, the hindbrain also seemed to keep a normal anterior–posterior pattern, as indicated by the restricted expression of hindbrain markers like *Hoxb1*, which is expressed in r4 (Fig. 4E,F; Frohman et al., 1990). These results indicate that, globally, the neuroectoderm of the *Bmp2* mutant embryos is correctly patterned along the anterior posterior axis, although expression of specific markers, most particularly *Wnt1*, seemed affected.

DISCUSSION

In this manuscript, we showed that, in the mouse, *Bmp2* is not required for the induction of neural crest cells, but it is essential for their migration from the neural tube. It is clear that migratory neural crest production is strongly compromised in the absence of *Bmp2*, which is in keeping with our previous data using biochemical blockage of BMP signaling in transgenic embryos (Kanzler et al., 2000; Ohnemus et al., 2002). However, all tests for neural crest cell induction, either using a variety of molecular markers or a transgenic approach, turned out positive in the *Bmp2* mutant embryos, indicating that *Bmp2* is not essential for the induction of this cell population, but rather for its migration from the neural tube. Interestingly, with the limitations inherent to the abnormal neural tube morphology of *Bmp2* mutant embryos, the spatial distribution of transcripts for the neural crest cell markers along the anterior–posterior axis was very similar to that observed in wild-type embryos. Thus, there were areas of strong expression, which corresponded to the neural crest-producing domains, and areas with very little or no expression, which corresponded to the neural crest-free areas of the hindbrain (Lumsden et al., 1991). This finding suggests that not only neural crest cell induction occurs in the absence of *Bmp2*, but also that the basic mechanisms are still in place in *Bmp2* mutant embryos. It should be noted that we cannot rule out that specific subsets of neural crest cells fail to be induced in *Bmp2* mutant embryos.

The absence of migratory neural crest cells seems not to be a consequence of increased cell death, as no increase in TUNEL-positive cells was detected associated with the lateral borders of the neuroectoderm in *Bmp2* null mutant embryos. It is still possible that the elimination of migratory cells occurs at a rate below the levels of detection of our assay. However, apoptotic cells were readily detected in embryos carrying mutations in other genes essential for survival of postmigratory neural crest cells (Solloway and Robertson, 1999; Trumpp et al., 1999). Therefore, given the large numbers of neural crest cells produced during the early stages of embryogenesis, an extent of cell death that could account for the absence of this migratory population should most probably be above the level of detection by TUNEL.

An alternative hypothesis for the absence of migratory neural crest cells in *Bmp2* mutants is that *Bmp2* is involved in triggering the migratory competence of the induced neural crest cells. A role for BMP (Dpp) signaling in the promotion of cell movement has already been reported in other systems (Vincent et al., 1997). Moreover, some of our data can be interpreted according to this hypothesis. In particular, we have observed that cells positive for some neural crest markers, like *Ap2α*, *Snail1*, or the RFP in *HtPA:RFP* transgenics, which are rarely detected in the dorsal neural tube but rather in migratory neural crest population, seem to accumulate in the lateral edges of the neuroectoderm, remaining as premigratory neural crest cells. It will be important to address this problem di-

rectly and determine the underlying mechanism.

It could be expected that, in the absence of migration, neural crest cells accumulate in the lateral neural tube of *Bmp2* mutant embryos. Although the domain positive for neural crest cell markers in *Bmp2* mutants may be slightly extended compared with wild-type embryos, it is clear that there is no overt accumulation of premigratory neural crest cells. Experiments in chicken and amphibian embryos indicate that neural crest cell induction requires interactions between the surface ectoderm and the neuroectoderm (Moury and Jacobson, 1990; Selleck and Bronner-Fraser, 1995). If the same is true for mouse embryos, the signals involved in this process could have a limited range of activity and, therefore, could not act much further than a few cells in distance. In this context, the induced neural crest cells that fail to migrate could act as a barrier for further neural crest induction in more medial cells within the neuroectoderm, thus maintaining the size of the neural crest compartment within normal limits. Another consequence of the absence of neural crest cell migration and their lack of elimination by death could be an abnormal accumulation of cells in the neuroepithelium. This explanation is consistent with the observation that neuroepithelium of *Bmp2* mutant embryos is clearly wider than those of control embryos and is abnormally folded. It should be noted, however, that increased apoptosis was also detected in specific areas of the neuroepithelium, which could contribute (at least partially) to the elimination of the extra cells accumulating as a result of the absence of migration of the induced crest cells. This cell death, of unclear origin, could also account for the lack of *Wnt1* expression in the midbrain/hindbrain boundary that we observed in the *Bmp2* mutants. Indeed, the observed domain of cell death contains the area of *Wnt1* expression in the neuroepithelium.

An important implication of our results is that the role of *Bmp2* in mouse neural crest development seems to be different to what has been reported for BMP signaling in other vertebrates. In chicken embryos, *Cad6B* and *Wnt1* are both downstream of BMPs in the signaling cascades that generate migratory neural crest cells (Sela-Donenfeld and Kalcheim, 1999; Burstyn-Cohen et al., 2004). Most particularly, it was proposed that *Wnt1* was an essential mediator of BMP signaling in the induction of migratory properties to neural crest cells (Burstyn-Cohen et al., 2004). In our case, it is clear that neither of the two genes was affected by the absence of *Bmp2*, but neural crest cells were still unable to migrate. There are several possible explanations for these inconsistencies. This may reflect another basic difference in the mechanisms that modulate production of migratory neural crest cells in the two vertebrates. The existence of such divergences has been clearly documented for the Snail family of transcription factors. It has been reported that *Snail2* (previously known as *Slug*) is required for the epidermal to mesenchymal transitions involved in the genesis of migratory neural crest cells in chicken embryos (Nieto et al., 1994). However, a recent report has clearly shown that mouse embryos carrying null mutations for both *Snail1* and *Snail2* still produce migratory neural crest cells, indicating that neither of these two genes is essential for this process in the mouse (Murray and Gridley, 2006). In this context, it is important to note that *Snail2* expression is maintained in the *Bmp2* mutants and neural crest cell delamination is still blocked. It is also clear that canonical Wnt signaling in the mouse cannot play the essential role in neural crest cell delamination reported for chicken embryos, as both *Wnt1;Wnt3A* double mutants and conditional mutants for β-*catenin* in the neural crest seem to have no problems in neural crest cell delamination (Ikeya et al., 1997; Brault et al., 2001). In the case of BMP signaling in the neural crest cells, additional differences have already been reported between mouse and chicken embryos. For instance, BMP4 seems to be the relevant molecule for the induction/migration of chicken neural crest cells (although an activity for BMP7 has also been reported), while *Bmp2* seemed irrelevant in this process (Liem et al., 1995). Conversely, inactivation of *Bmp2* alone is enough to block production of migratory neural crest cells in the mouse, while Bmp4 does not seem to play a major role in the process in this species (Kanzler et al., 2000). *Bmp5* and *Bmp7* also seem to play a role in the development of neural crest cells, but their function seems to be required at later stages (Solloway and Robertson, 1999). Another apparent BMP signaling-related difference between mouse and chicken neural crest is that mutant data in the mouse are not consistent with a role for the BMP inhibitor Noggin in the spatial and temporal control of neural crest cell delamination that has been proposed according to experiments performed in chicken embryos (McMahon et al., 1998; Sela-Donenfeld and Kalcheim, 1999).

Another possible explanation for the inconsistency of our results with those obtained for BMP signaling in chicken and *Xenopus* embryos is that, while most of our analyses have been performed in the cranial region, which is where our phenotypes were most easily scored, experiments performed to evaluate the relevance of BMP signaling in chicken neural crest delamination have been typically performed in the caudal neural tube. This finding would suggest that induction/delamination of cranial and caudal neural crest cells is controlled by different mechanisms. However, as far as we could evaluate from our expression analyses, what we documented for the cranial area seems to apply also for the trunk neural crest cells (our unpublished data).

In conclusion, while BMP signaling seems to be required for neural crest cell migration in various vertebrates, the molecular mechanisms for this process evidently diverge among species.

EXPERIMENTAL PROCEDURES

Mice

The *Bmp2* mutant mice were described previously (Zhang and Bradley, 1996). To generate the *HtPA-RFP* transgenic mice, the *RFP* cDNA was cloned downstream of the *HtPA* enhancer that drives expression in the neural crest (Pietri et al., 2003). The SV40 polyadenylation signal was cloned downstream of the *RFP* cDNA.

The purified construct was used to generate transgenic mice by pronuclear injection according to standard protocols. The *HtPA-RFP* transgenic animals and embryos were identified by polymerase chain reaction (PCR) using the primers 5′-TCCGAGGACGTCATCAGGGAG-3′ and 5′-ATGGTGTAGTCCTCGTTGTGG-3′.

In Situ Hybridization and Apoptosis

In situ hybridization was performed as previously described (Kanzler et al., 1998). At least three embryos for each genotype were analyzed per probe. The probes used were *Ap2*α (Mitchell et al., 1991), *Snail1* (Sefton et al., 1998), *Cad6B* (Ionue et al., 1997), *Wnt1* (Wilkinson et al., 1987), *En2* (Joyner and Martin, 1987), and *Otx2* (Simeone et al., 1992). The *Hoxb1* probe was obtained as a 1.1-kb fragment containing the whole open reading frame by reverse transcriptase-PCR, cloned into the *Eco*RI and *Bam*HI sites of pKS Bluescript. The probe for *Id2* was obtained from IMAGE clone 6515664. Stained embryos were embedded in gelatin/sucrose, sectioned to 30 μm with a Vibratome and photographed under Nomarski optics.

Apoptosis was determined by TUNEL as described in Kanzler et al. (2000) except for the use of an alkaline phosphatase-conjugated instead of horseradish peroxidase-conjugated antifluorescein antibody and subsequent detection of the activity with NBT and BCIP (nitroblue tetrazolium/5-bromo-4-chloro-3-indolyl phosphate) as performed in the in situ hybridization protocol. The RFP fluorescence was acquired by confocal microscopy using a Leica TCS SP2 system, and Z-projections of the confocal stacks were processed and colored using Imairs (v5.0.3) and ImageJ (v1.37).

ACKNOWLEDGMENTS

We thank Trish Labosky and Allan Bradley for the *Bmp2* mutant mice, Silvye Dufour for the *HtPA* enhancer, Angela Nieto for the *Snail1* probe, Andy McMahon for the *Wnt1* probe, Hubert Schorle for the *Ap1*α probe, Andreas Kispert for the *Cad6B* probe, José Belo for the *En2* and *Otx2* probes, Randy Cassada for reading the manuscript, and all members of the Mallo lab for support and discussion. This work was funded by the Centro de Biologia do Desenvolvimento and by FCT.

REFERENCES

Aybar MJ, Mayor R. 2002. Early induction of neural crest cells: lessons learned from frog, fish and chick. Curr Opin Genet Dev 12:452–458.

Aybar MJ, Nieto MA, Mayor R. 2003. Snail precedes slug in the genetic cascade required for the specification and migration of the Xenopus neural crest. Development 130:483–494.

Bally-Cuif L, Alvarado-Mallart RM, Darnell DK, Wassef M. 1992. Relationship between Wnt-1 and En-2 expression domains during early development of normal and ectopic met-mesencephalon. Development 115:999–1009.

Barembaum M, Bronner-Fraser M. 2005. Early steps in neural crest specification. Semin Cell Dev Biol 16:642–646.

Brault V, Moore R, Kutsch S, Ishibashi M, Rowitch DH, McMahon AP, Sommer L, Boussadia O, Kemler R. 2001. Inactivation of the beta-catenin gene by *Wnt1*-Cre-mediated deletion results in dramatic brain malformation and failure of craniofacial development. Development 128:1253–1264.

Burstyn-Cohen T, Stanleigh J, Sela-Donenfeld D, Kalcheim C. 2004. Canonical Wnt activity regulates trunk neural crest delamination linking BMP/noggin signaling with G1/S transition. Development 131:5327–5339.

Echelard Y, Vassileva G, McMahon AP. 1994. Cis-acting regulatory sequences governing Wnt-1 expression in the developing mouse CNS. Development 120: 2213–2224.

Frohman MA, Boyle M, Martin GR. 1990. Isolation of the mouse Hox-2.9 gene; analysis of embryonic expression suggests that positional information along the anterior–posterior axis is specified by mesoderm. Development 110:589–607.

Garcia-Castro MI, Marcelle C, Bronner-Fraser M. 2002. Ectodermal Wnt function as a neural crest inducer. Science 297:848–851.

Hollnagel A, Oehlmann V, Heymer J, Ruther U, Nordheim A. 1999. Id genes are direct targets of bone morphogenetic protein induction in embryonic stem cells. J Biol Chem 274:19838–19845.

Ikeya M, Lee SM, Johnson JE, McMahon AP, Takada S. 1997. Wnt signalling required for expansion of neural crest and CNS progenitors. Nature 389:966–970.

Inoue T, Chisaka O, Matsunami H, Takeichi M. 1997. Cadherin-6 expression transiently delineates specific rhombomeres, other neural tube subdivisions, and neural crest subpopulations in mouse embryos. Dev Biol 183:183–194.

Jiang X, Rowitch DH, Soriano P, McMahon AP, Sucov HM. 2000. Fate of the mammalian cardiac neural crest. Development 127:1607–1616.

Joyner AL, Martin GR. 1987. En-1 and En-2, two mouse genes with sequence homology to the Drosophila engrailed gene: expression during embryogenesis. Genes Dev 1:29–38.

Kanzler B, Kuschert SJ, Liu Y-H, Mallo M. 1998. *Hoxa-2* restricts the chondrogenic domain and inhibits bone formation during development of the branchial area. Development 125:2587–2597.

Kanzler B, Foreman RK, Labosky PA, Mallo M. 2000. BMP signaling is essential for development of skeletogenic and neurogenic cranial neural crest. Development 127:1095–1104.

Kee Y, Bronner-Fraser M. 2005. To proliferate or to die: role of Id3 in cell cycle progression and survival of neural crest progenitors. Genes Dev 19:744–755.

Le Douarin NM, Dupin E. 2003. Multipotentiality of the neural crest. Curr Opin Genet Dev 13:529–536.

Le Douarin NM, Kalcheim C. 1999. The neural crest. Cambridge, UK: Cambridge University Press.

Liem KF Jr, Tremmi G, Roelink H, Jessell TM. 1995. Dorsal differentiation of neural plate cells induced by BMP-mediated signals from epidermal ectoderm. Cell 82: 969–979.

Lumsden A, Sprawson N, Graham A. 1991. Segmental origin and migration of neural crest cells in the hindbrain region of the chick embryo. Development 113:1281–1291.

Martinsen BJ, Bronner-Fraser M. 1998. Neural crest specification regulated by the helix-loop-helix repressor *Id2*. Science 281:988–991.

McMahon JA, Takada S, Zimmerman LB, Fan CM, Harland RM, McMahon AP. 1998. Noggin-mediated antagonism of BMP signaling is required for growth and patterning of the neural tube and somite. Genes Dev 12:1438–1452.

Meulemans D, Bronner-Fraser M. 2004. Gene-regulatory interactions in neural crest evolution and development. Dev Cell 7:291–299.

Mitchell PJ, Timmons PM, Hebert JM, Rigby PW, Tjian R. 1991. Transcription factor AP-2 is expressed in neural crest cell lineages during mouse embryogenesis. Genes Dev 5:105–119.

Morales AV, Barbas JA, Nieto MA. 2005. How to become neural crest: from segregation to delamination. Semin Cell Dev Biol 16:655–662.

Moury JD, Jacobson AG. 1990. The origins of neural crest cells in the axolotl. Dev Biol 141:243–253.

Murray SA, Gridley T. 2006. Snail family genes are required for left-right asymmetry determination, but not neural crest formation, in mice. Proc Natl Acad Sci U S A 103:10300–10304.

Nieto MA, Sargent MG, Wilkinson DG, Cooke J. 1994. Control of cell behavior during vertebrate development by Slug, a zinc finger gene. Science 264:835–839.

Ohnemus S, Kanzler B, Jerome-Majewska LA, Papaioannou VE, Boehm T, Mallo M. 2002. Aortic arch and pharyngeal phenotype in the absence of BMP-dependent neural crest in the mouse. Mech Dev 119:127–135.

Pietri T, Eder O, Blanche M, Thiery JP, Dufour S. 2003. The human tissue plasminogen activator-Cre mouse: a new tool for targeting specifically neural crest cells and their derivatives in vivo. Dev Biol 259:176–187.

Sefton M, Sanchez S, Nieto MA. 1998. Conserved and divergent roles for members of the Snail family of transcription factors in the chick and mouse embryo. Development 125:3111–3121.

Sela-Donenfeld D, Kalcheim C. 1999. Regulation of the onset of neural crest migration by coordinated activity of BMP4 and Noggin in the dorsal neural tube. Development 126:4749–4762.

Selleck MA, Bronner-Fraser M. 1995. Origins of the avian neural crest: the role of neural plate-epidermal interactions. Development 121:525–538.

Selleck MA, Garcia-Castro MI, Artinger KB, Bronner-Fraser M. 1998. Effects of Shh and Noggin on neural crest formation demonstrate that BMP is required in the neural tube but not ectoderm. Development 125:4919–4930.

Shoval I, Ludwig A, Kalcheim C. 2007. Antagonistic roles of full-length N-cadherin and its soluble BMP cleavage product in neural crest delamination. Development 134:491–501.

Simeone A, Acampora D, Gulisano M, Stornaiuolo A, Boncinelli E. 1992. Nested expression domains of four homeobox genes in developing rostral brain. Nature 358:687–690.

Solloway MJ, Robertson EJ. 1999. Early embryonic lethality in *Bmp5;Bmp7* double mutant mice suggests functional redundancy within the 60A subgroup. Development 126:1753–1768.

Taneyhill LA, Coles EG, Bronner-Fraser M. 2007. *Snail2* directly represses cadherin6B during epithelial-to-mesenchymal transitions of the neural crest. Development 134:1481–1490.

Trumpp A, Depew MJ, Rubenstein JL, Bishop JM, Martin GR. 1999. Cre-mediated gene inactivation demonstrates that FGF8 is required for cell survival and patterning of the first branchial arch. Genes Dev 13:3136–3148.

Vincent S, Ruberte E, Grieder NC, Chen CK, Haerry T, Schuh R, Affolter M. 1997. DPP controls tracheal cell migration along the dorsoventral body axis of the Drosophila embryo. Development 124: 2741–2750.

Wilkinson DG, Bailes JA, McMahon AP. 1987. Expression of the proto-oncogene int-1 is restricted to specific neural cells in the developing mouse embryo. Cell 50: 79–88.

Zhang H, Bradley A. 1996. Mice deficient for *BMP2* are nonviable and have defects in amnion/chorion and cardiac development. Development 122:2977–2986.